

# CO<sub>2</sub> capture materials: a review of current trends and future challenges



Bartosz Dziejarski <sup>a, b,\*</sup>, Jarosław Serafin <sup>c</sup>, Klas Andersson <sup>b</sup>, Renata Krzyżyska <sup>a</sup>

<sup>a</sup> Faculty of Environmental Engineering, Wrocław University of Science and Technology, 50-370 Wrocław, Poland

<sup>b</sup> Department of Space, Earth and Environment, Division of Energy Technology, Chalmers University of Technology, SE-412 96 Gothenburg, Sweden

<sup>c</sup> Department of Inorganic and Organic Chemistry, University of Barcelona, Martí i Franqués, 1-11, 08028 Barcelona, Spain

## ARTICLE INFO

### Article history:

Received 15 April 2023

Accepted 20 July 2023

Available online 28 July 2023

### Keywords:

CO<sub>2</sub> adsorption

Sorption

Adsorbents

Greenhouse gases

CO<sub>2</sub> emission

Climate change mitigation

## ABSTRACT

Over the last decade, CO<sub>2</sub> adsorption technology has quickly gained popularity and is now widely applied in global CCUS projects due to playing an important role in achieving net-zero emissions by 2050. As a result, novel materials, or post-modification methods of those already available have been successively reported to enhance the efficiency of CO<sub>2</sub> capture from flue gases. This paper discusses a systematic understanding of fundamental aspects of current research trends in terms of developing selected solid CO<sub>2</sub> adsorbent, with a particular emphasis on the upcoming challenges. The candidates are reviewed considering the practical drawbacks of imposed by industrial scale and economics, including carbon-based materials, metal-organic frameworks (MOFs), polymers, zeolites, silica, alumina, metal oxides, amine-based adsorbents, and other composite porous materials. Sustainable sorbents derived from biomass and industrial residues are also studied due to the high need for cost-effective raw materials and their crucial role in the circular economy. Lastly, a techno-economic analysis (TEA) is included to provide the most important criteria that should be considered when adsorbents are implemented on an industrial scale. Consequently, the review is summarized, and recommendations are offered for future research in the advancement of CO<sub>2</sub> capture materials. The paper aims to establish a comprehensive theoretical basis of adsorption technologies currently progressed to reduce CO<sub>2</sub> emissions, along with highlighting the identification and precise articulation of the most important future research paths that could be beneficial to address over the next years.

© 2023 The Author(s). Published by Elsevier Ltd. This is an open access article under the CC BY license (<http://creativecommons.org/licenses/by/4.0/>).

## 1. Introduction

### 1.1. The impact of industrialization on CO<sub>2</sub> emissions and climate change

Since the beginning of the industrial revolution, there has been an exceptional boost in the amount of heavy pollution released from industrial facilities, mainly as a result of the burning of fossil fuels (coal, crude oil, and natural gas). Today, one of the most challenging and urgent environmental issues facing the world is the reduction of CO<sub>2</sub> concentration in the atmosphere, which is widely reported to be the main anthropogenic greenhouse gas that leads to global warming and climate changes [1]. For this reason,

the constant rise in average temperatures throughout the world and the associated frequency with greater intensity of the emergence of severe extreme weather events (heat waves, droughts, blizzards, and rainstorms) are among the most direct and immediately apparent effects that have resulted from this phenomenon [2,3]. It is anticipated that human activities have contributed to an escalation of global temperature of around 1 °C surpassing those of the pre-industrial period of time, with a probable range of 0.8–1.2 °C [4]. In 2020, CO<sub>2</sub> average annual level in the atmosphere was approximately 50% higher than in the 60's 18th century and has attained their greatest value recorded in the history of 412.5 ppm [5].

Unfortunately, the rapid development of the world's economic, and accelerating industrialization, with a soaring world population, will definitely cause a gradual growth of CO<sub>2</sub> emissions and will affect global warming to reach 1.5 °C in the next 30 years at the current state [1]. According to the Intergovernmental Panel on Climate Change (IPCC) latest report from 2022, to prevent this

\* Corresponding author.

E-mail addresses: [bartosz.dziejarski@pwr.edu.pl](mailto:bartosz.dziejarski@pwr.edu.pl), [bartoszd@chalmers.se](mailto:bartoszd@chalmers.se)  
(B. Dziejarski).

scenario, climate change mitigation efforts should be executed immediately. IPCC estimation indicates that the peak of GHG emissions must take place in 2025 at the latest, so by 2030 a 43% reduction of it will possibly be achieved. Otherwise, by the end of 2100 the average temperature on Earth and atmospheric concentration of CO<sub>2</sub> will increase by 3.2 °C and to 570 ppm, respectively [6]. In order to prevent this occurrence and meet the Paris Agreement climate ambition, specific system changes for energy management should be adopted. In particular, innovative transformation concerns industry, which is responsible for 25% of CO<sub>2</sub> emissions from energy and industrial processes, such as the cement, chemicals, iron and steel sectors [7]. Furthermore, it is associated with widespread electrification, better energy efficiency, aiming at rational supervision of fossil fuel exploitation, and intensification of the share of renewable energy sources (hydrogen, biomass-based fuels, solar energy, or nuclear power) in global energy consumption. Although the above long-term plans have enormous potential, they are currently unable to lessen the carbon footprint of humanity simply by mitigation of CO<sub>2</sub> emissions, burning fossil fuels, and R&D on total commercialization of clean energy requires large financial outlays and investments, and above all time.

In view of this, over the course of the last several decades, a concerted initiative has been launched all over the world to create new methods for point source carbon capture aiming to stop CO<sub>2</sub> emissions from entering the atmosphere. Especially one receives the most interest and is predicted to play a crucial part in the evolution toward the use of low-carbon energy, which is called carbon capture, utilization and storage (CCUS). The CCUS system specifies a group of technologies, such as carbon capture and storage (CCS), carbon capture and utilization (CCU), or bioenergy with carbon capture and storage (BECCS). Among the CCUS value chain, the CO<sub>2</sub> capture stage roughly represented around 70–90% of total operating expenditures, making it one of the key research areas for maturing the entire technologies and contributing to the achievement of net zero emissions [8]. Depending on the specific CO<sub>2</sub> manufacturing method, operating conditions, composition of flue gas and process parameters, there are three main capture approaches: pre-combustion capture, post-combustion capture, and oxy-fuel combustion [9]. Each of the above uses various CO<sub>2</sub> separation process, which are the most vital part of CO<sub>2</sub> capture, including: absorption, membranes, cryogenic method, chemical looping combustion (CLC), calcium looping (CaL), and adsorption.

## 1.2. A wide spectrum of CO<sub>2</sub> capture materials

The application of solid adsorbent materials is widely regarded as one of the most promising research directions and has garnered a high amount of attention for carbon capture in CCUS [10]. It delivers benefits such as, amongst others: considerably high CO<sub>2</sub> uptake efficiency, easy regeneration, simple handling, wide process operability range, material stability, the possibility of using broadly understood waste to produce materials [11]. Important definitions that should be used for the correct CO<sub>2</sub> adsorption characteristics are the formulations of the individuals participating in the process: adsorbent – a solid on which gas molecules from inside the gas phase are adsorbed, and adsorbate – a gas that has finally been adsorbed on the surface of the adsorbent [12]. There are two main types of gas molecule adsorption on the surface of a solid. If the accumulation of the adsorbate on the surface of the solid occurs due to weak intermolecular van der Waals interactions, then adsorption is termed physisorption or physical adsorption [12,13]. When gas molecules accumulate on the surface of the adsorbent by chemical bonds, the phenomenon occurring is called chemical adsorption or chemisorption [14]. Each of these two groups

contains specific materials that are commonly called physical and chemical adsorbents.

Generally, the most widely used solid materials for CO<sub>2</sub> capture are silica, zeolites, alumina, amine-based materials, metal oxides, metal-organic frameworks (MOFs), polymers, and carbon materials (activated carbon, graphite, graphene, fullerene, carbon nanotubes, biochar, and hydrochar). Moreover, it is crucial to elucidate the differentiation between amorphous and crystalline solids in terms of sorbents due to their substantial impact on CO<sub>2</sub> uptake performance, related strictly with their distinct physical and chemical characteristics. Crystalline materials exhibit distinct pore structures and surface areas, thus demonstrating the potential for significant CO<sub>2</sub> adsorption capacity. Their high stability under harsh process conditions and precise regulation of pore size and distribution can be optimized for practical purposes in CCUS projects. In contrast, materials characterized by the absence of a definite lattice pattern in the arrangement of its constituent atoms and molecules demonstrate an amorphous structure. The lack of a defined arrangement often results in elevated surface areas and porosities, making them highly suitable for CO<sub>2</sub> capture. However, it could also potentially lead to inadequate stability and diminished selectivity. Therefore, it is imperative to understand the properties while choosing and formulating CO<sub>2</sub> capture materials for particular uses. The optimal CO<sub>2</sub> adsorption efficiency can be achieved by utilizing either amorphous or crystalline materials, or a combination of both, depending on the specific requirements of the application. The number of publications since 2013 that have concerned solid materials for CO<sub>2</sub> capture is shown in Fig. 1.

As can be observed, over the last several years, there has been a substantial increase in the number of researchers interested in CO<sub>2</sub> capture by adsorption. This results directly in the publication of scientific articles related to the synthesis of different new materials or post-modification methods to optimize the efficiency of the CO<sub>2</sub> adsorption capacity. However, a generic overview that focuses on summarizing the current knowledge for beginner scientist in this field in sense of critical limitations, opportunities, or research trend for a specific adsorbent group, is not something that has been reported very often in the recent years.

In general, the aim of this review is to provide a comprehensive summary of advances that have been accomplished in the development of solid CO<sub>2</sub> capture materials with highly insightful current and future research directions. Furthermore, our work includes a compilation of up-to-date data on physicochemical measurements along with modification strategies to improve CO<sub>2</sub> adsorption capacity. Moreover, we also discuss the details of the techno-economic analysis (TEA), which is an essential procedure for introducing novel materials on an industrial level. Ultimately, several concluding perspectives are provided with proposed solutions for the existing challenges and upcoming barriers in commercial facilitation of discussed sorbents.

## 2. Desired properties and criteria for selecting CO<sub>2</sub> capture materials

To efficiently removing CO<sub>2</sub> from the flue gas mixture, the synthesized adsorbents should possess stringently specified good characteristics and satisfy technical and economic requirements that are favorable for CO<sub>2</sub> adsorption (Fig. 2). First and foremost, the material must be characterized by a high capacity to efficiently adsorb CO<sub>2</sub> under a variety of process conditions. Additionally, it is essential that the materials have superior application capability for commercial purposes. Regrettably, it is quite unusual to satisfy all crucial requirements. In this section, an evaluation of the most important adsorbent properties and criteria are listed below [12,14].

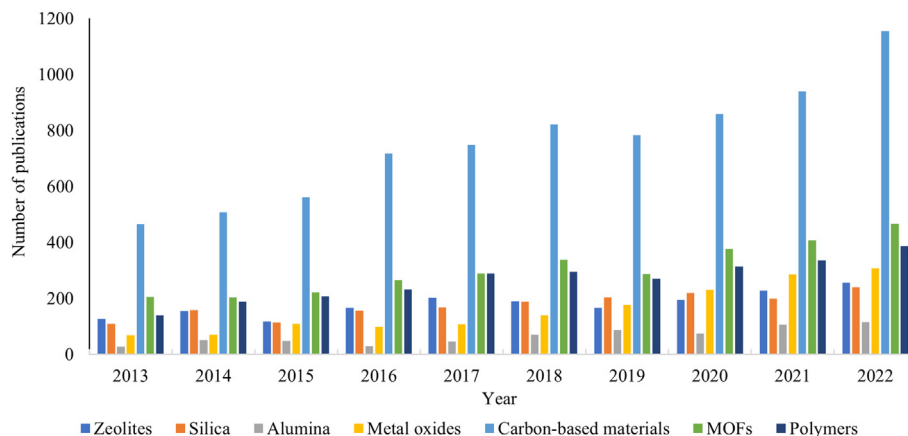


Fig. 1. Number of publications on CO<sub>2</sub> capture with various solid materials since 2013 (based on Scopus with keywords “CO<sub>2</sub> adsorption” or “CO<sub>2</sub> capture”).

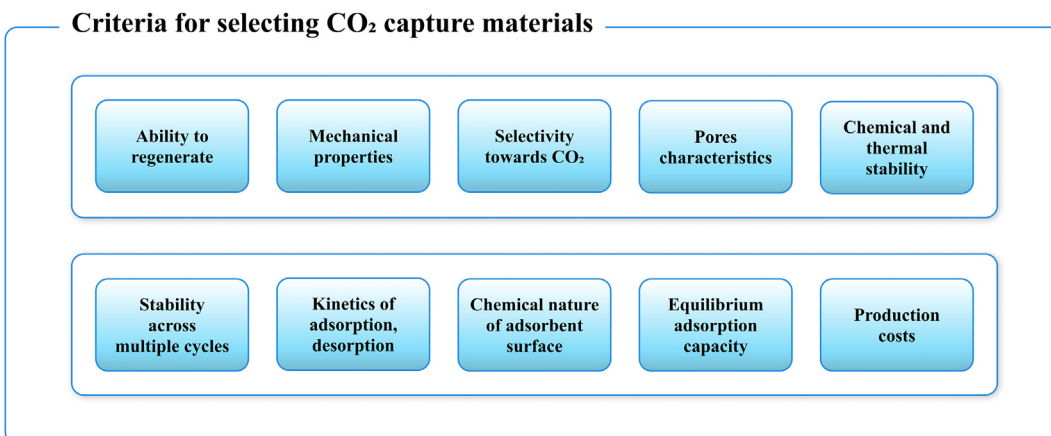


Fig. 2. The most important properties and criteria for selecting CO<sub>2</sub> capture materials.

- Equilibrium adsorption capacity is directly related to the specific surface, pore size, and surface chemistry of the adsorbent. The capacity value indicates the maximum amount of adsorbate related to the adsorbent mass unit that can be adsorbed at equilibrium (phase equilibrium at the solid–gas interface, where the adsorption rate is equal to the desorption rate) for a given temperature and pressure.
- CO<sub>2</sub> selectivity parameter serves as a theoretical metric for evaluating the practical effectiveness of an adsorbent, especially in scenarios involving the adsorption of multicomponent gaseous mixtures. It mainly depends on the size, shape, and distribution of pore network. The selectivity has a direct impact on the degree of purity of the obtained product, which in turn affects the economics of the adsorption installation. This criterion is the most important for physical adsorbents.
- Kinetics of adsorption and desorption are influenced by several factors, including the size of adsorbate molecules, the porosity of sorbent material, the concentration of adsorbate in the flue gas stream, and even the type of chemical bonding formed during the process, which also exerts a significant impact. Kinetics during CO<sub>2</sub> sorption should exhibit favorable and significantly fast behaviour, indicating that a short time is required to attain the equilibrium state between the adsorbate–adsorbent complex or to facilitate expedited regeneration of the adsorbent bed.
- Mechanical properties, the adsorbent should be mechanically strong, i.e., perfectly resistant to abrasion and crushing during its operation in process equipment (adsorption and chromatographic columns under various process conditions). These properties directly affect the efficiency of the process and the generation of additional costs.
- Chemical nature of surface is also an important determinant. The adsorption capacity of adsorbent may be enhanced by the presence of heteroatomic functional groups in the form of carbon–oxygen, carbon–nitrogen, or carbon–sulfur on its surface. The most significant functional groups contain oxygen atoms, so conferring a hydrophilic (polar) character to the outer surface, in addition to the hydrophobic (nonpolar) nature shown by the internal structure of the material. The dual nature of the adsorbent surface allows it to effectively adsorb a diverse range of gases, with a particular emphasis on CO<sub>2</sub> from flue gas streams containing moisture.
- Pores characteristics, there is a one-to-one correlation between the presence of micropores and the effectiveness of material in the adsorption process. Their widths are comparable to those of the CO<sub>2</sub> molecules that are capable of being adsorbed, falling within the range of <2 nm. Mesopores and macropores, which serve secondary functions, have the responsibility of transporting the adsorbed gaseous medium via a network of channels.

- Chemical and thermal stability, adsorbents are often exposed to harsh chemical conditions (the flue gas stream mainly contains water vapor and other impurities, such as CO<sub>2</sub>, trace elements, particulates, NO<sub>x</sub>, and SO<sub>x</sub>), as well as high pressure and elevated temperature. Robust stability and exceptional tolerance under these conditions ensure their proper lifetime, high equilibrium sorption capacity, and the possibility of subsequent regeneration and reuse in a greater number of adsorption–desorption cycles. The lack of an appropriate degree of chemical and thermal stability of the sorbent directly affects the economics of the entire CO<sub>2</sub> separation process.
- Regeneration capacity, adsorbents undergo a regeneration process after their adsorption capacity is exhausted, as a result of the maximum filling of the pore volume and occupying their surface with CO<sub>2</sub> molecules. The process of regeneration involves removal of the adsorbed CO<sub>2</sub> molecules from both the pores and the surface of adsorbent by desorption. This fully allows the restoration of the sorption capabilities of the material. Furthermore, the investigation of optimal sorbent regeneration conditions is now a key subject of current research in the selection of the suitable materials. Depending on their structure and physicochemical properties, the adsorption/desorption cycles are carried out considering parameters, such as temperature, pressure, and applying a specific adsorption technology or as a combination of several types: pressure swing adsorption (PSA), vacuum swing adsorption (VSA), vacuum pressure swing adsorption (VPSA), temperature swing adsorption (TSA), temperature pressure swing adsorption (TPSA), and electric swing adsorption (ESA).
- Stability in adsorption/desorption cycles and the lifetime of adsorbents play a crucial role in determining the frequency of material replacement, hence directly influencing the economic viability of industrial-scale installations.
- Production costs are another crucial parameter that is considered obligatorily in terms of the development of adsorbent production technology and the analysis of prospective research directions for materials suited to CO<sub>2</sub> sorption processes.
- Environmental implications, it is essential to appropriately dispose of adsorbents that are incapable of undergoing further regeneration. Therefore, they cannot possess a significant adverse influence on the environment.

The evaluation of the described criteria and attributes of adsorbent's effectiveness to capture CO<sub>2</sub> is based on an analysis of the initial characteristics of synthesized materials, as well as experimental investigations into CO<sub>2</sub> adsorption isotherms, breakthrough curves of adsorbent bed, and mass transport kinetics. The entire procedure is shown schematically Fig. 3.

### 3. CO<sub>2</sub> capture materials

#### 3.1. Amine-based adsorbents

One prevalent method used in the industrial sector so far involves the utilization of aqueous amine solutions with a concentration ranging from 20 to 30 wt% for the purpose of capturing post-combustion carbon dioxide [15–17]. This approach is primarily favored owing to the notable affinity shown by amines towards CO<sub>2</sub>. Nevertheless, the practicality of using amine is limited due to many drawbacks. One of these disadvantages is the high heat capacity of the liquid phase, which results in substantial energy consumption and increased costs during the regeneration process [18]. Another significant difficulty connected with aqueous amine absorption lies in its limited technological scalability, confining its applicability to CO<sub>2</sub> capture from coal or natural gas power plants

[19]. Additional complications encompass equipment corrosion and amine solvent degradation due to the presence of oxygen in the aqueous solution [20]. Therefore, to minimize these issues and potential elevated costs, research efforts are concentrated on the development of amine-functionalized solid materials, referred to as N-functionalized solid adsorbents (NFSAs). This approach aims to improve the CO<sub>2</sub> capture capacity of amine groups by increasing functional group availability and adsorption kinetics, concurrently ensuring stability and high porosity. Moreover, when compared to unmodified porous adsorbents, NFSAs exhibit improved CO<sub>2</sub> affinity and superior moisture tolerance. Thus, they have garnered attention as highly promising candidates for CO<sub>2</sub> adsorption from flue gas mixtures [21,22]. The excellent affinity of N-functionalized solid adsorbents towards CO<sub>2</sub> and their enhanced resistance to moisture can be attributed to the existence of nitrogen-containing functional groups on their surface. These functional groups possess the capability to interact with CO<sub>2</sub> molecules via diverse mechanisms such as electrostatic interactions, hydrogen bonding, and Lewis acid-base interactions. Furthermore, the nitrogen-containing functional groups confer hydrophobic characteristics to NFSAs, enabling them to withstand moisture and maintain CO<sub>2</sub> uptake efficiency even in high-humidity conditions.

The amine-based adsorbents are typically synthesized in two independent steps: initial preparation of solid supports and the subsequent integration of N-source sorbents with these supports. For the creation of high-performance NFSAs, a variety of different amine types can be employed, as listed in Table 1.

Further, numerous porous solid materials have also been investigated and documented for their ability to adsorb CO<sub>2</sub> from flue gas streams. These materials involve the functionalization of amines onto supports like activated carbons (ACs), carbon-based nanoadsorbents, mesoporous silica, zeolites, porous organic polymers, metal oxides, and others, all of which are extensively covered in this review. To date, three distinct classes of amine-based sorbent have been identified, based on the combination of the amine species/support material (bond structures), and nitrogen sources (types of amines) [23,24].

These classes are categorized as follows: Class 1 (impregnation method), Class 2 (grafting method), and a combination of the impregnation and grafting approaches, often referred to as Class 3 (direct synthesis method) [25,26]. Each of these classes offers unique synthesis paths, which are described below:

- Class I materials are prepared through the physically loading monomeric or polymeric amine species, amino acid, amino-containing ionic liquid, into accessible pores and on the surface of porous support [27,28]. This process involves the use of a solvent, typically water or organic solvents like methanol or ethanol, to combine the amine with the support. The solvent aids in dispersing amine molecules into the pores of the support material [27]. Within the pores and on the support surface, amine molecules that have formed bonds with each other serve as active adsorption sites for capturing CO<sub>2</sub>. Notably, the amine groups do not interact with the support in a chemical manner, meaning there is no substantial chemical bond or reaction between the loaded amines and the surface of the support. The total pore volume of the porous material, along with the amine density, plays a key role in determining the amount of amine that can be effectively dispersed into the porous structure [29]. Ideally, the support material should possess a larger pore volume, as this increases the potential capacity for impregnated amine. Once the impregnation step is complete, excess solvent is removed through filtration, followed by drying of the solution. The resulting amine-loaded adsorbent is then further dried in an oven at a temperature of around 40 °C [30].

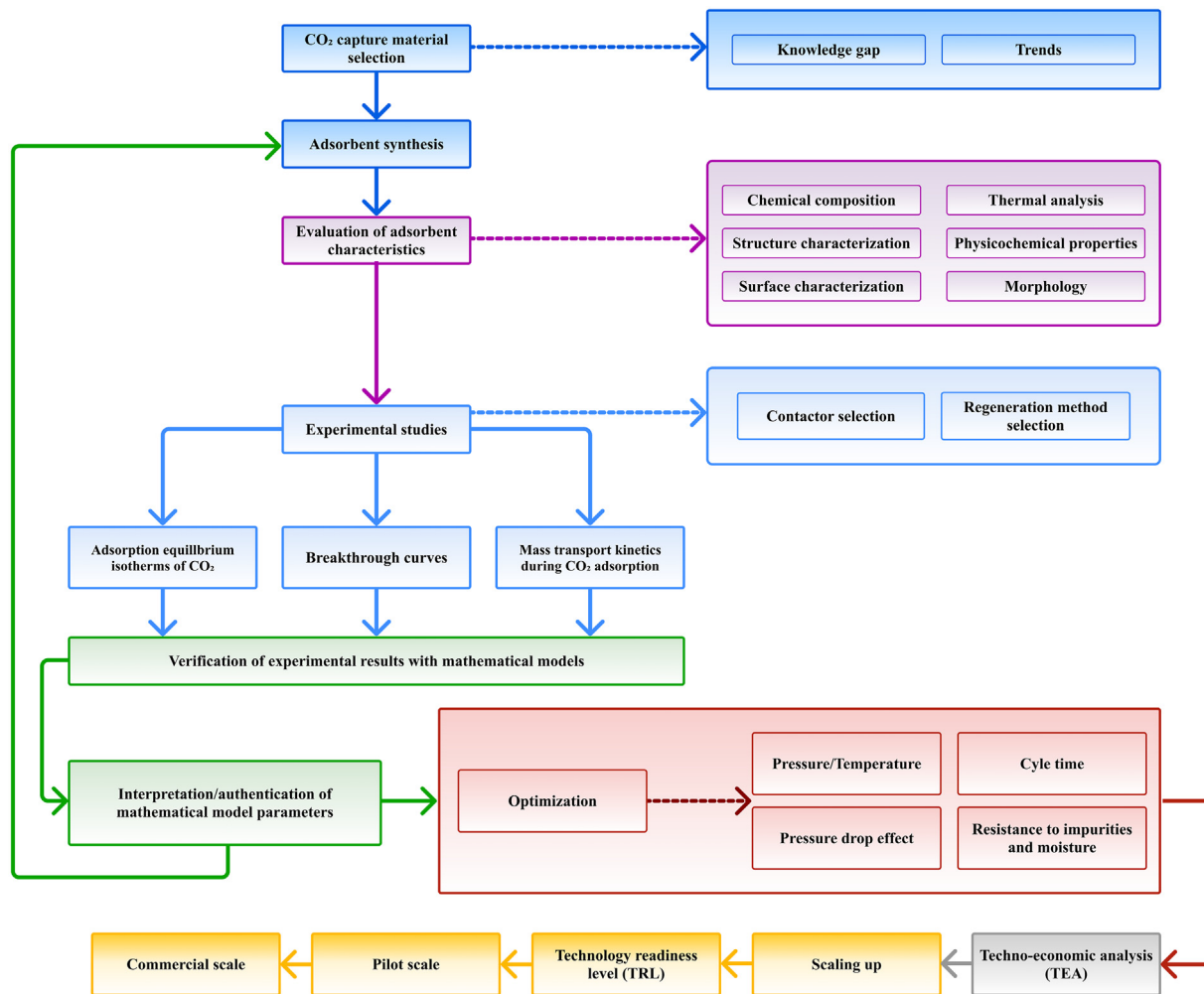


**Fig. 3.** The examination path to evaluate the suitability of materials for CO<sub>2</sub> capture application.

- In class II, materials are synthesized by dissolving the amine-containing organosilanes in a volatile solvent. The adsorbent is introduced into the solution and heated to facilitate covalent tethering. During this covalent bonding process, the amines of the silane group become attached to the surface functional groups of the support material. More specifically, hydroxyl groups (OH<sup>-</sup>) at the target interface form bonds with the central region of the organosilanes, leading to adhesion [31,32]. Therefore, it's crucial that the support material's surface contains a high concentration of these hydroxyl functional groups. Once the grafting process is complete, the primary solvent is replaced with a second volatile solvent. This step serves to activate the adsorbent by removing any remaining unreacted amine molecules [31,33]. Consequently, the number of active groups present on the substrate surface is critical in determining the quantity of loaded amine and the resulting adsorption performance [34]. This synthesis approach results in a stronger linkage between the support and the amine compared to the impregnation method.
- Class III materials are created through in situ polymerizations of the amine-containing precursor, which is the amine polymer monomer in the porous material. The direct synthesis method also relies on chemical bonding, resulting in materials featuring a single covalent bond for each amine molecule. Additionally, these materials are characterized by the

presence of C–O interface bonds [31]. Compared to the impregnation and grafting methods, the direct synthesis process is accomplished in a single step, reducing the complexity of the operation. Furthermore, the distribution of amino groups in the amine-based solid adsorbent is more uniform compared to the other methods [29]. This class of supported materials can be considered as a cross-over between the other two methods.

Considering the three major techniques mentioned above. Two different types of adsorbents can be synthesized, such as amine-loaded adsorbents (obtained by impregnation and grafting) and N-doped adsorbents (prepared by direct synthesis). In addition, a novel synthesis approach called double functionalization has been developed for the preparation of amine-based materials. This approach involves two functionalization steps, namely impregnation and grafting, combining the benefits of these two single synthesis techniques.

In conjunction with the numerous successes in the creation of NFSAs for increased CO<sub>2</sub> capture in recent years, several reviews have been compiled to provide the most up-to-date and relevant insights into their development. Therefore, the focus is particularly on review papers reported in 2020–2022. In 2020, Hu et al. [27] published a review that explored future research and development directions, as well as potential commercialization routes

**Table 1**

Commonly used types of amines in I, II, and III class.

Amine type	Abbreviation	Structure	Class
Monoethanolamine	MEA		I
Diethanolamine	DEA		II
Ethylenediamine	EDA		I
Diethylenetriamine	DETA		I
Tetraethylenepentamine	TEPA		III
Triethylenetetramine	TETA		I
Pentaethylenehexamine	PEHA		III
Polyethyleneimine	PEI		II
Isopropanol amine	IPA		III
2-Amino-2-methyl-1,3-propanediol	AMPD		III
2-Amino-2-methyl-1-propanol	AMP		III
(3-Aminopropyl)trimethoxysilane	APTMS		III

for amine-based adsorbents. The researchers emphasized two probable aspects of NFSAs development. The first objective is to overcome their disadvantages, making them more competitive with aqueous amines. The second objective is to investigate their practical applications, including the design of test equipment and technological methods applicable to current power plant systems and cost reduction. For amine-loaded adsorbents, one inherent drawback is their limited range of uses due to reduced adsorption capacity caused by factors, including ammonia loss during extended adsorption operations, oxidative degradation of amines, and degradation of porous supports due to irreversible adsorption of flue gas impurities like SO<sub>2</sub>, NO<sub>2</sub>, and O<sub>2</sub>. Regarding N-doped adsorbents, a fundamental challenge is controlling their adsorption capacity, either through the selection of materials or by improving the synthesis process. MOFs and polymers have been highlighted as the most promising options for the future. In conclusion, the authors point out the most important strategies for enhancing the adsorption performances of amine-loaded adsorbents, such as the following:

- The selection of appropriate amines for the synthesis of adsorbents with improved adsorption capacity or lower desorption temperatures (materials containing a mixture of two different amines often exhibit superior performance).

- Developing support features by increasing the pore diameters with specific reagents or selecting appropriate additives and solvents, using the most suitable treatment techniques.
- In the case of amine-impregnated adsorbents, it's preferable to choose supports with greater pore volumes and pore sizes, such as hierarchical pore structures or multilayered structures. Alternatively, for amine-grafted adsorbents, surfaces with a high concentration of hydroxyl groups are more convenient.
- Utilizing distinctive and well-structured supports, such as cage-structured zeolites, is recommended.
- Supports made of inexpensive materials that are abundant in nature, such as clay, are favored over more expensive alternatives.

In the same year, Gelles et al. [31] discussed the latest developments in the production and assessment of different kinds of amine functionalized materials, with the goal of presenting a thorough overview of current work and future trends in materials research and process implementation. The authors concluded that to adequately evaluate the potential of amine-based adsorbents for CO<sub>2</sub> capture, a comprehensive view must be employed, considering a variety of measurements that take both material and process performance into account. These data should be optimized as much as possible and can be categorized into main utilization criteria,

including CO<sub>2</sub> working capacity, adsorbent kinetics, regeneration requirements, cost, long-term stability, and formulation. In terms of future research, recent years have seen the development of class I-II and class I-III hybridized amine-materials. These hybrids have demonstrated superior working capability and cycle stability compared to their individual class counterparts. In consequence, it is highly likely that further advancements will be made in the development of hybridized materials. Additionally, it has been emphasized that, although VSA and TSA systems have demonstrated commercial viability, future research efforts should be directed towards conducting TEA. This analysis is essential for determining the costs associated with scaling up and ensuring the stability of amine-based adsorbents on an industrial scale. Over the years, various types of amines and adsorbent supports have been extensively investigated. In the future, the primary focus of research will be on identifying the optimal amine-adsorbent combination. This blend should be easy to synthesize and seamlessly integrate into process operations with minimal loss of CO<sub>2</sub> capture capacity.

Recently, in 2021, Zhao et al. [29] conducted a comprehensive review of the latest advancements in amine-functionalized solid adsorbents for post-combustion capture. Their recommendations for the development of NFSAs align with those proposed by Hu et al. [27] and Gelles et al. [31]. The authors highlighted the need to reduce preparatory costs and simplify the synthesis process, aiming to design a highly efficient and eco-friendly production method. They also stressed the importance of finding effective methods for introducing amines into practical support structures. Hence, the review noted that certain impurity gases, such as water vapor, can enhance CO<sub>2</sub> capture. Furthermore, most of the amine-based adsorbents studied so far exist in powder form, which can lead to challenges related to heat and mass transfer during CO<sub>2</sub> adsorption. Consequently, there is growing interest in monolithic adsorbents, which can improve heat and mass transfer rates and eliminate the need for the molding process. Finally, the review also mentioned the pressing need for research into the stability of these adsorbents on the commercial scale. Additionally, it's worth noting that amines are commonly employed as a post-modification method for solid CO<sub>2</sub> adsorbents, which are treated as supports. This category includes materials like graphene, graphite, activated carbons, and metal-organic frameworks. Among these materials, silica stands out as it represents the dominant research direction for amine functionalization [80,87]. Therefore, this review begins by focusing on this type of CO<sub>2</sub> capture materials.

**Fig. 4** illustrates the modification strategies, challenges, and current research directions of amine-based adsorbents. The size and color of the block sets change along the specialized investigation path, indicating that more specific areas of research are smaller in size compared to those representing broader ones. The order is consistently maintained: green > blue > purple > crimson. The same principle has been applied to other CO<sub>2</sub> capture materials as well.

### 3.1.1. Silica-based adsorbents

Silica is the collective term for a group of minerals found in various forms in the environment, typically as a crystalline solid with high hardness. It comprises silicon and oxygen, two of the most abundant elements in the Earth's crust. One of its most common forms is quartz, which is the planet's most prevalent mineral, constituting around 12% of its composition. The potential use of silica as an adsorbent for CO<sub>2</sub> capture lies in the synthesis of ordered mesoporous materials derived from it, possessing a precisely defined structure. However, amorphous silica presents challenges in supporting CO<sub>2</sub> adsorption. This is due to issues

related to pore control, problematic functionalization, and ineffective binding of CO<sub>2</sub> molecules.

A significant breakthrough in utilizing silica for sorption purposes occurred in the 1990s, marking a crucial moment in materials chemistry. Yanagisawa et al. [35,36] successfully synthesized mesoporous silica based on layered kanemite, which is a hydrated sodium silicate with the chemical formula NaHSi<sub>2</sub>O<sub>5</sub>·3H<sub>2</sub>O. This specific silicate showed a high ion exchange capacity, and its interlayer space was easily modifiable. The key innovation lay in the introduction of surface-active cationic organic compounds, often referred to as surfactants, between the layers of kanemite. This process enabled the creation of porous silica with remarkable characteristics, including a highly regular structure featuring a hexagonally ordered pore system. Moreover, this material boasted an exceptionally large specific surface area, reaching up to 900 m<sup>2</sup>/g, and pores with an average size of about 3 nm.

In 1992, the Mobile Research and Development Corporation achieved a notable advancement in creating materials similar to those developed by Japanese scientists [37,38]. This material family was named the M41S and comprised MCM-type materials (Mobil Composition of Matter), which were classified as MCM-41 (hexagonal), MCM-48 (cubic), and MCM-50 (lamellar, with surfactant molecules present between the lamellae). They showed variations in pore ordering. Especially, MCM-41 possesses a unidirectional pore system, featuring a regularly arranged hexagonal array of tubes. On the other hand, MCM-48 exhibits a three-dimensional pore system characterized by two non-intersecting gyroid pores. Among these, MCM-41 garnered the most attention due to its ordered and periodically repeating structure, even though it had an amorphous wall structure [39]. It was further distinguished by a specific surface area exceeding 1000 m<sup>2</sup>/g and relatively large pore sizes, some of which reached up to 10 nm. The development of M41S materials paved the way for the creation of new ordered mesoporous silicas, including SBA (Santa Barbara Amorphous) [40], MSU (Michigan State University), HMS (Hexagonal Mesoporous Silica), KIL (Kemijski Institut Ljubljana), FSM (Folded Sheet Materials), FDU (Fudan University), and KIT (Korean Advanced Institute of Science and Technology). These materials mainly differed in the arrangement of mesopores [41]. **Fig. 5** summarizes the collective efforts made in developing silica materials over the past few years, with their primary textural properties are presented in **Table 2**.

The unique properties of ordered mesoporous silica materials have broadened potential applications as solid sorbents for CO<sub>2</sub> capture in various scientific and technological disciplines. They offer several advantages, including high adsorption capacity under dry, high-pressure conditions (approximately 45 bar) and at ambient temperature, large surface area and pore volumes, tunable pore size, low production cost, superior regeneration stability with low regeneration energy requirements, good selectivity over CH<sub>4</sub> and N<sub>2</sub>, fast kinetics, or strong thermal and mechanical stability [45–47]. However, a distinct barrier associated with these materials, and an ongoing research focus to overcome it, is their limited hydrothermal stability, which involves the hydrolysis of Si—O—Si bonds. This limitation can affect their economic feasibility [48].

The final textural characteristics, including specific surface area, pore volume, pore size, and their distribution, can be modified by adjusting the synthesis process. This offers significant potential for increasing CO<sub>2</sub> adsorption capacity and addressing specific defects, particularly through surface modification [49]. Moreover, silica materials possess morphological flexibility and porosity, making them amenable to the integration of a wide range of organic and inorganic groups through the functionalization process [50,51]. Another avenue of research involves the development of composite/hybrid materials by dispersing nanoparticles of different metals within the porous structure of silica. This approach is advantageous

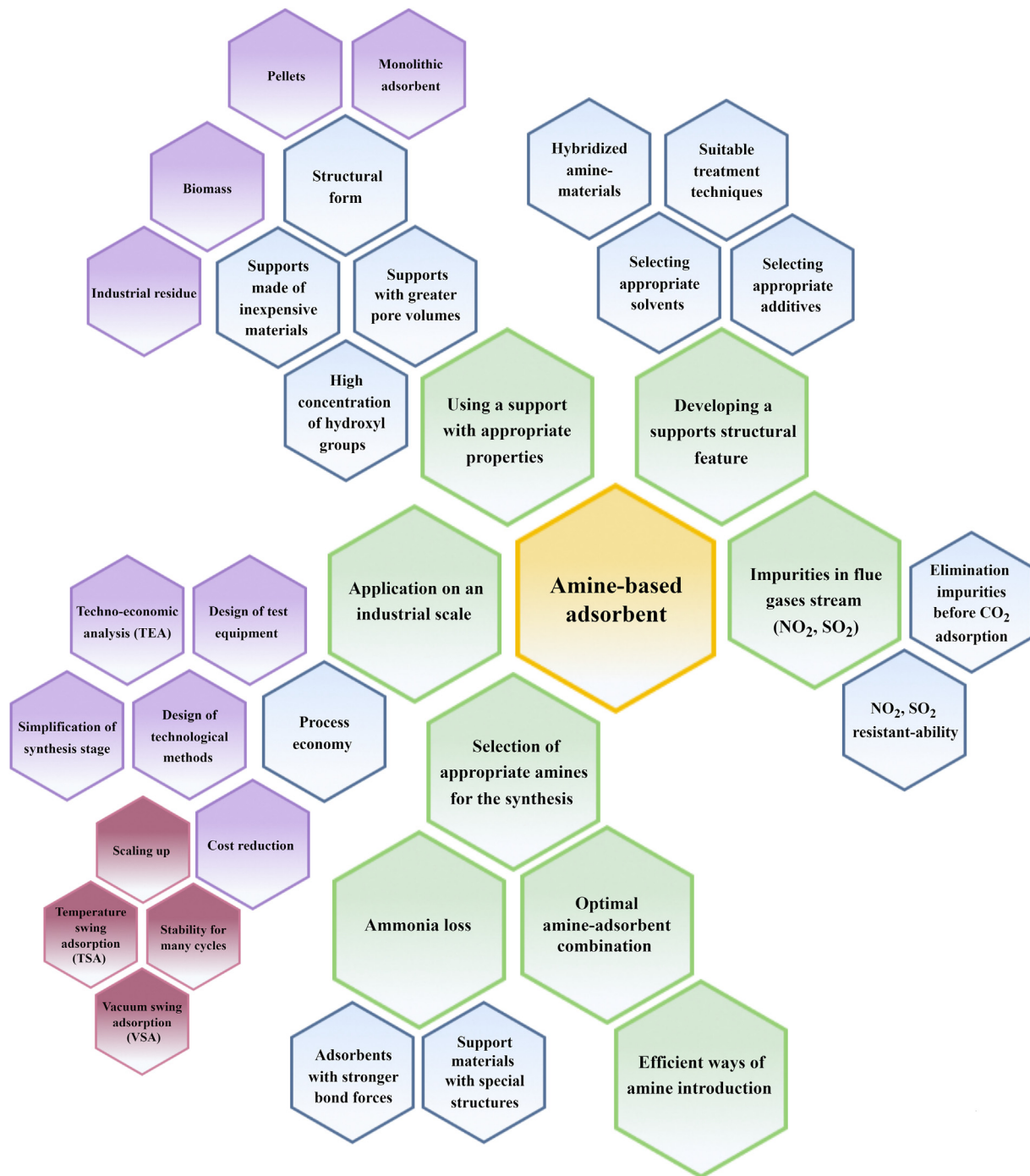


**Fig. 4.** The modification strategies and research directions of amine-based adsorbents.

when these materials are used as catalysts [52–54]. Additionally, silica can be combined with various adsorbents, such as carbon nanotubes (CNTs) [270], or MOFs [380], as discussed later in this review.

According to the literature, silica is mainly exploited as a support material for amine aimed at enhancing CO<sub>2</sub> capture, which is a strategy for designing new adsorbents. Numerous studies have also investigated the impact of moisture on CO<sub>2</sub> adsorption revealing that its content in the feed gas is beneficial for CO<sub>2</sub> uptake. As a result, a significant portion of research activity related to silica-based adsorbents focuses on developing various types of

silica materials, including silica nanoparticles, silica hollow spheres, silica nanotubes, silica fumes, mesocellular silica foams, macroporous silica, and aerogels [296]. Researchers investigate the selection of suitable amine functionalities. The modification of silica surfaces can be achieved through post-synthetic methods, such as chemical grafting or physical impregnation, which have been extensively discussed before [55–57]. On the other hand, amine functionalization can be accomplished by combining the above methods. This involves impregnating amine onto silica that has previously undergone grafting with amine-containing organosilanes [58].

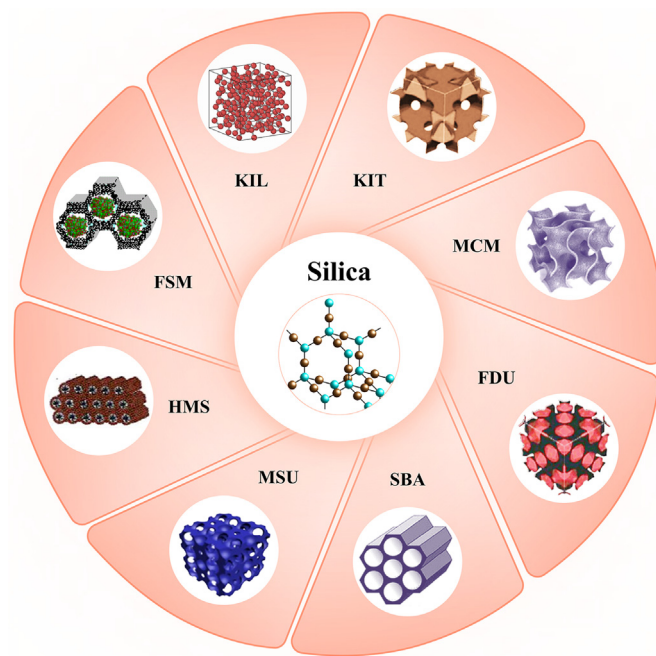


**Fig. 5.** Comparative overview of silica-based materials for CO<sub>2</sub> capture.

**Table 2**

Textural properties of different types of mesoporous silica-based materials [42–44].

Silica-based material	BET surface area, m <sup>2</sup> /g	Total pore volume, cm <sup>3</sup> /g	Pore diameter, nm
MCM-41	1229	1.15	2.7
SBA-15	950	1.31	6.6
MSU-1	1021	0.40	—
HMS	561	1.44	9.8
KIT-6	895	1.22	6.0
FDU-15	660	0.44	10.2
KIL-2	702	1.61	9.55

Zhang et al. [57] summarized recent advances between 2017 and 2019 in amine-functionalized silica for CO<sub>2</sub> capture. In their systematic review of the literature, the authors found few issues which need to be addressed for future practical applications. In the case of the amine-impregnated silica, while functionalization with high concentrations of amines is advantageous for easy sorbent preparation, a significant problem with these materials is their stability during many adsorption-desorption cycles. This matter is related to the leaching and degradation of amines, which can potentially be solved by introducing amines with higher boiling points or by reducing the operating temperature. In contrast, amine-grafted silica is stable throughout the cycles, but the amine loading is limited, and the synthesis method is more rigorous, resulting in lower CO<sub>2</sub> adsorption capacity. In addition, the authors noted that there is an insufficient number of research results on one-pot synthesis, which should receive more attention as a research direction. Chen et al. [56] drawn similar conclusions in their paper, which focused on contemporary progress in amine–silica composites, including the preparation and characterization of adsorbents, CO<sub>2</sub> capture under dry and moisture conditions, and stability after many cyclic adsorption–desorption runs. Furthermore, it was shown that although there are several successful methods for immobilizing amine species on a silica surface through a chemical grafting process, innovative procedures capable of achieving larger amine loadings are still required.

Future research paths should also consider the potential effects of silica functionalization by an amine moiety in ionic liquids (ILs),

as new advanced materials that show excellent CO<sub>2</sub> adsorption properties. Fatima et al. [55] collected data on the development and progress of silica functionalized with ILs, the mechanism of interaction, and the kinetics of CO<sub>2</sub> adsorption. The authors stated that traditional amines may readily be replaced with ionic liquids, which offer tunable physicochemical features such as cation/anion pairing, viscosity, and vapor pressure, among other properties. Some crucial topics that should be addressed were also identified, including the inability of ILs to be recycled along with the lack of life cycle assessment, limited knowledge of the adsorption mechanism, and the design of equipment for use on an industrial scale.

**Fig. 6** illustrates current and future research directions of silica-based adsorbents. **Tables 3** and **4** summarize the CO<sub>2</sub> uptake and textural properties of silica-based materials with specific amine functionalization methods.

### 3.2. Carbon-based adsorbents

The success of the CO<sub>2</sub> adsorption process essentially depends on the adsorbent material used. The rising levels of CO<sub>2</sub> emissions into the atmosphere have spurred significant interest among scientists and researchers in developing technologically advanced materials for gaseous media storage. Carbon-based materials have gained a wide interest due to their rather unusual physical and chemical properties highly related with the CO<sub>2</sub> uptake abilities.

They are characterized by low-cost precursor materials, low density, diverse carbon structural forms (powder, fibers, aerogels, composites, sheets, monoliths, tubes), high surface area, tailored surface chemistry (O, N, S, P, F, or other heteroatom doping), extensive pore morphology, large pore volumes, and very high resistance to rapid changes in temperature and pressure [94–96]. Among other attributes, they are distinguished by fine reproducibility and electronic properties [97,98]. Additionally, they possess the following unique features, which are especially highly relevant for CO<sub>2</sub> capture, as follows: (1) excellent stability, particularly in high and humid environments; (2) a hydrophobic surface, where CO<sub>2</sub> sorption on their surface is not affected by moisture; (3) a reversible nature of physical adsorption, where regeneration consumes less energy (weak van der Waals forces); (4) effectively suitable for adsorption usage under atmospheric pressure [94]. Carbon-based adsorbents comprise a diverse range of materials with varying morphologies, structures, and precursor sources. These materials can be broadly categorized into several basic groups, such as activated carbons, hydrochar, biochar, graphene, fullerenes, graphite, and carbon nanotubes (**Fig. 7**).

#### 3.2.1. Biochar and hydrochar

There has been a notable rise in demand for biomass-derived products along with industrial waste containing char across various economic sectors. This response stems from the pressing environmental challenges we currently face, encompassing CO<sub>2</sub> emissions, the climate crisis, and industrial contamination.

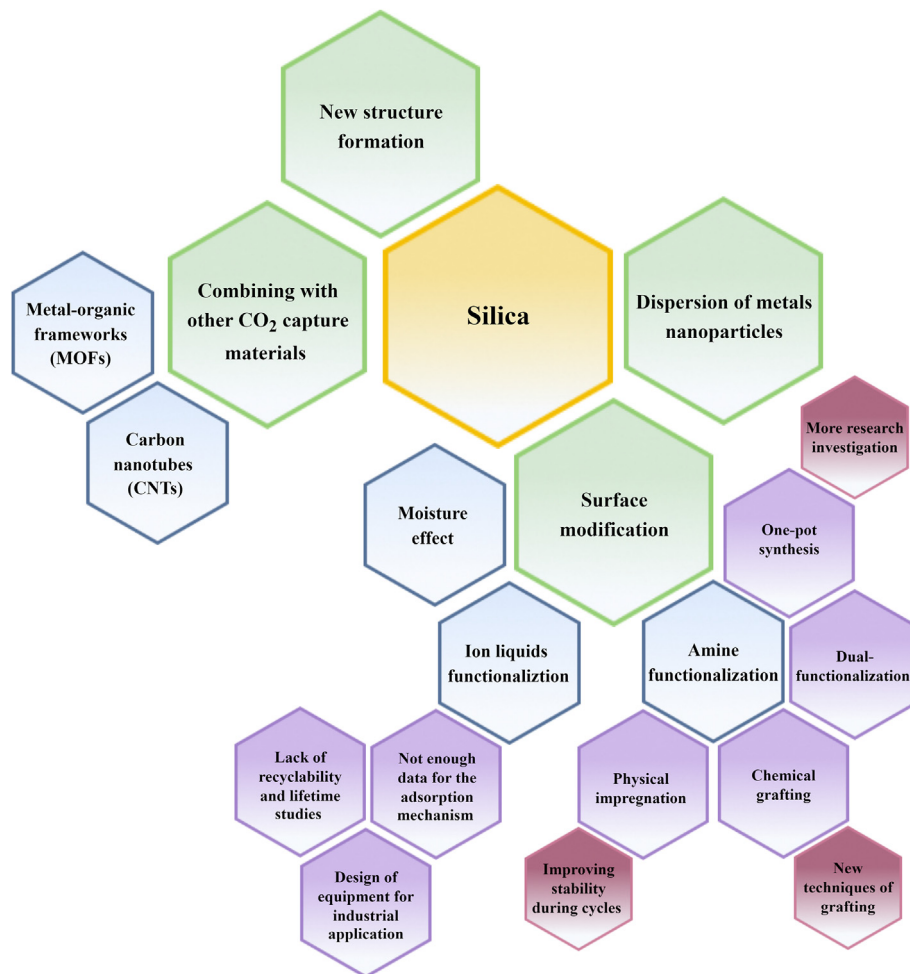


**Fig. 6.** The modification strategies and research directions of silica-based adsorbents.

Nowadays, scientists are concentrating their efforts on developing biochar and hydrochar, mainly due to the cost-effectiveness and sustainability merits [99].

Therefore, the focus has been highly diverted from other carbonaceous materials for the purpose of CO<sub>2</sub> capture. The classification of feedstock employed in the synthesis of biochar and hydrochar is one of the greatest paramount importance in determining the most optimal production method for the conversion process. In view of this, there are many different types of carbon-rich biomass that can serve as perspective, abundant and sustainable sources. These sources include residues from agriculture or forestry, food and energy crops, animal by-products, wood residues, as well as municipal wastes (Fig. 8) [99,100].

Many studies have explored thermal conversion as an alternative path to biomass processing, aiming to generate value-added products for CO<sub>2</sub> applications. This approach can break the chemical bonds in organic matter and directly convert its intermediates into char, bio-oil, and syngas [101]. Consequently, the biomass processing procedure strives to obtain char as a potential adsorbent, increasing the carbon content within the solid product [102]. The most common ways to produce biochar and hydrochar, respectively, are through the processes of pyrolysis and hydrothermal carbonization (HTC).

**3.2.1.1. Hydrochar.** Hydrochar is synthesized through hydrothermal carbonization, abbreviated as HTC, which may be used to produce low-cost CO<sub>2</sub> capture materials. This conversion process

relies on thermochemical decomposition of organic matter present in waste biomass into structural carbons within a high pressure and temperature water environment [103]. HTC is typically performed at temperatures ranging from 180 to 260 °C. During this step, biomass and water are combined, then subjected to high pressures of around 2–6 MPa for a duration of 5–240 min [104,105]. Among the specific parameters of HTC, process water exhibits characteristics akin to those of organic solvents and function as a catalyst in the biomass transformation through decarboxylation, condensation, aromatization, hydrolysis, and dehydration [106]. The resulting product based on converting organic material consists of carbonized material (hydrochar), liquid bio-oil, and gaseous volatile vapors. The final solid product preserves a considerable percentage of the original biomass structure, making it particularly valuable for carbon dioxide storage applications [107]. HTC char generally retains between 55 and 90% of the original mass of the feedstock while possessing 80–95% of its energy content [108].

Recently, a few reviews related to this research scope were published between 2018 and 2021. Goel et al. [103] examined factors necessary for achieving higher yields of biochar and hydrochar suitable for CO<sub>2</sub> capture. The authors highlighted several crucial process parameters affecting the sorption properties of the final HTC product, including the type of feedstock, temperature, pressure, residence time, biomass-to-process water ratio, and the use of a catalyst. Fang et al. [109] presented a concise summary of the potential applications of hydrochar and outlined the primary steps involved in the hydrothermal carbonization of biomass. They

**Table 3**Influence of amine functionalization on textural properties and CO<sub>2</sub> uptake of silica-based adsorbents.

Silica-based adsorbents	Functionalization agent	Amine loadings (Nitrogen)	BET surface area, m <sup>2</sup> /g	Total pore volume, cm <sup>3</sup> /g	CO <sub>2</sub> uptake, mmol/g	CO <sub>2</sub> , vol%	Adsorption temperature, °C	Pressure, bar	Reference
<b>Physical impregnation method</b>									
SiO <sub>2</sub> -NS	Polyethyleneimine	50 wt%	463.5	1.3	4.01	100	75	1	[59]
SBA-15	Polyethyleneimine	50 wt%	49.0	0.09	0.83	100	25	1	[60]
					1.70		45		
					2.04		75		
SBA-15	Polyethyleneimine	50 wt%	—	—	3.94	100	75	1	[61]
MCM-41	Polyethyleneimine	50 wt%	1254	2.44	3.19	100	75	1	[62]
Si-MCM-41	Polyethyleneimine	50 wt%	6	0.00	2.26	—	100	1	[63]
Silica monoliths	Tetraethylenepentamine	11.5 mmol N/g	13	0.07	2.23	10	25	1	[64]
Silica powder	Tetraethylenepentamine	12.8 mmol N/g	35	0.17	2.56	10	25	1	[64]
KIT-6	Polyethyleneimine	50 wt%	—	—	3.07	100	75	—	[65]
KIL-2	Tetraethylenepentamine	50 wt%	177	0.46	3.37	—	25	1	[44]
					4.35		95		
KIL-2	Polyethyleneimine	50 wt%	127	0.35	2.19	—	25	1	[44]
					3.60		95		
MSU-J	Tetraethylenepentamine	50 wt%	185	0.54	3.73	100	25	1	[66]
Platelet mesoporous silica	Branched polyethyleneimine	50 wt%	29.2	0.115	5.65	10	75	—	[67]
Granular silica	Polyethyleneimine	50 wt%	44	0.41	2.39	95	25	1	[68]
					3.06		55		
					3.11		85		
Microspherical silica	Polyethyleneimine	50 wt%	29	0.22	2.27	95	25	1	[68]
					3.07		55		
					3.26		85		
Silica	Tetraethylenepentamine; 1,2-epoxybutane	—	5.9	0.0	2.00	15	30	—	[69]
Mesoporous silica	Polyethyleneimine/diethanolamine (PEI/DEÄ50:50)	7.4 mmol N/g	74	0.46	2.93	100	35	—	[70]
ILs-SBA-15	Tetraethylenepentamine ([TEPA] [NO <sub>3</sub> ])	66 wt%	21.90	0.008	2.15	15	60	0.15	[71]
<b>Chemical grafting method</b>									
MCM-41	N <sup>1</sup> -(3-trimethoxysilylpropyl) diethylenetriamine	6.39 mmol N/g	38.75	0.4096	2.10	10	75	0.2	[72]
Silica monolith	3-aminopropyltrimethoxysilane	4.83	62	0.22	1.13	10	25	1	[64]
Silica powder	3-aminopropyltrimethoxysilane	4.95	103	0.32	1.14	10	25	1	[64]
SBA-15	N <sup>1</sup> -(3-trimethoxysilylpropyl) diethylenetriamine	3.14 mmol N/g	434	1.13	1.88	5	25	1	[73]
SBA-15	Diethylenetriamine alkoxysilane	—	81	0.15	2.00	100	45	1	[74]
Spherical silica gel	3-Aminopropyltriethoxysilane	—	203.59	0.49	1.56	1	35	—	[75]
Silica gel, dry grafted	N <sup>1</sup> -(3-trimethoxysilylpropyl) diethylenetriamine	3.39 mmol N/g	152	0.62	1.35	100	25	1	[76]
Silica gel, wet grafted	N <sup>1</sup> -(3-trimethoxysilylpropyl) diethylenetriamine	5.12 mmol N/g	73.1	0.31	1.97	100	25	1	[76]
					2.3		75		
KIT-6	(3-Aminopropyl)triethoxysilane	2.44 mmol N/g	90	0.22	1.56	—	30	1	[77]
HMS "as made"	Polyethyleneimine	50 wt%	11	0.02	2.40	100	45	1	[78]
HMS "calcined"	Polyethyleneimine	70 wt%	2.1	<0.01	2.19	100	45	1	[78]
Hierarchical bimodal silica, dry grafted	Diethylenetriamine alkoxysilane	28 wt%	203	0.96	1.72	70	25	1	[79]
Hierarchical bimodal silica, wet grafted	Diethylenetriamine alkoxysilane	49 wt%	28	0.19	2.31	70	25	1	[79]
MCM-41	Aminopropyl organosilanes	—	544	0.74	0.87	100	45	1	[80]
MCM-41	Ethylenediamino organosilanes	—	421	0.60	1.51	100	45	1	[80]
MCM-41	Diethylenetriamino organosilanes	—	373	0.54	1.75	100	45	1	[80]
SBA-15	Diethylenetriamine	—	204	0.36	1.90	100	45	1	[81]
Silica particles (0.5–1.5 nm)	Si-[P <sub>8883</sub> ]TFSI	—	263.9	0.1208	0.99	100	40	1	[82]
<b>One-pot synthesis</b>									
ILs-Silica aerogels	(3-Aminopropyl)triethoxysilane	—	6.37	—	5.53	50	—	1	[83]
Precipitated silica	(3-Aminopropyl)triethoxysilane	30 wt%	7.34	0.12	1.025	100	50	1	[84]
Silsesquioxane aerogel	(3-Aminopropyl)triethoxysilane	—	146.3	1.52	3.04	1	50	1	[85]
Mesoporous silica powder	Polyethyleneimine	54.09 wt%	413.9	0.27	2.82	15	75	1	[86]
<b>Double functionalization</b>									
Pore expanded MCM-41	Aminopropyl/Tetraethylenepentamine	50 wt%	169	0.20	2.37	100	45	1	[80]
Pore expanded MCM-41	Diethylenetriamino/Tetraethylenepentamine	50 wt%	162	0.18	2.13	100	45	1	[80]
Pore expanded MCM-41	Aminopropyl/Pentaethylenehexamine	30 wt%	88	0.16	1.53	100	45	1	[80]
MCM-41	3-aminopropyltrimethoxysilane/Tetraethylenepentamine	30/40 wt%	33.7	0.05	3.50	15	70	1	[87]

**Table 4** Comparison of CO<sub>2</sub> adsorption capacity of several functionalized silica-based adsorbents in dry and humid feed streams.

Silica-based adsorbent	Type of the surface modification	Functionalization agent	Amine loadings (Nitrogen)	BET surface area, m <sup>2</sup> /g	CO <sub>2</sub> uptake, mmol/g		CO <sub>2</sub> vol%	Adsorption temperature, °C	Pressure, bar	Reference
					Dry CO <sub>2</sub>	Humid CO <sub>2</sub>				
Macroporous silica	Physical impregnation	Polyethyl/eneimine Polyethyl/eneimine	50 wt% 60 wt%	261 0.09	1.80 4.07	2.44 3.84	15 15	40 75	0.15 1	[88] [89]
Mesoporous multiamellar silica vesicle	Physical impregnation	Polyethyl/eneimine Polyethyl/eneimine	11.5 mmol N/g 13.2 mmol N/g	13 8	0.07 0.03	2.23 1.21	10 1.96	25 10	1 25	[64] [64] [90]
Silica monoliths	Physical impregnation	Tetraethyl/enepentamine Polyethyl/eneimine Polyethyl/eneimine	30 wt%	16	0.01	1.63	5.05	15	25	1
Silica monoliths	Physical impregnation									
Core-shell 5A@mesoporous silica	Physical impregnation	Tetraethyl/enepentamine Tetraethyl/enepentamine Polyethyl/eneimine (3-Aminopropyl)triethoxysilane	63.8 wt% 50 wt% — —	90 3 — 146.3	0.28 0.02 — 1.52	3.52 3.45 2.2 3.04	4.02 4.28 2.27 3.84	15 10 75 1	75 10 70 50	1 1 1 1
Fibrous nanosilica	Physical impregnation									
Mesoporous silicas	Physical impregnation									
Mesoporous silica	Physical impregnation									
Silsesquioxane aerogel	One-pot synthesis									

brought attention to the necessity for unique syntheses and creative manufacturing techniques that are crucial for the development of value-added tailored carbon products from hydrochar. Moreover, to promote the practical implementation of hydrochar on an industrial scale, support for the concept of engineered hydrochar is also necessary in the research field. Unfortunately, there is still a noticeable lack of a critical literature review closely related to hydrochar for CO<sub>2</sub> capture and its utilization in cyclic regeneration systems at different scale. Precise systematization of current knowledge would significantly improve the scaling process of using these materials and increase their technological maturity.

Hydrochar itself obtained exclusively from the HTC process often exhibits a poorly developed microporosity and a low specific surface area, posing challenges for its use in CO<sub>2</sub> sorption purposes [110]. To improve the above properties, physical or chemical activation is widely reported as essential step to synthesize biomass-derived activated carbons (Fig. 9). As section 3.2.2 is devoted to ACs and the activation processes, the most important theoretic aspects of this material will be covered there.

**3.2.1.2. Biochar.** Biochar is a carbonaceous material obtained by pyrolysis, which involves the thermal decomposition of biomass under the influence of elevated temperature (ranging from 300 to 650 °C) in the absence of oxygen or other oxidizing agents. Following the completion of this process, three distinct groupings of products are created: gaseous (volatile parts), liquid (polycyclic aromatic hydrocarbons and water, the so-called bio-oil), and solid (high-carbon solid residue as well as ash, termed as biochar) [111]. A solid char, as in the case of hydrothermal carbonization, due to its porous structure, the prospect for a large storage capacity, and the existence of fundamental functional groups, has been recognized as an ecologically favorable and sustainable material in terms of CO<sub>2</sub> capture [112]. Considering a supply of biomass, it is approximately 10 times less expensive than other CO<sub>2</sub> adsorbents on the market and the cost of production is approximately one-sixth of that of ACs [113]. First and foremost, biochar is stable and does not degrade easily, its carbon half-life is between 100 and 10<sup>7</sup> years during exposition to ambient oxidation [114]. The ability of biochar to adsorb CO<sub>2</sub> is largely determined by its physicochemical characteristics, such as specific surface area, pore sizes, total pore volume, basicity of biochar surface, presence and type of surface functional groups, appearance of alkali and alkali earth metals, hydrophobicity, polarity, and aromaticity [115]. The aforementioned properties are inherently interconnected with the composition of the feedstock used in its formation as well as the thermochemical conditions. Biochar main component is obviously carbon, but there is also hydrogen, oxygen, nitrogen, a mineral substance, and trace amounts of sulfur [116]. Low-mineral biochars with a high content of carbon element are used for energy applications and the production of ACs. Consequently, the substantial concentration of mineral substances in biochars may potentially provide a beneficial effect on fertilizer and sorption utilization [117].

Many review articles have described the current state of knowledge on biochar between 2019 and 2022, with a particular emphasis on its use in CO<sub>2</sub> adsorption, as opposed to hydrochar. Jung et al. [118] devoted significant attention to advancing current research on activated biochars for CO<sub>2</sub> adsorption, derived from various biomass sources. According to the final findings of authors, the production of activated biochars from biomass holds promise as a viable approach for creating the required CO<sub>2</sub> capture materials. However, consideration needs to be given to the optimization of pyrolysis and activation parameters to enhance energy efficiency, reduce chemical usage, and minimize reaction time. This can be achieved through methods such as microwave-assisted pyrolysis or combining pyrolysis and activation into one step. Other aspects that

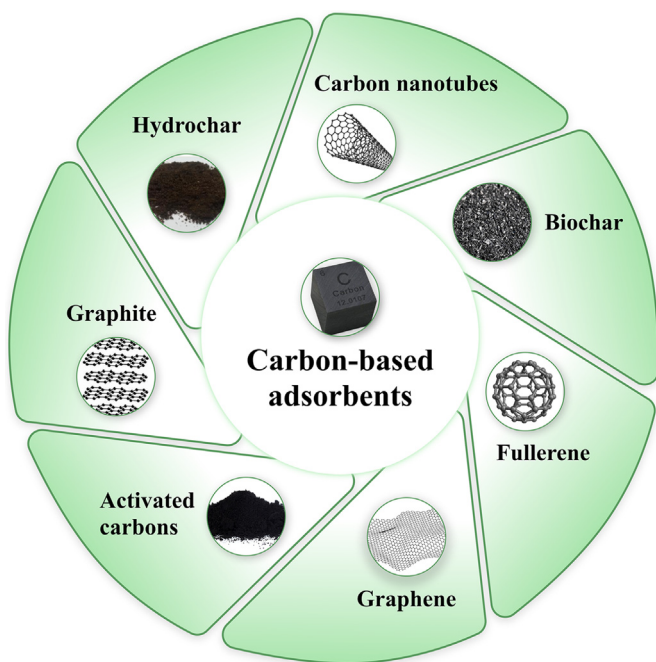


**Fig. 7.** Applicable carbon-based materials for CO<sub>2</sub> capture.

deserve future exploration include in-depth practical research on CO<sub>2</sub> separation from flue gas mixtures under varying conditions, and the discovery of appropriate examination methods for potentially abundant biomass to lower sorbent production costs (naturally heteroatom-doped and metal-impregnated biomass precursors can reduce the need for surface treatment processes).

The regulation of thermochemical process parameters and the implementation of specific modification strategies are also crucial considerations for biochars. The main objective is to modify surface characteristics such as mesoporosity, microporosity, basicity, and

alkalinity to enhance the CO<sub>2</sub> adsorption capacity. Additionally, biochar can undergo various post-treatment modifications, including chemical activation (NaOH, KOH) [119], physical activation (CO<sub>2</sub>, steam) [119,120], amine functionalization [121], high-temperature treatment with chemical mixtures of CO<sub>2</sub> with ammonia [120,122], ammonification with ammonia (NH<sub>3</sub>) [120,122], and metal incorporation [123,124] (Fig. 10). Shafawi et al. [125] provided an overview of current research directions on the production of engineered biochar by various modifications to increase its CO<sub>2</sub> capture capacity. The present study evaluated and discussed the influence of several modification strategies involving physical, chemical, and physicochemical treatments, on the modified biochar. Authors suggested that future studies aimed at improving CO<sub>2</sub> uptake, by significantly increasing surface area, micropore volume, and surface chemistry, could benefit from combining multiple modifications. These could consist of functionalization with alkali and amines or doping with metal or metal oxide, which can be empirically and conceptually proven to be significant. Moreover, density functional theory (DFT) was identified as a feasible way to uncover relevant details associated with biochar modifications and the CO<sub>2</sub> adsorption mechanism. In conclusion, it was recommended that further research be conducted to investigate the stability and regeneration of spent biochar, expanding its role in green chemistry and climate change mitigation. Dissanayake et al. [126] also summarized an assessment of the potential use of both pristine and tailored biochar as CO<sub>2</sub> adsorbent. In particular, they discussed the variables affecting CO<sub>2</sub> adsorption capacity and the challenges connected with biochar synthesis. The final conclusions emphasized the importance of future research in creating cost-effective and environmentally friendly biochar-based composites (incorporating metal-organic frameworks, and carbon-based nanomaterials) for extensive implementation in large-scale CO<sub>2</sub> capture technologies. On top of that, the primary importance should be placed on the development of innovative techniques for regenerating and recycling captured CO<sub>2</sub>.

Among the research on modification of biochars, several important studies can be identified. Lahijani et al. [123] studied

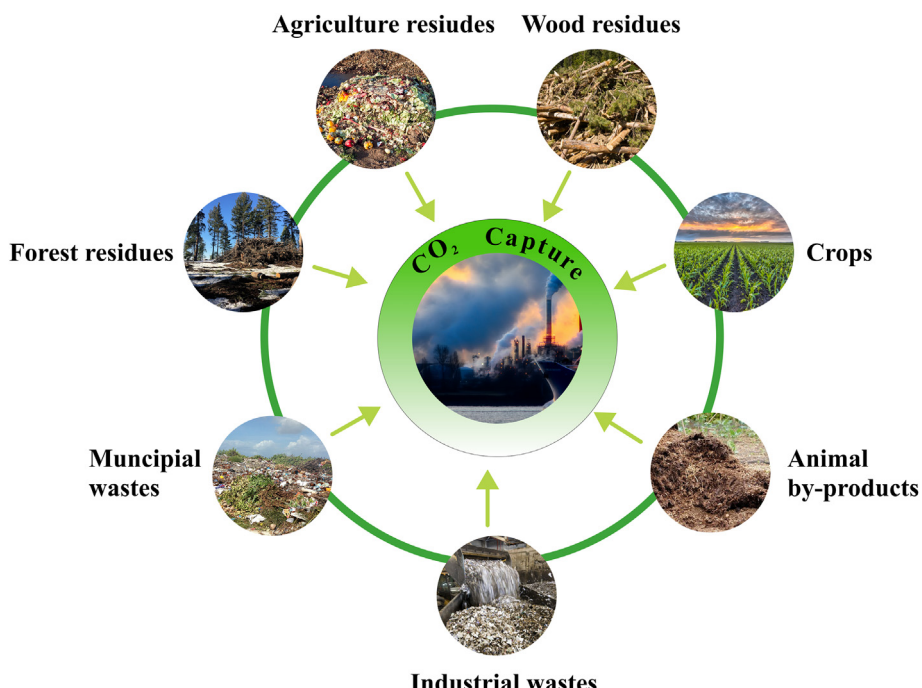


**Fig. 8.** Suitable types of biomass for the production of biochar and hydrochar.

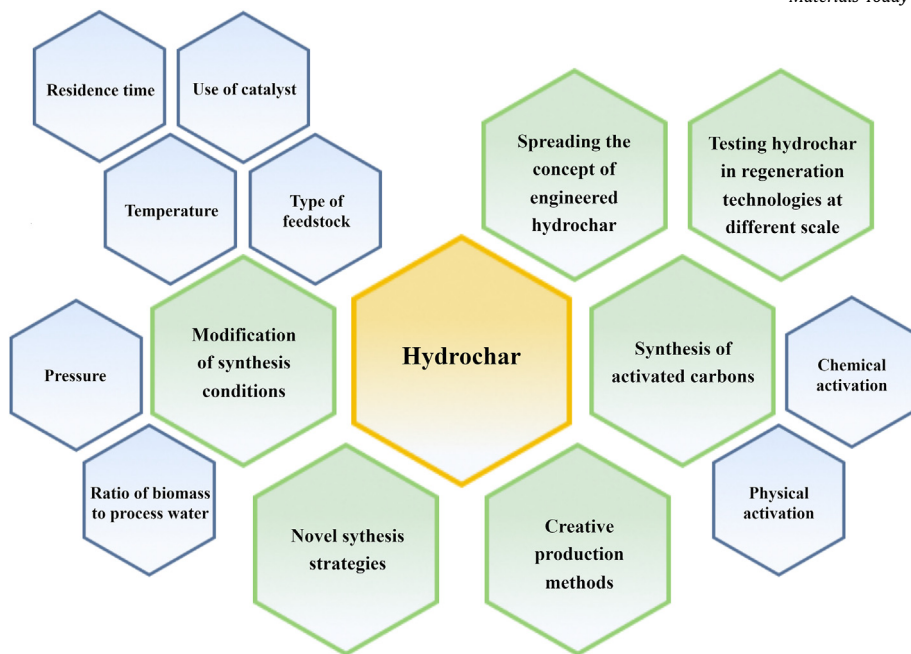


**Fig. 9.** The modification strategies and research directions of hydrochar.

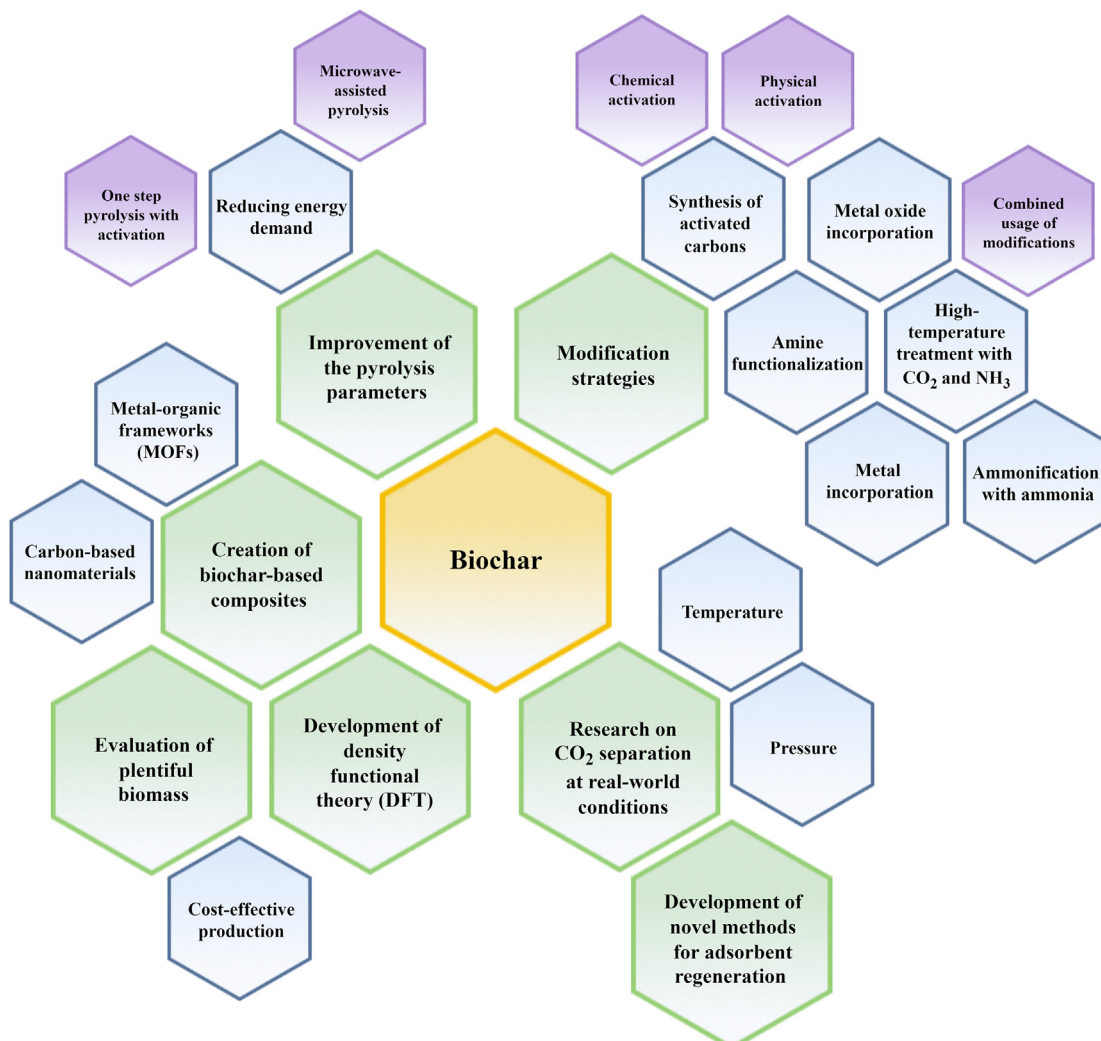


**Fig. 10.** The modification strategies and research directions of biochar.

the development of metal incorporated biochar as an inexpensive and durable adsorbent for CO<sub>2</sub> capture at ambient temperatures. Biochars were created from walnut shell using a simple one-step pyrolysis procedure, and then different metals were introduced into the biochar skeleton using a simple impregnation approach followed by heat treatment to increase the CO<sub>2</sub> adsorption capacity. The Mg-loaded biochar exhibited the greatest CO<sub>2</sub> uptake of 1.82 mmol/g when compared to the other metalized biochars.

Creamer et al. [124] synthesized and described aluminum hydroxide, magnesium hydroxide, and iron oxide–biochar composites, as well as evaluated their capacity to capture CO<sub>2</sub> at ambient temperature and atmospheric pressure. They subjected biomass feedstocks to pretreatment with various metal ions and subsequently pyrolyzed them at 600 °C. This resulted in a greater CO<sub>2</sub> uptake in the composites, especially in those with optimum metal-to-biomass ratios, when compared to unmodified biochar. Each composite possessed a reasonably high surface area and primarily absorbed CO<sub>2</sub> by physical adsorption. While Fe<sub>2</sub>O<sub>3</sub>–biochar composites showed the maximum surface area, AlOOH–biochar composites demonstrated the highest adsorption capacity, reaching 1.61 mmol/g at 25 °C, equivalent to that of commercial adsorbents.

Zhang et al. [122] used soybean straw as a raw material to synthesize highly efficient adsorbents, specifically nitrogen-doped porous modified biochars. The authors evaluated three distinct modification methods for manufacturing these materials, namely CO<sub>2</sub> activation, ammonification with ammonia, and high temperature treatment with a combination of carbon dioxide and ammonia. Combining the CO<sub>2</sub> activation and NH<sub>3</sub> ammonification processes not only enhanced the formation of micropore structures in soybean straw-modified biochar but also increased the introduction of nitrogen functional groups onto the surface. The micropore structure of modified biochars was found to be the most critical attribute influencing their CO<sub>2</sub> capture capability at lower adsorption temperatures, when comparing the physicochemical parameters of modified biochars. In contrast, as the adsorption temperature increases, the influence of the micropore structure gradually diminishes, and the chemical characteristics, particularly

the presence of nitrogen functional groups, become more prominent. The same author conducted additional research on the effect of the same modification at different temperatures on CO<sub>2</sub> adsorption [120].

Madzaki et al. [121] examined the properties of raw sawdust biochar and amine treated sawdust biochar. The highest CO<sub>2</sub> capture capacity of amine treated biochar was 1.09 mol/g, at temperature of 30 °C. The incorporation of nitrogen functionalities into the carbon surface of the treated biochar resulted in lower CO<sub>2</sub> adsorption than that of untreated biochar. In addition, the incorporation of nitrogen functionalities onto the carbon surface may lead to a reduction in the exposed surface area of the biochar.

**Table 5** presents a comparative analysis of modification strategies impact on the CO<sub>2</sub> adsorption capacity and textural properties of biochar. The following data presents a concise overview of the principal results obtained from current research using modified biochar for the purpose of carbon dioxide adsorption. The scope of biochar activation is presented in section 3.2.2 on activated carbons, so it will not be present here deeply.

### 3.2.2. Activated carbons (ACs)

Activated carbons are indisputably the most thoroughly researched, extremely effective, and attractive material among carbon materials for capturing CO<sub>2</sub> from the flue gas stream [129]. Their main advantages as adsorbent include cost-effectiveness, low temperature required for desorption, straightforward regeneration process, low energy consumption, fast CO<sub>2</sub> sorption kinetics, high thermal and chemical stability, mechanical strength, or exceptional thermal conductivity [130–132].

The production of activated carbons (Fig. 11) is based on the use of large amounts of waste biomass or industrial waste rich in high carbon concentration and low inorganic content [133,134]. ACs can also be manufactured from natural charcoal resources such as coal and lignite [135,136]. Moreover, the synthesis method may also use synthetic polymers, although at a notable rise in manufacturing costs. These synthetic polymers may include mixes of cellulose with polystyrene, waste resins, or polyvinylidene chloride. Therefore, the low price and widespread availability of carbon-rich raw

**Table 5**

The effect of biochar modification strategies on textural properties and CO<sub>2</sub> uptake of biochar.

Biochar precursor	Temperature of pyrolysis, °C	Residence time, h	BET surface area, m <sup>2</sup> /g	Total pore volume, cm <sup>3</sup> /g	CO <sub>2</sub> selectivity at 1 bar	CO <sub>2</sub> uptake, mmol/g	CO <sub>2</sub> adsorption temperature, °C	Adsorption pressure, bar	Reported treatment sources/chemicals	Purpose of modification method	Reference
Walnut shell	900	1.5	292	0.157	—	1.86	25	1	Metal incorporation (Mg)	Improving the surface properties and enhancing the interaction with CO <sub>2</sub>	[123]
Cottonwood	600	3	275	0.01	—	1.45	25	1	Metal incorporation (Mg:biochar = 0.01)	[124]	
Cottonwood	600	3	367	0.37	—	1.61	25	1	Metal incorporation (Al:biochar = 4)	[124]	
Cottonwood	600	3	654	0.19	—	1.48	25	1	Metal incorporation (Fe:biochar = 4)	[124]	
Rambutan peel	900	1.5	505	0.28	—	1.72	25	1	Metal incorporation (Mg)	[127]	
Soybean straw	500	—	365	—	—	~1.80	30	1	High temperature NH <sub>3</sub> treatment	Increasing basicity and level-up N-contents	[122]
Soybean straw	500	—	491	—	—	~2.02	30	1	High temperature NH <sub>3</sub> and CO <sub>2</sub> treatment	Developing porosity, increasing basicity along with level-up N-contents	[122]
Cotton stalk	600	—	627	—	—	~2.16	—	1	High temperature NH <sub>3</sub> treatment	[122]	
Cotton stalk	600	—	436	—	—	~1.77	—	1	High temperature NH <sub>3</sub> treatment	basicity along with level-up N-contents	[122]
Chicken manure	450	1	302	0.22	79.1	10.15	20	1	HNO <sub>3</sub> and NH <sub>3</sub> treatment	[128]	
Sawdust	750	—	0.61	—	—	0.90	30	1	Amine functionalization	[121]	
Sawdust	850	—	3.17	—	—	1.02	70	1	(monoethanolamine)	[121]	

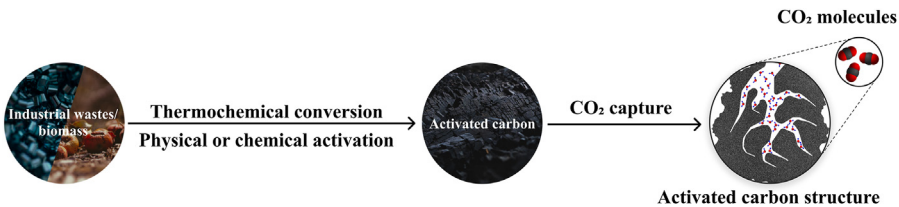


**Fig. 11.** Schematic diagram of activated carbons pre-treatment steps.

material sources, along with the production on an industrial scale, offer a significant competitive edge to ACs compared to other adsorbents. However, due to the quite diverse properties of raw materials, activated carbons are characterized by a different structure (porosity and specific surface area), implying that the overall course of the CO<sub>2</sub> adsorption process is changeable [131].

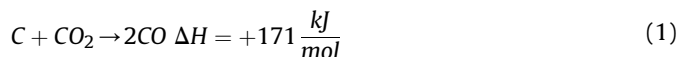
Activated carbons offer a wide distribution of an extensive porous structure, mainly microporous and mesoporous, where the size of the specific surface ranges from 500 to about 3000 m<sup>2</sup>/g [137]. The pores within the ACs structure may have different shapes depending on the type of hysteresis loop present in the multilayer range of physisorption isotherms. In most cases, they correspond to H1 (nearly vertical and parallel adsorption and desorption branches) and H2 (sloping adsorption branch and nearly vertical desorption branch) types, defining the shape of the pores as cylinders open on both sides, or alternatively, as ink bottle-shaped pore.

The CO<sub>2</sub> adsorption capacity of ACs can also be increased by the presence of heteroatomic functional groups in the form of connections: carbon–oxygen, carbon–nitrogen or carbon–sulfur on its surface. They can be categorized into acidic, such as carboxyl, lactone, or phenolic groups, and basic, including chromene, ketone, or pyrone groups [138]. The most important functional groups contain oxygen atoms, which contribute the outer surface a hydrophilic (polar) nature, in addition to the hydrophobic (nonpolar) character shown by the internal structure. The inherent duality of ACs surfaces enables them to effectively adsorb a diverse array of gases, with a particular emphasis on greenhouse gases (GHGs), therefore mitigating their release into the atmosphere.

**3.2.2.1. Physical activation.** Thermochemical conversion (hydrothermal carbonization, or pyrolysis) and activation are the two basic steps in the preparation of ACs. The char structure with undeveloped porosity (especially microporosity) and a small specific surface, which for a significant useful applications of CO<sub>2</sub> adsorption, are unsatisfactory, as highlighted before [131,139]. To improve the above parameters, the activation process (physical or chemical) is performed, by using a specific thermal treatment, which ultimately facilitates the improvement of carbon dioxide storage efficiency. Specifically, this treatment leads to the expansion or creation of new pores at both the micro and meso sizes.

Physical activation entails the partial gasification of raw materials in the presence of oxidizing gases at a temperature of 800 °C–1000 °C, such as water vapor, CO<sub>2</sub>, air, or their mixtures [140]. The process can be classified into two distinct ways, either in combination with thermochemical conversion or as an independent operation, i.e., the direct approach and the two-step approach. In the direct way, thermochemical conversion is performed in the presence of nitrogen flow until the reaction is complete. The N<sub>2</sub> flow is then stopped, and the activation gas is immediately introduced at the temperature. In the case of the second method, the activation process is divided into two steps. During it, the conversion of feedstock is carried out while maintaining a continuous supply of nitrogen flow. The process mentioned continues until an adequate amount of carbonaceous material is generated and collected afterward, then the activation is processed [141,142].

Among the activating gases, CO<sub>2</sub> is considered one of the most advantageous factors due to its ability to create narrow micropores of large volume, suitable for the kinematic diameter of the CO<sub>2</sub> molecule [143]. In the case of AC activation with steam, the existing pores are enlarged [140]. In the case of activation with steam, the existing pores are enlarged [140]. On the other hand, using a gas mixture of H<sub>2</sub>O + O<sub>2</sub> as an activating agent leads to rapid reaction kinetics, resulting in an active carbon structure with random porosity and substantial char losses. Consequently, its use is not recommended [144–146]. The effect of activation gases is also chemical in nature and involves the elemental carbon oxidation of material. For activation with CO<sub>2</sub>, the general reaction, also known as the Boudouard reaction, may be described as follows [140]:



The above reaction can be written in more details by separating it into two distinct phases, i.e., dissociative chemisorption (involving the dissociation of CO<sub>2</sub> on the surface of carbon material along with the formation of an oxide on its surface) and desorption of the surface oxide (in which the oxide is desorbed from the surface, and CO is produced) [147]:

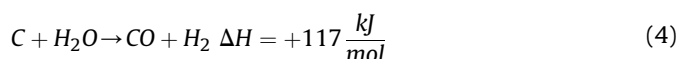
- Dissociative chemisorption



- Surface oxide desorption

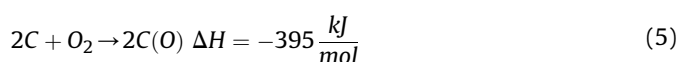


For activation using H<sub>2</sub>O, the general reaction can be presented as follows [148]:

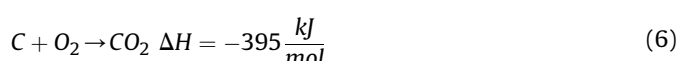


In the physical activation mechanism of O<sub>2</sub>, it runs according to the following reactions [149,150]:

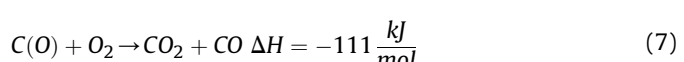
- Chemisorption



- Carbon gasification



- Oxide gasification on the surface of carbon material



The development of char porosity, specifically the capillary structure, as a direct outcome of physical activation occurs through the reaction of oxidizing gases with amorphous carbon. These activating gases penetrate the internal structure of the precursor surface, resulting in the opening and widening of previously inaccessible pores and the creation of new ones [151]. This process is the effect of complex mechanisms, including the diffusion of reactants to the surface of the carbon material and into the pores, their chemisorption on the surface, chemical reactions, and the subsequent desorption of reaction products. Additionally, physical activation promotes the presence of functional groups containing oxygen atoms, such as phenolic, ketone, and carboxyl groups [152].

To date, CO<sub>2</sub> capture has been achieved using various of physically activated carbon adsorbents from char, as given in Table 6. The majority of research findings highlight the potential of biomass as a viable and sustainable raw material for AC synthesis through physical activation. Currently, laboratory-scale research primarily concentrates on identifying new precursors and optimizing activation parameters to enhance CO<sub>2</sub> uptake.

Li et al. [153] synthesized AC from rice husk that was leached with potassium carbonate after being activated with CO<sub>2</sub>. The resulting material was then examined for its CO<sub>2</sub> adsorption capacity, kinetics, and regeneration. The studies revealed that the activated carbon possessed a dual pore structure comprising micropores and mesopores. The BET specific surface area, mesopores volume, and micropores volume were 1097 m<sup>2</sup>/g, 0.49 cm<sup>3</sup>/g, and 0.34 cm<sup>3</sup>/g, respectively. The developed AC demonstrated both a high CO<sub>2</sub> adsorption capacity, reaching 3.1 mmol/g, and excellent CO<sub>2</sub> selectivity of 7.6 at 25 °C and 1 bar, respectively. These values were comparable to those of AC produced by chemical activation with KOH serving as the activator.

Rashidi et al. [154] conducted research on the volumetric CO<sub>2</sub> adsorption utilizing AC made from palm kernel shells. The carbon was directly activated at 850 °C for 1 h. The obtained AC demonstrated a satisfactory CO<sub>2</sub> adsorption capacity of 2.13 mmol/g along with excellent regeneration performance of 7.0 and stability after many cycles.

Ogungbenro et al. [156] investigated the preparation of AC from date fruits as a promising adsorbent material. The AC synthesis involved pyrolysis in a furnace, followed by activation in a carbon dioxide environment at temperatures ranging from 600 to 900 °C. Among the samples, the one pyrolyzed at 800 °C and activated at 900 °C for 1 h exhibited the highest CO<sub>2</sub> adsorption capacity, reaching 3.21 mmol/g. This can be attributed to its superior textural properties, including a BET specific surface area of 798.38 m<sup>2</sup>/g, a micropore area of 712.87 m<sup>2</sup>/g, and a micropore volume of 0.28 cm<sup>3</sup>/g.

Puig-Gamero et al. [159] studied the influence of physical activation parameters involving CO<sub>2</sub> and steam on the production of AC derived from olive stones and its CO<sub>2</sub> adsorption capabilities. For H<sub>2</sub>O activation, the determined conditions were 900 °C, 30 min, 0.15 ml/min, and 1 bar. In the case of CO<sub>2</sub> activation, the optimal conditions were found to be 900 °C, 30 min, 300 ml/min, and 1 bar. Furthermore, the ACs demonstrated respectable CO<sub>2</sub> adsorption capacity of 4.28 and 4.66 mmol/g at 30 °C and 10 bar, with BET specific surface area of 955.06 and 1190.65 m<sup>2</sup>/g, and total pore volumes of 0.44 and 0.69 cm<sup>3</sup>/g for CO<sub>2</sub> and H<sub>2</sub>O activation, respectively.

To sum up, several comparative studies have been conducted in recent years to evaluate various activating agents for physical activation. The physical activation method of steam activation is widely utilized, yielding activated carbon possessing a substantial surface area and micropore volume. However, the process necessitates elevated temperatures and prolonged activation periods,

**Table 6**  
Influence of precursors, physical activation process conditions on textural properties and CO<sub>2</sub> uptake of activated carbons.

Precursor	Activating agent	Activation approach	Activation temperature °C	BET surface area, m <sup>2</sup> /g	Total pore volume, cm <sup>3</sup> /g	Micropore volume, cm <sup>3</sup> /g	Mesopore volume, cm <sup>3</sup> /g	CO <sub>2</sub> selectivity at 1 bar	CO <sub>2</sub> uptake, mmol/g		Reference
									0 °C	25 °C	
Rice husk char	CO <sub>2</sub>	Direct	900	1097	—	0.34	0.49	7.60	—	3.1	[153]
Peat	Steam	Direct	850	660.7	0.67	—	—	7.00	—	1.88	[154]
Palm kernel shell	CO <sub>2</sub>	Direct	850	367.8	0.22	—	—	—	—	2.13	[154]
Date stone	CO <sub>2</sub>	Two-step	600	821.7	0.45	—	—	—	—	1.7	[155]
Date seeds	CO <sub>2</sub>	Two-step	900	798.38	—	0.28	—	—	—	2.94	[156]
Palm kernel shell	CO <sub>2</sub>	Two-step	800	167.08	0.09	0.08	—	—	—	1.66	[157]
Olive stones	O <sub>2</sub> (3%)	Direct	650	697	—	0.27	—	~42.00	3.10	2.02	[150]
Olive stones	CO <sub>2</sub>	Direct	800	1215	0.51	—	—	18.00	—	3.1	[158]
Olive stones	Steam (H <sub>2</sub> O)	Direct	900	1190.65	0.69	0.52	0.17	—	4.28 (30 °C)	10	[159]
Olive stones	CO <sub>2</sub>	Direct	1000	955.06	0.44	0.40	0.04	—	4.66 (30 °C)	10	[159]
Olive mill waste	CO <sub>2</sub>	Two-step	850	424	0.476	0.373	0.014	24.20	2.945	—	[160]
Coconut shell	CO <sub>2</sub>	Direct	800	1327	0.65	0.55	0.10	—	5.60	3.90	[161]
Coconut shell	CO <sub>2</sub>	Direct	800	371	0.15	0.11	—	—	—	1.8	[162]
Coffee grounds	CO <sub>2</sub>	Two-step	700	593	0.24	0.24	—	13.00	3.50	2.20	[163]
Vine shoots	CO <sub>2</sub>	Two-step	800	767	0.374	0.245	0.049	—	68.50	4.07	[164]
Nutshell	CO <sub>2</sub>	Two-step	900	573	0.171	—	—	12.30	—	3.48	[165]
Almond shell	CO <sub>2</sub>	Direct	750	862	0.36	—	—	—	—	2.7	[158]
Almond shell	O <sub>2</sub> (3%)	Direct	650	557	—	0.21	—	~73.00	3.11	2.11	[150]
Palm date seeds	CO <sub>2</sub>	Two-step	900	858	0.39	0.34	—	—	—	4.38	[166]
Amazonian andiroba shell	CO <sub>2</sub>	Two-step	880	1296	0.63	0.53	—	—	15.00	6.1	[167]
Pine cones	Steam	Two-step	700	424	0.34	0.18	—	36.10	~3.28	3.2	[168]
Walnut shell	CO <sub>2</sub>	Direct	500	810.85	0.34	—	—	—	—	1.58 (20 °C)	[169]

resulting in a high demand for energy and a prolonged duration. On the other hand, the use of CO<sub>2</sub> as an activating agent requires less energy and can be carried out at lower temperatures compared to steam activation. The process yields activated carbon that exhibits substantial surface area and pore volume, albeit potentially leading to a reduced micropore volume relative to steam-activated carbon. Further, air activation has the capability to generate activated carbon featuring diverse pore sizes and surface areas. Its application is not as frequent owing to the potential hazard of oxidation and combustion of the precursor material. In general, the selection of physical activating agent is contingent upon the intended characteristics of the resultant activated carbon. Although steam activation remains the predominant technique, CO<sub>2</sub> activation is increasingly being adopted owing to its reduced energy demands. Although less frequently employed, air activation has the potential to provide a broader spectrum of pore sizes and surface areas.

**3.2.2.2. Chemical activation.** Chemical activation concerns the reaction of char with chemical reagents, followed by subjecting it to heat treatment under neutral conditions. This method leads to the production of ACs within a temperature range of 450–900 °C [170]. The two most common chemical activation procedures are a single step approach, known as dry mixing, and a two step approach referred to as wet impregnation [171]. The difference between the two is related to the environment for carrying out the activation reaction and the number of sequential steps required in achieving the final product. The wet impregnation method involves the addition of an AC precursor to a saturated solution of an activating agent, followed by heating and drying. The dried mixture is then activated under a nitrogen gas atmosphere in a furnace. Subsequently, the activated material undergoes a washing process prior to a further drying step. On the other hand, the dry mixing approach is characterized by its simplicity, involving mixing of a solid activating agent with the particular raw material. Then, the mixture also is directly subjected to carbonization and activation in a single step, maintaining an atmosphere of N<sub>2</sub> gas [172].

The development of porous structure through chemical activation is influenced by several factors, including the content of organic or synthetic raw material, activation temperature, residence time, heating rate, type of activating agent, and the weight ratio between AC precursor and activating agent [173–175]. Chemical activation provides a number of benefits over physical activation, such as a reduction in temperature and activation time [176,177], higher carbon yield, more porous structure of activated carbon, low energy and operating cost, or easier development of microporosity [132,178]. It has also been observed that chemically activated chars have higher carbon yields and surface areas than physically activated ones [179]. Conversely, the chemical activation has several drawbacks, including an additional rinse step to remove excess chemical agent, and secondary contamination issues along with their ecological disposal [180].

Commercially available ACs have a relatively low CO<sub>2</sub> adsorption capacity due to the wide pore size distribution [181,182]. In order to achieve high CO<sub>2</sub> adsorption, various chemicals are utilized in the chemical activation to regulate the pore network, which fall into three main classes, namely alkaline (KOH, NaOH, K<sub>2</sub>CO<sub>3</sub>, Na<sub>2</sub>CO<sub>3</sub> and K<sub>3</sub>PO<sub>4</sub>), which are most commonly used, acidic (H<sub>3</sub>PO<sub>4</sub>, H<sub>2</sub>SO<sub>4</sub>, HNO<sub>3</sub>) and neutral (FeCl<sub>3</sub>, ZnCl<sub>2</sub>, K<sub>2</sub>SO<sub>4</sub>, NaNH<sub>2</sub>, NH<sub>4</sub>Cl) [183,184]. Their main goal is to serve as a hydrating agent, affecting the breakdown process and preventing the formation of tar to restrict it to a minimum [185,186]. Cao et al. [187] recommended the use of chemical activation instead of physical activation using the steam method because it consumes less energy. Among the activators, they proposed the utilization of KOH for its less harmful influence on the environment than ZnCl<sub>2</sub> or H<sub>3</sub>PO<sub>4</sub>.

Generally, CO<sub>2</sub> adsorption mechanism depends on the type and volume of pores in the ACs structure. Carbon materials with micropores, especially pores with diameters less than 1 nm, were found to show a high capacity to adsorb CO<sub>2</sub> [188,189]. In addition, these pore sizes favor the diffusion of CO<sub>2</sub> in the materials, which makes the adsorption kinetics very fast [190]. For several years, the interest of researchers has focused on the use of waste residues and biomass as a precursor to produce activated carbons. Among the works published between 2010 and 2022, there are several that have contributed in particular to this field of research.

Hu et al. [191] obtained activated carbons for CO<sub>2</sub> adsorption using petroleum coke as a precursor. The authors employed various ratios of KOH to carbon, and the most favorable CO<sub>2</sub> adsorption results were achieved when the ratio of KOH to the carbon precursor was 3. Under these conditions, the material adsorbed 3.5 mmol/g of CO<sub>2</sub> at a temperature of 25 °C and a pressure of 1 bar. This carbon was shown to be characterized by a significant advantage in micropore volume with diameters less than 1 nm compared to other pores.

Ouzzine et al. [192] prepared activated carbon from pomegranate peel (PP). Optimal conditions for CO<sub>2</sub> adsorption were evaluated by controlling the activation temperature. KOH was used as an activating agent in a KOH/PP activating ratio of 1:1. Four activated carbons were synthesized at activation temperatures in the range of 600–900 °C, and their surface and pore characteristics were examined along with CO<sub>2</sub> adsorption. The results showed that with the increase of the activation temperature from 600 to 800 °C, the total pore volume and the specific surface area increased considerably from 0.78 to 1.28 cm<sup>3</sup>/g and from 1311 to 2141 m<sup>2</sup>/g, respectively. However, the values of these two parameters decreased at temperatures above 900 °C. The best CO<sub>2</sub> adsorption capacity of 4.44 mmol/g and 5.53 mmol/g was obtained for activated carbon prepared at 800 °C at 25 and 0 °C at 1 bar, respectively. This result highlights the importance of the structural and textural characteristics of activated carbons, prepared at different activation temperatures, on the CO<sub>2</sub> adsorption behavior.

Acevedo et al. [193] investigated the preparation of porous activated carbon from the chemical activation of African palm shells sourced from crops in the Guajira region, Colombia. They utilized solutions of Fe(NO<sub>3</sub>)<sub>3</sub> and Cu(NO<sub>3</sub>)<sub>2</sub> with varying concentrations and conducted the activation process at two different temperatures of 700 °C and 800 °C. The obtained material presented micro-mesoporosity with surface area between 5 and 1300 m<sup>2</sup>/g. The fixed carbon content ranged from 47.1% to 78.4%. These results indicated that the activation process had notable effects on the textural parameters, elemental composition, and proximal composition of the obtained solids. Additionally, the CO<sub>2</sub> uptake values at low pressures were between from 1.82 to 5.68 mmol/g.

Ello et al. [194] prepared microporous activated carbon from palm shells for CO<sub>2</sub> capture. The volume of micropores and the specific surface area of the obtained carbons varied depending on the ratio of KOH to the carbon precursor, ranging from 0.16 cm<sup>3</sup>/g (365 m<sup>2</sup>/g) to 0.82 cm<sup>3</sup>/g (1890 m<sup>2</sup>/g). Among these carbons, the one with a specific surface area of 1250 m<sup>2</sup>/g and an ultramicropore volume (diameter less than 0.7 nm) of 0.29 cm<sup>3</sup>/g proved to be the most effective CO<sub>2</sub> capture material. At 1 bar and 0 °C, it exhibited CO<sub>2</sub> adsorption capacity of 6.3 mmol/g. Interestingly, activated carbon with a higher specific surface area (1890 m<sup>2</sup>/g) showed lower CO<sub>2</sub> uptake and a reduced ultramicropore volume.

Similar research results were presented by Zhu et al. [197], who tested the carbon obtained from sawdust in the CO<sub>2</sub> adsorption process. They noted that the carbon material with the highest specific surface area of 2435 m<sup>2</sup>/g was not characterized by the best CO<sub>2</sub> adsorption capacity. The authors concluded that the reason was the relatively low volume of the micropores, which

represented only 29% of the total pore volume. On the other hand, the maximum CO<sub>2</sub> uptake of 8.0 mmol/g at a pressure of 1 bar at a temperature of 0 °C was obtained on activated carbon with a much lower specific surface, but with a high volume of micropores, constituting 73% of the pore volume. Therefore, the proper micro-pore fraction in the carbon structure was found to be the main factor contributing to CO<sub>2</sub> adsorption.

Sevilla et al. [222] used eucalyptus sawdust, cellulose, and potato starch as precursors to produce KOH-activated carbons. They prepared several series of activated carbons that differed in the ratio of KOH to the carbon precursor and in the activation temperature. The carbon samples obtained at the activation temperature of 600 °C showed the highest CO<sub>2</sub> capture capacity at room temperature (4.8 mmol/g, 250 °C and 1 bar). The authors associated the high adsorption of CO<sub>2</sub> with the presence of narrow micropores (diameter < 1 nm). The specific surface area was found to play a less significant role. In addition, there was an observation made that the obtained carbons under mild activation conditions at temperatures of 600–800 °C, are characterized by higher CO<sub>2</sub> uptake. It was found that using the ratio of KOH to precursor equal to 2 led to the formation of materials characterized by an increased number of pores with widths below 0.8 nm.

The increase in pore diameters causes a decrease in CO<sub>2</sub> uptake, in line with the previously discussed concept that pores with volumes less than 1 nm play a predominant role in CO<sub>2</sub> adsorption under ambient conditions. Presser et al. [195] found that the volume of pores with diameters less than 0.8 nm correlated with the amount of CO<sub>2</sub> adsorbed at 0 °C and a pressure of 1 bar. Therefore, the authors stated that micropores smaller than 0.8 nm play a dominant role in CO<sub>2</sub> adsorption under these conditions.

Wei et al. [196] also conducted studies on activated carbons derived from biomass for CO<sub>2</sub> adsorption and arrived at similar conclusions. Activated carbons with a high CO<sub>2</sub> adsorption capacity were produced from bamboo using KOH as the activator. The maximum amount of CO<sub>2</sub> adsorbed at the temperature of 0 °C and the pressure of 1 bar was 7.0 mmol/g. The study aimed to identify the pores responsible for CO<sub>2</sub> adsorption, revealing a strong linear correlation between the amount of CO<sub>2</sub> uptake and the size of pores with diameters less than 0.82 nm. The authors found that pores in the range of 0.33–0.82 nm were mainly responsible for CO<sub>2</sub> adsorption at 0 °C and 1 bar pressure.

Based on the literature review and the findings presented in Table 7, KOH emerges as the most frequently used reagent in chemical activation for CO<sub>2</sub> adsorption compared to the others. It is widely considered as one of the chemicals for improving CO<sub>2</sub> adsorption capacity and selectivity, enhancing the microporosity, increasing surface area, and subduing the generation of tar. However, an excess of KOH blocks pores and reduces the surface area [197–200]. The superior performance of KOH is evident in the research examples carried out with the utilization of other activating agents. For example, Shen et al. [201] used coal pitch as a precursor of activated carbons, activated with steam. The ACs showed low CO<sub>2</sub> uptake at the level of 1.9 mmol/g at a temperature of 30 °C and a pressure of 1 bar. Plaza et al. [202] produced a series of ACs by the activation of olive pits with carbon dioxide. The maximum CO<sub>2</sub> adsorption capacity value that could be obtained on these carbons was 2.4 mmol/g at a temperature of 25 °C and a pressure of 1 bar. The use of carbon dioxide as activating agent resulted in ACs with lower CO<sub>2</sub> adsorption performance compared to KOH-ACs. Lastly, Goel et al. [103] in their review identified the ideal synthesis and process working conditions for chemical activation via KOH, such as a KOH/char ratio of 2–3, an activation temperature of 700 °C, and an optimal CO<sub>2</sub> adsorption temperature of below 50 °C. They also emphasized that increasing the KOH/char ratio beyond 3 may enhance the surface area, but larger pore sizes

may render some sites inaccessible to adsorption, resulting in reduced CO<sub>2</sub> uptake.

In summary, the utilization of KOH is frequently favored over alternative chemical agents owing to its capacity to generate structures that are highly porous and possess extensive specific surface areas. The heightened chemical reactivity of KOH facilitates a more efficient reaction with the precursor material at lower temperatures, ultimately resulting in the generation of a greater quantity of micropores and mesopores. Furthermore, potassium hydroxide is a cost-effective and easily accessible option, rendering it a feasible alternative for mass manufacturing.

**3.2.2.3. Modification strategies of activated carbons.** By applying specific strategy methods, the key disadvantages of ACs merit attention, i.e., susceptibility to SO<sub>x</sub>, NO<sub>x</sub>, and H<sub>2</sub>O impurities in the flue gas stream, low balance, less effective adsorption capacity at low partial CO<sub>2</sub> pressures, and a decrease in adsorption efficiency with increasing process temperature [131]. Therefore, to eliminate the influence of the above drawbacks on CO<sub>2</sub> adsorption, many studies described in the scientific literature focused primarily on: (1) modification of the synthesis condition (thermochemical conversion, or activation process), which were previously discussed; (2) surface modifications (high temperature NH<sub>3</sub> treatment [224,225], amine functionalization [226,227]); (3) development of activated carbon composites (carbon-based nanomaterials [228], polymers [229–231], metal oxides/metal impregnation [232,233], zeolites [234–237], metal-organic frameworks [238,239]) (Fig. 12). The combinations of the above modification strategies have also been reported in the literature and seems to be a very promising solution for increasing CO<sub>2</sub> capture. They are closely related to the optimization of the synthesis conditions with high temperature NH<sub>3</sub> treatment [205], amine functionalization [240], or metal impregnation.

Zhang et al. [205] improved CO<sub>2</sub> adsorption by biochar synthesis modification (chemical activation of KOH) in conjunction with surface modification by heat treatment of NH<sub>3</sub> resulted in the development of microporosity and the introduction of basic nitrogen-containing groups into biomass-based carbon material. The high CO<sub>2</sub> uptake of 7.19 mmol/g and 5.05 mmol/g at 0 and 25 °C were achieved due to the development of the micropore structure and the abundance of basic nitrogen-containing functionalities, which enhanced CO<sub>2</sub> adsorption at higher adsorption temperatures. According to the findings, the modified activated carbon contained a high surface area, measuring 2511 m<sup>2</sup>/g, as well as a significant micropore volume, reaching 1.16 cm<sup>3</sup>/g.

Liu et al. [240] reported an effective synthesis of hierarchical ultra-micro/mesoporous biocarbons by chemical activation and amine functionalization (MEA). At ambient temperature and low CO<sub>2</sub> partial pressure, the biocarbons displayed high adsorption capacities (1.90 mmol/g) at 25 °C and 15 kPa CO<sub>2</sub> and record high Henry's law CO<sub>2</sub>/N<sub>2</sub> selectivity up to 212. The final results established that the unique surface textural features high mesoporosity and ultra-microporosity of 0.175 cm<sup>3</sup>/g with a restricted pore size distribution, large specific surface area of 1190 m<sup>2</sup>/g and increased surface chemistry. These factors combined to provide favorable conditions for CO<sub>2</sub> adsorption with strong selectivity for CO<sub>2</sub>/N<sub>2</sub> at low partial pressures of CO<sub>2</sub>, while the presence of mesoporosity significantly enhanced CO<sub>2</sub> adsorption kinetics.

In recent years, researchers have been more interested in producing AC composites, which are very effective path for increasing CO<sub>2</sub> uptake and selectivity. The utilization of AC composites is principally noteworthy due to their synergistic impact on the CO<sub>2</sub> adsorption efficiency of the constituent materials.

Othman et al. [241] combined activated carbon nanofibers (ACNFs) with four different types of metal oxides, including

**Table 7**Influence of precursors, chemical activation process conditions on textural properties and CO<sub>2</sub> uptake of activated carbons.

Precursor	Activating agent	Activation temperature, °C	Residence time, h	Activation approach	Weight ratio (precursor:agent)	BET surface area, m <sup>2</sup> /g	Total pore volume, cm <sup>3</sup> /g	CO <sub>2</sub> selectivity at 1 bar	CO <sub>2</sub> uptake, mmol/g		Adsorption pressure, bar	Reference
									0 °C	25 °C		
Urea and tobacco stem	KOH	600	1	Dry mixing	1:2	3839	2.30	—	—	29.5	30	[203]
Pomegranate peels	KOH	700	1	Wet impregnation	1:1	585	0.28	15.10	6.03	4.11	1	[204]
Carrot peels	KOH	700	1	Wet impregnation	1:1	1379	0.58	8.10	5.64	4.18	1	[204]
Fern leaves	KOH	700	1	Wet impregnation	1:1	1593	0.74	6.50	4.52	4.12	1	[204]
Black locust	KOH	830	1.5	Wet impregnation	1:6	2064	0.98	—	5.86	3.75	1	[205]
Rice husk char	KOH	780	1	Wet impregnation	1:3	2965	1.14	—	6.24	3.71	1	[206]
Jujun grass	KOH	700	1	Dry mixing	1:2	3144	1.56	—	—	4.10	1	[207]
Camellia japonica	KOH	600	1	Dry mixing	1:2	1353	0.67	—	—	5.00	1	[207]
Pristine gelatin	KOH	700	0.17	Dry mixing	1:4	1294	0.63	—	4.25	3.30	1	[208]
Starch	KOH	700	0.17	Dry mixing	1:4	714	0.40	—	3.02	2.81	1	[208]
Pristine gelatin and starch	KOH	700	0.17	Dry mixing	1:4	1636	0.51	—	7.49	3.84	1	[208]
Slash pine	KOH	580	2	Wet impregnation	1:4	906	0.35	—	4.93	—	1	[209]
Slash pine	ZnCl <sub>2</sub>	580	2	Wet impregnation	1:1	1384	0.37	—	4.32	—	1	[209]
Longan shell	KOH	800	2	Wet impregnation	1:2	3139	2.5	~40.61	4.5	3.4	1	[210]
Paulownia sawdust	KOH	700	1	Wet impregnation	1:4	1643	0.857	—	8.00	5.80	1	[197]
Bituminous coal	NaOH	800	2	Wet impregnation	1:4	1511	0.75	—	8.25	—	1	[211]
Bituminous coal	KOH	800	2	Wet impregnation	1:4	2599	1.16	—	9.09	—	1	[211]
Bituminous coal	ZnCl <sub>2</sub>	700	2	Wet impregnation	1:4	1568	1.06	—	5.54	—	1	[211]
Argan hard shells	NaOH	850	1	Wet impregnation	1:4	1827	0.96	—	—	3.73	1	[212]
Argan hard shells	NaOH	850	1	Dry mixing	1:4	1463	0.74	—	—	3.64	1	[212]
Argan hard shells	KOH	850	1	Dry mixing	1:4	1890	0.87	—	—	5.63	1	[212]
Argan hard shells	KOH	850	1	Wet impregnation	1:4	2251	1.04	—	—	5.51	1	[212]
Vine shoots	KOH	700	1	Dry mixing	1:5	1439	0.674	56.80	6.08	—	1	[164]
Vine shoots	KOH	700	1	Wet impregnation	1:2	1671	0.67	8.50	5.40	—	1	[164]
Coffee grounds	KOH	600	1	Dry mixing	1:2	876	0.40	18.00	4.40	3.00	1	[163]
Coffee grounds	KOH	700	1	Dry mixing	1:4	2785	1.36	—	4.00	6.89	1	[213]
Wooden chopstick	KOH	700	1.5	Wet impregnation	1:1.5	—	—	17.60	—	2.63	1	[214]
Assai seeds	KOH	600	2	Dry mixing	1:2	1857	0.75	—	7.13	4.38	1	[215]
Brazilian nutshell	KOH	600	2	Dry mixing	1:2	1824	0.68	—	6.99	4.79	1	[215]
Andiroba seeds	KOH	600	2	Dry mixing	1:2	1894	0.79	—	7.18	4.80	1	[215]
Cupuassu nutshell	KOH	600	2	Dry mixing	1:2	2004	0.68	—	6.51	4.18	1	[215]
Polypodium vulgare	KOH	800	1	Wet impregnation	1:1	1994	0.998	66.30	9.05	5.67	1	[216]
Common oak leader	KOH	700	1	Wet impregnation	1:1	1842	0.91	74.36	6.17	5.44	1	[217]
Walnut shell	KOH	800	1	Wet impregnation	1:1	1868	1.06	163.00	9.54	5.17	1	[218]
Corn stover	KOH	800	2	Dry mixing	1:2	2442	1.56	15.50	7.14	—	1	[219]
Corn stover	KOH	800	4	Dry mixing	1:2	1862	0.81	—	6.32	—	1	[219]
Corn stover	KOH	600	2	Dry mixing	1:2	955	0.43	—	4.93	—	1	[219]
Corn stover	KOH	700	2	Dry mixing	1:2	1539	0.72	—	6.80	—	1	[219]
Corn stover	KOH	800	2	Dry mixing	1:1	1543	0.71	—	5.06	—	1	[219]
Corn stover	KOH	800	2	Dry mixing	1:3	2201	1.31	—	6.22	—	1	[219]
Sugarcane bagasse	KOH	800	0.75	Wet impregnation	1:6.25	2080	1.316	12.00	2.00	—	1	[220]
Lignin waste	KOH	700	1	Dry mixing	1:2	1551	0.77	—	7.40	4.60	1	[221]
Lignin waste	KOH	800	1	Dry mixing	1:2	1924	0.95	—	—	6.5	1	[221]
Lignin waste	KOH	700	1	Dry mixing	1:4	2038	1.00	—	—	3.2	1	[221]
Lignin waste	KOH	900	1	Dry mixing	1:4	2750	1.66	—	—	2.4	1	[221]
Palm date seeds	KOH	900	2	Wet impregnation	1:1	1906	1.06	—	—	5.44	1	[166]
Palm date seeds	KOH	900	2	Wet impregnation	1:2	2335	1.54	—	—	4.67	1	[166]
Palm date seeds	H <sub>3</sub> PO <sub>4</sub>	900	2	Wet impregnation	1:2	1439	0.60	—	—	4.40	1	[166]
Palm date seeds	H <sub>3</sub> PO <sub>4</sub>	900	2	Wet impregnation	1:1	1218	0.50	—	—	4.00	1	[166]
Starch, cellulose and sawdust	KOH	800	1	Dry mixing	1:2	1940	0.82	—	5.80	3.90	1	[222]
Starch, cellulose and sawdust	KOH	600	1	Dry mixing	1:2	1260	0.55	5.40	6.10	4.80	1	[222]
Starch, cellulose and sawdust	KOH	600	1	Dry mixing	1:4	2370	0.91	—	5.20	2.90	1	[222]
Garlic peel	KOH	800	1	Dry mixing	1:2	1206	0.70	—	4.33	2.82	1	[223]
Garlic peel	KOH	600	1	Dry mixing	1:2	947	0.51	—	6.25	4.22	1	[223]

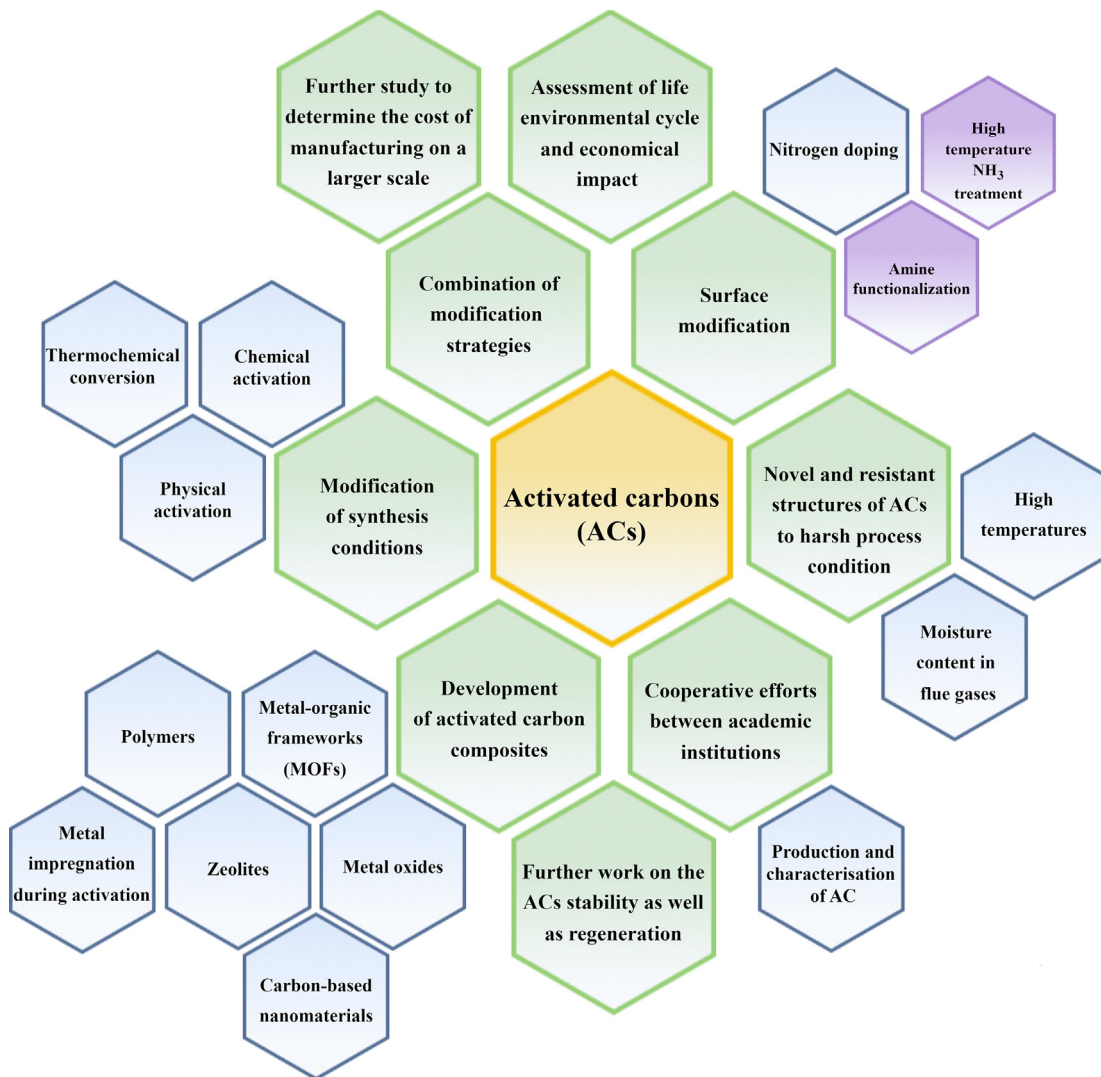


**Fig. 12.** The modification strategies and research directions of activated carbons.

magnesium oxide ( $\text{MgO}$ ), manganese dioxide ( $\text{MnO}_2$ ), zinc oxide ( $\text{ZnO}$ ), and calcium oxide ( $\text{CaO}$ ). Among the composites tested, it was discovered that ACNFs with  $\text{MgO}$  had the highest specific surface area ( $413 \text{ m}^2/\text{g}$ ) and micropore volume ( $0.1777 \text{ cm}^3/\text{g}$ ), when compared to pristine material and other composites. It also exhibited the maximum  $\text{CO}_2$  adsorption at  $25^\circ\text{C}$ , with a capacity of  $2.08 \text{ mmol/g}$ . According to these findings, the integration of  $\text{MgO}$  into ACNFs led to the greatest improvement in the physicochemical qualities of all treatments. Metal impregnation mainly increased  $\text{CO}_2$  adsorption capacity due to the high affinity between metals and  $\text{CO}_2$  molecules, especially at elevated temperatures.

Liu et al. [242] created innovative composites by combining Cu-BTC with porous carbon materials, including ordered mesoporous activated carbon. All composites formed were recognized as microporous materials having an adsorption isotherm of type I. Additional micropores that were created during the synthesis of these composites, significantly increasing their specific surface area and porosity. These unique porous carbon/MOF composites had a significant application of  $\text{CO}_2$  adsorption. In particular, the nitrogen-containing microporous carbon composite demonstrated the highest  $\text{CO}_2$  capacity, with  $8.24$  and  $4.51 \text{ mmol/g}$  under  $1 \text{ bar}$  pressure at  $0$  and  $25^\circ\text{C}$ , respectively. In the case of the AC composite, the  $\text{CO}_2$  uptake was equal to  $8.03$  and  $4.49 \text{ mmol/g}$ . Further,

the highest BET surface area ( $1368 \text{ m}^2/\text{g}$ ) and micropore volume ( $0.60 \text{ cm}^3/\text{g}$ ) were observed for the AC sample. Additionally, the  $\text{CO}_2$  adsorption capacity were shown to have a correlation with the specific surface area, the volume of micropores (less than  $2 \text{ nm}$ ), and the volume of ultra-micropores (less than  $0.7 \text{ nm}$ ).

From recent reviews on ACs for  $\text{CO}_2$  capture, in 2021 Abd et al. [138] made attempts to examine the adsorption characteristics of carbon dioxide on activated carbons produced from a variety of sources. They drew attention to the current performance, preparation, and surface modification of ACs for future research progress or improvement. They outlined several important directions that future research should focus on, including: novel structures of AC materials that are resistant to harsh process environment conditions (high temperatures and moisture level in flue gas stream); necessary academic cooperation for the manufacturing, characterization, and performance modeling of AC; more investigation on the price of producing AC at a larger scale, since it is crucial to evaluate their potential applications in the commercial level; analysis of the life environmental cycle impact as well as the financial implications of AC manufacturing; or more in-depth research on AC stability and the regeneration requirements for flue gas mixtures that may contain not only  $\text{N}_2$  or  $\text{CH}_4$ , but also different impurities.

**Table 8** summarizes the modification strategies applied to improve textural properties and the CO<sub>2</sub> capture capabilities of activated carbons.

### 3.2.3. Carbon nanotubes (CNTs)

Carbon dioxide adsorption on carbon nanotubes is receiving a growing experimental and theoretical focus due to their structure similar to activated carbons, favorable surface properties, topological hollow tube structures, high mechanical strength, very low weight, thermal and chemical stability, and beneficial pore size distribution [254–256]. The cross-sectional diameter of CNTs may reach magnitudes of tens of nanometers, although their length can extend to several thousand times more. Their internal structure focuses on the interactions between graphene layers, rolled up into a uniform cylinder, which is empty inside. This tubular geometry enables the gas distribution and residence time to be controlled. The amount of adsorbed CO<sub>2</sub> in carbon nanotubes is determined by gas pressure, temperature, their diameter in the entire volume of the material, and the distance between adjacent layers graphene [257].

The main possibility of the systematic division of carbon nanotubes can be based on the number of graphene layers present in their spatial structure (walls), therefore the following are distinguished: single walled carbon nanotubes (SWCNTs), double walled carbon nanotubes (DWCNTs), multi walled carbon nanotubes (MWCNTs). The three-dimensional representations of SWCNTs, DWCNTs, MWCNTs, are given in Fig. 13. Each of the above forms has been found to be an effective adsorbent material for specific gaseous media. The number of graphene layers additionally affects the properties of nanotubes, i.e., mechanical (tensile strength) and thermal parameters. Moreover, single-walled carbon nanotubes (SWCNTs) are distinguished by a large specific surface area, usually between 400 and 3000 m<sup>2</sup>/g, which is comparable to the activated carbons [258]. Nonetheless, MWCNTs are considered to be a superior CO<sub>2</sub> capture materials than SWCNTs [259,260].

The CNTs also offer the possibility of modifying their surface by adding chemical groups [261,262]. All ways of functionalizing carbon nanotubes fall into one of two categories: internal functionalization and external chemical functionalization (based on the mechanism of attaching compounds and groups). Chemical functionalization can be further divided into three subgroups as follows: (1) adding functional groups to defects or ends of carbon nanotubes for covalent functionalization, (2) “side wall functionalization” for covalent functionalization, and 3) non-covalent functionalization, such as the use of surfactants to wrap carbon nanotubes in polymers [256].

Many studies on modification strategies to enhance CO<sub>2</sub> adsorption capacity of CNTs, have focused on the nitrogen doping via amines on the surface of CNTs [263–266]; treatment methods by chemical agents [267,268]; synthesis of hybrid materials with MOFs (creation of hierarchical structures composed of functionalized MWCNTs and zeolitic imidazolate frameworks) [269], silica [270], deposition of layered double hydroxides (LDHs) [271], and carbon foams [272]; or the combination of approaches listed above. The generic CNTs modification strategies and research paths are presented in Fig. 14.

Based on the review, the amine functionalized CNTs are suggested to be very suitable, non-toxic, materials for further development of CO<sub>2</sub> capture processes from flue gas streams. Keller et al. [263] functionalized highly porous multi-walled carbon nanotube based microtubes with polyethylenimine. In the case of low PEI fractions in the impregnating solution, the carbon material was characterized by a large specific surface and porosity of the microtubes, and the sorption of CO<sub>2</sub> increased with the increase in the amount of PEI. Thus, a CO<sub>2</sub> uptake maximum value of

2.11 mmol/g at 20 wt% was observed, respectively. On the other hand, higher amounts of PEI (>20 wt%) caused decreasing the efficiency of CO<sub>2</sub> adsorption. Lee et al. [264] also used MWCNTs to impregnate them with PEI. They reached the same conclusions, finding that attaching amino groups to the carbon surface in the impregnation process leaves oxygen affinity sites, which increases sorption efficiency. Rahimi et al. [256] instead, used diamine precursor (1,3-diaminopropane) for the modification of multi-walled carbon nanotubes, which improved the CO<sub>2</sub> adsorption capacity of MWCNTs from 1.10 to 2.11 mmol/g.

Additionally, Keller et al. [270] noticed the high potential usefulness of a composite based on CNTs and silica, due to the reduced pressure drop, lower energy consumption, higher CO<sub>2</sub> recovery, and thermal and chemical stability. Silica particles were dispersed in the CNTs network, and polyethylenimine was immobilized in the hollow fibers to increase the efficiency of CO<sub>2</sub> sorption. The application of silica particles improved the specific surface area of the composite to 283.2 m<sup>2</sup>/g. Nevertheless, the impact of the increase in PEI loading was more pronounced, resulting in a higher CO<sub>2</sub> uptake of 1.92 mmol/g.

Another interesting direction is the development of composite materials is a synthesis of hierarchically porous MWCNTs/carbon foam (CF) nanocomposites based on biomass. The results obtained by Zhang et al. [272], which determined the influence of the amount of MWCNTs on the mechanical properties, the pore structure of CF and the composite, showed a unique potential both in terms of CO<sub>2</sub> capture and energy storage of these materials. Due to a more developed hierarchical porosity, in particular ultramicroporosity with a pore size from 0.50 to 0.80 nm and mesopores with an average size of about 3.70–3.90 nm. The MWCNTs contained in the foam significantly increased the compressive strength of CF (by 113%), and also improved the thermal stability and the degree of graphitization. The CO<sub>2</sub> adsorption capacity of the nanocomposite reached a high value of 4.58 and 3.19 mmol/g at 0 and 25 °C, respectively.

**Table 9** outlines the modification strategies used to enhance CO<sub>2</sub> uptake and optimize the textural properties of carbon nanotubes.

### 3.2.4. Fullerenes

Fullerenes are also one of the allotropic forms of carbon that has been shown to be effective in separation and storage of a wide range of gases from simple monoatomic to polyatomic, including H<sub>2</sub>, and CO<sub>2</sub> [283–286]. They possess interesting physicochemical properties, considering their carbon atom bonding structure, which is uniform and demonstrates sp<sup>2</sup> hybridization. The structure of fullerenes can additionally be illustrated as a twisted layer of a graphene sheet, in which the carbon atoms form pentagonal or hexagonal configurations, resulting in a three-dimensional spatial architecture [287]. The most frequently considered as a potential adsorbent is icosahedral fullerene, composed of 60 carbon atoms (C<sub>60</sub>), due to its exceptional chemical stability [288]. However, other forms of fullerenes are also being explored in the context of improving CO<sub>2</sub> capture, such as B<sub>40</sub> [289–292], B<sub>80</sub> [293], or C<sub>24</sub>N<sub>24</sub> [294].

Studies with fullerene primarily concern the utilization of DFT approaches (Fig. 15). The methodology for investigating fullerenes via DFT entails the optimization of geometry, selection of a suitable level of theory and basis set, computation of electronic structure and properties, and examination of vibrational modes, electron density, and charge distribution. Upon completion of the DFT calculations, a range of properties pertaining to the fullerene structure can be computed, including but not limited to the electronic density of states, the HOMO-LUMO gap, and the vibrational spectra. Recently, that method was used in few research regarding fullerene to investigate the potential of them to capture and store CO<sub>2</sub>

**Table 8**Influence of modification strategies on textural properties and CO<sub>2</sub> uptake of activated carbons.

Activated carbon	BET surface area, m <sup>2</sup> /g	Total pore volume, cm <sup>3</sup> /g	Micropore volume, cm <sup>3</sup> /g	Average pore diameter, nm	CO <sub>2</sub> selectivity at 1 bar	CO <sub>2</sub> uptake, mmol/g	Adsorption temperature, °C	Adsorption pressure, bar	Reported treatment sources/chemicals	Purpose of modification method	Reference
NH <sub>3</sub> -AC (biomass residue)	788	0.369	0.305	0.9	—	2.23	25	1	High temperature NH <sub>3</sub> treatment at 400 °C	Increasing basicity, affinity between CO <sub>2</sub> molecules-adsorbent	[224]
NH <sub>3</sub> -AC (palm shell)	889	0.474	0.442	—	—	1.67	30	1	High temperature NH <sub>3</sub> treatment at 800 °C	surface and level-up N-contents	[225]
NH <sub>3</sub> -AC (black locust)	2511	1.35	1.16	2.15	30.75	5.05	25	1	High temperature NH <sub>3</sub> treatment at 600 °C		[205]
NH <sub>3</sub> -AC (cane or beet sugar)	611	0.890	—	4.7	—	1.41	35	1	High temperature NH <sub>3</sub> treatment at 600 °C		[243]
NH <sub>3</sub> -AC (biomass corncob)	1154	0.57	—	—	—	2.8	25	1	High temperature NH <sub>3</sub> treatment at 800 °C		[244]
MEA-AC (dried rice husk)	1190	0.777	0.422	—	115.00	1.90	25	1	Amine functionalization (Monoethanolamine)		[240]
TETA-AC (broom sorghum stalks)	1098	0.642	0.525	2.33	—	3.2	25	1	Amine functionalization (Triethylenetetramine)		[226]
Urea-AC (broom sorghum stalks)	614	0.383	0.274	2.49	—	2.33	25	1	Amine functionalization (Urea)		[226]
PEI-AC (bagasse)	483.86	0.280	0.258	2.18	—	0.20	75	1	Amine functionalization (Polyethylenimine)		[227]
DEA-AC (palm shell)	652.6	0.38	—	2.34	—	5.3	70	4	Amine functionalization (Diethanolamine)		[245]
PEI-AC (biomass derived waste)	—	—	—	—	—	2.0	30	1	Amine functionalization (Polyethylenimine)		[246]
AC/MgO–CaO	331	—	—	—	—	0.15	30	1	Loading of metal oxides (MgO, CaO)	Improving the surface properties and promoting the	[232]
AC/MgO	615	0.496	0.147	—	—	1.11	25	1	Loading of metal oxide (MgO)		[233]
AC/Cu–Zn	599.41	—	0.399	—	—	2.26	30	1	Loading of metals (Cu, Zn)	interaction with CO <sub>2</sub> ;	[247]
AC/Cu	638	0.30	0.24	—	—	4.93	0	1	Loading of metal (Cu)	Composite formation	[248]
AC/Ni	595.97	0.33	0.22	2.20	—	2.36	25	1	Loading of metal (Ni)		[249]
AC nanofibers/MgO	413	0.22	—	—	—	2.08	25	1	Loading of metal oxides (MgO)		[241]
AC/CuO–MgO	727.7	0.50	0.26	2.8	—	1.91	30	1	Loading of metal oxides (CuO, MgO)		[250]
AC/CuO	1954	1.63	1.60	1.56	—	6.78	30	1	Loading of metal oxide (CuO)		[251]
AC/NiO	1945	1.63	1.59	1.79	—	6.48	30	1	Loading of metal oxide (NiO)		[251]
PEI-K <sub>2</sub> CO <sub>3</sub> /AC	160.34	0.105	—	2.62	—	3.60	60	—	Amine functionalization (Polyethylenimine); Alkali metal loading (K <sub>2</sub> CO <sub>3</sub> )	Improving the surface properties and promoting the interaction with CO <sub>2</sub> ; Increasing basicity and level-up N-contents	[252]
AC/Zeolite 13X	656	0.315	0.267	—	—	5.31	30	0.05	Zeolite 13X	Composite formation	[234]
AC/Na-A zeolite	182	0.047	—	—	—	1.14	25	1	Na-A zeolite		[235]
AC/hydrotalcite	441	0.21	—	1.95	—	1.638	200	3	Hydrotalcite		[253]
AC/expanded graphite	523	0.205	—	—	18.10	2.89	25	1	Expanded graphite		[228]
AC/HKUST-1 (MOF)	1,1456	—	0.4363	—	—	3.52	25	1	HKUST-1 (MOF)		[238]
AC/Cu-BTC (MOF)	1368	0.66	0.60	—	16.80	4.49	25	1	Cu-BTC (MOF)		[242]
Pd-AC/MOF-74(Ni)	1115	0.78	—	0.823	14.60	12.24	25	32	MOF-74(Ni)		[239]
Pd-AC/MOF-74(Co)	1088	0.75	—	0.815	12.40	11.42	25	32	MOF-74(Co)		[239]
AC/polydopamine	1841	0.74	—	—	25.10	4.05	25	1	Polydopamine		[230]
AC/molecularly imprinted polymer	3010	1.506	1.289	2.6	22.60	3.00	25	1	Molecularly imprinted polymer		[229]
AC/phenolic resin/carbon fibers	79.83	0.148	—	—	12.30	3.578	25	1	Phenolic resin, carbon fibers		[165]

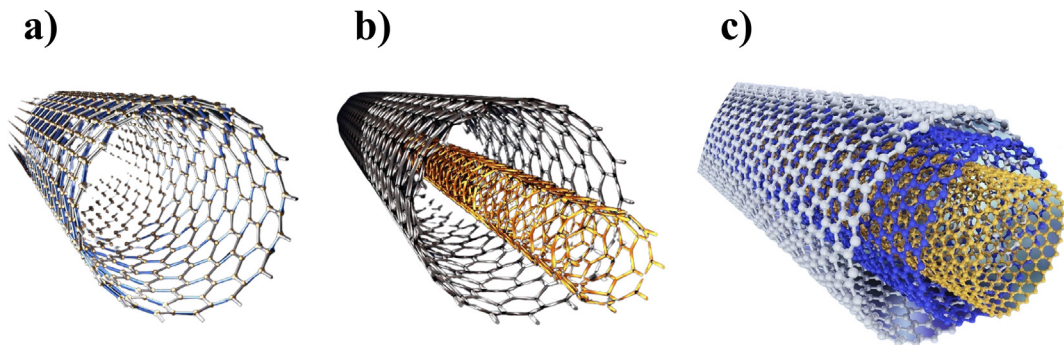


**Fig. 13.** Spatial models of single-walled (a), double-walled (b), and multi-walled (c) carbon nanotubes.

molecules. One of the newest directions of research on fullerene as adsorbents is the simultaneous sorption and reduction of CO<sub>2</sub> to compounds that can be reused in industry (MOFs materials are applied in a similar strategy). Qu et al. [293] sought to produce photocatalysts for CO<sub>2</sub> reduction with high efficiency and selectivity, which is important from both an energy and environmental standpoint. They discovered through comprehensive density functional theory calculations that fullerene B<sub>80</sub> is an excellent metal-free photocatalyst for CO<sub>2</sub> reduction to HCOOH (the activation and reduction mechanisms have been thoroughly investigated). Formic acid, which is frequently used in organic synthesis, beekeeping, and as a strong fungicidal preservative, can be reused in this manner. Their work provided significant insight into adsorption of CO<sub>2</sub> and its possible reduction products on B<sub>80</sub>.

Further, the adsorption behavior of the calcium coated fullerene B<sub>40</sub> by DFT method was studied by Esrafil et al. [292]. The Ca atom has been discovered to be able to stably adsorb CO<sub>2</sub> molecules, with

polarization and charge transfer processes governing the adsorption of CO<sub>2</sub> on the Ca-coated B<sub>40</sub>. In this way, each coated Ca atom could adsorb up to four CO<sub>2</sub> molecules with an average adsorption energy of 0.54 eV, which is within the range proposed for an ideal CO<sub>2</sub> adsorbent. Furthermore, because of the considerable difference in adsorption energy between CO<sub>2</sub> and H<sub>2</sub>, CH<sub>4</sub>, or N<sub>2</sub>, Ca-coated B<sub>40</sub> has proven to be effective in separating CO<sub>2</sub> from CH<sub>4</sub>/H<sub>2</sub> in natural gas or from N<sub>2</sub> in flue gas mixture (high selectivity towards CO<sub>2</sub>). DFT approach was also implemented in research regarding electric field in CO<sub>2</sub> adsorption, where it consisted in achieving a specific process mechanism in order to facilitate the uptake and regeneration of CO<sub>2</sub> capture material. Khan et al. [295] used an electric field to study the behavior of carbon dioxide storage by phosphorus-doped fullerene (P-doped C<sub>60</sub>-fullerene). They demonstrated that CO<sub>2</sub> is physisorbed without the application of an electric field by using the predicted adsorption energy. However, when it is employed, it induced a change from physical to chemisorption of

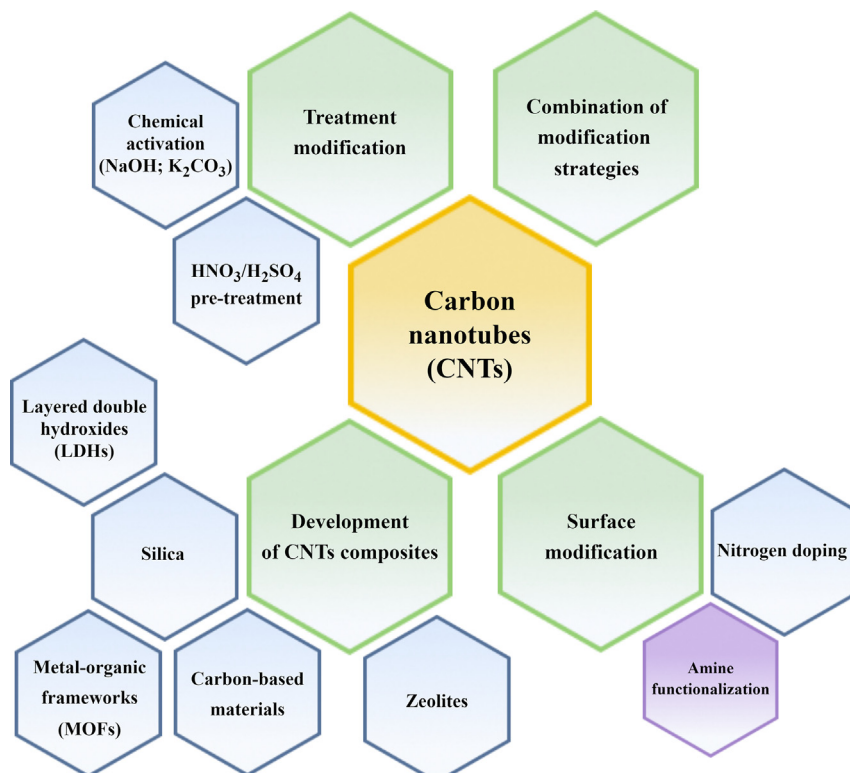


**Fig. 14.** The modification strategies and research directions of carbon nanotubes.

carbon dioxide as a stronger chemical bond is formed between the P atom and the CO<sub>2</sub> molecule. Consequently, by eliminating the electric field, the adsorbent may be easily regenerated for reuse. Moreover, P-doped fullerene has been discovered to be an excellent adsorbent for CO<sub>2</sub> removal from a N<sub>2</sub>/CO<sub>2</sub> mixture. Khan et al. [294] conducted the same research for P-decorated C<sub>24</sub>N<sub>24</sub> fullerene for selective separation of CO<sub>2</sub> from N<sub>2</sub>/CO<sub>2</sub> mixture in the presence of an electric field. The estimated geometric parameters revealed that under the electric field, bond lengths and angles (O=C=O) (O=C=O) are vastly reduced, converting physisorption to chemisorption by raising the electric field. This research discovered that P-decorated C<sub>24</sub>N<sub>24</sub> was a selective adsorbent and can aid in the development of a controlled, and regenerable sorption for the CO<sub>2</sub> separation from a gas mixture in the presence of an electric field.

### 3.2.5. Graphite-based adsorbents

Graphite in light of its internal structure, properties similar to those of carbonaceous adsorbents, and the economic advantage of being low cost is also considered a unique material for CO<sub>2</sub> capture [296]. Its structure is characterized by a multilayer arrangement whereby carbon atoms exhibit sp<sup>2</sup> hybridization and occur in the configuration of closed six-membered rings [297]. These rings are composed of graphene layers that form a complex spatial structure connected by relatively weak intermolecular interactions known as van der Waals forces. The strength of these forces may be precisely represented by appropriate modeling techniques (Fig. 16). Therefore, the storage of gas molecules between the graphene layers is possible by adjusting their mutual distances. However, graphite has a weak affinity towards CO<sub>2</sub> and a low surface area, limiting its CO<sub>2</sub> adsorption capacity [298].

The formation of new graphite structures is one of method to overcome these limitations, apart from graphite exfoliation (conversion to graphene oxide), chemical/physical activation, surface functionalization, or composites synthesis (Fig. 17). Several examples of them have been reported in the literature, e.g., graphite nanofibers (Yuan et al. [299] studied the effect of KOH activation on its surface), graphite nanoplatelets (Mishra et al. [300] proved that this particular structure has the potential as an effective CO<sub>2</sub> capture material under high pressure conditions, such as fumes from thermal power plants, or the cement industry sector).

The most commonly form of graphite utilized in CO<sub>2</sub> adsorption is graphite oxide, which is a product by applying the Hummer method [301]. This approach introduces oxygen-containing functional groups, namely epoxide and hydroxyl groups, into the crystal structure of graphite. To date, researchers have successfully synthesized several types of adsorbents, including amine-based adsorbents [302–305] and hybrid materials [306–308], by employing graphite oxide as an initial component. Shin et al. [302] developed CO<sub>2</sub> adsorbents based on graphite oxide modified with polyethylenimine. The study showed that the CO<sub>2</sub> adsorption capacity and CO<sub>2</sub>/N<sub>2</sub> selectivity increased with increasing polyethylenimine content (enhanced acid-base interaction between CO<sub>2</sub> gases with nitrogen functional groups) and exceeded pristine graphite oxide. The results obtained indicated that the maximum CO<sub>2</sub> uptake and selectivity were 0.75 mmol/g and 37.13, respectively, with a polyethylenimine content of 60% by weight. Hong et al. [305] modified the graphite oxide with 3-aminopropyl-triethoxysilane, which ensured the enhancement of the affinity for CO<sub>2</sub> and increased its adsorption capacity. The aminated material also showed high stability during the adsorption/desorption cycles. Zhang et al. [304] achieved noteworthy findings of their research involving the modification of graphite oxide by 3, 5, 10, and 50 wt% TEPA, where CO<sub>2</sub> adsorption experiments were carried out over a wide range of pressures and temperatures. The graphite oxide samples with 3 and 5 wt% of TEPA exhibited superior CO<sub>2</sub> uptake

compared to the pristine material. Conversely, the samples with 10 and 50 wt% of TEPA shown worse performance in terms of CO<sub>2</sub> uptake. In this particular scenario, it was observed that an optimal quantity of TEPA loading resulted in an enhanced CO<sub>2</sub> adsorption capacity. However, excessive TEPA loading yielded a contrary outcome, mostly owing to the decrease in the specific surface area of the adsorbent and the reduced accessibility of the amine groups.

It is noteworthy that research has also been undertaken on the modification of the graphite surface using other chemical compounds than amines as an alternative. Espinosa-Jiménez and Domínguez [309] used an anionic surfactant, sodium dodecyl sulfate to promote CO<sub>2</sub> adsorption on a graphite surface. The results showed that the addition of surfactants increased confinement of CO<sub>2</sub> and the amount of gas retention on adsorbent. Other studies also concern an investigation of sulfur doping effects and humidity influence on the adsorption performance of graphite. Li et al. [310] demonstrated that sulfur doping significantly increased the adsorption of pure CO<sub>2</sub> (graphite split graphite pore showed a 39.85% growth in the adsorption capacity by the impregnation with 33.12% sulfur at 27 °C and 1 bar). Significantly, it was observed that split graphite pores demonstrated a notably greater CO<sub>2</sub> uptake compared to sorbents without sulfur admixture, particularly in the presence of water.

As previously mentioned, graphite oxides have been utilized in the synthesis of composites, especially with MOFs. Policicchio et al. [307] studied CO<sub>2</sub> adsorption on the parent MOFs and their composites with graphite oxide and amine-based versions. The composite of metal-organic frameworks and amine-based graphite oxide with the highest content of nitrogen, showed the best performance, in terms of both adsorption capacity and process reversibility. The CO<sub>2</sub> capacity on this material reached 4.65 and 7.27 mmol/g at 25 and 4 °C at 0.1 MPa, which is competitive with many best performing adsorbents addressed in the literature. In the case of promising strategy for designing and fabricating composites using copper-based MOF, Zhao et al. [308] examined graphite oxide modified with urea. The composite with the highest nitrogen content exhibited an excellent CO<sub>2</sub> uptake (4.23 mmol/g) at 25 °C. The results indicated that CO<sub>2</sub> was mainly physisorbed on the composites under dry conditions and the primary adsorption sites were the open Cu centers. Then the small micropores on the interface between MOF units and the modified graphene layers, were occupied by the adsorbate molecules. The analysis of the adsorption heats suggested that the unsaturated copper sites were stronger adsorption centers than the small micropores and the interactions between copper and CO<sub>2</sub> were highly specific. In addition, a prominent research direction in composite synthesis is the application of graphite electrode waste together with cerium oxide or iron oxide as adsorbents. These materials exhibit stability and selectivity towards carbon dioxide, hence minimizing the negative impacts on the environment [311,312].

**Table 10** summarizes the modification strategies employed to improve CO<sub>2</sub> uptake and textural properties of graphite-based adsorbents. So far, there has been no review closely related to graphite, fullerene, the same as for carbon nanotubes. Therefore, a critical review of the literature is recommended, which would contribute to the organization of current knowledge on a laboratory scale to facilitate the technological maturity of these carbon-based materials.

### 3.2.6. Graphene-based adsorbents

Graphene is a carbon allotrope in the form of a single-layer two-dimensional honeycomb lattice (a 2D structure composed of carbon atoms connected in hexagons with sp<sup>2</sup> hybridization) [315]. In the pursuit for a highly efficient sorption materials, graphene-based adsorbents have been discovered to offer amazing

**Table 9**  
Influence of modification strategies on textural properties and CO<sub>2</sub> uptake of carbon nanotubes.

Carbon nanotube-based adsorbent	BET surface area, m <sup>2</sup> /g	Total pore volume, cm <sup>3</sup> /g	Micropore volume, cm <sup>3</sup> /g	Average pore diameter, nm	CO <sub>2</sub> selectivity at 1 bar	CO <sub>2</sub> uptake, mmol/g	Adsorption temperature, °C	Adsorption pressure, bar	Reported treatment sources/chemicals	Purpose of modification method	Reference
TEPA-CNT	2.20	0.03	—	—	—	5.00	60	—	Amine functionalization (Tetraethylenepentamine); Chemical activation (KOH)	Increasing basicity, affinity between CO <sub>2</sub> molecules-adsorbent surface and level-up N-contents; Increasing surface area and porosities	[267]
K <sub>2</sub> CO <sub>3</sub> -APF-CNT	1005	0.61	0.45	0.92	8.80	4.50	0	1	Amine functionalization (3-aminophenol/formaldehyde resin); Chemical activation (K <sub>2</sub> CO <sub>3</sub> )	[273]	
TEPA-CNT	8.94	0.0565	—	19.04	—	3.56	40	—	Amine functionalization (Tetraethylenepentamine)	Increasing basicity, affinity between CO <sub>2</sub> molecules-adsorbent surface and level-up N-contents	[254]
PEI-MWCNT	34.7	23.4	—	—	196.00	2.11	25	1	Amine functionalization (Polyethylenimine)	Increasing basicity, affinity between CO <sub>2</sub> molecules-adsorbent surface and level-up N-contents	[263]
PEI-MWCNT	174	1.646	0.015	—	—	2.14	25	0.15	HNO <sub>3</sub> /H <sub>2</sub> SO <sub>4</sub> pre-treatment; Amine functionalization (Polyethylenimine)	Carboxylation, oxidation of MCNT; Increasing basicity, affinity between CO <sub>2</sub> molecules-adsorbent surface and level-up N-contents	[264]
BPEI-CNT	14.1	0.10	—	—	—	2.43	70	—	Amine functionalization (Polyethylenimine)	Increasing basicity, affinity between CO <sub>2</sub> molecules-adsorbent surface and level-up N-contents	[274]
PEI-purine-CNT	—	—	—	—	—	3.875	50	1	Amine functionalization (Polyethylenimine); Purine	Increasing specific area of CNTs, basicity, affinity towards CO <sub>2</sub> and level-up N-contents	[266]
APS-CNT	198	0.63	—	12.2	—	2.19	25	1	Amine functionalization (3-aminopropyltriethoxysilane)	Increasing basicity, affinity between CO <sub>2</sub> molecules-adsorbent surface and level-up N-contents	[275]
PAA-MWCNT	60.44	0.40	—	13.76	—	1.59	25	1	Amine functionalization (Polyaspartamide)	Building bonding between amino-containing compound and substrate material to enhance the surface area and pore volume	[276]
HNO <sub>3</sub> /H <sub>2</sub> SO <sub>4</sub> -DAP-MCNT	112.8	0.65	—	11.6	—	2.11	30	17.3	HNO <sub>3</sub> /H <sub>2</sub> SO <sub>4</sub> pre-treatment; Amine functionalization (1,3-diaminopropane)	Carboxylation, oxidation of MCNT; Increasing basicity, affinity between CO <sub>2</sub> molecules-adsorbent surface and level-up N-contents	[256]
HNO <sub>3</sub> /H <sub>2</sub> SO <sub>4</sub> -PDA-MCNT	90.7	0.53	—	23.80	—	0.54	25	2	HNO <sub>3</sub> /H <sub>2</sub> SO <sub>4</sub> pre-treatment; Diamine functionalization (phenylenediamine)	[277]	
HNO <sub>3</sub> /H <sub>2</sub> SO <sub>4</sub> -MCNT	100.93	0.05	1.59	2.73	~12.00	0.32	25	1	HNO <sub>3</sub> /H <sub>2</sub> SO <sub>4</sub> pre-treatment	Carboxylation, oxidation of MCNT	[268]
PEI-CNT/Silica	283.2	—	—	—	217.00	1.92	25	0.15	Amine functionalization (Polyethylenimine); Silica	Composite formation	[270]
PAN-CNT/Carbon nanofibers (CNF)	390	0.40	0.33	—	78.00	6.3	25	1	Amine functionalization (Polyacrylonitrile as amine source); Carbon nanofibers	[278]	
CNT/N-doped AHPC	561	—	—	—	18.04	3.91	25	1	N-doped acicular hollow porous carbon	[279]	
MWCNT/Carbon foam	805.91	0.35	0.31	—	8.44	3.19	25	1	Carbon foam	[272]	
N-doped CNT/PAN-ACF	709	0.3577	0.2312	2.019	—	1.75	25	1	Amine functionalization; Polyamide-based activated carbon fibers	[280]	
PEI-MWCNT/Cd-nanozeolite	365	0.39	—	2.65	—	5.70	25	20	Amine functionalization (Polyethylenimine); Nanozeolite modified with Cd <sup>2+</sup>	Increasing basicity, affinity between CO <sub>2</sub> molecules-adsorbent surface and level-up N-contents; Composite formation	[281]
MWCNT/MIL-101 (MOF)	—	—	—	—	—	0.003	25	1	MIL-101 (MOF)	[282]	

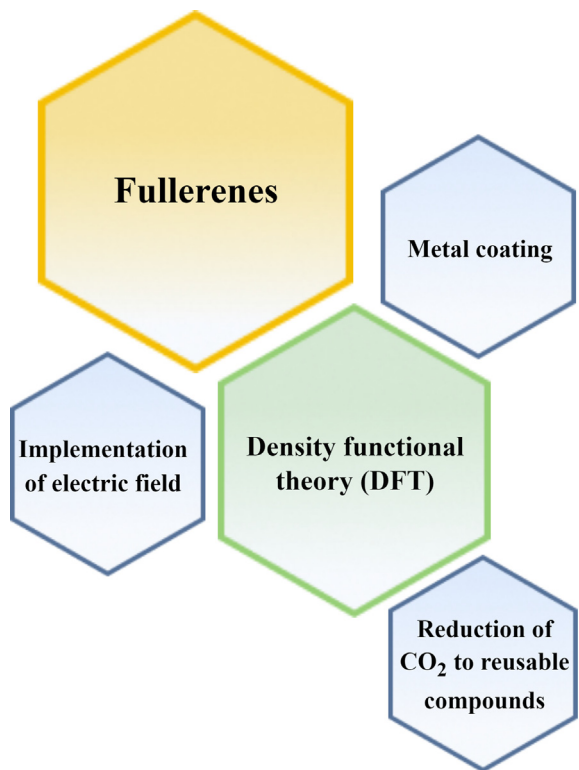


**Fig. 15.** The modification strategies and research directions of fullerenes.

attributes, including large specific surface area, high proclivity for gas adsorption, extraordinary electrical conductivity, good mechanical stability, and easy surface modification [316–318]. Furthermore, it is well acknowledged as a powerful adsorbent, particularly in terms of its ability to demonstrate a high adsorption capacity for carbon dioxide, surpassing that of methane and nitrogen [319]. The intimate relationship between graphene and its dense single-atom structure contributes to its ability to serve as a high-speed transport channel with exceptional gas selectivity [320].

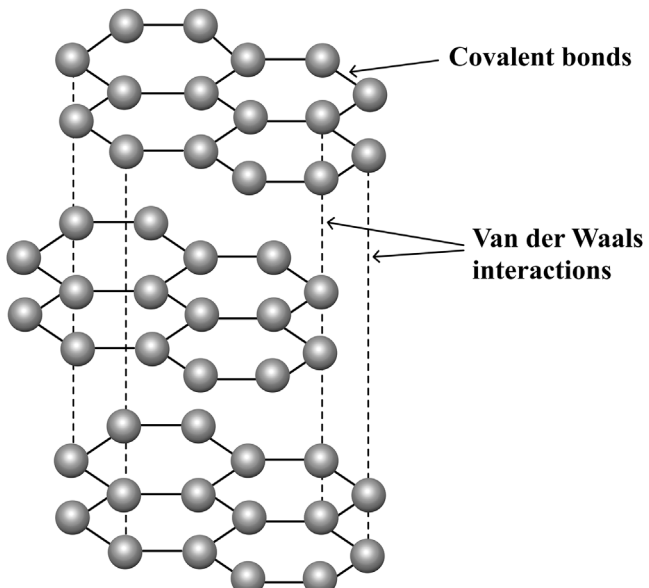


**Fig. 16.** Schematic structure of graphite.

However, because of the highly strong intermolecular interaction and the limited number of functional groups, pristine graphene has poor dispersibility and compatibility [321]. In this sense, graphene oxide (GO), an alternative form of graphene, exhibits remarkable characteristics attributed to the abundance of hydrophilic oxygenated functional groups. These groups offer numerous active sites for the joining of additional functional groups or molecules, thereby enabling functionalization through both covalent and non-covalent bonding mechanisms [322,323]. In addition to that, the adaptability of surface modification allows the use of graphene-based materials for CO<sub>2</sub> capture [324]. Another form of graphene used in CO<sub>2</sub> adsorption application, *inter alia*, for the synthesis of composites, is reduced graphene oxide (rGO). rGO is produced by the chemical or thermal reduction of graphene oxide. It is considered to possess a structure that is between that of a graphene sheet and highly oxidized graphene oxide [325]. The three structures of graphene are schematically shown in Fig. 18.

Currently, research on graphene as a CO<sub>2</sub> capture material concerns similar modifications as in the case of graphite, such as synthesis of hybrid materials/composites (MOFs [326–328], carbon-based materials [329], polymers [330,331], incorporation of metal oxides [332,333], clays [334]), creating new material structures based on graphene (aerogels [335], cryogels [336,337]), and treatment methods related to the improvement of the surface morphology (oxidation [338], physical and chemical activation [339–341]) (Fig. 19). Xia et al. [339] tuned the pore structure and surface chemistry of porous graphene materials (PGMs) for CO<sub>2</sub> capture, which was achieved by activating CO<sub>2</sub> and KOH in thermally exfoliated graphite oxide. CO<sub>2</sub>-activated PGMs (CPGM) had a three-dimensional morphology with a hierarchical pore structure, while KOH-activated PGMs (KPGM) had a two-dimensional morphology with large number of micropores and small mesopores. Specifically, CPGM exhibited a substantial presence of quinone and carbonyl functional groups, while KPGM demonstrated a significant concentration of hydroxyl groups. These distinctions in surface chemistry were confirmed through pore structure analysis and gas adsorption experiments. Additionally, the CO<sub>2</sub> adsorption by PGM was influenced by both the pore structure and the surface chemistry. At 0 °C and 1 bar, the highest adsorption value reached 4.06 mmol/g.

Another popular modification of graphene-based adsorbents is attaching organic functional groups to the graphene surface. Nitrogen doping [342–344] has been found to be a promising strategy to improve CO<sub>2</sub> adsorption capability. The developed materials were characterized by excellent stability and recyclability, high selectivity of CO<sub>2</sub> in relation to N<sub>2</sub>, suitable heat of adsorption, high dynamic adsorption, as well as fast CO<sub>2</sub> adsorption kinetics. As a result of their exceptional characteristic, GO has been fully exploited as a suitable framework for the fabrication of an amine-functionalized adsorbents for selective CO<sub>2</sub> capture. Moreover, there are many advantages associated with this specific research path, which are as follows: (1) reduced energy consumption during regeneration, (2) no corrosion susceptibility of instruments, (3) low creation of harmful byproducts due to amine groups incorporated in the solid matrix. Hosseini et al. [342] modified the surfaces of graphene oxide with 3 different amines, including triethylenetetraamine (TETA), pentaethylenehexamine (PEHA) and *meta*-phenylenediamine (MPD). At 298 K and 1 bar, CO<sub>2</sub> adsorption improved dramatically from 0.39 mmol/g for graphene oxide (GO) to 0.61, 0.74, and 0.91 mmol/g for GO-PEHA, GO-TETA, and GO-MPD samples, respectively. Furthermore, based on the ideal adsorbed solution theory (IAST), the predicted CO<sub>2</sub>/N<sub>2</sub> selectivity of the investigated solid sorbents revealed an outstanding value, particularly for the GO/MPD, reaching around 21.21 under ambient conditions. An et al. [345] examined graphene-derived N-enriched

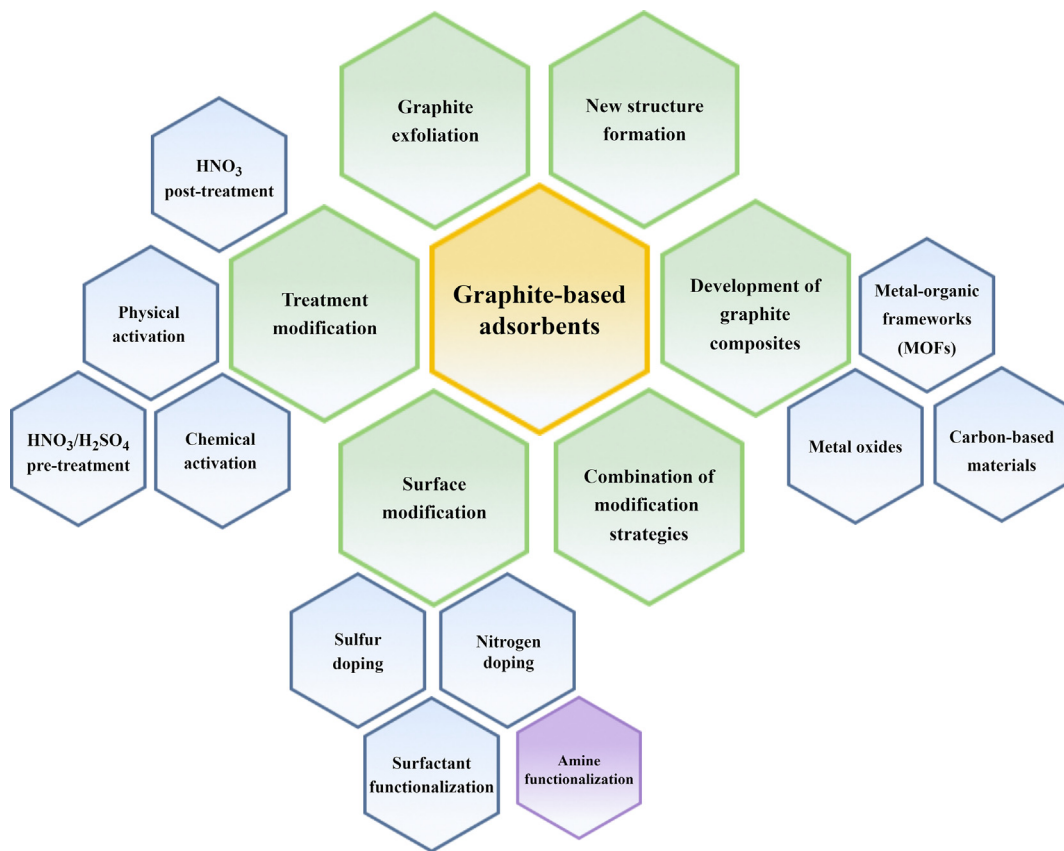


**Fig. 17.** The modification strategies and research directions of graphite-based adsorbents.

carbonaceous materials as well, although with an alternative nitriding agent, namely urea. The experimental setup included the usage of GO as the precursor and KOH as the activator. Subsequently, the samples were exposed to a thermal shock treatment, which aimed to enhance the structural features of the adsorbent. The results demonstrated that thermal expansion of the GO precursor improved the porosity and nitrogen enrichment of the porous carbons. At atmospheric pressure, the produced adsorbents demonstrated good CO<sub>2</sub> adsorption, with 2.40 and 3.24 mmol/g at 25 and 0 °C, respectively. Furthermore, investigations have shown that under ambient conditions, both narrow microporosity and N-doping are favorable for CO<sub>2</sub> capture.

In summary, this type of CO<sub>2</sub> capture materials must exhibit a range of desired properties in order to be considered economically viable and ecologically sustainable for sorption applications. These include a substantial surface area and pore volume, the presence of a porous structure (specifically microporosity), and the effective modification of surface chemistry through the incorporation of functional groups or heteroatoms. Lately, Ruhaimi et al. [346] systematically provided a comprehensive overview of the most recent scientific research concerning the utilization of graphene-based adsorbents in CO<sub>2</sub> adsorption technologies, as well as a discussion of that investigation. The authors highlighted several significant challenges that must be addressed in order to fully harness the promise of graphene-based adsorbents in the present moment. First, most of the current fabrication techniques, apparatus, and supplies are both expensive and time consuming, which limits their usefulness in the industrial sector. The significance of manufacturing costs in the context of large CO<sub>2</sub> capture systems cannot be overstated. Consequently, it is imperative to explore alternative recyclable waste residues for the purpose of processing

and functionalizing carbon-based adsorbents, with the aim of fostering a beneficial influence on the circular economy. Additional barriers that should be taken into consideration refer to the demand for more extensive research and an in-depth analysis of the CO<sub>2</sub> adsorption mechanism. Furthermore, it is crucial to place greater emphasis on conducting CO<sub>2</sub> sorption tests in both wet and dry environments to enhance the diffusion of CO<sub>2</sub> molecules into the porous structure of the material. Additionally, there is a necessity for further advancement in hybrid materials incorporating graphene-based adsorbents to enhance CO<sub>2</sub> uptake, while also considering other criteria for the selection and optimization of CO<sub>2</sub> capture materials.

The previously published review in 2015 by Balasubramanian and Chowdhury [347] also presented an in-depth evaluation of the emerging field of graphene-based adsorbents, highlighting notable areas for future research. Its primary objective was to compile the latest advancements in this rapidly evolving field. In particular, the authors highlighted the importance of defining the work path development on a laboratory scale and their practical transfer to a commercial application. Due to this, there is an unavoidable need for an expansive research endeavor that is both multidisciplinary and interconnected. Further future perspectives and recommendations have been proposed in relation to the measurement of CO<sub>2</sub> uptake on a volumetric basis, assessment of working capacity, determination of multicomponent gas adsorption isotherms, investigation of the impact of water vapor, in situ characterization of adsorbed CO<sub>2</sub>, and the development of molecular models along with force fields that accurately simulate realistic conditions.

The CO<sub>2</sub> capture performance and textural properties of graphene-based adsorbents associated with specific modification strategies are compared in Table 11.

**Table 10**Influence of modification method on textural properties and CO<sub>2</sub> uptake graphite-based adsorbents.

Graphite-based adsorbent	BET surface area, m <sup>2</sup> /g	Total pore volume, cm <sup>3</sup> /g	Micropore volume, cm <sup>3</sup> /g	CO <sub>2</sub> selectivity at 1 bar	CO <sub>2</sub> uptake, mmol/g	Adsorption temperature, °C	Adsorption pressure, bar	Reported treatment sources/chemicals	Purpose of modification method	Reference
PEI-graphite oxide	16	0.051	0.004	37.13	0.75	25	1	Amine functionalization (Polyethyleneimine)	Increasing basicity, affinity between CO <sub>2</sub> molecules-adsorbent	[302]
APTS-graphite oxide	19	—	—	—	1.16	30	1	Amine functionalization (3-Aminopropyl-Triethoxysilane)	surface and level-up N-contents	[305]
EDA-graphite oxide	2.73	—	—	—	1.22	30	—	Amine functionalization (Ethylenediamine)		[303]
TEPA-graphite oxide	42.68	—	—	—	2.08	25	30	Amine functionalization (Tetraethylenepentamine)		[304]
Graphite nanoplatelets (GNP)	—	—	—	—	4.9	25	12	Acid intercalation (HNO <sub>3</sub> /H <sub>2</sub> SO <sub>4</sub> pre-treatment); Thermal exfoliation; HNO <sub>3</sub> post-treatment	Graphite oxidation; Introducing hydrophilic functional groups (−COOH, −C=O, and −OH)	[300]
Graphite nanoplatelets (GNP)/Fe <sub>3</sub> O <sub>4</sub>	102.35	0.1509	—	—	8.5	25	11.5	Acid intercalation (HNO <sub>3</sub> /H <sub>2</sub> SO <sub>4</sub> pre-treatment); Thermal exfoliation; HNO <sub>3</sub> post-treatment; Loading of metal oxide (Fe <sub>3</sub> O <sub>4</sub> )	Graphite oxidation; Introducing hydrophilic functional groups (−COOH, −C=O, and −OH); Composite formation	[312]
Graphite waste/Fe <sub>3</sub> O <sub>4</sub>	18.48	0.07	—	—	5.36	30	8	Loading of metal oxide (Fe <sub>3</sub> O <sub>4</sub> )	Composite formation	[312]
Graphite waste/CeO <sub>2</sub>	20.03	—	—	—	3.58	30	20	Loading of metal oxide (CeO <sub>2</sub> )		[311]
S-doped graphite oxide/Porous carbon	831	0.589	0.38	—	5.00	0	1.2	Porous carbon; Sulfur doping	Composite formation; Enhancing the interaction strength between CO <sub>2</sub> and composite surface.	[313]
Graphite oxide/Cu <sub>3</sub> (BTC) <sub>2</sub> (MOF)	837	0.19	—	—	3.30	25	1	Cu <sub>3</sub> (BTC) <sub>2</sub> (MOF); Presence of humidity	Composite formation	[306]
Aminated graphite oxide/Cu-BTC (MOF)	1367	0.663	0.572	24.77	4.65	25	1	Amine functionalization by urea treatment; Cu-BTC (MOF)	Increasing basicity, affinity between CO <sub>2</sub> molecules-adsorbent surface and level-up N-contents; Composite formation	[307]
KOH-activated graphite nanofibers	919	1.057	0.226	—	1.61	25	1	Chemical activation with KOH	Improving the development of microporous structures and increasing surface area	[299]
KOH-activated graphite nanofibers	567	0.708	0.274	—	1.35	25	1	Chemical activation with KOH		[314]

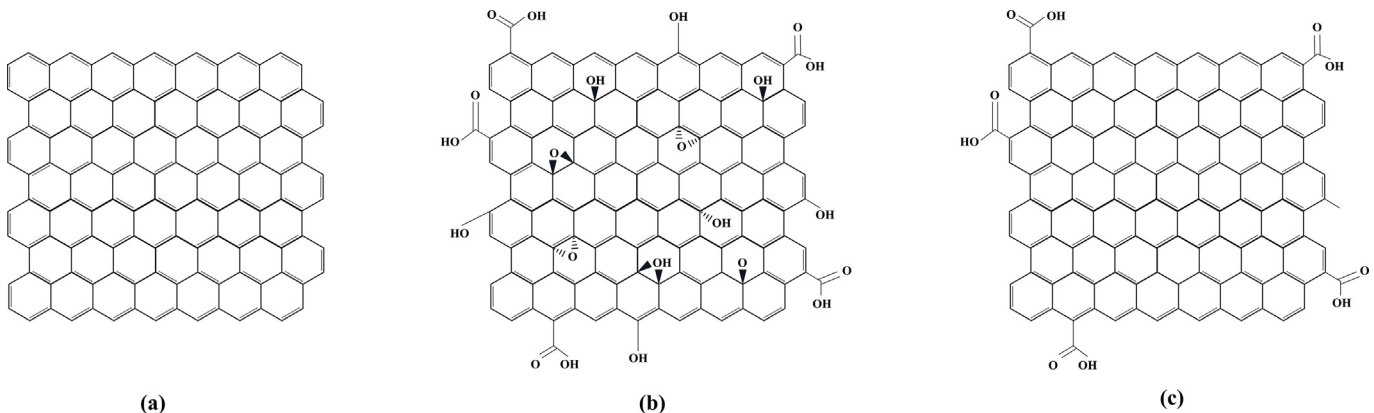


**Fig. 18.** Schematic representation of structures of graphene sheet (a), graphene oxide (GO) (b), and reduced graphene oxide (rGO) (c).



**Fig. 19.** The modification strategies and research directions of graphene-based adsorbents.

**Table 11**Influence of modification method on textural properties and CO<sub>2</sub> uptake of graphene-based adsorbents.

Graphene-based adsorbents	BET surface area, m <sup>2</sup> /g	Total pore volume, cm <sup>3</sup> /g	Micropore volume, cm <sup>3</sup> /g	Average pore diameter, nm	CO <sub>2</sub> selectivity at 1 bar	CO <sub>2</sub> uptake, mmol/g	Adsorption temperature, °C	Adsorption pressure, bar	Reported treatment sources/chemicals	Purpose of modification method	Reference
MPD-graphene oxide	44.33	0.046	0.031	4.23	21.21	0.91	25	1	Amine functionalization ( <i>Meta</i> -phenylenediamine)	Increasing basicity, affinity between CO <sub>2</sub> molecules-adsorbent	[342]
TETA-graphene oxide	14.40	0.016	0.011	4.65	16.37	0.74	25	1	Amine functionalization (Triethylenetetramine)	surface and level-up N-contents	[342]
PEHA-graphene oxide	9.39	0.012	0.008	5.27	9.54	0.61	25	1	Amine functionalization (Pentaethylenehexamine)		[342]
PEI-graphene oxide	—	1.822	—	—	—	2.91	75	1	Amine functionalization (Polyethylenimine)		[343]
EDA-graphene oxide cryogels	21.37	—	—	—	—	2.0	25	1	Amine functionalization (Ethylenediamine)		[336]
EDA-graphene oxide cryogels	167.66	—	—	—	—	1.18	25	1	Peroxidation step; Amine functionalization (Ethylenediamine)	Improving adsorption property; Increasing basicity, affinity between CO <sub>2</sub> molecules-adsorbent	[337]
Chitosan- graphene oxide cryogels	33.32	0.129	—	—	—	0.257	25	1	Chitosan grafting	N-contents	[348]
Urea-KOH-graphene oxide	1032	0.82	—	—	12.00	2.40	25	1	Thermal shocking; Urea modification (a source of amines); KOH activation	Providing the large surface area, high porosity, and a large number of amine group	[345]
CO <sub>2</sub> -activated porous graphene	2518	1.65	1.32	—	—	4.06	0	1	KOH activation	Improving the development of microporous structures	[339]
NaOH-activated porous graphene	843	2.71	0.12	—	—	1.74	0	1	CO <sub>2</sub> activation	and increasing surface area	[339]
3D crumpled graphene-based porous adsorbent	1.316	1.07	0.21	—	162.00	2.45	25	1	CO <sub>2</sub> activation of reduced graphene oxide		[340]
Monolithic reduced graphene oxide-based aerogels	1622	7.15	—	—	—	6.31	25	10	Steam activation of reduced graphene oxide		[335]
Triply oxidized graphene oxide	—	—	—	—	—	3.54	30	9	Multiple oxidations	Tuning the composition of GO functionalities (increasing the amount of oxygen containing groups)	[338]
Graphene oxide/MOF-200	3359	—	—	—	18.37	1.34	25	1	MOF-200	Composite formation	[326]
Graphene oxide/Cu-BTC	1820	0.88	0.88	—	21.00	9.05	0	1	Cu-BTC (MOF)		[327]
Graphene oxide/Cu-BTC	1772	0.718	0.593	—	43.80	8.90	0	1	Cu-BTC (MOF)		[328]
Graphene oxide/Cu-BTC	1015	0.4996	—	—	—	2.50	32	5	Cu-BTC (MOF)		[349]
UV-irradiated graphene oxide/Cu <sub>3</sub> (BTC) <sub>2</sub>	1324	0.777	0.676	2.304	14.35	5.14	25	1	UV-irradiation of GO; Cu <sub>3</sub> (BTC) <sub>2</sub> (MOF)	Enhancing critical parameters of GO adsorbents associated	[350]

(continued on next page)

Table 11 (continued)

Graphene-based adsorbents	BET surface area, m <sup>2</sup> /g	Total pore volume, cm <sup>3</sup> /g	Micropore volume, cm <sup>3</sup> /g	Average pore diameter, nm	CO <sub>2</sub> selectivity at 1 bar	Adsorption temperature, °C	Reported treatment sources/chemicals	Purpose of modification method	Reference
Graphene oxide/Cu <sub>3</sub> (BTC) <sub>2</sub>	1097	0.632	0.524	2.336	—	2.53	25	1	Cu <sub>3</sub> (BTC) <sub>2</sub> (MOF)
Graphene oxide/Uio-66	1184	0.384	0.304	—	—	3.37	25	1	UiO-66 (MOF)
Reduced graphene oxide/Polymer	110	0.197	0.036	13.6	12.00	3.85	25	1	Polymer monolithic material
Graphene oxide/Polyaniline (PANI)	<5	—	—	—	—	~19.00	1.31	30	1
Graphene oxide/TiO <sub>2</sub> nanoparticles	99.54	0.382	<0.01	—	30.856	22.00	1.88	25	Incorporation of metal oxide (TiO <sub>2</sub> )
Graphene oxide/MgO	12	0.10	—	—	—	3.34	60	60	Incorporation of metal oxide nanoparticles (MgO)
Reduced graphene oxide/PMMT	50.77	0.0788	—	6.7	—	0.49	25	1.18	Polyphosphoric acid modified clay (PMMT)

### 3.3. Metal-organic frameworks (MOFs)

Organic-inorganic hybrid porous materials, such as metal-organic frameworks, are solid CO<sub>2</sub> adsorbents with benefits including excellent thermodynamic stability, customizable chemical functionality, extra high porosity, easily programmable pore characteristics, high purity, well-defined crystallographic geometric properties, and large-scale production capability, among other materials [352–354]. Generally, MOFs are composed of metal-containing nodes that are connected together by organic linking groups (organic ligand bridges) principally through strong covalent bonds (coordination bonds) that form a one-, two- or three-dimensional coordination network [355–357]. MOFs can be classified into different groups based on their structural properties, such as rigid MOFs, dynamic/flexible MOFs, surface functionalized MOFs, open metal sites MOFs, Lewis basic sites MOFs, both open metal and Lewis basic sites MOFs, microporous MOFs, post-synthetically modified MOFs, and MOF composites [356]. Additionally, a combination of the above groups can be distinguished, i.e., MOFs with micropores and a functionalized surface, or micropores and open metal sites. The generic classification is shown in Fig. 20.

To date, a significant number of publications have been dedicated to the improvement of CO<sub>2</sub> capture by MOFs. Modifying the type and quantity of organic linkers or changing the connectivity of metal ions (both of the two fundamental building components) may be used to continuously improve a CO<sub>2</sub> adsorption performance and quality of MOFs structures [358,359]. As a result, various modifications of MOFs synthesis and their influence on the efficiency of carbon dioxide uptake were investigated, including the selection of organic linker [360], activating and removing the solvent molecule [361], and altering the open metal sites and Lewis basic sites [362,363]. Therefore, those materials possess a high degree of simplicity in terms of their production and adaptability for CO<sub>2</sub> capture application. The schematic illustration of CO<sub>2</sub> storage mechanism in MOFs structure is given in Fig. 21. By comparing metal-organic frameworks with other porous materials like zeolites and activated carbons, it becomes transparent that MOFs exhibit the ability to readily optimize their porosity, surface characteristics, and other properties. This versatility renders them highly suitable for a diverse range of specific and precise applications as solid material for CO<sub>2</sub> adsorption [364]. Nevertheless, the main challenge in achieving a high degree of crystallinity in the synthesis of MOFs lies in the optimization of multiple reaction parameters. These parameters include the concentration of reactants, the ratio of metal to ligand, the concentration of cosolvents, the pH of the solution, as well as the temperature and time of the reaction [356,365].

The amount of CO<sub>2</sub> captured by porous MOF materials is dependent on a number of parameters, including adsorption capacity, surface morphology, selectivity, and the amount of energy used during adsorption. Generally, the robust ability of MOFs to capture CO<sub>2</sub> can be attributed to their unique chemical and physical properties of frameworks, which are appropriately changed and adjusted to increase the interaction forces between the material surface and the CO<sub>2</sub> molecules [357]. These distinguishing characteristics primarily include pore size, porosity, specific surface area, unsaturated or open metal sites, and integration of polar functional groups into the pore channels (–NH<sub>2</sub>, –OH, –NO<sub>2</sub>, and –COOH) [366,367]. In order to modify these parameters, extensive research has been performed in recent decades. As an instance, Furukawa et al. [366] developed ultrahigh porosity in MOFs by synthesizing crystalline solids with extended non-interpenetrating three-dimensional crystal structures supported well-defined pores. Series of MOFs showed exceptional

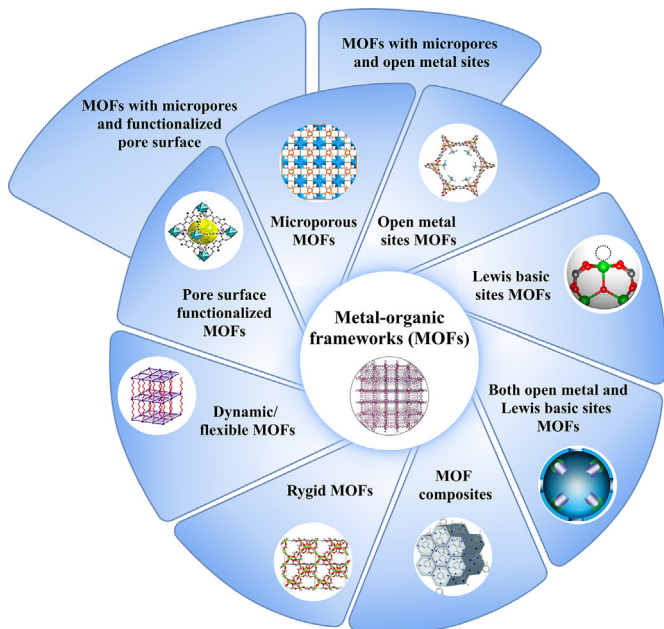


**Fig. 20.** Classification of metal-organic frameworks for  $\text{CO}_2$  capture.

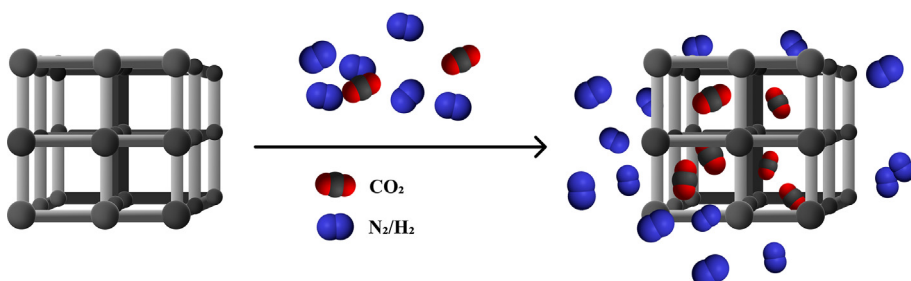


**Fig. 21.** Adsorption process of  $\text{CO}_2$  molecules within the structure of MOFs.

porosities and  $\text{CO}_2$  uptake with the maximum BET surface area reaching of almost  $6240 \text{ m}^2/\text{g}$ . Further, Farha et al. [367] focused on combining MOFs featuring ultrahigh surface via de novo approach entailing computational design and simulations before experimentation. The obtained adsorbent had a high BET surface ( $6143 \text{ m}^2/\text{g}$ ) with high  $\text{CO}_2$  storage capacity.

Currently, R&D projects on MOFs mainly focus on investigating the impact of process conditions and flue gas composition on  $\text{CO}_2$  adsorption. This research mainly concentrates on the influence of moisture, as well as pollutants. Other areas of interest include altering and fixing pore shape and size, modifying metal sites and Lewis basic bases, doping with metal ions, creating novel structures, optimizing regeneration and recycling procedures, exploring various methods of functionalizing the pore surfaces of MOFs, and synthesizing MOF composites (Fig. 22) [296,355,356]. The main objective of the above modifications is to further enhance the  $\text{CO}_2$  uptake, selectivity towards  $\text{CO}_2$ , and stability of the framework itself, according to the researchers [368]. Therefore, the majority of studies concern the evaluation of  $\text{CO}_2$  adsorption capacity by determining the adsorption equilibrium [369].

A large number of microporous metal–organic frameworks (MMOFs) have been developed as  $\text{CO}_2$  capture materials. Chen et al. [370,371] emphasized that the tuning of micropores inside MOFs is critical for their application in the separation of small molecules. Since metal-containing secondary building units and organic

linkers may be selectively added to MOFs, the pores within these materials can be tuned more precisely than standard porous zeolites. Wu et al. [372] presented flexible MMOFs as remarkable adsorbent with high  $\text{CO}_2$  selectivity of over other gaseous molecules at relative low pressure and high temperature, which are comparable to those present in flue gas mixtures.

However, developing MMOFs with exceptionally high  $\text{CO}_2$  capture capacity and gas selectivity while still simultaneously requiring low regeneration energy, remains a formidable obstacle to overcome. Recently, Wen et al. [373] designed and synthesized a MMOF with suitable pore size and dual functionalities. That material displayed excellent  $\text{CO}_2$  capture capacity ( $3.56 \text{ mmol/g}$  at  $0.15 \text{ bar}$  and  $23^\circ\text{C}$ ) as well as strong  $\text{CO}_2/\text{N}_2$  selectivity (600), both of these values were considerably higher than those observed in most other MMOFs previously reported. The research findings further indicated that the outstanding  $\text{CO}_2$  uptake at low pressure and mild heat of  $\text{CO}_2$  adsorption may be related to the appropriate pore size and dual functionalities, which not only interact with  $\text{CO}_2$  molecules but also enable them to dense pack inside the framework. Other studies on MMOFs concern pore environment modifications to enhance  $\text{CO}_2$  adsorption. Fan et al. [374] alter multifunctional ligands with  $-\text{F}$ ,  $-\text{Cl}$ ,  $-\text{NH}_2$ ,  $-\text{CH}_3$ ,  $-\text{OCH}_3$ , and organic secondary building units with bipy-N ligands (dimethylamine, pyridine, 4-aminopyridine, and isonicotinic acid) based on

microporous Ni-MOFs. Fluorine modified MOFs showed the highest  $\text{CO}_2$  uptake of  $3.81 \text{ mmol/g}$  at  $0^\circ\text{C}$  and  $1 \text{ atm}$ . The conclusive findings indicated successful synthesis of innovative porous materials that offer significant efficacy as  $\text{CO}_2$  adsorbent, hence contributing to the development of a systematic approach for enhancing gas adsorption and separation abilities.

Several research have been conducted to investigate the rational modification of open metal sites and Lewis nitrogen sites, aiming to enhance the  $\text{CO}_2$  sorption performance. These studies provide vital insights for the design and synthesis of novel materials in the field of MOFs. Song et al. [375] conceived and produced three diisophthalate organic ligands containing nitrogen and utilized them to synthesize three isostructural NbO-type MOFs with varying numbers and orientations of nitrogen sites. The results of the investigation established that the  $\text{CO}_2$  adsorption characteristics of MOFs are influenced not only by the amount of Lewis basic nitrogen sites but also by their accessibility. Additionally, the introduction of functional groups does not have a restricted impact on improving  $\text{CO}_2$  uptake.

Accordingly, ligand functionalization or post-synthetic modification has been explored by many researchers. Xu et al. [376] developed two N-oxide functionalized linear diisophthalate ligands and used them to create their corresponding NbO-type MOFs under acceptable solvothermal conditions. Their  $\text{CO}_2$  adsorption capacities and selectivity towards  $\text{CO}_2$  shown considerable levels of

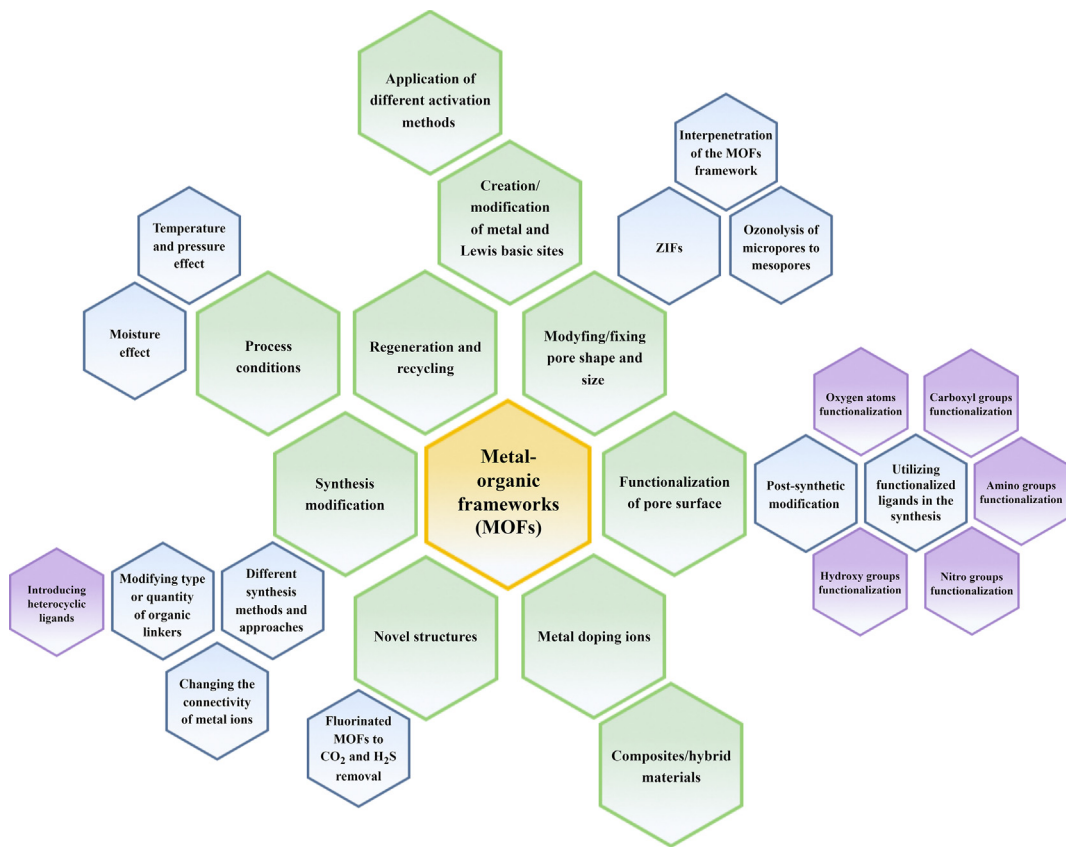


**Fig. 22.** The modification strategies and research directions of metal-organic frameworks.

effectiveness for NbO-type MOF counterparts. Furthermore, structure–property relationship investigations demonstrated that the N-oxide functionality is highly critical for increasing CO<sub>2</sub> adsorption efficiency.

As previously stated, metal-organic frameworks are typically utilized together with other materials to form composite structures. Typically, the production of these MOF-based composites requires the dissolution of the raw components or as-processed materials in the precursor solutions of MOFs prior to initiating the reactions. As a consequence of the synergistic effects, the resulting multi-component composites not only exhibit the inherent strength of the original materials, but also possess unique physicochemical characteristics and functional properties. In recent years, carbon-based materials have been extensively used to fabricate such composites. The addition of these components has the potential to regulate particle sizes and drive the formation of MOF crystals in a certain direction, hence leading to improved adsorption capacity [377]. Kayal and Chakraborty [378] designed and developed carbon-based MOF composite, which was synthesized by in situ incorporation of activated carbon powder (type Maxsorb-III) in MOF (MIL-101(Cr)). In comparison to the parent MOF, it was seen that the composite exhibited greater CO<sub>2</sub> adsorption capacity. Specifically, the composite demonstrated a 10% and 15% increase in CO<sub>2</sub> uptake on a volumetric and gravimetric basis, respectively. Qian et al. [379] aimed to improve the structural features of hierarchical porous carbon monolith (HCM) by incorporating the advantages of metal–organic frameworks (Cu<sub>3</sub>(BTC)<sub>2</sub>) to optimize the CO<sub>2</sub> capture on a volumetric basis. The obtained composite was characterized by a significant CO<sub>2</sub> adsorption capacity value, notable CO<sub>2</sub>-over-N<sub>2</sub> selectivity and a good regeneration capability.

Recently, the ordered mesoporous silica has also been selected for use in the fabrication of MOF-based composite materials, according to the researchers [380–383]. The introduction of ordered mesoporous structure, in addition to providing functional attributes that are comparable to those of carbon-based materials, also offers the reduction of mass transfer resistance of guest molecules and boosts the diffusion efficiency [379]. Chen et al. [380] attempted to create hybrid composites based on mesoporous silica and MOFs that exhibited both high CO<sub>2</sub> adsorption capacity and rapid adsorption kinetics. The composite was constituted of MIL-101(Cr) and mesoporous silica through an in-situ hydrothermal method. The synthesis led to reduced particle size, enhanced micropore volume, and increased specific surface area of the composite, resulting in a considerable improvement in its CO<sub>2</sub> uptake (2.09 mmol/g at 0 °C and 1 bar), about 79% higher than that of parent MOF. Further, the application of MCM-41 contributed to a decrease in the mass transfer resistance and facilitated the CO<sub>2</sub> diffusion. Consequently, there was an apparent reduction in the time required to achieve adsorption equilibrium and an increase in the adsorption rate. Moreover, the synergistic impact of mesoporous silica and MOFs strengthened the interactions between CO<sub>2</sub> molecules and the composite, as indicated by the isosteric heats of CO<sub>2</sub> adsorption and desorption activation energy.

Further, the chemical composition of the flue gases, which are separated for the purpose of carbon dioxide capture, is a crucial factor to consider in relation to MOFs. Especially, the presence of moisture can substantially impact on the CO<sub>2</sub> adsorption capacity of MOFs. Llewellyn et al. [384] highlighted the difference in the adsorption behavior between the polar and nonpolar nature of the molecules that are being adsorbed on MOFs. In general, different molecules with various degrees of polarity need to be investigated

to productively recover CO<sub>2</sub> in mixed-gas streams, particularly those with a substantial water content. Yu and Balbuena [385] evaluated water effects on post-combustion CO<sub>2</sub> capture in MOFs by using a combination of grand canonical Monte Carlo (GCMC) and DFT simulations. Their findings indicated that the presence of water molecules linked to coordinatively unsaturated metal sites (CUMs) reduces the CO<sub>2</sub> adsorption capacity of MOFs. This resulted from a decrease in the binding energy between CO<sub>2</sub> and the water-coordinated MOFs. Simultaneously, it was revealed that the CUMs in MOFs are critical for their CO<sub>2</sub> uptake in realistic streams that incorporate water and other contaminants. Nevertheless, these data are especially noteworthy in light of the recovery of carbon dioxide in multicomponent gas mixtures.

In summary, MOFs are potentially extremely interesting innovation for large-scale commercialization of CO<sub>2</sub> adsorbent materials. Unfortunately, there are several drawbacks associated with MOFs that need to be addressed in order to facilitate their scalability and enhance technological maturity. Aniruddha et al. [386] in their review on utilization of MOFs in CO<sub>2</sub> capture, highlighted several important aspects, including difficulty in large-scale synthesis (majority of synthesis techniques are suitable for small-scale and laboratory experiments), lack of thermal stability (enhancing it through manipulation of MOFs morphology is crucial), excessive attraction of moisture (total disintegration of the crystalline structure), further study to increase the desorption temperature and the spontaneity of the CO<sub>2</sub> adsorption, or development of parameters for screening MOFs. The other barriers are related to high cost on an industrial scale, low selectivity of CO<sub>2</sub>/N<sub>2</sub>, poor chemical, mechanical, and hydrothermal stability. These challenges still persist for their application under humid conditions [387]. Furthermore, to assess their virtues and demerits, metrics such as cyclic stability, regenerability, and kinetics must be evaluated under real/harsh operating conditions. Therefore, as stated by Youmas et al. [355], integrating the economics of the manufacturing process with the molecular-level properties of MOFs is essential path to create materials that are technically viable as well as commercially successful.

Table 12 provides a comprehensive analysis of the impact of modification strategies on the textural properties and CO<sub>2</sub> uptake of various metal-organic frameworks.

### 3.4. Polymers

#### 3.4.1. Porous organic polymers (POPs)

Porous organic polymers (POPs) constitute an emerging class of porous materials, composed of lightweight components linked by robust covalent bonds. They have showcased significant potential across various applications, including gas storage and separation [409,410]. Several classes of POPs have been developed, including conjugated microporous polymers (CMPs), covalent organic frameworks (COFs), hyper-crosslinked polymers (HCPs), covalent triazine frameworks (CTFs), porous aromatic frameworks (PAFs), and polymers of intrinsic microporosity (PIMs), presented schematically in Fig. 23. In the context of widespread utilization for CO<sub>2</sub> capture, three fundamental groups of POPs can be highlighted, such as CMPs, COFs, and HCPs.

POPs exhibit a combination of advantageous characteristics, including low density, extensive surface areas, adjustable pore sizes with numerous channels, and abundant active sites available for chemical reactions. They also offer easily customizable functionality, exceptional physicochemical stability, and a wide array of design options and synthetic approaches (Fig. 24). Hence, POPs have arisen as highly promising CO<sub>2</sub> capture materials [411–416]. Typically, diverse network reactions are employed in the preparation of each type of POPs. With the sole exception of CTFs and COFs,

which stand as crystalline materials featuring ordered structures formed under thermodynamic control, all other POPs show an amorphous nature [417,418].

Until recently, considerable endeavors have been dedicated to formulating and creating high-performance POPs adsorbents, yielding promising outcomes. According to the latest reviews published between 2017 and 2022 by Mohamed et al. [416], Gao et al. [421], Bhanja et al. [422], and Wang et al. [423], the key research fields for improving the CO<sub>2</sub> capture properties of POPs can be characterized as follows: (1) increasing the CO<sub>2</sub> adsorption capacity of materials, (2) enhancing CO<sub>2</sub>/N<sub>2</sub> selectivity, and (3) considerations the real application conditions. The all authors highlighted that mainly, due to the micropore filling process, large specific surface areas [424,425] and appropriate micropore sizes [426,427] are considered as influential factors with regard to CO<sub>2</sub> uptake and selectivity. Alternatively, the metal sites [428,429] and the morphology of POPs have been reported to be important determinants that impact CO<sub>2</sub> storage process. Therefore, some aspects of the above properties should be investigated further. The creation of 3D POPs with a large surface is one of them [426]. This strategy could allow modification of POPs to occur while still retaining a part of the BET surface area. Secondly, it's advisable to employ post-synthesis conditions that are milder and more efficient. This approach can incorporate the functional moiety while preserving the porous structure of POPs. Furthermore, enhancing the affinity between CO<sub>2</sub> and the material surface can be achieved through the introduction of heteroatoms (N, O, S, F) or the integration of functional groups (–NH<sub>2</sub>, –OH) within POPs. This can be realized by using diverse monomers or implementing post-functionalization techniques. Unfortunately, the insertion of functional groups could potentially diminish the CO<sub>2</sub> capture efficiency of POPs. This could occur due to the added volume of functional groups obstructing the available pore space or leading to an increase in the density of porous polymers, among other possible factors. Diverse strategies can be applied to address these challenges. These include utilizing low-density functional groups, controlling pore sizes to enhance CO<sub>2</sub> surface interaction, and expanding the specific surface area of polymers [416,421–423].

In the case of industrial application, the subsequent aspects have been examined and continue to pose challenges, especially within post-combustion capture technology. Those issues involve CO<sub>2</sub> capture performance at high temperatures and low pressures (developing POPs with multiple adsorption sites for binding CO<sub>2</sub> molecules), material stability in the presence of moisture and at high temperatures, cost-effectiveness and scalability (investigating novel synthesis techniques that use non-noble metal catalysts, low-cost monomers, and mild reactions) [421,423].

Fig. 25 illustrates a comparison of modification strategies applied to POPs in relation to various ongoing research trends.

#### 3.4.1.1. Conjugated microporous polymers (CMPs).

Conjugated microporous polymers are three-dimensional semiconducting polymers in which rigid aromatic groups are connected together, either through direct bonds or double or triple bonds, to form π-conjugated microporous structure [430]. Due to molecular rigidity and expansion of their conjugated parts, creating the inherent porous characteristics, they aroused great interest [431]. The CMPs can be synthesized by a wide range of synthetic building blocks and enormously different synthesis routes, such as Sonogashira-Hagihara coupling reaction, Suzuki-Miyaura reaction, Yamamoto reaction or Heck reaction [432]. This diversity results in CMPs having distinctive properties, different structures with unique skeleton, and highly modifiable nature.

Numerous CMPs have been developed in recent years to optimize CO<sub>2</sub> capture by various research approaches, e.g., tailoring

**Table 12**Influence of modification strategies on textural properties and CO<sub>2</sub> uptake of metal-organic frameworks.

Metal-organic frameworks (MOFs)	BET surface area, m <sup>2</sup> /g	Total pore volume, cm <sup>3</sup> /g	CO <sub>2</sub> selectivity at 1 bar	CO <sub>2</sub> uptake, mmol/g	Adsorption temperature, °C	Adsorption pressure, bar	Reported modification	Purpose of modification method	Reference
Zn(ADC)(4,4'-Bpe)0.5'xG	100	—	—	5.8	−78.15	1	Novel structures	Tuning the micropores by triple-framework interpenetration	[370]
Cu(FMA)(4,4'-Bpe)0.5	—	—	—	4.41	−78.15	1.0	Novel structures		[371]
PCN-5	225 (Langmuir)	0.13	—	4.80	−78.15	1.0	Novel structures		[388]
Flexible microporous MOF	—	—	116.00	1.11	25	1	Novel structures	Increasing high selectivity in capturing and separating CO <sub>2</sub> from a gas mixture	[372]
3D MOF (UPC-21)	1117	—	34.30	3.87	0	1	Novel structures	Improving CO <sub>2</sub> adsorption selectivity	[389]
UTSA-120 [Cu(dpt) <sub>2</sub> (SiF <sub>6</sub> )] <sub>n</sub>	638	—	~600.00	3.56	23	0.15	Novel structures; Functionalizing pore surface	Tuning the pore size; Enhancing the interaction strength between CO <sub>2</sub> and MOFs surface	[373]
2D MOF	340.8	—	—	1.9	25	1	Novel structures; Functionalizing pore surface	Obtaining thermal stability and moisture resistance; Increasing CO <sub>2</sub> affinity	[390]
Dehydrated-MIL-53 (Cr)	—	—	—	8.5	30.85	20	Adsorption conditions	Influence of hydration on the adsorption capacity and selectivity	[384]
Hydrated-MIL-53(Cr)	—	—	—	7.7	30.85	20	(moisture effect)		[384]
Hydrated 6.5 wt%‐Mg‐MOF‐74	—	—	~110	6.18	25	1			[385]
Hydrated 13 wt%‐Mg‐MOF‐74	—	—	~130	4.73	25	1			[385]
MOF-177 [Zn <sub>4</sub> O(BTB) <sub>2</sub> ]	4508	—	—	33.5	25	35	Adsorption conditions	Influence of room temperature and high pressure on CO <sub>2</sub> capacity (isotherms analysis)	[391]
IRMOF-1 [Zn <sub>4</sub> O(BDC) <sub>3</sub> ]	2833	—	—	21.79	25	30	(temperature and pressure effect)		[391]
IRMOF-6 [Zn <sub>4</sub> O(C <sub>2</sub> H <sub>4</sub> :BDC) <sub>3</sub> ]	2516	—	—	19.45	25	30			[391]
IRMOF-3 [Zn <sub>4</sub> O(NH <sub>2</sub> BDC) <sub>3</sub> ]	2160	—	—	18.70	25	30			[391]
IRMOF-11 [Zn <sub>4</sub> O(HPDC) <sub>3</sub> ]	2096	—	—	14.73	25	30			[391]
Cu <sub>3</sub> (BTC) <sub>2</sub> [Zn <sub>4</sub> O(HPDC) <sub>3</sub> ]	1781	—	—	10.62	25	30			[391]
MOF-74 [Zn <sub>2</sub> (DHBDC)]	816	—	—	10.41	25	30			[391]
MOF-505 [Cu <sub>2</sub> (BPTC)]	1547	—	—	10.21	25	30			[391]
MOF-2 [Zn <sub>2</sub> (BDC) <sub>2</sub> ]	345	—	—	3.22	25	30			[391]
MIL-53(Al)	—	—	—	10.53	30.85	30	Metal ions doping	Improving the surface area, pore volume; Creating rich adsorptive sites for CO <sub>2</sub> adsorption	[392]
MIL-53(Cr)	—	—	—	10.04	30.85	25			[392]
[Ni <sub>6</sub> (OH) <sub>4</sub> (BTB) <sub>8/3</sub> (H <sub>2</sub> O) <sub>6</sub> ·4H <sub>2</sub> O·9DMF] <sub>n</sub>	819.3	—	—	1.3	25	1			[393]
Li-HKUST-1	985.8	0.46	—	7.89	25	18			[394]
Na-HKUST-1	1006	0.45	—	8.11	25	18			[394]
K-HKUST-1	1189	0.52	—	8.64	25	18			[394]
Cu <sub>3</sub> (BTC) <sub>2</sub>	1734	—	—	2.94	42	1.1	Metal ions doping; Improving activation procedures and syntheses	Improving the surface area, pore volume, and CO <sub>2</sub> affinity towards MOFs surface	[395]
Cr <sub>3</sub> (BTC) <sub>2</sub>	1689	—	—	1.82	42	1.1			[395]
Ni <sub>3</sub> (BTC) <sub>2</sub> (DMF) <sub>2</sub> (H <sub>2</sub> O)	847	—	—	2.32	42	1.1			[395]
Mo <sub>3</sub> (BTC) <sub>2</sub> (DMF) <sub>0.5</sub>	1689	—	—	1.82	42	1.1			[395]
[Ru <sub>3</sub> (BTC) <sub>2</sub> ][BTC] <sub>0.5</sub>	1180	—	—	2.46	42	1.1			[395]
SNU-110'	411	0.248	35.00	0.58	25	1	Synthesis modification (selecting or modifying organic linker)	Improving the selectivity over H <sub>2</sub> , N <sub>2</sub> , CH <sub>4</sub>	[396]
Noninterpenetrated-SNU-70'	5290	2.17	—	0.80	25	1		Improving a pore size, surface area, and CO <sub>2</sub> uptake	[397]
Interpenetrated-SNU-71'	1770	0.709	—	1.05	25	1			[397]
MOF-505 [JNU-Bai12]	3038	—	24.60	19.85	25	20		Improving the specific surface area and pore volume	[398]
MOF-177	4500	1.89	—	35.23	25	50		Developing ultrahigh porosity	[366]
MOF-210	6240	3.60	—	65.23	25	80			[366]
NU-100	6143	2.82	—	52.61	25	40		Improving surface area	[367]
PCN-68	5109	2.13	—	41.00	25	100			[399]
ZNJU-43a	2243	0.8943	—	4.60	25	1	Synthesis modification (selecting or modifying organic linker); Creating Lewis basic sites	Increasing basicity, affinity between CO <sub>2</sub> molecules-adsorbent surface	[375]
PCN-124	1372	0.579	—	5.01	22	1	Synthesis modification (selecting or modifying organic linker); Metal site modification; Functionalizing pore surface	Improving the micro-porosity, and the selectivity over CH <sub>4</sub>	[400]

SNU-31'	704	0.28	—	0.59	25	1.0	Synthesis modification (selecting or modifying organic linker); Functionalizing pore surface	Improving the selectivity over H <sub>2</sub> , O <sub>2</sub> , N <sub>2</sub> , CH <sub>4</sub>	[401]
UPC-105	2082	—	2.50	2.37	25	1		Optimization of the pore environment for enhanced C <sub>2</sub> H <sub>2</sub> /CO <sub>2</sub> storage and separation performances	[374]
UPC-106	1984		2.49	2.42	25	1			[374]
UPC-107	1865		2.56	2.06	25	1			[374]
UPC-108	1837	—	2.84	2.04	25	1			[374]
UPC-109	1601	—	2.71	1.08	25	1			[374]
UPC-110	1384	—	5.10	1.08	25	1			[374]
UPC-111	1732	—	2.56	1.88	25	1			[374]
UPC-112	1559	—	2.76	1.83	25	1			[374]
pt-Uio-66(Zr)(OH) <sub>2</sub>	1230	—	105.00	5.63	25	1	New synthesis approach	Improving a pore size, surface area, CO <sub>2</sub> uptake, selectivity over H <sub>2</sub> , N <sub>2</sub> , CH <sub>4</sub>	[402]
amino-MIL-53	400	1.03	42.30	2.16 1.88	0 23	1	Amine functionalization	Increasing basicity, affinity between CO <sub>2</sub> molecules-adsorbent surface and level-up N-contents	[403]
amino-MIL-53-dimethylformamide/ethanol	356	0.71	637.00	2.98 2.01	0 23	1	Amine functionalization; New synthesis approach	Increasing basicity, affinity between CO <sub>2</sub> molecules-adsorbent surface; Enhancing CO <sub>2</sub> adsorption and selectivity of CO <sub>2</sub> /N <sub>2</sub>	[403]
amino-MIL-53-dimethylformamide/ethanol/acetic acid	321	0.65	637.00	2.42 1.81	0 23	1			[403]
amino-MIL-53-dimethylformamide/methanol	348	0.51	153.00	3.17 2.10	0 23	1			[403]
amino-MIL-53-dimethylformamide/methanol/acetic acid	632	0.33	42.30	3.35	0	1			[403]
TEPA-HKUST-1	327	0.25	—	0.225	45	0.15	Amine functionalization (Tetraethylenepentamine)	Increasing basicity, affinity between CO <sub>2</sub> molecules-adsorbent surface and level-up N-contents	[404]
TEPA- MIL-53 (Al)	286	0.30	—	0.159	45	0.15			[404]
TEPA- ZIF-8	9	0.01	—	1.52	45	0.15			[404]
ZJNU-13	1352	0.502	5.76	3.92	25	1	Oxygen atoms functionalization	Increasing separation and purification with high adsorptivity and impressive selectivity	[405]
dmpn-Mg <sub>2</sub> (dobpdc)	948	—	—	2.42	40	1	Diamine functionalization (2,2-dimethyl-1,3-diaminopropane)(dmpn) N-oxide groups functionalization	Increasing basicity, and affinity between CO <sub>2</sub> molecules-adsorbent surface	[406]
ZNJU-19	2165	0.882	6.40	4.75	25	1		Increasing affinity between CO <sub>2</sub> molecules-adsorbent surface;	[376]
ZNJU-20	2154	0.902	6.20	4.63	25	1		Enhancing CO <sub>2</sub> /CH <sub>4</sub> separations	[376]
SNU-77H	3670	1.52	—	0.89	25	1	Different activation method approaches (high temperature evacuation)	Discarding unreacted precursors and solvents from synthesized MOFs	[407]
HCM-Cu <sub>3</sub> (BTC) <sub>2</sub> /Hierarchical porous carbon monoliths	516	0.26	10.60	2.75	25	1	MOF incorporation in hierarchical porous carbon monoliths	Composite/hybrid materials formation	[379]
MIL-101(Cr)/Activated carbon (type Maxsorb-III)	2670	1.27	—	7.14	27	5	Activated carbon incorporated in MOF		[378]
MIL-101(Cr)/MCM-41	2843	1.30	8.53	2.09	25	1	MCM-41 as the structure-directing agent for MOF		[380]
MIL-101(Cr)/MIL-53(Al)	1746	0.80	59.34	16	25	40	Hybrids of nanoporous MOFs synthetization		[408]

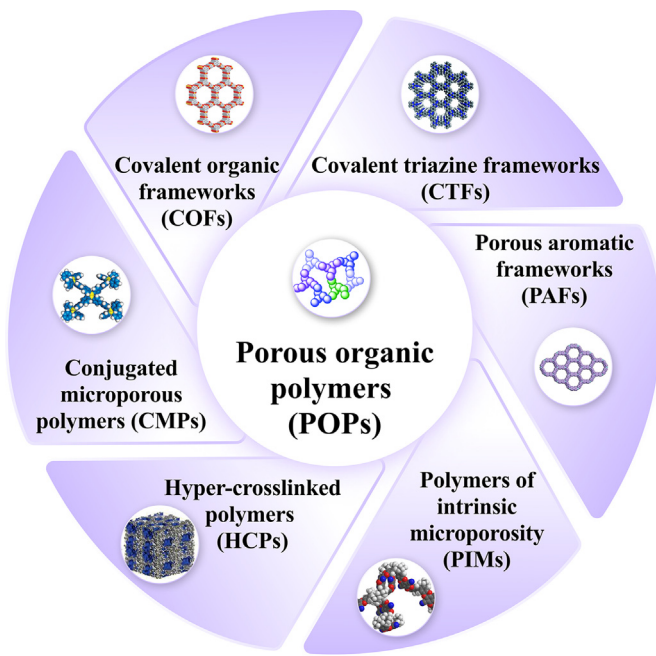


**Fig. 23.** Classification of different types of porous organic polymers for  $\text{CO}_2$  capture application.

size and shape of the pores [433–436], incorporation of functional groups [437–440], introduction of heteroatoms into the skeleton [441,442], and metal functionalization [413]. Due to that, CMPs can be customized for utilization across a diverse spectrum of  $\text{CO}_2$  capture applications, owing to the wide range of variability in the selection and design of components, as well as the control over other characteristics. Jiang et al. [443] showed that, the surface area and pore size can be regulated by the monomer structure of the network. In addition, these features may be fine-tuned in a continuous way by copolymerization of monomers with varying lengths. This provides an unparalleled level of direct synthetic control over micropore characteristics in an organic network.

CMPs also encounter many challenges that need resolutions, Gao et al. [421] in their review highlighted that one of the most significant considerations for the future involves discovering cost-effective synthesis methods, attributed to the difficulties of scalability. Other issues relate achieving a high surface area, which

remains an ongoing obstacle in synthetic chemistry because of the complicated creation process of the porous morphology. Newly, Liu et al. [444] improved  $\text{CO}_2$  adsorption capacity by developing a simple post-knitting process to enhance the surface area. The obtained CMPs had a high Brunauer–Emmett–Teller surface area and total pore volume up to  $2267 \text{ m}^2/\text{g}$  and  $3.27 \text{ cm}^3/\text{g}$ , respectively, which was 2.3 and 8.8 times greater than that of the precursors. These CMPs demonstrated significant  $\text{CO}_2$  uptake improvements, achieving  $3.98 \text{ mmol/g}$  at 1 bar and  $0^\circ\text{C}$ . Moreover, it has been reported that non-functionalized microporous organic polymers (MOPs) typically exhibit a significantly low  $\text{CO}_2$  uptake at ambient temperatures and pressures. This is due to their low  $\text{CO}_2$  adsorption enthalpies resulting from the absence of robust  $\text{CO}_2$  binding sites. To accomplish high-performance  $\text{CO}_2$  capture, novel MOPs with rationally modified skeletons and varied functionalities are desirable. Zhang et al. [445] used sulfone and hydroxyl groups as functionalities in a synthesis of biofunctionalized CMPs via palladium-catalyzed Sonogashira-Hagihara cross-coupling reaction. The synthesized polymers showed a significant BET surface area up to  $1470 \text{ m}^2/\text{g}$ , along with a carbon dioxide uptake of  $2.77 \text{ mmol/g}$  at  $0^\circ\text{C}$  and 1.13 bar. Likewise, Wang et al. [446] proposed to use thiophene as a base for two novel CMPs. The obtained adsorbents displayed good physicochemical stability and outstanding  $\text{CO}_2$  adsorption capacity ( $14.73 \text{ mmol/g}$  at 50 bar and  $44.85^\circ\text{C}$ ).

**Fig. 26** provides a current overview of the recent modification strategies and research trends for CMPs. The  $\text{CO}_2$  uptake and textural properties of CMPs associated with distinct methodologies are summarized in **Table 13**, providing a comprehensive overview of the data.

**3.4.1.2. Covalent organic frameworks (COFs).** Covalent organic frameworks are synthesized based on the principles of reticular chemistry, where organic building blocks with pre-designed geometries and radicals are connected through the formation of covalent bonds to produce extended networks [451]. Fine regulation pore sizes, shapes with specific distribution, alongside achieving low density and precise control of skeleton structure, emerge as the most attractive characteristics of COFs for  $\text{CO}_2$  adsorption. This distinction is particularly apparent when comparing COFs with crystalline structures to their amorphous counterparts [452]. Recent findings suggested that materials featuring pore sizes close to the kinetic radius of  $\text{CO}_2$  tend to exhibit notable  $\text{CO}_2$  uptake [423], emphasizing the effectiveness of COFs with precisely controlled pore sizes as promising  $\text{CO}_2$  capture materials [453].

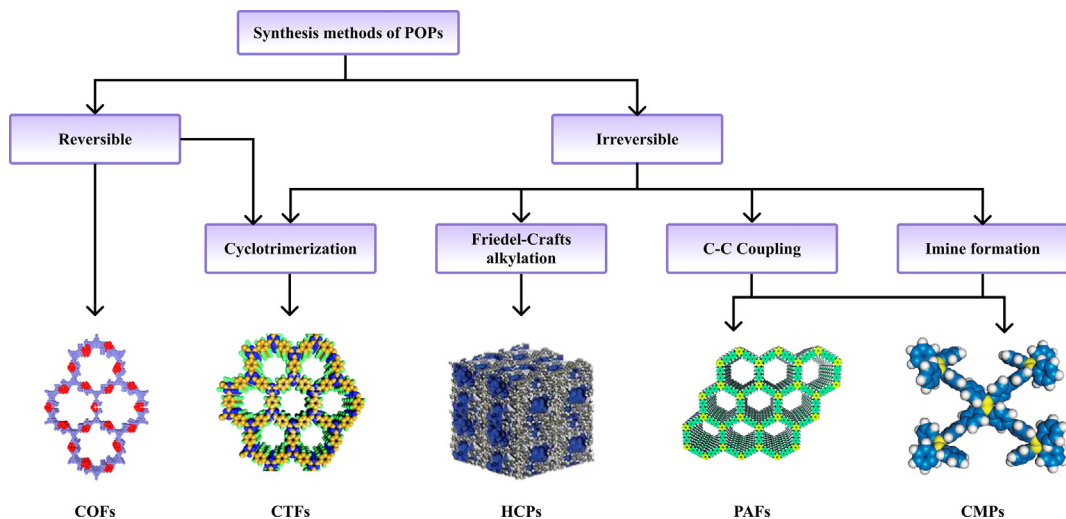


**Fig. 24.** Synthetic methodologies widely used for the preparation of POPs [419,420].

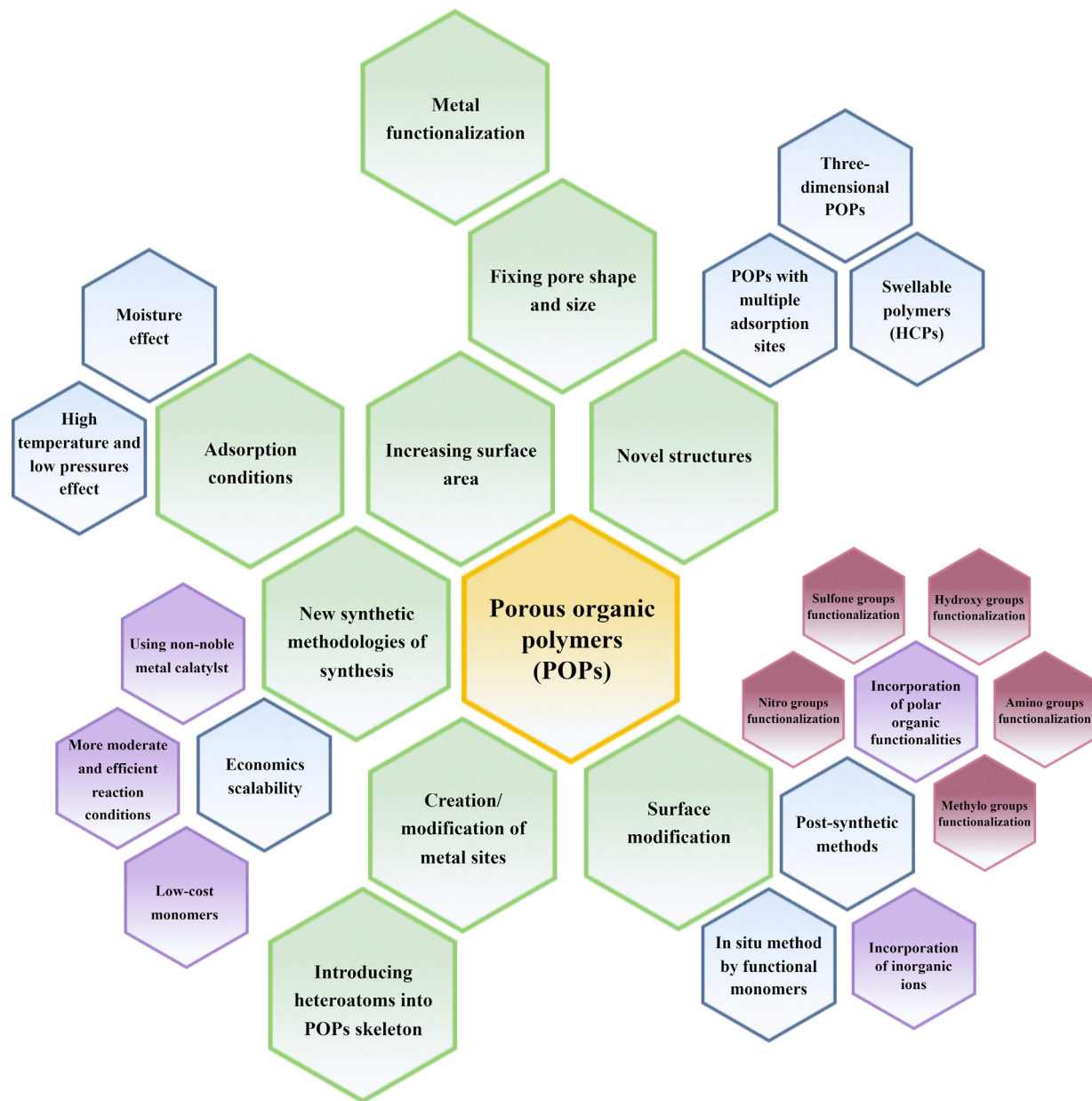


**Fig. 25.** The modification strategies and research directions of porous organic polymers.

Similar conclusions were drawn by Furukawa and Yaghi [454], demonstrating that COFs hold an advantageous standing in comparison to common carbon-based materials, zeolites, and MOFs. This positions COFs firmly within the category of valuable porous materials and highlights their efficacy as effective CO<sub>2</sub> adsorbents.

A significant number of ongoing research concern the exploration for innovative COFs through diverse different synthetic methods, aiming to capture CO<sub>2</sub> from a variety of sources and transform it to valuable products. These applications involve CO<sub>2</sub> fixation to epoxides for cyclic carbonate synthesis and CO<sub>2</sub> reduction to CO [455]. Additionally, it is very desirable to combine the criteria for high crystallinity, robust stability, and increasing porosity with the requirements for high specific surface area and small pore size for gas storage. In consequences, the precise regulation of control of internal pore structure becomes crucial for COFs. Considering these trends, Tian et al. [456] managed to develop a strategy to construct heteropores COFs. These COFs with

heteropores possessed two kinds of micropores characterized by varying shapes and sizes, with one being a quadrangle and the other an inequilateral hexagon. They exhibited favorable adsorption capacities for CO<sub>2</sub> and H<sub>2</sub>, with CO<sub>2</sub> uptake reaching up to 19.8 wt% (0 °C, 1 bar), positioning them as one of the top-performing COFs for CO<sub>2</sub> capture.

An alternative approach for developing COFs is the functionalization of pore surfaces, specifically through channel wall functionalization. This can be achieved by incorporating chemical moieties, such as polar functional groups [457], immobilizing ionic liquids or introducing specific special active sites into polymer networks [458], such as heteroatoms [459], charged units [460] and unsaturated metal sites [461]. The objective of these modifications is to enhance the affinity between the material surface and CO<sub>2</sub>.

Huang et al. [457] reported a strategy for converting a conventional 2D COF into an outstanding platform for carbon dioxide capture through channel-wall functionalization. Through the

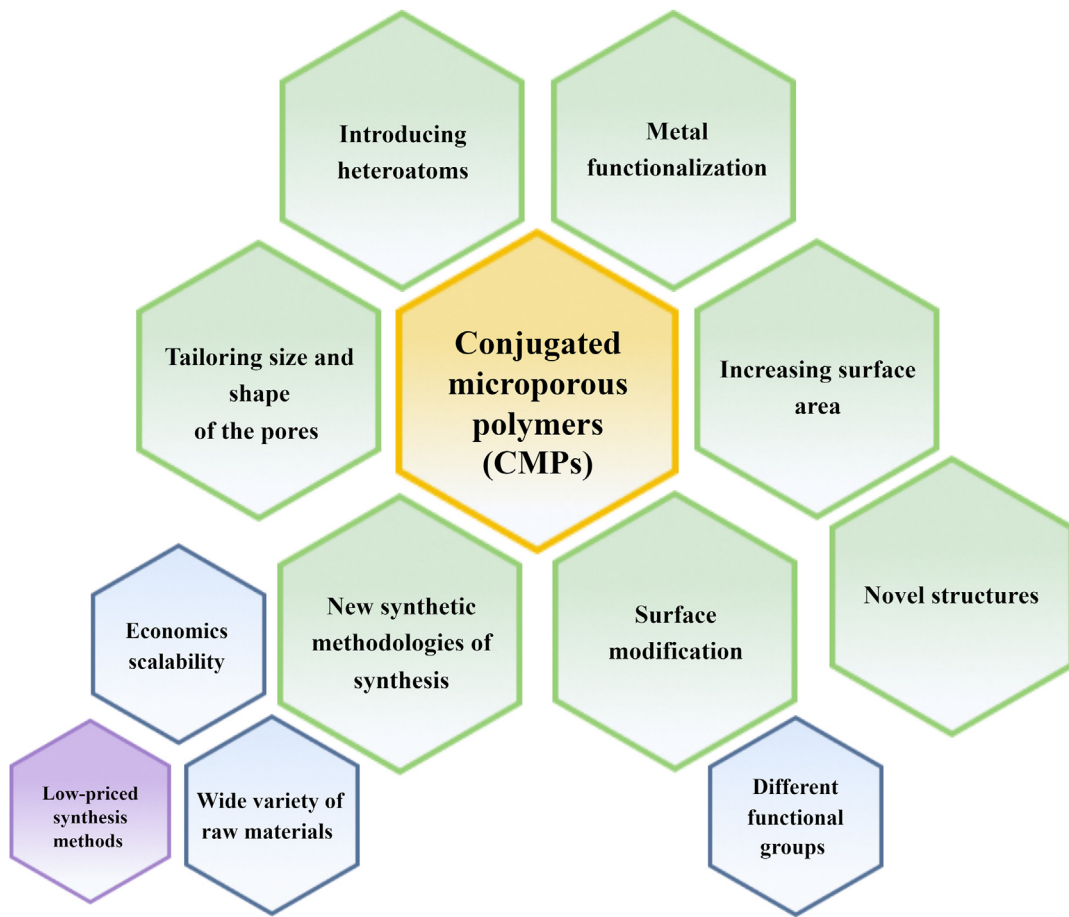


**Fig. 26.** The modification strategies and research directions of conjugated microporous polymers.

adoption of a dense layer structure, the integration of carboxylic-acid groups onto the channel walls was successfully achieved, leading to the emergence of an advanced version of COF with enhanced  $\text{CO}_2$  uptake, reusability, selectivity, and separation productivity for flue gas treatment. The results indicated that channel-wall functionalization effectively transformed typical COFs into  $\text{CO}_2$  adsorption materials with exceptional performance.

Dong et al. [458] presented immobilization of ionic liquid on the channel walls of COF using a post-synthetic strategy. According to authors, the ionic COF exhibited an excellent  $\text{CO}_2$  adsorption capacity of 3.74 mmol/g (1 bar, 0 °C) and was very stable. Furthermore, it has been established as an efficient heterogeneous catalyst for the transformation of  $\text{CO}_2$  into high-value-added formamides under ambient conditions.

Buyukcakir et al. [460] developed and synthesized the first charged covalent triazine frameworks (CTFs) with temperature-dependent surface area and hierarchical porosity by incorporation of ionic functional moieties. The ionic character of CTFs, in addition to their large surface area, thermal and chemical durability, resulted in considerable increases in  $\text{CO}_2$  adsorption capacity, due to the extra electrostatic interactions between  $\text{CO}_2$  molecules and charge centers of viologen units. The resulting CTFs showed high BET surface area up to 1247 m<sup>2</sup>/g and  $\text{CO}_2$  uptake approximately around 3.02 mmol/g at 1 bar and 0 °C.

Liu et al. [462] constructed the triazine-based COF (highly heteroatom-functionalized COF) with a 2D structure by the condensation reaction. The adsorbent exhibited a notable level of crystallinity, along with remarkable chemical and thermal stabilities. The BET surface area and a pore volume measured 1407 m<sup>2</sup>/g

and 0.97 cm<sup>3</sup>/g, respectively. The resulting COF demonstrated a selectivity value of 19, indicating its ability for moderately selective  $\text{CO}_2/\text{N}_2$  adsorption, with a  $\text{CO}_2$  uptake of 1.71 mmol/g.

Collectively, these data indicate that it is imperative to dedicate substantial resources towards investigating the synthesis and characterization of COFs. This research should aim to integrate the desirable attributes of stability, crystallinity, and porosity in COFs, with the ultimate goal of optimizing their efficacy as  $\text{CO}_2$  capture materials. Furthermore, considering the analysis of various reviews about COFs, it is possible to provide supplementary objectives for enhancing this category of POPs. Olajire et al. [463] used a wide range of sources to present an in-depth look of potential research paths for COFs. According to the author, research endeavors should be concentrated on the following areas, such as the exploration of novel synthetic methodologies, 3D COFs construction, improving the synthesis parameters of COFs and scaling them for commercial applications, constructing hybrid membranes based on COFs, and conducting experiments on separation of  $\text{CO}_2$  from other gases in flue gas streams. In addition, Gao et al. [421] highlighted an additional significant challenge, which involves synthesizing COFs with high  $\text{CO}_2$  uptake under humid conditions.

**Fig. 27** presents the current status of modification strategies and research directions for COFs. **Table 14** offers an overview of  $\text{CO}_2$  uptake and textural properties exhibited by COFs in relation to specific modification strategies.

**3.4.1.3. Hyper-crosslinked polymers (HCPs).** Hyper-crosslinked polymers are commonly synthesized from a wide range of low-cost monomers and electrophiles that serve as cross-linking agents. The

**Table 13**Influence of modification strategies on textural properties and CO<sub>2</sub> uptake of conjugated microporous polymers.

Conjugated microporous polymer	BET surface area, m <sup>2</sup> /g	Average pore size, nm	Total pore volume, cm <sup>3</sup> /g	Micropore volume, cm <sup>3</sup> /g	V <sub>mic</sub> /V <sub>tot</sub> , %	CO <sub>2</sub> selectivity at 1 bar	CO <sub>2</sub> uptake, mmol/g	Adsorption temperature, °C	Pressure, bar	Reported modification	Purpose of modification method	Reference
CMP@1	346	—	0.22	—	—	—	1.52 1.03	0 25	1	New synthetic methodologies of synthesis (imidization reaction)	Novel structures	[447]
CMP@2	325	—	0.60	—	—	—	2.28 1.47	0 25	1			[447]
CMP@3	343	—	0.70	—	—	—	1.43 0.71	0 25	1			[447]
BTCMP-1	4.37	—	0.0046	—	—	—	14.73	44.85	50	New synthetic methodologies of synthesis (cross-coupling polycondensation)		[446]
BTCMP-2	5.13	—	0.0019	—	—	—	6.57	44.85	50			[446]
CMP	772	—	1.21	0.117	9.7	—	1.61	25	1	Metal functionalization (Co, Al)	Creating rich adsorptive sites for CO <sub>2</sub> adsorption	[413]
Co-CMP	965	—	2.81	0.419	14.9	—	1.80	25	1			[413]
Al-CMP	798	—	1.41	0.298	21.1	—	1.74	25	1			[413]
ZnP-50%F-CMPs	240	—	0.376	—	—	—	2.05	25	1	Introduction of chemical functionalities (fluoride functionalization)	Increasing affinity between CO <sub>2</sub> molecules-adsorbent surface	[448]
BFCMP-1	1316	—	1.20	0.31	25.83	31.90	2.45 1.39	0 25	1.13	Introduction of chemical functionalities (sulfone and —OH groups)		[445]
BFCMP-2	1470	—	1.35	0.29	21.48	29.60	2.77 1.64	0 25	1.13			[445]
CMP-1	837	—	0.45	0.32	71	—	1.18	25	1	Introduction of chemical functionalities (carboxylic acids, amines, hydroxyl groups, and methyl groups)		[438]
CMP-1-COOH	522	—	0.30	0.22	73	—	1.60	25	1			[438]
CMP-1-NH <sub>2</sub>	710	—	0.39	0.27	69	—	—	—	—			[438]
CMP-1-(CH <sub>3</sub> ) <sub>2</sub>	899	—	0.75	0.34	45	—	0.94	25	1			[438]
CMP-1-(OH) <sub>2</sub>	1043	—	0.71	0.40	56	—	1.07	25	1			[438]
NCMP-2	900	—	0.55	0.32	58.18	10.50	2.10 1.15	0 25	1	Introduction of heteroatoms (N)		[449,450]
TPA-BD-CMP	543	—	1.11	—	—	—	3.25	0	1			[441]
TCMP-0	963	—	0.98	0.38	39	9.60	2.38 1.34	0 25	1	Synthetic control of the micropore size and surface area;	Improving the pore and surface properties; Increasing affinity between CO <sub>2</sub> molecules-adsorbent surface	[450]
TNCMP-2	995	—	0.55	0.30	73	7.60	2.62 1.45	0 25	1	Introduction of chemical functionalities into CMPs skeleton (nitrogen-rich triazine units)		[450]
TCMP-3	961	—	0.36	0.28	78	25.20	2.25 1.26	0 25	1			[450]
TCMP-5	494	—	0.51	0.19	37	17.00	0.37 1.22	0 25	1			[450]
CMP-0	1018	—	0.56	0.38	67.86	—	2.10 1.21	0 25	1	Synthetic control of the micropore size and surface area	Improving the pore and surface properties to promote the interaction with CO <sub>2</sub>	[443]
CMP-3	522	—	0.26	0.18	69	—	1.22 0.68	0 25	1			[443]
CMP-5	512	—	0.47	0.16	34	—	1.11 0.63	0 25	1			[443]
KCMP-F1	1433	2.9	1.04	0.32	30.8	—	0.58 2.70	0	0.15	Synthetic control of the micropore size and surface area		[444]
KCMP-M1	1845	3.6	1.66	0.35	21.1	—	0.88 3.77	0	0.15			[444]
KCMP-F2	1632	5.1	2.08	0.34	16.3	—	0.86 3.51	0	0.15			[444]
KCMP-M2	2267	5.3	3.00	0.31	10.3	—	0.80 3.69	0	0.15			[444]
KCMP-F3	494	5.1	0.64	0.12	18.8	—	0.42 1.59	0	0.15			[444]
KCMP-M3	1321	3.6	1.20	0.30	25.0	29.10	0.97 3.61	0	0.15			[444]
KCMP-F4	1245	6.9	2.16	0.20	9.3	—	0.46 2.14	0	0.15			[444]
KCMP-M4	2157	6.1	3.27	0.34	10.4	—	0.90	0	0.15			[444]

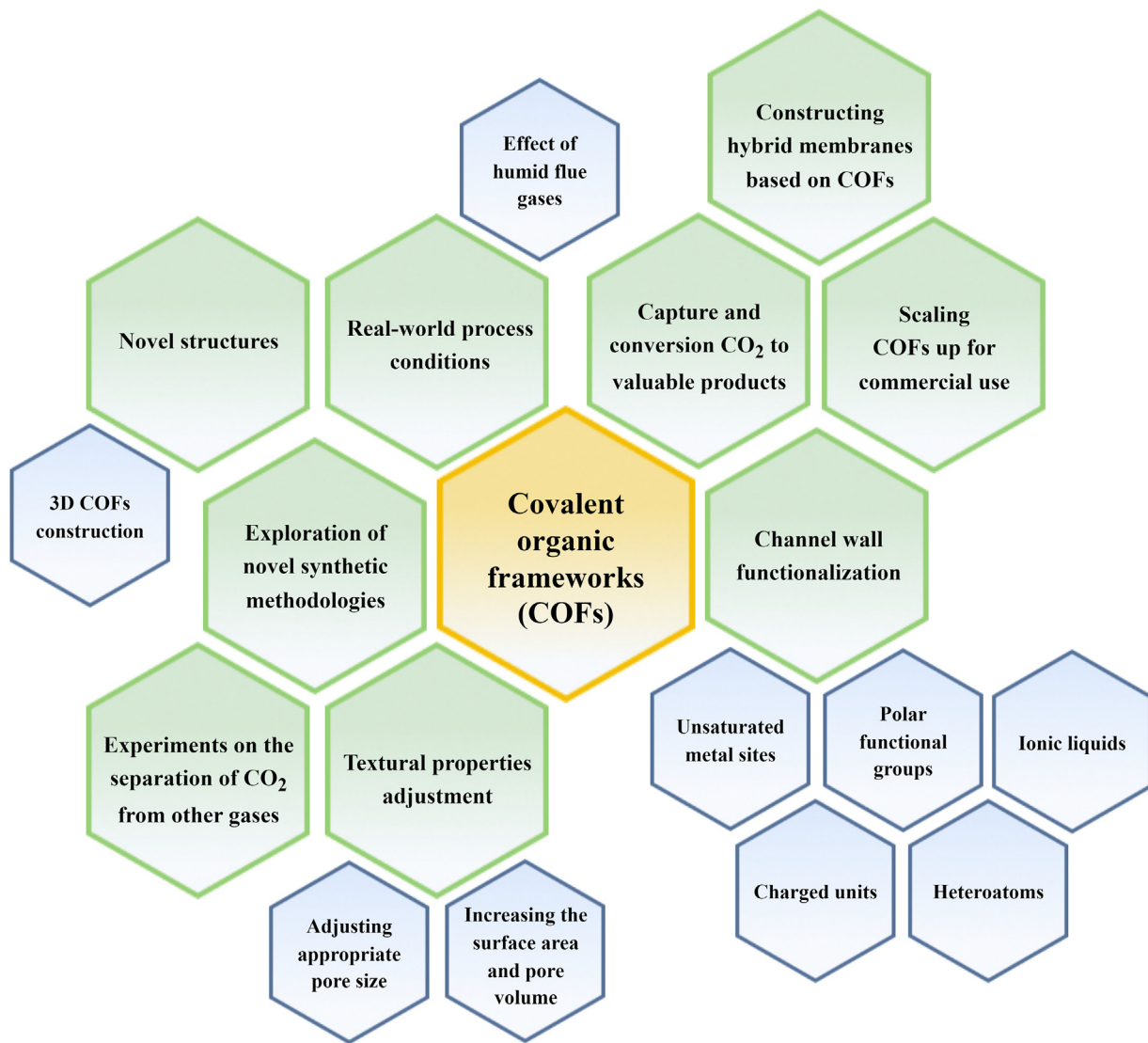


**Fig. 27.** The modification strategies and research directions of covalent organic frameworks.

Friedel-Crafts alkylation reaction, employed in the production of HCPs, allows the attainment of desired properties without necessitating the use of precious metal coupling catalysts [467]. Moreover, a variety of precursors has been used in the synthesis process of HCPs. A noticeable trend is observed in repurposing waste materials [468], including biomass-based aromatic compounds [469]. That is closely related to the broad adaptability of monomers, and the processability of their structures. For example, Fu et al. [468] proposed a facile strategy for synthesizing HCPs using expanded polystyrene foam. The HCPs that were produced exhibited high specific surface areas and excellent thermal stability. At 0 °C and 1.13 bar, HCP demonstrated the maximum CO<sub>2</sub> adsorption capacity, reaching 1.987 mmol/g, along with the highest adsorption selectivity ratio (CO<sub>2</sub> over N<sub>2</sub>) of 23.4. Additionally, Fayemiwo et al. [470] used monomers for the environmentally friendly fabrication of HCPs using hydrocarbons sourced from fossil fuels.

Compared to other types of microporous polymers, HCPs offer a straightforward synthesis procedure, a diverse selection of monomer sources, and a relatively inexpensive and widely accessible catalyst [471]. One of the most significant advantages of these organic polymers for CO<sub>2</sub> capture is the substantial surface area created through the interconnected aromatic structures. Among

other characteristics, HCPs exhibit robustness and scalability, exceptional thermal stability, outstanding chemical resistance (e.g., to strong acids and bases), and exceptionally facile manufacturing process on a large scale. Nevertheless, a significant challenge encountered by HCPs is associated with their molecular design-based synthesis, requiring carefully control over pore structure [421].

A considerable body of literature has focused on the exploration of strategies to improve CO<sub>2</sub> capture by COFs. The conventional approach adopted to enhance the CO<sub>2</sub> adsorption capacity of these materials involves increasing the specific surface area and modifying the pore size through various synthetic methods. In recent years, studies have shown that HCPs containing active sites can achieve higher CO<sub>2</sub> adsorption capacity while having a smaller specific surface area compared to traditional HCPs. For this reason, several endeavors have been undertaken with the aim of increasing the CO<sub>2</sub> uptake and selectivity of HCPs by the introduction of polar functional groups or heteroatoms (N, O, Si). Fayemiwo et al. [472] synthesized a series of nitrogen-rich, hyper-crosslinked polymers (HCP-MAAMs) through bulk co-polymerization. The polymers were initially functionalized with amide groups and demonstrated a remarkable CO<sub>2</sub>/N<sub>2</sub> selectivity of 104 at ultra-low CO<sub>2</sub> partial

**Table 14**Influence of modification strategies on textural properties and CO<sub>2</sub> uptake of covalent organic frameworks.

Covalent organic frameworks	Covalent bond type	BET surface area, m <sup>2</sup> /g	Total pore volume, cm <sup>3</sup> /g	CO <sub>2</sub> selectivity at 1 bar	CO <sub>2</sub> uptake, mmol/g	Adsorption temperature, °C	Pressure, bar	Reported modification	Purpose of modification method	Reference
SIOC-COF-5	Imine	707	0.59	—	4.5	0	1	Synthetic control of new topological structure	Novel structures	[456]
SIOC-COF-6	Imine	1617	0.92	—	3.2	0	1	Novel synthetic methodologies	Broadening the synthetic scope for making tunable framework structures	[464]
TPE-COF-II	Imine	2168	2.14	—	5.27	0	1		Tuning the porosity, pore volume/size, surface area and increasing number of heteroatom active sites	[459]
COF-JLU2	Azine	410	0.56	77.0	4.93	0	1		Tuning the porosity, pore volume/size, surface area, and functionalization of COFs frameworks	[465]
COF-JLU6	Imine	1450	0.96	—	2.93	0	1		Tuning the porosity, pore volume/size, surface area, and functionalization of COFs frameworks	[465]
COF-JLU7	Imine	1392	1.78	—	3.43	0	1			[458]
ACOF-1	Azine	1176	0.91	—	4.02	0	1		Tuning the porosity, pore volume/size, surface area	[452]
TDCOF-5	Boronate	2497	—	—	2.1	0	1			[466]
[Et <sub>4</sub> NBr]50%-Py-COF	Imine	700	—	—	3.74	0	1	Functionalization of COFs frameworks (immobilization of ionic liquids)	Tuning the pore size, surface area, and increasing affinity between CO <sub>2</sub> molecules-adsorbent surface	[458]
cCTF-500	Triazine	1247	1.04	—	3.02	0	1	Functionalization of COFs frameworks (incorporation of charged units)	Tuning the porosity, and surface area to promote the interaction with CO <sub>2</sub>	[460]
cCTF-450	Triazine	861	0.59	—	1.82	25	1			[460]
43	cCTF-400	Triazine	744	0.36	2.25	0	1			[460]
	[HO]25%- H <sub>2</sub> P-COF	Imine	1054	0.89	1.41	25	1	Functionalization of COFs frameworks (introduction of polar functional group)	Tuning the porosity, and increasing affinity between CO <sub>2</sub> molecules-adsorbent surface	[457]
[HO]50%- H <sub>2</sub> P-COF	Imine	1089	0.91	—	54	0	1			[457]
[HO]75%- H <sub>2</sub> P-COF	Imine	1153	0.96	—	31	25	1			[457]
[HO]100%- H <sub>2</sub> P -COF	Imine	1153	0.96	—	46	0	1			[457]
[HO]100%- H <sub>2</sub> P -COF	Imine	1284	1.02	8.00	32	25	1			[457]
[HO <sub>2</sub> C]25%- H <sub>2</sub> P-COF	Imine	786	0.78	—	52	0	1			[457]
[HO <sub>2</sub> C]50%- H <sub>2</sub> P-COF	Imine	673	0.66	—	58	25	1			[457]
[HO <sub>2</sub> C]75%- H <sub>2</sub> P-COF	Imine	482	0.54	—	134	0	1			[457]
[HO <sub>2</sub> C]100%-H <sub>2</sub> P-COF	Imine	364	0.43	77.00	67	25	1			[457]
TMFPT-COF	Triazine	1407	0.97	17.00	157	0	1	Functionalization of COFs frameworks (introduction of heteroatoms)		[462]
MCTF@500	Triazine	1510	2.674	—	72	25	1	Functionalization of COFs frameworks (introduction of unsaturated metal sites)		[461]
COF-1	Boronate	750	0.30	—	17.00	0	55			[454]
COF-5	Boronate	1670	1.07	—	5.23	0	55			[454]
COF-6	Boronate	750	0.32	—	19.17	0	55			[454]
COF-8	Boronate	1350	0.69	—	7.05	0	55			[454]
COF-10	Boronate	2080	1.44	—	14.32	0	55			[454]
COF-102	Boronate	4650	1.55	—	22.95	0	55			[454]
COF-103	Boronate	4630	1.54	—	27.27	0	55			[454]

pressures. At 0 °C, the maximum CO<sub>2</sub> adsorption capacity was 1.56 mmol/g, while the corresponding isosteric heat of adsorption ranged from 28 to 35 kJ/mol, respectively.

Another extensively reported nitrogen-containing functional group used in HCP synthesis is carbazole [473–477]. Chang et al. [475] created two distinct types of indolo[3,2-b] carbazole-based building blocks, differing in the different number of reactive sites. The synthesized nitrogen-rich polymers demonstrated a substantial BET surface area of up to 1421 m<sup>2</sup>/g, coupled with a CO<sub>2</sub> uptake of 3.58 mmol/g at 0 °C and 1.13 bar. These values are comparable to those seen in several other POPs, indicating their competitive nature. Ramezanipour Penchah et al. [477] investigated the influence of operating parameters (crosslinker ratio, synthesis time, and catalyst type) on CO<sub>2</sub> adsorption capacity of carbazole-based HCP, synthesized through a Friedel–Crafts reaction. At a temperature of 25 °C and a pressure of 5 bars, the CO<sub>2</sub> uptake reached its optimum value of approximately 4.35 mmol/g.

HCPs can also serve as precursors for producing porous carbons. The wide variety of aromatic compounds available as raw materials makes it appealing to synthesize porous carbons from HCPs, especially those that are highly porous or entirely microporous

Shao et al. [478] developed a series of NDPC with tunable porosity and polarity derived from the N-containing HCPs, prepared from 4-vinylbenzyl chloride and 4-vinyl pyridine by the suspension polymerization and Friedel-Crafts reaction. It was found that the current NDPC could be good candidates for CO<sub>2</sub> capture, and a new idea was proposed for the design of porous carbons – the ultramicropore walls modified with plentiful heteroatoms. The volume of ultramicropores was shown to be a critical element in CO<sub>2</sub> adsorption. The developed material exhibited satisfactory CO<sub>2</sub> uptake (6.11 mmol/g at 0 °C and 1 bar) and CO<sub>2</sub>/N<sub>2</sub> selectivity (11.2) of the developed material were satisfactory. Similar outcomes were achieved in the experiment using imidazole-based HCPs. In the other study, Shao et al. [479] observed that the NDPCs exhibited a large BET surface area (1248–2059 m<sup>2</sup>/g) and pore volume (0.80–1.12 cm<sup>3</sup>/g). At low pressure, these NPCs adsorbed a large amount of CO<sub>2</sub> (4.09–5.86 mmol/g at 0 °C and 1 bar, 0.93–1.66 mmol/g at 0 °C and 0.15 bar). In conclusion, it was determined that in comparison to porosity, the nitrogen concentration has a minor impact on CO<sub>2</sub> uptake.

A comprehensive overview of the paths for modifying HCPs and the direction of ongoing research is presented in Fig. 28.

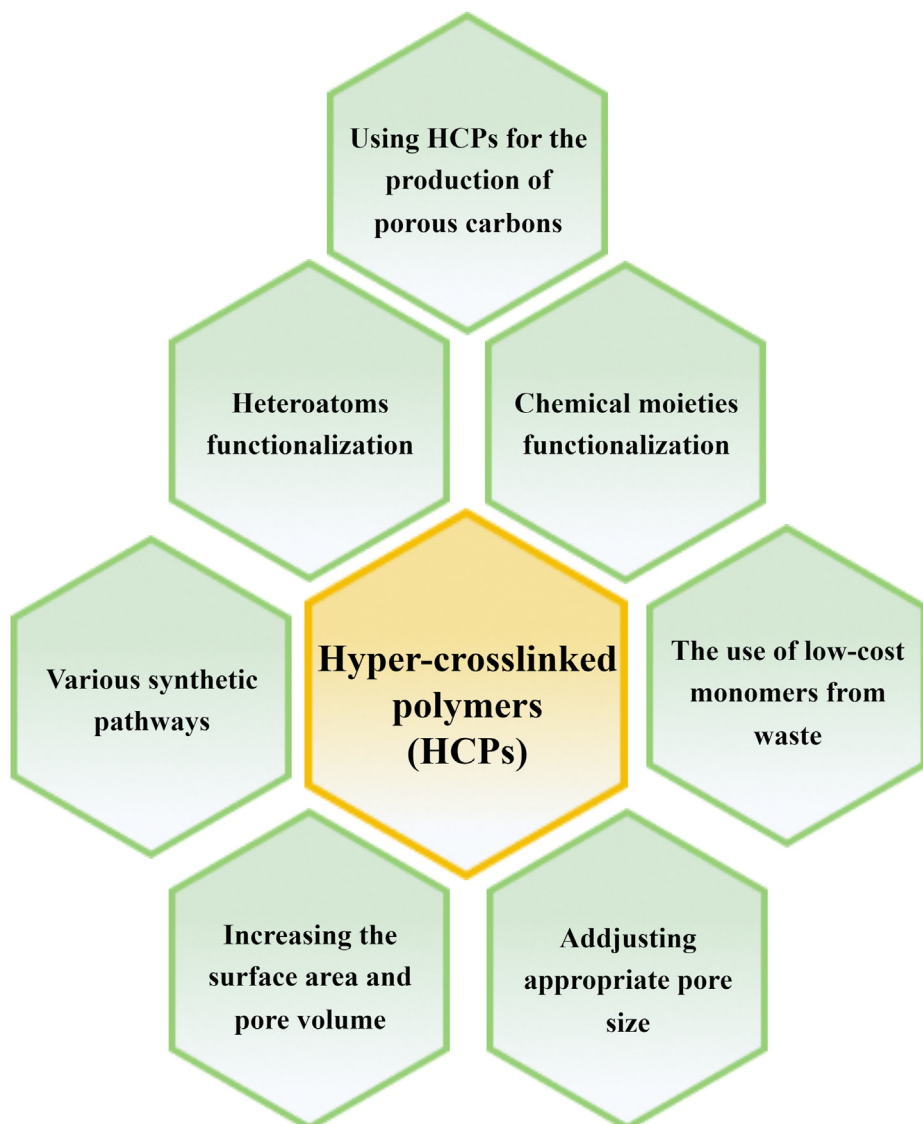


**Fig. 28.** The modification strategies and research directions of hyper-crosslinked polymers.

**Table 15** presents a thorough analysis of how various strategies have impacted the textural properties and CO<sub>2</sub> adsorption capabilities of hyper-crosslinked polymers, showcasing their potential for advancing carbon capture technologies.

### 3.5. Zeolites

Since the seminal discovery made by Cronstedt in 1756, zeolites have attracted significant scholarly interest, leading to several practical applications in recent decades. Zeolites offer several advantages, including cyclic stability, high surface area, and extremely fast kinetics of CO<sub>2</sub> adsorption compared to other solid sorbents [483,484]. They additionally possess robust adsorption sites and show favorable mechanical properties, including high abrasion resistance, density, and mechanical strength, enabling their formation into granules, spheres, and extrudates [485–487]. Furthermore, these CO<sub>2</sub> capture materials have an immense adsorption capacity under moderate operating conditions (0–100 °C, 0.1–1 bar) [488], which is strongly influenced by temperature and is positively correlated with their pore size [489]. Unfortunately, if the temperature approaches 100 °C, the CO<sub>2</sub> uptake of zeolites drops dramatically. According to lately review of Kumar et al. [489], it was indicated that the optimal temperature for CO<sub>2</sub> adsorption on zeolites is 70 °C, which is lower than the typical flue gas temperature (normally 90 °C). Therefore, either cooling the flue gas or modifying the adsorbents to render them suitable for high-temperature adsorption is necessary before their industrial-scale implementation. On the other hand, introduction an additional process, such as cooling, could lead to increased energy consumption and higher costs in CO<sub>2</sub> capture technology. Hence, addressing this aspect effectively in the future is crucial. Fig. 29 provides a schematic representation of the zeolites most frequently mentioned in the literature for applications in CO<sub>2</sub> adsorption.

In last years, more publications have been published in zeolite discipline, and it is apparent that researchers are concentrating their efforts on a few key areas, including: (1) searching for new raw materials, (2) new synthetic methodologies of synthesis, (3) designing of textural properties and material composition (by changing the Si/Al ratio, development of porosity), (4) cation exchange, (5) amine functionalization, (6) reduction of adverse moisture-related impacts, and (7) developing composite/hybrid materials. Furthermore, regarding the latest first-principles modeling for the design of materials in CO<sub>2</sub> capture technologies, Yuan et al. [490] stated that utilizing DFT fundamentals to analyze CO<sub>2</sub> adsorption behavior on zeolites can be applied to predict multiple factors, such as adsorption capacity, preferred sites, and selective adsorption between different gaseous mixtures. The same quantum-mechanical method for modeling non-covalent interactions and thermochemistry, has been reported in many other papers [491–495]. Currently, molecular simulations play a crucial role in advancing understanding of the correlation between microscopic and macroscopic characteristics within zeolites. Gaining insights into the adsorption characteristics of zeolites could enhance knowledge of the underlying processes of adsorption and diffusion phenomena. Also, it can contribute to identifying further potential applications of zeolites as CO<sub>2</sub> adsorbents. The generic methodology was comprehensively described by García-Pérez et al. [496].

Zeolites can be categorized into natural and synthetic. Natural ones are used as dryers, deodorants, for air separation, ion exchange (in water treatment, especially heavy metal ions), and soil improvement. Synthetics are exploited primarily for research and industry and possess several distinct advantages over those that occur in nature. One of them is the possibility of achieving unprecedented levels of control over the material porosity and

crystallinity that are not achievable in nature. On the contrary, in terms of CO<sub>2</sub> capture, synthetic zeolites tend to be more expensive compared to more affordable natural zeolites, which, despite their lower cost, often display inferior sorption properties, varying composition, and reduced purity [497].

Over the last few decades, waste management and the reduction of costs in the synthesis process of zeolites have gained importance in many sectors of the industry. A substantial amount of research has been dedicated to both the reuse of fly ash as a raw material and the exploitation of natural material. Garshasbi et al. [498] prepared zeolite 13X synthesized by hydrothermal treatment using natural clays. The zeolite 13X demonstrated a superior BET surface area (591.22 m<sup>2</sup>/g), CO<sub>2</sub> uptake (6.9 mmol/g) and micropore volume (0.250 cm<sup>3</sup>/g) compared to the other materials studied. Chen et al. [499] prepared zeolite 13X using bentonite as raw material by alkaline fusion followed by hydrothermal treatment. It was determined that the newly synthesized zeolite 13X had high BET surface area of 688 m<sup>2</sup>/g, a large micropore volume of 0.30 cm<sup>3</sup>/g, and exhibited substantial CO<sub>2</sub> capture capacity (4.80 mmol/g) along with selectivity (CO<sub>2</sub>/N<sub>2</sub> = 37) at 25 °C and 1 bar. Considering these details, the variety of natural and synthetic zeolites makes them appealing for use in the CO<sub>2</sub> adsorption process due to their unusual versatility.

Zeolites are a class of highly porous crystalline aluminosilicates, composed of tetrahedrons formed by shared oxygen atoms of alumina and silica, characterized by the formula T<sub>4</sub>O<sub>4</sub> (T = Si or Al) [500]. Such a substitution leads to the accumulation of negative charge in their pore structure, leading to an increase in basicity when incorporating a higher concentration of aluminum atoms in the framework [501]. This is owing to the weaker electronegativity of aluminum compared to silica, which causes this effect. Furthermore, cations (Li<sup>+</sup>, Na<sup>+</sup>, Ca<sup>2+</sup>, etc.) are present in the zeolite's channels and chamber systems, with strictly defined molecular sizes to compensate for this negative charge. This gives rise to another key aspect of zeolites, namely, ion exchange [502]. Consequently, the alteration of the Si/Al ratio is of significant importance, as higher basicity corresponds to greater CO<sub>2</sub> adsorption capacity of zeolites [503]. The different Si/Al ratios in zeolites determine their properties. Low-silica zeolites (Si/Al < 2) exhibit considerable acid resistance and thermal stability, as well as hydrophilic properties. Conversely, high-silica zeolites (Si/Al > 50) are characterized by an increased degree of ion exchange, and hydrophobicity [504]. Overall, this parameter signifies the focus of research endeavors concerning zeolite-based adsorbents, specifically centered around optimizing material composition through diverse synthesis approaches. Further, due to the defined crystal structure, zeolites show a very narrow pore size range from 0.5 to 1.2 nm [505]. As a direct consequence of possessing that property, zeolites can effectively separate CO<sub>2</sub> molecules through a molecular sieving process, because of their tailorabile cavities and tunable pore sizes. The presence of microporosity in zeolites classifies them as molecular sieves, enabling pore size-dependent adsorption selectivity (Fig. 30) [506]. In this case, only gas molecules with a kinetic diameter smaller than the pore size of the zeolite can be adsorbed. Hence, the topologies and pore diameters within the crystal lattice are important criteria in the research for developing CO<sub>2</sub> capture materials based on zeolites. Introducing mesopores into microporous zeolites, achieved through the synthesis of hierarchical porous materials, stands as one of the most promising approaches for creating novel structures with tailored chemical and textural attributes [507–510]. It offers the combined benefits of improved CO<sub>2</sub> adsorption properties and enhanced mass transfer through the mesoporous channels, due to adaptable porous structure that effectively addresses limitations in molecule diffusion [511,512].

**Table 15**Influence of modification strategies on textural properties and CO<sub>2</sub> uptake of hyper-crosslinked polymers.

Hyper-crosslinked polymers	BET surface area, m <sup>2</sup> /g	Total pore volume, cm <sup>3</sup> /g	Micropore volume, cm <sup>3</sup> /g	CO <sub>2</sub> selectivity at 1 bar	CO <sub>2</sub> uptake, mmol/g	Adsorption temperature, °C	Pressure, bar	Reported modification	Purpose of modification method	Reference
HCPs-5%	1165	0.98	0.37	32.30	2.25 0.56	0	1 0.15	Novel synthetic methodologies (new synthesis strategy)	Tuning the porosity, and surface area to promote the interaction with CO <sub>2</sub>	[480]
HC-Pcz-8	1688	1.11	0.37	17.00	3.50	25	1	Novel synthetic methodologies (new synthesis strategy)		[476]
HCTPP	582	0.32	—	—	-1.65	25	1	Novel synthetic methodologies (selecting external crosslinker)		[481]
HCTPA	921	0.53	—	—	-2.13	25	1			[481]
HCTPM	670	0.37	—	—	-1.70	25	1			[481]
InCz-HCP2	1421	1.48	0.42	29.00	3.58	0	1.13	Heteroatoms functionalization (N)	Enhancing adsorbent surface binding affinity to CO <sub>2</sub> molecules	[475]
46	HCP	992	1.06	0.1188	49.00 2.72 25	0	1	Heteroatoms functionalization (N, O)		[471]
	HCP-MAAM	142	0.87	—	53.00	1.45	0	Introduction of chemical functionalities (amide groups)		[470]
HCP-MAAMs -1	856	1.00	0.25	~20.00	1.56	0	1			[472]
BAHCP	1101	—	—	42.00	3.03	0	1	Introduction of chemical functionalities (-OH groups)		[482]
HCP-1	434	0.25	0.19	56.60	1.95 0.61	25	1 0.1	HCP as precursor N-doped porous carbon	Providing the possibility to large-scale production;	[479]
NPC-700-KOH	2616	1.37	1.14	14.20	5.45 0.80	25	1 0.1		Employing the large number of containing N aromatic compounds	[479]
NDPC-10%	1226	0.70	0.57	20.20	6.11 3.89 25	0	1			[478]
NPC-700-ZnCl <sub>2</sub>	1105	0.58	0.50	42.60	4.02 1.09	25	1 0.15			[479]

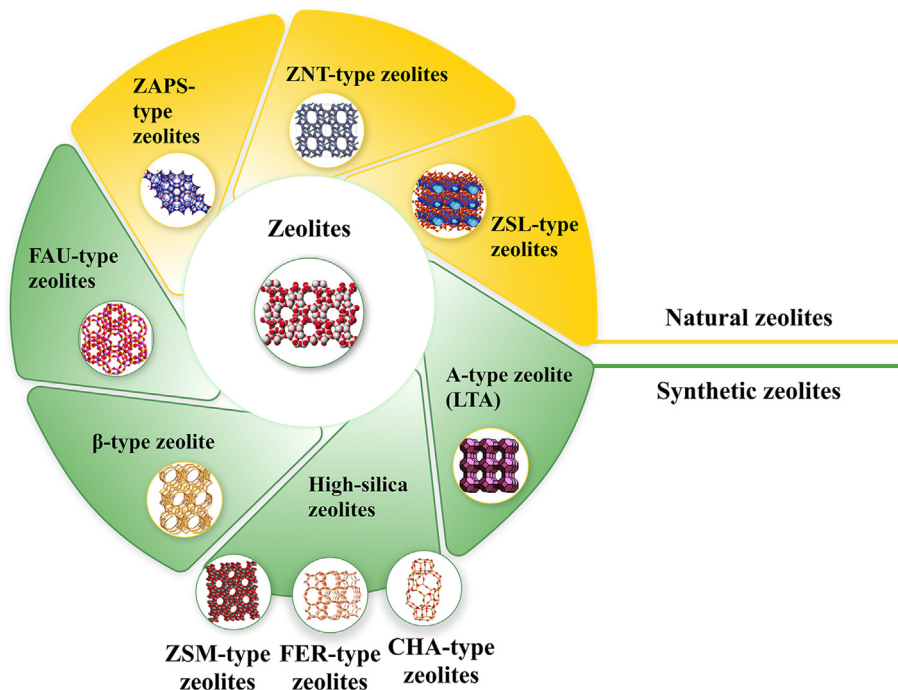


**Fig. 29.** Classification of zeolites for CO<sub>2</sub> capture application.

Panda et al. [513] created hierarchical zeolites 4A (HZ4A) by introducing mesoporosity into zeolites Z4A bodies using a urea treatment under hydrothermal conditions. The obtained zeolites showed adjustable physicochemical properties, including expanded surface area (126 m<sup>2</sup>/g), increased mesopore volume (0.44 cm<sup>3</sup>/g), and coexistence of micropores (about 0.4 nm) with mesopores (5.5 nm). Moreover, compared to Z4A bodies, the presence of mesopores increased the rapid gas diffusion within the pores during both adsorption and desorption. As an outcome, the CO<sub>2</sub> adsorption efficiency was improved, while maintaining an acceptable regeneration energy requirement. Dabbawala et al. [514] designed the synthesis of hierarchical porous zeolite-Y by employing cationic polymer polydiallyldimethylammonium chloride (PDDA) as a bifunctional mesopore directing template. It was reported that the hierarchical zeolite-Y had a higher CO<sub>2</sub> adsorption capacity (ranging from 5.4 to 5.9 mmol/g) and better selectivity (reaching up to 160) than microporous zeolite-Y. Liu et al. [515] prepared hierarchical porous zeolite (HP-ZSM-5) combining both micro and mesoporous structures using organosilanes. The synthesized material showed an improved CO<sub>2</sub> adsorption capacity, achieving a maximum value of up to 2.6 g/mol at 0 °C and 1 bar. The HP-ZSM-5 also demonstrated a faster physical adsorption process compared to the pristine zeolite (ZSM-5). Further, it was determined that the microstructure and morphology of the hierarchical zeolite were the most important parameters influencing the CO<sub>2</sub> adsorption performance.

CO<sub>2</sub> separation on zeolites can also occur through a mechanism of selective adsorption, where CO<sub>2</sub> molecules interact with the electric field generated by the presence of ions within the zeolite framework. This interaction creates a strong affinity between the acidic adsorbate and the adsorbent surface [516]. Thus, the coordination and distribution of exchangeable cations within the zeolite framework can influence the adsorption equilibrium and gas diffusion, directly impacting the strength of the electric field they create. Sun et al. [517] verified the CO<sub>2</sub> capture efficiency of transition metal cation-exchanged SSZ-13 zeolites. Among the tested transition metals

(Co(II), Ni(II), Zn(II), Fe(III), Cu(II), Ag(I), La(III), and Ce(III)) exchanged SSZ-13, Co(II)/SSZ-13 and Ni(II)/SSZ-13 demonstrated the greatest CO<sub>2</sub> uptake (4.49 and 4.45 mmol/g, respectively) and the best CO<sub>2</sub> selectivity over N<sub>2</sub> (52.55 and 42.61, respectively) at 0 °C and 1 bar. The findings revealed a significant difference between performance of alkali metal-form. The exceptional CO<sub>2</sub> capture capacity was attributed to the pi-complexation effect.

As previously observed in other material types, the influence of moisture also poses an added challenge for zeolite-based adsorbents in real-world applications. The presence of another gas, which potentially competes with CO<sub>2</sub> molecules for active adsorption sites along with exposure to water vapor, can considerably diminish the adsorption capacity and stability in an adverse manner [516,518]. Under acidic conditions that arise from contact with water and carbon dioxide, there can be alterations in the

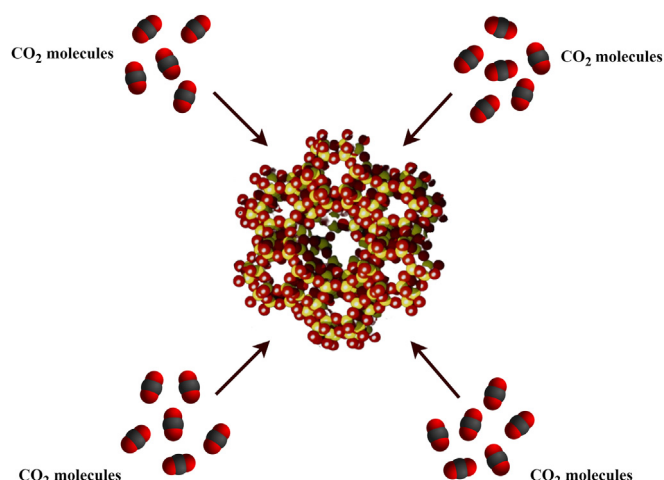


**Fig. 30.** Schematic mechanism of CO<sub>2</sub> adsorption in the zeolite Y structure.

dealumination of zeolite structures, leading to the disintegration of the framework [519]. Other impurities within the flue gas stream can also negatively affect CO<sub>2</sub> capture. Panda et al. [513] investigated the CO<sub>2</sub> adsorption performance of HZ4A under humid conditions, with HZ4A-1–3 exhibiting a CO<sub>2</sub> uptake of 1.36 mmol/g at 40 °C and retaining 34.67% of CO<sub>2</sub> adsorption (0.61 mmol/g) in comparison to the dry state at 0.15 bar. Significantly, HZ4A-13 shown superior performance in mitigating the negative effects of moisture within the low flue gas pressure range. Furthermore, the authors highlighted that the CO<sub>2</sub> adsorption capacity of HZ4A-13 surpassed that of other tested adsorbents, including zeolite 13X, amine-functionalized LTA-125-NH<sub>2</sub>, and zeolite 5A, providing a distinct advantage. Consequently, HZ4A-13 holds promise for CO<sub>2</sub> capture in humid flue gas environments within extensive coal-fired power plant operations.

Zeolites act as an excellent case in which intricate research can be succinctly outlined through a list of research requirements and potential development pathways as CO<sub>2</sub> capture materials. Given this perspective, they establish the groundwork for a comprehensive methodological overview of the current advancements in novel adsorbent production. The comparison of modification strategies reported for zeolite-based adsorbents regarding their impact on CO<sub>2</sub> adsorption performance and textural properties is presented in Table 16. Fig. 31 provides a broad overview of the modification strategies and their associated research directions for zeolites in CO<sub>2</sub> capture.

### 3.6. Alumina

Basic alumina, also referred to as aluminum oxide, is a well-recognized support material utilized in CO<sub>2</sub> adsorption applications, existing in multiple crystallographic forms (with approximately 27 forms reported to date). Substrates associated with the synthesis of Al<sub>2</sub>O<sub>3</sub> encompass aluminum-containing minerals, such as aluminum hydroxide and oxyhydroxide, the most known are bayerite ( $\alpha$ -Al(OH)<sub>3</sub> or  $\beta$ -Al(OH)<sub>3</sub>), gibbsite (Al<sub>2</sub>O<sub>3</sub>·3H<sub>2</sub>O or Al(OH)<sub>3</sub>), boehmite ( $\gamma$ -AlO·OH), diasporite ( $\alpha$ -AlO·OH), and pseudoboehmite [536]. These chemical compounds differ in the arrangement sequence of atomic layers and the distance between them. Subsequently, they are subjected to the Bayer process as raw materials for alumina production. This procedure can be categorized into three steps: extraction, precipitation, and calcination [537]. The various metastable phases of Al<sub>2</sub>O<sub>3</sub> obtained through this method are primarily influenced by the temperature of thermal treatment, the type of natural ore, and the pH of solution during the neutralization process of aluminum salt [538]. The most recognizable crystal types of alumina are alpha ( $\alpha$ ), rho ( $\rho$ ), gamma ( $\gamma$ ), eta ( $\eta$ ), chi ( $\chi$ ), theta ( $\theta$ ), delta ( $\delta$ ), and kappa ( $\kappa$ ). The  $\gamma$ -,  $\rho$ - and  $\alpha$ -types are the most frequently observed on an industrial scale [539]. Fig. 32 presents an overview of the commonly utilized alumina phases in CO<sub>2</sub> adsorption applications.

The use of an all-alumina support for CO<sub>2</sub> adsorption offers many prominent benefits. These advantages include cost-effectiveness, exceptional crystallinity, high specific surface area, well-tailored mesoporosity, large pore volumes, as well as superior chemical, mechanical, and thermal stability [319,540,541]. Current research trends mainly focus on enhancing the physicochemical properties of Al<sub>2</sub>O<sub>3</sub>-based supports to improve CO<sub>2</sub> adsorption capacity, stabilize adsorption-desorption cycles, and increase CO<sub>2</sub> selectivity over CH<sub>4</sub>/N<sub>2</sub> in flue gas streams. These covers optimizing texture characteristics, periodicity, long-range order, the distribution, or number of active sites, as well as adjusting basicity to strengthen the interaction between the adsorbent surface and CO<sub>2</sub> molecules. According to the modifications reported in the literature

between 2018 and 2021, these improvements can be achieved by creating composites/hybrid materials, and more specifically through [542–554]:

- new synthesis approaches and modification of the process conditions;
- functionalization by ionic liquids;
- functionalization by metal oxides/carbonates;
- impregnation with metal hydroxides;
- impregnation or grafting with amines;
- use of different structure of Al<sub>2</sub>O<sub>3</sub>-based supports;
- use carbon waste for aluminum extraction as an adsorbent.

By combining an alumina-aerogel support with K<sub>2</sub>CO<sub>3</sub>, Bararpour et al. [542] developed a unique process for the production of solid sorbents in the post-combustion CO<sub>2</sub> capture process with very high CO<sub>2</sub> capture capacity and stability. Compared to previous investigations on alumina-based materials, the alumina-aerogel support showed a significantly higher BET surface area of 2019 m<sup>2</sup>/g, an achievement that had not been attained in previous studies for this specific type of material. Under optimal conditions, the sorbent achieved a notable CO<sub>2</sub> capture capacity of 7.2 mmol/g at 56.1 °C, which was statistically significant. In another research, Bararpour et al. [546] investigated the influence of textural qualities on the performance of the mesoporous alumina supported K<sub>2</sub>CO<sub>3</sub>. Al<sub>2</sub>O<sub>3</sub> was synthesized using a surfactant-assisted technique. The support constructed with a surfactant-to-Al ratio of 0.5 possessed the highest CO<sub>2</sub> uptake of 5.7 mmol/g and stayed stable during 15 cycles of carbonation/regeneration. This increase was related to the existence of numerous active sites for carbonation reactions, leading to an enhanced CO<sub>2</sub> capture capacity. Studies on the functionalization of aluminum support with ionic liquids have also been reported by Sun et al. [552].

Hiremath et al. [553] presented a facile, green, and template-free synthesis of mesoporous Al<sub>2</sub>O<sub>3</sub> for effective insertion of MgO to generate strong basicity. Significantly, the material was endowed with strong basicity, thereby eliminating the loss of active surface area. The approach showed a scalable mesoporous structure with an excellent surface area of 315 m<sup>2</sup>/g, characterized by a narrow pore size distribution (PSD). Furthermore, the incorporation of MgO as a heteroatom into the mesoporous alumina framework resulted in an improved surface area of 357 m<sup>2</sup>/g, while maintaining PSD. An advantageous aspect of the developed material was its improvement in basicity, increasing from 1.13 to 2.73 mmol/g. This improvement increased the affinity of the adsorbent surface for CO<sub>2</sub> molecules.

Zhou et al. [549] synthesized and immobilized polymeric ionic liquids (PILs) on mesoporous  $\gamma$ -Al<sub>2</sub>O<sub>3</sub> (MA) using the ultrasonic immersion method. The experimental results showed that P[VCIm] Cl/MA demonstrated the highest CO<sub>2</sub> adsorption capacity among all adsorbents. The maximum value reached 0.562 mmol/g and occurred under optimal working conditions, including a loading ratio of 1:1, a temperature of 40 °C, a pressure of 5 bar, and a CO<sub>2</sub> flow rate of 10 mL/min.

Another noteworthy research direction is the extraction of alumina from coal-based solid waste, which serves as a means to mitigate environmental hazards. Li et al. [550] prepared amine-functionalized CO<sub>2</sub> adsorbents by grafting APTES with the alumina residue and the alumina-extracted residue. The findings indicated that under conditions of 25 °C and 100 vol% CO<sub>2</sub> feed flow, the sample treated with 12 mmol of APTES exhibited a peak CO<sub>2</sub> adsorption capacity of 1.23 mmol/g. The sorbent was successfully regenerated at 110 °C and maintained a stable uptake over 5 repeated adsorption-desorption cycles. Fig. 33 highlights related to alumina that have been published in the literature.

**Table 16**Influence of modification strategies on textural properties and CO<sub>2</sub> uptake of zeolites.

Zeolite	BET surface area, m <sup>2</sup> /g	Total pore volume, cm <sup>3</sup> /g	Micropore volume, cm <sup>3</sup> /g	Mesopore volume, cm <sup>3</sup> /g	Si/Al ratio	CO <sub>2</sub> selectivity at 1 bar	CO <sub>2</sub> uptake, mmol/g	Adsorption temperature, °C	Pressure, bar	Reported modification	Purpose of modification method	Reference
Zeolite 4A	—	—	—	—	0.74	—	4.8	25	20.7	—	—	[181]
Zeolite 13X	—	—	—	—	1.08	—	5.2	25	20.7	—	—	[181]
Zeolite 13X	164.3	0.21	—	—	—	—	4.54	25	30	—	—	[485]
Zeolite 5A	—	—	—	—	—	—	4.5	25	1	—	—	[520]
NaY	723	—	0.35	—	—	—	4.8	30	1	—	—	[521]
Nano-zeolite	698.19	0.369	—	—	—	18.65	4.81	20	1	Novel synthetic methodologies of synthesis	Enhancement of CO <sub>2</sub> capture	[419]
Silicalite-1 (CON)	390.14	0.24	—	—	—	~2.75	2.36	30	0.8	—	—	[420]
Silicalite-1 (SON)	382.83	0.31	—	—	—	~3.20	2.12	30	0.8	—	—	[420]
A5 Zeolite	179.44	—	—	—	11.9	—	5.2	0	30	—	—	[522]
Z4A	39	0.14	—	0.13	—	—	3.77	0	1	Novel synthetic methodologies of synthesis; Textural properties adjustment; Moisture effect	Implementation of mesoporosity into zeolite structure	[513]
Humid-Z4A	—	—	—	—	—	—	3.00	40	1	—	—	[513]
HZ4A-1-3	126	0.45	—	0.44	—	—	3.41	0	1	—	—	[513]
Humid-HZ4A-1-3	—	—	—	—	—	—	3.09	25	1	—	—	[513]
HZ4A-1-1	112	0.42	—	0.41	—	—	2.72	0	1	—	—	[513]
HZ4A-3-1	65	0.53	—	0.52	—	—	1.36	40	1	—	—	[513]
ZY	662	0.30	0.28	0.02	2.2	—	5.1	25	1	Novel synthetic methodologies of synthesis; Textural properties adjustment	Improving structural properties (increasing the pore volume and surface area)	[514]
PDY-3	699	0.36	0.27	0.09	2.3	—	5.2	25	1	—	—	[514]
PDY-6	705	0.38	0.26	0.12	2.1	~100.00	5.9	0	1	—	—	[514]
PDY-7	773	0.39	0.26	0.13	2.0	160.00	5.4	25	1	—	—	[514]
ZSM-5	383	0.21	0.19	0.02	25	~72.50	2.37	0	1	Novel synthetic methodologies of synthesis; Textural properties adjustment; Moisture effect	Improving structural properties (combining micro- and mesoporous structures)	[515]
Cl-HP-ZSM-5	438	0.29	0.17	0.12	26	~67.50	1.81	25	1	—	—	[515]
Humid-Cl-HP-ZSM-5	—	—	—	—	—	—	0.26	50	1	—	—	[515]
N-HP-ZSM-5	405	0.25	0.18	0.07	25.5	~65.00	2.60	0	1	—	—	[515]
LTA-000	656	0.35	0.29	—	—	—	1.91	25	1	Textural properties adjustment;	Implementation of mesoporosity into zeolite structure; Increasing basicity, affinity between CO <sub>2</sub> molecules-adsorbent surface and level-up N-contents	[523]
APTMS-LTA-050	708	0.64	0.23	—	—	—	1.4	60	0.15	—	—	[523]
APTMS-LTA-100	708	0.58	0.14	—	—	—	1.9	60	0.15	Amine functionalization (3-aminopropyl)trimethoxysilane	Increasing basicity, affinity between CO <sub>2</sub> molecules-adsorbent surface and level-up N-contents	[523]
APTMS-LTA-125	499	1.02	0.11	—	—	—	2.3	60	0.15	—	—	[523]
TEPA-ZSM-5	19.045	—	0.049	—	—	—	1.80	100	1	Amine functionalization (Tetraethylenepentamine)	Increasing basicity, affinity between CO <sub>2</sub> molecules-adsorbent surface and level-up N-contents	[524]
Meso-13X	728	0.46	0.25	0.21	—	—	—	100	1	Amine functionalization (Polyethylenimine)	—	[525]
PEI-Meso-13X	1	0.001	—	—	—	—	1.82	100	1	—	N-contents	[525]
Ag(I)-SSZ-13	770.88	0.33	0.26	—	11.9	18.80	3.14	25	1	Cation exchange (Ag <sup>+</sup> , Co <sup>2+</sup> , Ni <sup>+</sup> )	Increasing basicity, affinity between CO <sub>2</sub> molecules-adsorbent surface	[517]
Co(II)-SSZ-13	786.75	0.44	0.23	—	9.92	52.55	4.49	25	1	—	—	[517]
Ni(I)-SSZ-13	836.01	0.44	0.23	—	10.04	42.61	4.45	25	1	—	—	[517]
Li-LSX	662	0.32	0.31	—	1.00	128.00	400	60	0.15	Cation exchange (Li <sup>+</sup> )	—	[526]
LiX	560.25	0.30	—	—	—	103.00	—	—	—	Cation exchange (Li <sup>+</sup> , Ag <sup>+</sup> , Pd <sup>2+</sup> )	—	[527]
LiPdAgX	549.19	0.29	—	—	—	128.00	—	—	—	—	—	[527]
Clino	37	0.14	0.005	—	4.79	—	2.25	10	1	Cation exchange (Na <sup>+</sup> )	Increasing basicity, affinity between CO <sub>2</sub> molecules-adsorbent surface	[528]
Na-Clino	32	0.14	0.004	—	5.75	—	2.17	10	1	Natural materials as zeolite precursor	Reducing production costs	[528]
Na-Zeolite β	508	0.52	—	—	7.4	16.80	3.45	0	1	Cation exchange (Na <sup>+</sup> , K <sup>+</sup> , Li <sup>+</sup> )	—	[529]

(continued on next page)

**Table 16 (continued)**

Zeolite	BET surface area, m <sup>2</sup> /g	Total pore volume, cm <sup>3</sup> /g	Micropore volume, cm <sup>3</sup> /g	Mesopore volume, cm <sup>3</sup> /g	Si/Al ratio	CO <sub>2</sub> selectivity at 1 bar	CO <sub>2</sub> uptake, mmol/g	Adsorption temperature, °C	Pressure, bar	Reported modification	Purpose of modification method	Reference
K-Zeolite β	446	0.41	—	—	7.4	14.70	2.96 3.57 2.70	25 0 25	1		Increasing basicity, affinity between CO <sub>2</sub> molecules-adsorbent surface	[529]
Li-Zeolite β	474	0.45	—	—	7.4	20.00	3.08 2.39	0 25	1			[529]
Z-Y-3	819	0.33	0.32	—	2.25	—	2.59	30	1	Solid wastes as zeolite precursor (gasified rice husk)	Reduction of production costs	[530]
Coal fly ash zeolites (CFAZ)	486	0.31	0.13	0.17	—	—	3.02	0	1	Solid wastes as zeolite precursor		[531]
Zeolite 13X	643	—	0.35	—	3.0–5.0	—	5.07	25	1	Solid wastes as zeolite precursor (fly ash)		[532]
Fly ash zeolite (F)	414	0.251	0.188	—	—	—	4.16	50	—	Solid wastes as zeolite precursor;	Reduction of production costs; Enhancement of CO <sub>2</sub> capture	[533]
Fly ash zeolite (H)	39	0.138	0.016	—	—	—	1.2	50	—			[533]
Fly ash zeolite (TS)	34	0.069	0.013	—	—	—	0.24	50	—	Novel synthetic methodologies of synthesis		[533]
Zeolite 13X (13X-C)	588	—	0.240	—	—	—	6.9 6.3	25 35	1	Natural materials as zeolite precursor (kaolin, bentonite, feldspar)	Reduction of production costs	[498]
Zeolite 13X (13X-K)	591	—	0.250	—	—	6.88	5.5 6.2	25 35	1			[498]
Zeolite 13X (13X-B)	505	—	0.160	—	—	—	4.9 4.2	25 35	1			[498]
Zeolite 13X (13X-F)	472	—	0.140	—	—	—	3.9 3.2	25 35	1			[498]
C-13X	876	0.35	0.35	—	—	26.00	6.18	25	1	Natural materials as zeolite precursor (bentonite)		[499]
B-13X	688	0.38	0.30	—	—	37.00	4.80	25	1			[499]
50 Silicalite-1/TOCNF/gelatin	~272	-0.22	—	—	—	—	~1.24	25	1	Materials based on the gelatin/nanocellulose	Composite/hybrid materials formation	[534]
Zeolite-Y/Chitosan	795	—	—	—	—	—	1.64	25	1	Chitosan biopolymer		[535]
ZSM-5/Chitosan	444	—	—	—	—	—	2.39	25	1			[535]

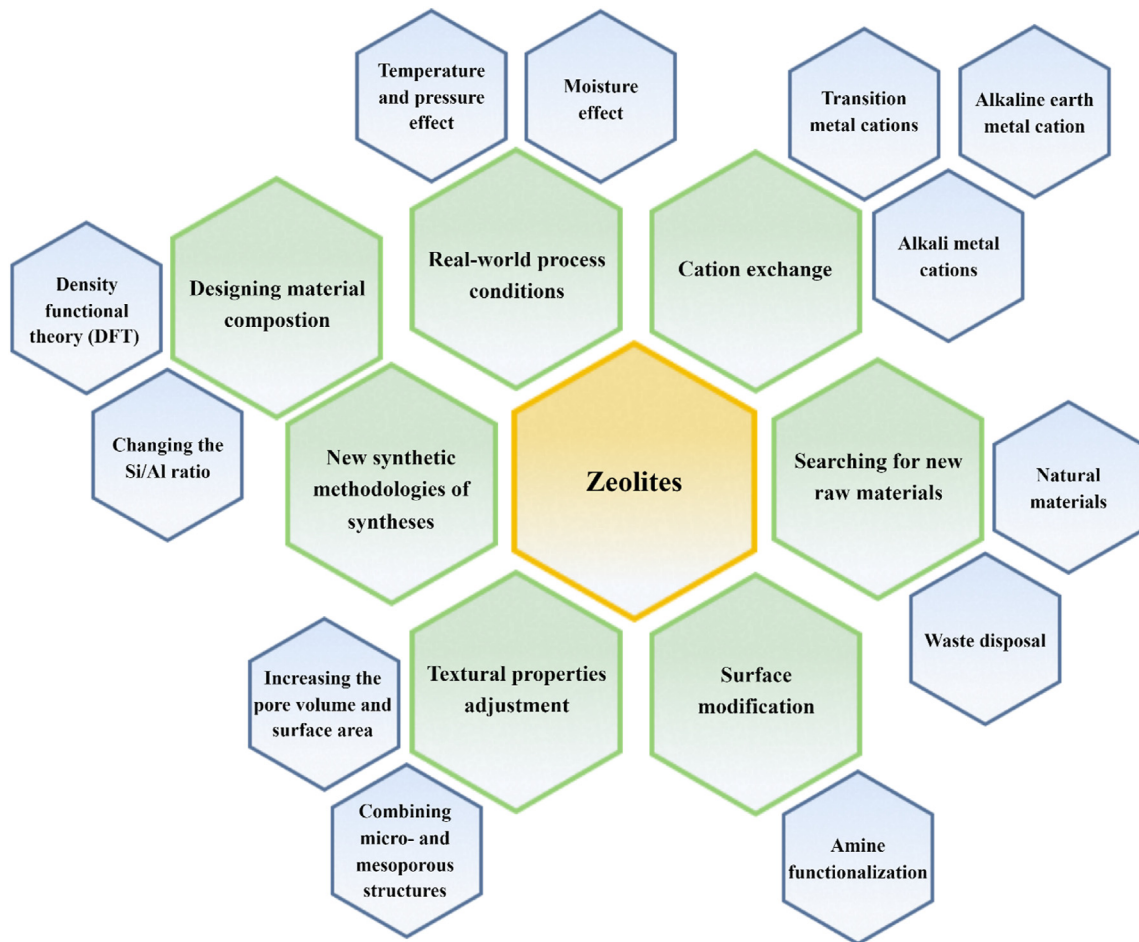


**Fig. 31.** The modification strategies and research directions of zeolites.

The CO<sub>2</sub> uptake and textural properties of alumina-supported adsorbents resulting from various modification approaches are summarized in [Table 17](#).

### 3.7. Metal oxides

One of the strategies for CO<sub>2</sub> capture involves the utilization of metal oxides as adsorbents. These materials, including calcium oxide (CaO), magnesium oxide (MgO), titanium dioxide (TiO<sub>2</sub>), iron oxides (F<sub>x</sub>O<sub>x</sub>), and their various combinations, can be directly applied in a CO<sub>2</sub>-solid reaction to form metal carbonates ([Fig. 34](#)). The choice of these particular metal oxides is deeply interrelated by the objective of producing a thermodynamically stable carbonized material as the end product [\[555\]](#). Consequently, it is feasible to thermally desorb CO<sub>2</sub> molecules that have been adsorbed and then regenerate the adsorbent. Carbonation reactions generally release heat (exothermic), whereas carbonate breakdown reactions require heat input (endothermic), enabling the establishment of a cyclic process [\[556–559\]](#).

#### 3.7.1. Titanium dioxide

Titanium dioxide has attracted considerable interest among researchers due to its efficacy as an adsorbent, with distinctive characteristics making it suited to a range of industrial and environmental applications. Remarkably, it demonstrates a strong affinity towards CO<sub>2</sub> [\[560\]](#), high adsorption capacity, and selective adsorptions based on the size of absorbate molecules due to its unsaturated surface atoms [\[332\]](#). Hence, TiO<sub>2</sub> has also been widely

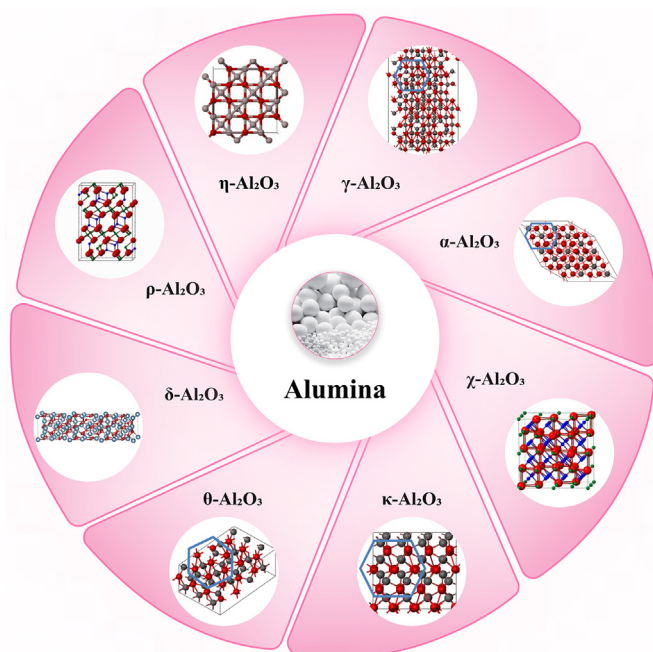


**Fig. 32.** Alumina phases used as support materials for CO<sub>2</sub> adsorption.

utilized in the separation of CO<sub>2</sub> from flue gas streams. Furthermore, its significant surface area and tight range of pore sizes result in a shorter time period required to achieve adsorption equilibrium [561]. It is closely related to the high regularity in mesopore channels with access to active sites, which significantly improves the diffusion rate, ensuring the rapid uptake of gas molecules during adsorption [562].

Currently, titanium dioxide is primarily exploited as a catalyst, giving rise to the development of new hybrid materials for CO<sub>2</sub> conversion processes. Research in this field mainly centers on the photocatalytic reduction of CO<sub>2</sub> into valuable chemical compounds, such as solar fuels [563–569]. The literature has documented investigations into the direct implementation of TiO<sub>2</sub> for CO<sub>2</sub> capture. These studies concern optimizing amine functionalization [332,570–575], incorporating phosphorus [576], and developing composite materials with other solid adsorbents. This leads to increased adsorption capacity and improved cyclic stability compared to the parent materials [556,577,578].

According to Ota et al. [575], while the wide variety of TiO<sub>2</sub> structures exist, including particulate, tube, rod, sheet, and sponge, there is relatively limited research comparing amine functionalization to other porous materials. This is due to a low concentration of OH groups on the surface of TiO<sub>2</sub>, which makes it challenging to achieve significant modifications with high levels of amines. Consequently, the authors developed a technique to synthesize new amorphous TiO<sub>2</sub> nanoparticles with a diameter of 3 nm, a large surface area of 617 m<sup>2</sup>/g, and a higher concentration of OH groups. Compared to conventional TiO<sub>2</sub>, amorphous TiO<sub>2</sub> nanoparticles treated with ethylenediamine demonstrated a higher CO<sub>2</sub> adsorption capacity (2.90 mmol/g at 0 °C and 1 bar). The tuning of the ethylenediamine quantity bound to the particles enhanced their CO<sub>2</sub> uptake without impeding pore accessibility.

Regarding a potential CO<sub>2</sub> composite adsorbent, Chowdhury et al. [332] studied mesoporous titanium dioxide/graphene oxide (TiO<sub>2</sub>/GO) nanocomposites using varying ratios of GO to TiO<sub>2</sub> mass. The material with the lowest GO to TiO<sub>2</sub> mass ratio, due to its wide specific surface area (99.536 m<sup>2</sup>/g) and total pore volume (0.382 cm<sup>3</sup>/g), displayed the highest adsorption rate. The achieved maximum CO<sub>2</sub> adsorption capacity was 1.88 mmol/g at 25 °C and 1 bar, a value significantly surpassing that of various other CO<sub>2</sub> adsorbents, including zeolite, activated carbon, and specific MOFs, among others. Furthermore, the TiO<sub>2</sub>/GO composite exhibited rapid CO<sub>2</sub> uptake kinetics and excellent CO<sub>2</sub>/N<sub>2</sub> selectivity, suggesting its potential for further exploration in CO<sub>2</sub> capture applications.

Mixed oxides represent an alternative option for CO<sub>2</sub> adsorption performance enhancement. Jeon et al. [556] synthesized mixed oxides of mesoporous MgO/TiO<sub>2</sub> containing spherical nanoparticles through a sol–gel process. Nitrogen adsorption/desorption research demonstrated an increase in the surface area and total pore volume of mixed MgO/TiO<sub>2</sub> oxide, as well as the formation of bimodal pores. Because of this, the CO<sub>2</sub> adsorption capacity of the MgO/TiO<sub>2</sub> was found to be substantially higher (0.477 mmol/g at 25 °C and 1 bar) compared to the individual pure oxides. Wu et al. [578] focused on the preparation of TiO<sub>2</sub> coated nano CaO-based adsorbent. The results revealed a considerable increase in the endurance of the adsorption capacity. After 40 cycles of carbonation–calcination, nano CaO-based adsorbent with an optimal TiO<sub>2</sub> concentration of 10% exhibited considerably more stable CO<sub>2</sub> adsorption capacity (5.3 mmol/g) than CaO without TiO<sub>2</sub> coating (3.7 mmol/g).

**Fig. 35** compares the reported modification strategies and their related research directions for TiO<sub>2</sub> in CO<sub>2</sub> capture.

### 3.7.2. Iron oxides

Iron oxides have been shown to possess exposed active sites on their surfaces, capable of interacting with gaseous CO<sub>2</sub> molecules

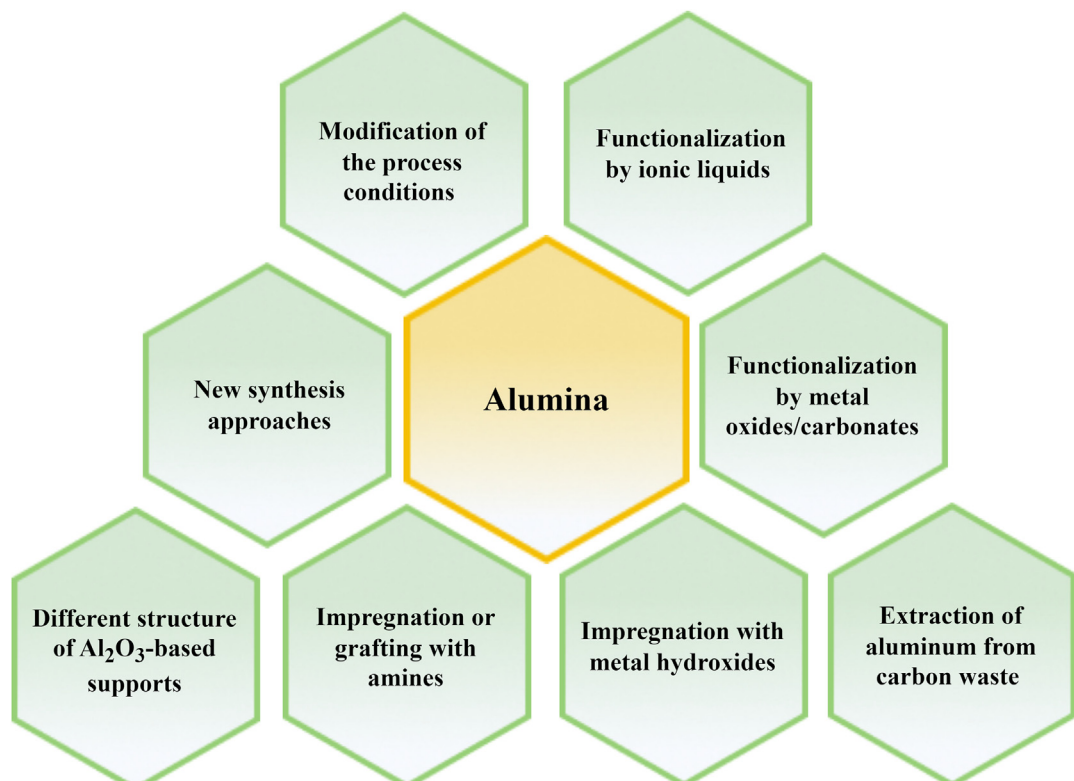


**Fig. 33.** The modification strategies and research directions of alumina-supported adsorbents.

**Table 17**Influence of modification strategies on textural properties and CO<sub>2</sub> uptake of alumina-based adsorbents.

Alumina-based adsorbent	Alumina support	BET surface area, m <sup>2</sup> /g	Total pore volume, cm <sup>3</sup> /g	Average pore diameter/width, nm	CO <sub>2</sub> uptake, mmol/g	CO <sub>2</sub> vol%	Adsorption temperature, °C	Pressure, bar	Reported modification	Reference
Alumina-aerogel/K <sub>2</sub> CO <sub>3</sub> γ-Alumina/K <sub>2</sub> CO <sub>3</sub>	Alumina-aerogel γ-Alumina	2019 49.6	6.3 0.173	8.3–9.5 11.9–13.9	7.20 —	— —	56.1 —	— —	New synthesis approach and modification of the process conditions; Carbonates functionalization	[542] [542]
γ-Alumina/K <sub>2</sub> CO <sub>3</sub> γ-Alumina/K <sub>2</sub> CO <sub>3</sub>	γ-Alumina	90 62.61	0.27 0.200	8.7 —	0.66 5.5	5 —	60 —	— —	Carbonates functionalization	[545]
Boehmite/K <sub>2</sub> CO <sub>3</sub>	Boehmite	88.03	0.130	—	—	—	—	—	Comparison of the synthesis approach; Carbonates functionalization	[543] [543]
Alumina-aerogel/K <sub>2</sub> CO <sub>3</sub>	Alumina-aerogel	188.66	0.212	—	—	—	—	—	New synthesis approach;	[543]
Activated alumina/K <sub>2</sub> CO <sub>3</sub>	Activated alumina	6.23	0.003	—	2.29	10	60	1	Carbonates functionalization	[544]
Activated alumina/K <sub>2</sub> CO <sub>3</sub> /15 wt% urea	Activated alumina	10.62	0.004	—	3.10	10	60	1	New synthesis approach and modification of the process conditions; Carbonates functionalization	[546]
Mesoporous alumina/K <sub>2</sub> CO <sub>3</sub>	Mesoporous alumina	87	0.11	6.7	2.82	2.33	—	—	Carbonates functionalization	[547]
Ordered mesoporous Al <sub>2</sub> O <sub>3</sub>	Mesoporous alumina	305	0.33	—	1.69	—	0	1	New synthesis approach	[548]
Mesoporous alumina/sodium tripolyphosphate/chitosan	Mesoporous alumina	448.6	0.46	5.59	6.34	5	50	1	Ionic liquids functionalization	[549]
Mesoporous alumina/Polymeric ionic liquids	Mesoporous γ-Al <sub>2</sub> O <sub>3</sub>	171.87	0.87	22.26	0.562	—	40	5	Metal oxide functionalization	[550]
Mesoporous alumina/Bi-functionalized ionic liquid	Mesoporous alumina	91	0.16	5.85	2.02	—	25	1	Amine functionalization ((3-aminopropyl)triethoxysilane)	[551]
Mesoporous alumina/Bi-functionalized ionic liquid	Mesoporous alumina	0.03	~0	—	3.27	—	40	1	Metal hydroxide functionalization	[551]
Mesoporous alumina/MgO	Mesoporous alumina	357	0.6	7.1	0.82	—	150	—		
Alumina-extracted residue/APTES	Alumina-extracted residue	151.73	0.26	—	1.23	100	25	1		
Activated alumina/NaOH	Activated alumina	92.40	0.24	10.31	3.33	—	20	6		
Activated alumina/KOH	Activated alumina	103.02	0.25	9.83	2.97	—	20	6		

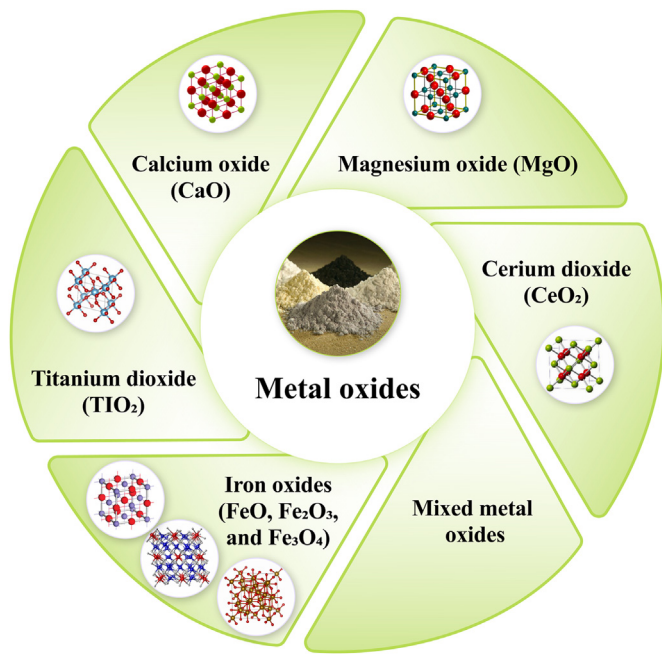


**Fig. 34.** Metal oxides explored as materials for  $\text{CO}_2$  adsorption in the literature.

[579]. Iron-based solid sorbents offer several key advantages, including their accessibility, favorable thermodynamics, cost-effectiveness, straightforward synthesis, abundance, and sustained adsorption capacity with slow degradation over time [580]. Iron oxides, especially, present an attractive option for  $\text{CO}_2$  capture in iron mills due to the potential for multiple cycles of carbonation and regeneration within the same ironmaking facility, allowing for seamless integration with steel production processes. Furthermore,

this sector consumes a substantial quantity of fossil fuels and accounts for approximately 7% of global  $\text{CO}_2$  emissions [581].

Unfortunately, the catalytic role of iron oxide in  $\text{CO}_2$  adsorption and desorption has not been conclusively proved yet. The surface interaction of iron oxide gradually revealed various carbonate species, including monodentate carbonate, bidentate carbonate, bicarbonate, and carboxylate [582]. In order to gain a deeper understanding of the  $\text{CO}_2$  adsorption mechanism, it is essential to provide detailed explanations. Hakim et al. [582] studied  $\text{CO}_2$  adsorption and desorption properties using  $\text{FeO}$ ,  $\text{Fe}_2\text{O}_3$ , and  $\text{Fe}_3\text{O}_4$  as absorbents, mainly due to the basicity and porosity of the morphology. In the case of  $\text{Fe}_2\text{O}_3$ , the study revealed the presence of various basic sites, including weak, medium, strong, and very strong phases.  $\text{Fe}_3\text{O}_4$ , despite its potential for use in  $\text{CO}_2$  capture, showed instability in adsorbing higher concentrations of carbon dioxide, resulting in its oxidation to form  $\text{Fe}_2\text{O}_3$ . On the other hand, among the other oxides,  $\text{Fe}_2\text{O}_3$  exhibited the most significant increase in BET specific surface area and the highest  $\text{CO}_2$  adsorption capacity after undergoing four cycles of adsorption-desorption (0.50 mmol/g). The authors concluded that enhancing  $\text{CO}_2$  capture efficiency can be achieved through chemical modification of the  $\text{Fe}_2\text{O}_3$  surface, either by increasing its basicity through the addition of basic metal oxides or by optimizing the surface through the use of appropriate support materials.

Recently, Mendoza et al. [583] presented a novel method for capturing  $\text{CO}_2$  by mixtures of raw materials used in the steel industry ( $\text{Fe}_3\text{O}_4 + \text{Fe}$  and  $\text{Fe}_2\text{O}_3 + \text{Fe}$ ). Based on  $\text{CO}_2$  pressure and planetary ball mill process parameters, they examined the kinetics of mechanically stimulated chemical reactions between iron oxides and  $\text{CO}_2$ . By applying increased  $\text{CO}_2$  pressure (10–30 bar) and room temperature, it was assumed that total carbonation of iron oxides may be accomplished. Under the same pressure, temperature, and reaction time as the  $\text{Fe}_2\text{O}_3$  and  $\text{Fe}$  system, the  $\text{CO}_2$  capture capacity of  $\text{Fe}_3\text{O}_4$  and  $\text{Fe}$  was 13.87 mmol/g, which was comparatively lower.

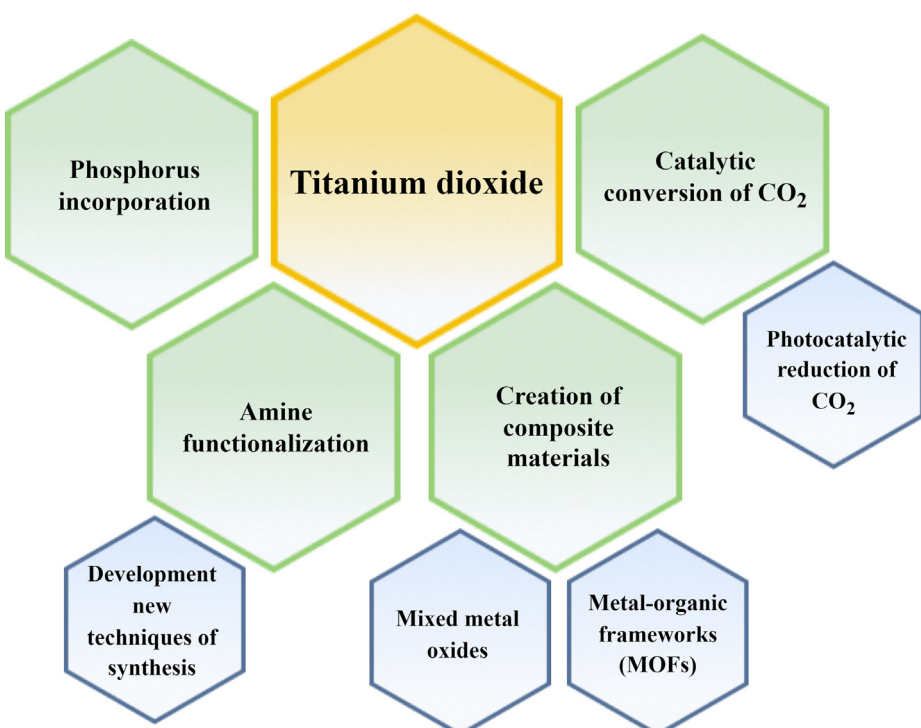


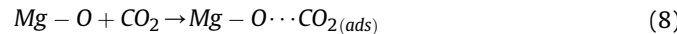
**Fig. 35.** The modification strategies and research directions of titanium dioxide-based adsorbents.

As a result of these findings, iron oxides are considered to be potential and efficient reversible solid sorbents for CO<sub>2</sub> capture.

The current research directions and modification strategies of iron oxides are given in Fig. 36.

### 3.7.3. Magnesium oxide

The general adsorption mechanism on MgO is based on the reversible interaction between CO<sub>2</sub> molecules and O<sup>2-</sup> sites of magnesium oxide, as presented in equation (8):



As a result, depending on the adsorption conditions and the structure of solid surface, several types of complexes are formed, such as bicarbonate, unidentate carbonate, and bidentate carbonate [584–586]. Fast physisorption occurs at low temperatures, whereas slower chemisorption takes place at high temperatures.

Initially, MgO was deemed unsuitable for high temperature CO<sub>2</sub> capture applications due to its inherent drawbacks. They partly include a limited practical CO<sub>2</sub> adsorption capacity at elevated temperatures due to restricted CO<sub>2</sub> access to the internal cavities, which is constrained by a small specific surface area and very sluggish kinetics [587]. Furthermore, MgO-based adsorbents frequently raise concerns about thermal stability since they require very high temperatures during the desorption stage [588,589]. This phenomenon is related to sintering processes taking place within the adsorbent, leading to the formation of a carbonate termination layer on the surface when the temperature surpasses a specific threshold. Consequently, this leads to a decrease in surface area and a decline in both CO<sub>2</sub> capture performance and recyclability. Due to these limitations, MgO-based materials are less cost-effective for industrial applications [519,590].

Nonetheless, there is a growing interest in reevaluating the suitability of MgO for CO<sub>2</sub> adsorption, owing to its lower energy consumption (<500 °C) in comparison to alternatives like Li<sub>2</sub>O and CaO [584,587], its affordability, abundant precursors, and advancements in materials science. Furthermore, magnesium oxide presents itself as a promising option for CO<sub>2</sub> capture applications owing to its distinctive attributes, such as appropriate surface basicity leading to the creation of oxygen vacancies that directly impact adsorption performance [591–595]. As a result, several investigations have been conducted to improve efficient CO<sub>2</sub> adsorption by MgO-based adsorbents, including their distribution on porous supports, metal doping, using different synthesis methods (precipitation method, double-replicate, aerogel method, sol-gel method, and many others), influence of surfactants, effect of the magnesium precursors, amine functionalization, synthesizing molten salt-modified MgO (alkali metal nitrate/carbonate), and mixed metal oxides.

Recently, Ruhaimi et al. [596] provided the most in-depth analysis to date of the review on MgO-based adsorbents prepared through diverse modification strategies using different approaches of synthesis and promoters. The authors suggested that merging innovative concepts and trends from other separation processes could enhance the economic viability and optimization of promoters in the adsorbent preparation. One approach could involve creating adsorbents with distinct morphological characteristics derived from biomass, along with the application of promoter optimization techniques like spray coating and aerosol impaction-driven assembly. Moreover, inclusion of promoters, hybrid adsorbents, and amine functionalization with the aid of a stabilizer may help to increase the cycle stability even further. It is also crucial to consider real-world industrial conditions, which often involve gaseous impurities like NO<sub>x</sub> and SO<sub>x</sub> in the flue gas stream, as well as the presence of moisture.

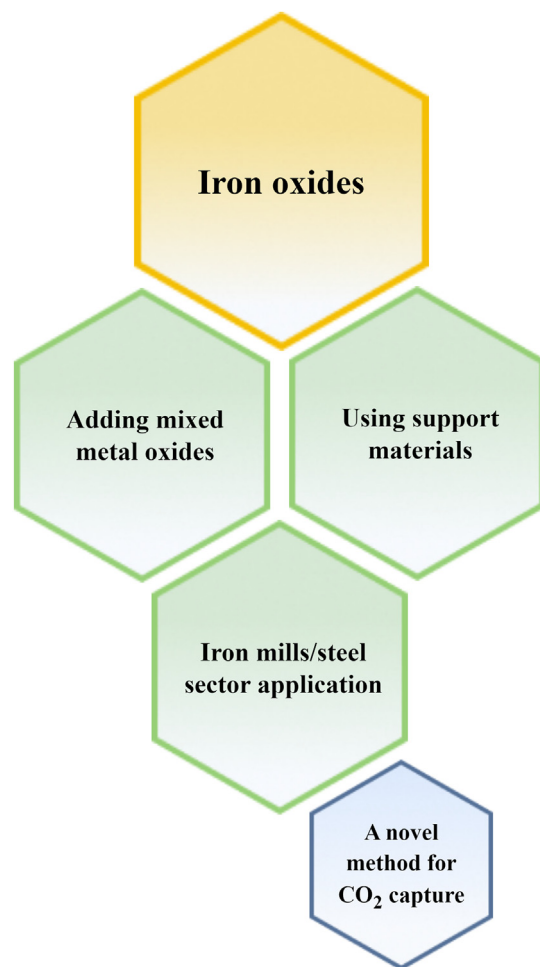


**Fig. 36.** The modification strategies and research directions of iron oxides-based adsorbents.

**Fig. 37** illustrates the current status of modification strategies for MgO-based adsorbents, as well as future research directions. Further, the CO<sub>2</sub> capture performance is summarized in Table 18 and Table 19.

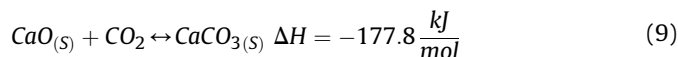
### 3.7.4. Calcium oxide

Calcium oxide has been widely investigated for CO<sub>2</sub> adsorption due to its superior thermodynamic and chemical properties, enhanced regeneration capabilities, as well as its affordability and natural abundance in the form of carbonates like limestone and dolomite [628]. Furthermore, CaO offers durability, low toxicity, recyclability of spent materials, environmental friendliness, the potential for CO<sub>2</sub> removal from flue gases in hydrogen generation processes, high reactivity towards CO<sub>2</sub> across a broad temperature range of 500–900 °C (allowing for heat recovery possibilities), and versatility in fluidized bed applications. Consequently, CaO has been a subject of research for many years [629–634]. The adsorption capacity of calcium oxide is affected by several parameters, including partial pressure of CO<sub>2</sub>, particle size, material morphology, and precursor nature [519,635].

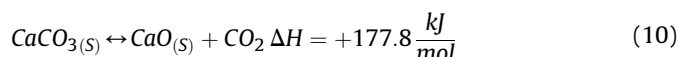
Upon exposure to elevated temperatures, CaO undergoes a reaction with CO<sub>2</sub> on its surface, involving the nucleation and growth of CaCO<sub>3</sub>. The carbonation process of CaO can be divided into two stages: a rapid phase controlled by kinetics, followed by a slower phase controlled by diffusion [636]. Carbonation of CaO concludes once a layer of CaCO<sub>3</sub> accumulates and forms over the unreacted

adsorbent. The carbonated sorbent can be regenerated through calcination, leading to the restoration of CaO, which can be reused for subsequent CO<sub>2</sub> sorption. This approach, known as calcium looping, involves the cyclic utilization of CaO. The underlying chemisorption mechanisms during CO<sub>2</sub> adsorption (carbonation) and desorption (decarbonation/calcination) by CaO are shown below:

Carbonation:



Decarbonation/calcination:



Regrettably, the utilization of calcium oxide as a CO<sub>2</sub> capture material presents several challenges, including the need for a high energy input during regeneration (typically exceeding 800 °C for CaCO<sub>3</sub> decomposition), leading to sintering and mechanical degradation over successive cycles of CaO carbonation and calcination [637]. Additionally, there is a decrease in carbonation kinetics after the initial layer of calcium carbonate forms on the oxide surface, attributed to restricted CO<sub>2</sub> diffusion (a rate-determining step) [638,639]. Ultimately, complications also arise from the structure of high-specific surface area CaO powder during adsorption processes, resulting in increased pressure drop, flow

entrainment, and material attrition in some cases [630]. Extensive research efforts have aimed to address these challenges related to CaO as a CO<sub>2</sub> adsorbent, focusing on improving its stability and recyclability through a variety of techniques.

In 2018, Sun et al. [640] reviewed the progress in the development and application of CaO-based adsorbents for CO<sub>2</sub> capture and provided an understanding of the basic elements of cyclic carbonation/calcium in a systematic way. The authors identified four main strategies for enhancing CO<sub>2</sub> uptake of CaO-based materials, which include producing synthetic CaO with high surface area (employing diverse CaO precursors and refining synthesis techniques), dispersing CaO on inert supports (utilizing bimetallic metal oxides, other metal oxides), applying surface modifications (using organic acids, mineral acids), and improving CO<sub>2</sub> capture during rigorous calcination conditions. Furthermore, they identified several issues that need to be thoroughly addressed during the creation of novel adsorbents. In terms of material stability, nanoparticles with a stable framework and porous structure are critical. Additionally, new CaO-based adsorbents are rarely evaluated under exceptional conditions, such as regeneration at 100% CO<sub>2</sub>, and the challenge of their attrition is infrequently reported. Another consideration is also whether the synthesis is both cost-effective and environmentally friendly.

In the same year, Salaudeen et al. [628] discussed current advances in metal-based solid sorbents with a particular focus on calcium oxide and presented the use of biomass as competitive sources of CaCO<sub>3</sub>. This review showed that adsorbent hydration is

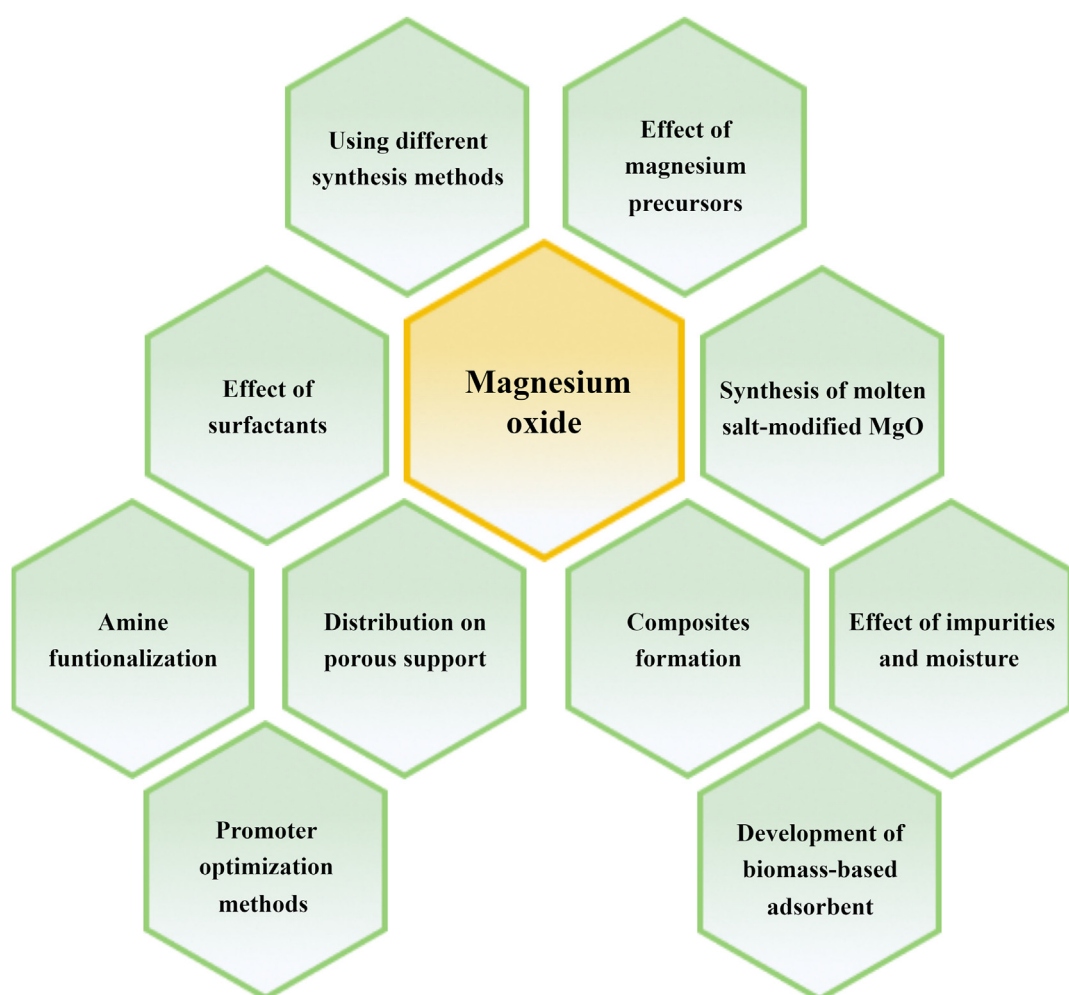


**Fig. 37.** The modification strategies and research directions of magnesium oxide-based adsorbents.

**Table 18**  
An overview of textural properties and CO<sub>2</sub> capture performance of magnesium oxide-based adsorbents synthesized via various methods.

MgO-based adsorbent	BET surface area, m <sup>2</sup> /g	Total pore volume, cm <sup>3</sup> /g	Average pore size (nm)	CO <sub>2</sub> uptake, mmol/g	CO <sub>2</sub> vol %	Adsorption temperature, °C	Pressure, bar	Description of synthesis method	Reference
Rod-like MgO	331	0.575	7.06	1.56	100	25	1	Precipitation method	[597]
Meso-MgO	250	0.53	5.2	1.82	100	25	1	Double-replicate	[598]
Lamellar shaped MgO	686	2.11	4.90	2.34	100	30	1	Aerogel method	[599]
Irregular plateletlike MgO-A	350	0.414	5	0.681	100	30	1	Sol-gel method	[600]
MgO nanoparticles	177	0.823	—	1.49	30	60	1	Flame aerosol method	[601]
MgO	123	0.32	4.11	0.73	10+H <sub>2</sub> O	120	1	Direct calcination (effect of moisture)	[602]
Foam-like MgO	130	0.36	9.9	2.61	100	100	1	One-pot hydrothermal method	[603]
Leaf-like MgO	321	0.3	2.19	0.83	100	300	1	Hydrothermal method (effect of surfactants)	[604]
Nanosheets								Urea hydrolysis	[605]
Mesoporous leaf like MgO	372	0.38	1.84	1.18	100	200	1	Solid state chemical reaction	[606]
Thin sheet-like MgO	100	0.67	—	2.39	10	200	1	Extrusion-spheronisation technique	[607]
Pellet-MgO	33	—	—	0.602	40	232	1	Solution-combustion method	[608]
MgO-SC	5.71	0.0289	12.12	0.39	—	25	1		

an efficient method for regenerating and optimizing multiple reaction cycles. Furthermore, while the stability of CaO-based solid sorbents has been described in literature in the presence of various inert supports or dopants, the fundamental mechanisms of this phenomenon are not yet fully comprehended. To gain a deeper understanding of the principles and potential factors that impact the relationship between sorbent performance and inert support, further research is needed. Concerning the utilization of biomass as a precursor for calcium oxide production, animal shell waste emerges as a potential source. However, conflicting results exist regarding the comparative advantages of calcined shells versus calcined limestone. Addressing this discrepancy might require further experimentation and the application of kinetic modeling. Numerous other studies have also highlighted the potential value of waste biomass. Recently, Nawar et al. [641] exploited waste eggshells to synthesize modified structure CaO through the use of organic acids, demonstrating that eggshells could serve as a cost-effective option for CO<sub>2</sub> adsorption.

In the field of novel research directions in CaO-based materials, there is a discernible increase in the attention being given to the wide exploration of biomass and industrial residues as potential sources for CaCO<sub>3</sub> and support materials. Moreover, the addition of anionic surfactants, or the amine functionalization during synthesis, appears to be a promising approach for enhancing the characteristics. Finally, the impact of process conditions, particularly the influence of moisture on the CO<sub>2</sub> capture efficiency, is being extensively investigated.

Fig. 38 illustrates the existing improvement strategies and ongoing research pathways for CaO-based adsorbents for CO<sub>2</sub> adsorption. Table 20 provides an overview of the performance of CaO-based adsorbents in CO<sub>2</sub> capture applications, categorized based on the main modification strategies employed.

### 3.7.5. Cerium oxide

Cerium oxide, also referred to as ceria, has been extensively studied and has garnered significant attention within the field of catalysts and catalytic supports [658]. Ceria demonstrates distinctive attributes in relation to its structural and thermal properties. These characteristics encompass extensive accessible surface area, rigid frameworks, notable interaction with CO<sub>2</sub> molecules at ambient conditions (exhibiting Lewis-base active site properties), orderly distribution of pore sizes, substantial capacity for oxygen storage, and straightforward redox reaction [659–663].

Numerous efforts have been made to enhance the catalytic activity of ceria by increasing its thermal stability and surface area through the use of organized porous structures. The interaction of cerium oxide with carbon dioxide has also been thoroughly characterized [664–667]. However, despite ceria's ability to adsorb and desorb CO<sub>2</sub> under ambient conditions, its practical application in CO<sub>2</sub> capture hasn't been adequately investigated, particularly in terms of adsorption capacity and the influencing factors.

In 2014, Yoshikawa et al. [668] detailed the synthesis and analysis of cerium oxide-based adsorbents, providing the first coherent measurement of CO<sub>2</sub> uptake. The authors investigated CO<sub>2</sub> capture materials derived from various single metal oxides (SiO<sub>2</sub>, Al<sub>2</sub>O<sub>3</sub>, ZrO<sub>2</sub>). CeO<sub>2</sub> exhibited the highest CO<sub>2</sub> adsorption capacity, achieving 0.132 mmol/g at 50 °C, along with its specific surface area of 166 m<sup>2</sup>/g. Furthermore, the experimental results have revealed essential insights into the factors that play a significant role in influencing the number of available CO<sub>2</sub> adsorption sites as well as the overall CO<sub>2</sub> uptake of metal oxide materials. It was emphasized that these encompass synthesis conditions, precursor choices that could introduce surface contaminants hindering CO<sub>2</sub> adsorption, and material attributes including morphology, particle sizes, porosity, and surface area.

**Table 19**

A summary of the modification strategies applied to magnesium oxide-based adsorbents and their impact on textural properties and CO<sub>2</sub> adsorption uptake.

MgO adsorbent	BET surface area, m <sup>2</sup> /g	Total pore volume, cm <sup>3</sup> /g	Average pore size (nm)	CO <sub>2</sub> uptake, CO <sub>2</sub> , vol % mmol/g	Adsorption temperature, °C	Pressure, bar	Description of promoter used in modification	Reported modification	Reference
Mesoporous MgO	95.8	0.22	9.09	6.25	100	350	10	—	[609]
Mesoporous MgO	250	0.53	4.3	1.81	100	25	1	Mesoporous carbon obtained from mesoporous SBA-15	Effect of the magnesium precursor [598]
MgO–Fe	15.85	0.1387	9.20	0.90	—	25	1	Fe	Metal doping [608]
MgO–Ni	30.83	0.1588	4.20	1.50	—	25	1	Ni	[608]
MgO–mPC	306	0.156	2.03	5.45	100	80	—	Mesoporous carbon	Distribution on porous supports [610]
MgO–OMC	598.9	0.58	2.20	2.09	100	25	1	Mesoporous carbon	[611]
MgO (20 wt%)-RHA	39.5	0.12	—	4.56	10	200	—	Biomass wastes (rice husk ash)	[612]
MgO (20 wt%)/MCM-41	390	0.27	2.24	1.06	100	25	1	Mesoporous silica	[613]
Mesoporous carbon supported MgO	421	0.40	3.8	1.68	—	25	1	Mesoporous carbon derived from biomass	[614]
MgO/γ-Al <sub>2</sub> O <sub>3</sub>	225.5	0.52	3.41	2.10	10	60	1	γ-Al <sub>2</sub> O <sub>3</sub>	[615]
MgO/Al <sub>2</sub> O <sub>3</sub>	200.91	0.60	17.3	0.97	13	60	1	Al <sub>2</sub> O <sub>3</sub>	[557]
PAC4/15%MgO	1623	1.43	3.53	3.86	10	25	1	Biomass-derived activated carbon	[616]
MgO/Al <sub>2</sub> O <sub>3</sub>	200.91	0.60	17.3	1.36	13	60	1	Al <sub>2</sub> O <sub>3</sub>	Distribution on porous supports; Moisture effect [557]
PAC4/10%MgO–5%Al <sub>2</sub> O <sub>3</sub>	1605	1.33	3.31	4.50	10	25	1	Biomass-derived activated carbon; Al <sub>2</sub> O <sub>3</sub>	Distribution on porous supports; Mixed metal oxides formation [616]
Ordered mesoporous MgO/carbon spheres composites	355.6	0.22	2.7	3.08	—	0	1.2	Carbon spheres	Composite formation [617]
MgO–ZrO <sub>2</sub>	180	—	5–10	1.15	100	300	1	ZrO <sub>2</sub>	Mixed metal oxides formation [618]
MgO/CaO	21.4	0.173	38.4	9.49	20	650	1	CaO	[619]
MgO/FeO	177	0.20	3.0	0.795	14	200	1	FeO	[620]
Mg–Na double salts	1.26	—	—	3.48	100	375	1	Na <sub>2</sub> CO <sub>3</sub>	Synthesis of molten salt-modified MgO [621]
(Li <sub>0.3</sub> Na <sub>0.6</sub> K <sub>0.1</sub> )NO <sub>3</sub> ·MgO	65.8	0.438	—	16.8	100	300	1	LiNO <sub>3</sub> , NaNO <sub>3</sub> , KNO <sub>3</sub>	[622]
MgO-[Li <sub>0.44</sub> K <sub>0.56</sub> ]NO <sub>3</sub> ] <sub>2</sub> [(Na <sub>0.5</sub> K <sub>0.5</sub> )CO <sub>3</sub> ]	—	—	—	19.06	100	325	1	KNO <sub>3</sub> , LiNO <sub>3</sub> , K <sub>2</sub> CO <sub>3</sub> , Na <sub>2</sub> CO <sub>3</sub>	[623]
MgO–NaNO <sub>2</sub>	16	—	—	15.7	100	350	1	NaNO <sub>2</sub>	[624]
MgO–NaNO <sub>3</sub>	67	0.29	—	11.2	10	260	1	NaNO <sub>3</sub>	[625]
MgO–CaCO <sub>3</sub>	29.9	0.16	26.1	13.18	100	350	1	CaCO <sub>3</sub>	[626]
TEPA-MgO	19	0.22	1.9	4.98	40	30	1	Tetraethylenepentamine	Amine functionalization [627]
APTES-MgO	134	0.301	9	1.49	100	30	1	(3-Aminopropyl)triethoxysilane	[600]
DETA-MgO	91	0.203	9	1.08	100	30	1	Diethylenetriamine	[600]
PEI-MgO	72	0.178	10	0.54	100	30	1	Polyethylenimine	[600]

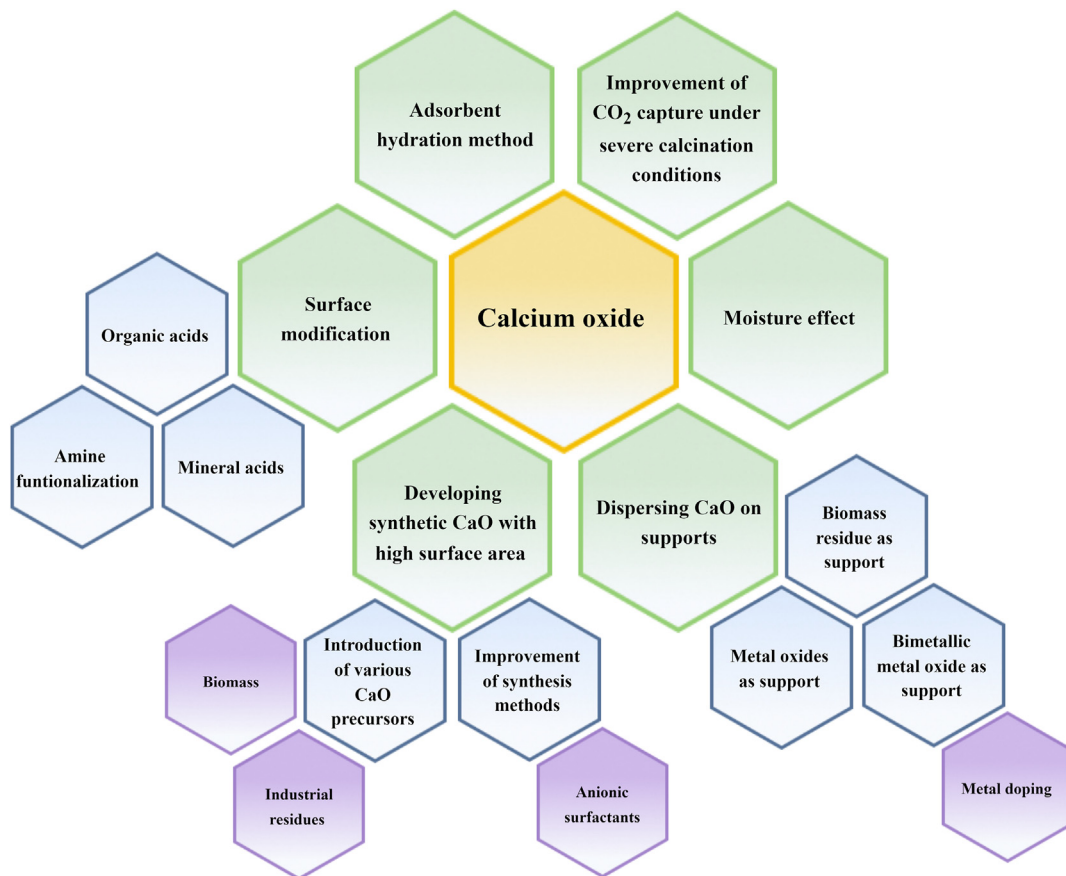


**Fig. 38.** The modification strategies and research directions of calcium oxide-based adsorbents.

In 2015, Li et al. [669] studied mesostructured ceria and ceria doped with Mg, Zr, La, and Cu for CO<sub>2</sub> adsorption prepared using a surfactant-templated method and tested at room temperature. The findings indicated that the adsorption characteristics of the materials are influenced not only by their textural properties but also by their surface chemistry, including acid–base sites and oxygen vacancies. These aspects are affected by the type and content of dopants in the CeO<sub>2</sub>.

In 2017, Słostowski et al. [670] investigated the potential of CeO<sub>2</sub> nanoparticles as CO<sub>2</sub> adsorbents in the form of nanopowders, focusing on their specific surface area. This method resulted in a solid sorbent with a specific surface area of 199 m<sup>2</sup>/g. Additionally, it showed a maximum CO<sub>2</sub> adsorption capacity of approximately 1.13 mmol/g at 25 °C and 1 pressure. The possibility of cycling CO<sub>2</sub> adsorption/desorption was also explored. Initial research indicated the feasibility of adsorbing CO<sub>2</sub> at 25 °C and nearly completely regenerating the material at 150 °C in an inert gas environment without compromising the CO<sub>2</sub> capture capability. Therefore, CeO<sub>2</sub> with substantial specific surface areas hold great promise as potential candidates for low-temperature reversible CO<sub>2</sub> capture materials in the future.

In 2020, Azmi et al. [671] further elaborated on the amine functionalization (APTMS) of mesoporous ceria nanoparticles (MCN) for CO<sub>2</sub> capture. The introduction of APTMS functional groups onto MCN enhanced the availability of CO<sub>2</sub> binding sites, evident through the formation of carbamate species upon CO<sub>2</sub> interaction with the NH groups. As a result, the adsorption capacity increased by up to tenfold compared to the pristine oxide. However, the addition of APTMS to the MCNs led to a reduction in their textural properties. This decrease is attributed to the functionalization and blocking effect of APTMS molecules within the MCN support.

**Fig. 39** presents an up-to-date overview of the current modification strategies and research trends of CeO<sub>2</sub>-based adsorbents.

#### 4. Techno-economic analysis (TEA) of CO<sub>2</sub> capture materials

A CO<sub>2</sub> sorption-based process utilizing the efficient and cost-effective adsorbents has the potential to yield significant technological and economic advantages. In line with ongoing theoretical and practical research, there appear to be distinct categories of materials exhibiting remarkable CO<sub>2</sub> capture capabilities. Primarily, newly synthesized materials intended for industrial applications must demonstrate efficacy within specific technological regeneration configurations (in terms of pressure, temperature, electricity, or combined cycles) and in various gas–solid contactors (such as fixed, fluidized, moving, or rotating beds). This assessment is pivotal, as it ultimately determines whether a technology based on a particular adsorbent type can be economically viable for CO<sub>2</sub> capture from flue gas in power plants. Integrated capture and separation processes incur the most costs, making careful analysis imperative prior to scaling up and introducing the technology at manufacturing scale. Consequently, in order to facilitate a systematic and equitable comparison of CO<sub>2</sub> separation technologies, and to comprehensively understand the techno-economic impacts associated with implementing CO<sub>2</sub> capture systems across diverse industries, techno-economic analysis is extremely essential.

In many cases of TEA, it's important to adopt a real model of a coal-fired power plant at a specific scale, proportionally reflecting the electricity generation rate. This is closely associated with the amount of fossil fuel consumption and, consequently, the resulting CO<sub>2</sub> emissions into the atmosphere. The Emissions and Generation Resource Integrated Database (eGRID) of U.S. EPA (Environmental

**Table 20**A summary of the modification strategies applied to calcium oxide-based adsorbents and their impact on textural properties and CO<sub>2</sub> adsorption capacity.

Calcium oxide-based adsorbents.	Methods	BET surface area, m <sup>2</sup> /g	Total pore volume, cm <sup>3</sup> /g	Average pore size (nm)	Carbonation conditions (adsorption)			Calcination conditions (desorption)			Number of implemented cycles to test adsorbent	CO <sub>2</sub> uptake mmol/g	Material	Improvement strategy	Reference
CaO-based pellets	—	15.6	0.063	—	650	15% CO <sub>2</sub> (N <sub>2</sub> balance)	20	850	100% N <sub>2</sub>	120	—	11.4	Powdered limestone	Introduction of various CaO precursor	[642]
CaO-based carbide sledge	Bubbling methods	~11.3	—	—	750	100% CO <sub>2</sub>	60	900	100% He	90	15	14.09	Carbide slag		[643]
Eggshell-Ca(OH) <sub>2</sub> -CaO	Calcination Sol-gel method	84.37	0.25	7.6	700	100% CO <sub>2</sub>	10	900	100% CO <sub>2</sub>	5	10	14.32	Eggshell waste		[644]
CaO		—	—	—	650	15% CO <sub>2</sub> (N <sub>2</sub> balance)	15	800	100% N <sub>2</sub>	10	20	11.59	CaO by sol-gel process	Improvement of synthesis method	[645]
CaO-gemini surfactant	Precipitation method	16.3	0.059	14.5	600	15% CO <sub>2</sub> (N <sub>2</sub> balance)	—	850	—	—	5	6.59	Sodium dodecyl sulfate (SDS) surfactant		[646]
CaO-SDS surfactant	Precipitation method	9.4	0.036	15.0	600	15% CO <sub>2</sub> (N <sub>2</sub> balance)	—	850	—	—	5	6.14	Gemini surfactant		[646]
Mn-promoted CaO	Sol-gel method	17.72	0.0222	4.88	600	100% CO <sub>2</sub>	60	700	100% H <sub>2</sub>	60	10	15.43	Mn	Dispersing CaO on inert supports	[647]
CaO/Y <sub>2</sub> O <sub>3</sub>	Sol-gel combustion method	25	0.115	—	650	20% CO <sub>2</sub> (N <sub>2</sub> balance)	30	900	100% N <sub>2</sub>	5	10	11.1	Y <sub>2</sub> O <sub>3</sub>		[648]
CaO/Ca <sub>9</sub> Al <sub>6</sub> O <sub>18</sub>	Citric acid method	958	0.85	5	600	20% CO <sub>2</sub> (N <sub>2</sub> balance)	20	850	100% N <sub>2</sub>	10	100	13.64	Al <sub>2</sub> O <sub>3</sub>		[649]
Mesocellular siliceous foam (MCF)-supported CaO	—	12.9	0.06	—	700	100% CO <sub>2</sub>	30	900	100% N <sub>2</sub>	15	5	4.00	Mesocellular siliceous foam		[650]
CaO/KIT-6	Non-ionic surfactant templating method	2.9	0.007	—	600	15% CO <sub>2</sub> (N <sub>2</sub> balance)	30	800	100% N <sub>2</sub>	10	10	7.6	Mesoporous silica (KIT-6)	Dispersing CaO on inert supports	[651]
CaO/Ca <sub>12</sub> Al <sub>14</sub> O <sub>33</sub>	Hydrothermal method	9.2	0.08	—	500	15% CO <sub>2</sub> , 47% H <sub>2</sub> O (N <sub>2</sub> balance)	10	920	21% CO <sub>2</sub> , 78% H <sub>2</sub> O (N <sub>2</sub> balance)	3	40	4.77	Al <sub>2</sub> O <sub>3</sub>		[652]
CaO/Ca <sub>12</sub> Al <sub>14</sub> O <sub>33</sub> nanoCaO/CaTiO <sub>3</sub>	Sol-gel method	13	0.09	—	750	50% CO <sub>2</sub> (N <sub>2</sub> balance)	6	750	100% N <sub>2</sub>	—	30	7.05	Al <sub>2</sub> O <sub>3</sub>		[653]
CaO/MgO	Coating method	6.13	—	10.15	600	20% CO <sub>2</sub> (N <sub>2</sub> balance)	10	750	100% N <sub>2</sub>	10	40	5.3	TiO <sub>2</sub>		[578]
	Wet mixing combustion synthesis	—	—	—	650	15% CO <sub>2</sub> (N <sub>2</sub> balance)	15	850	100% N <sub>2</sub>	10	50	9.09	MgO		[633]
CaO/Ca <sub>12</sub> Al <sub>14</sub> O <sub>33</sub> -gemini surfactant	Precipitation method	17	0.0035	8.42	600	15% CO <sub>2</sub> (N <sub>2</sub> balance)	—	850	—	—	5	7.05	Al <sub>2</sub> O <sub>3</sub>		[646]
Charcoal-supported CaO (1:4 mass ratio)	Sol-gel method	63.6	0.166	10.45	600	15% CO <sub>2</sub> (N <sub>2</sub> balance)	25	650	100% N <sub>2</sub>	30	10–30	15.1	Charcoal		[654]
Charcoal-supported CaO (1:4 mass ratio)	Wet impregnation method	18.0	0.044	9.88	600	15% CO <sub>2</sub> (N <sub>2</sub> balance)	25	650	100% N <sub>2</sub>	30	10–30	5.7	Charcoal		[654]
Al-doped CaO	Precipitation method	12	0.066	—	650	14.9% CO <sub>2</sub> , 3.6% O <sub>2</sub> , 8.8% H <sub>2</sub> O (N <sub>2</sub> balance)	20	900	100% N <sub>2</sub>	5	30	5.4	Al <sub>2</sub> O <sub>3</sub>		[655]
CaO/NiO	Sol-gel combustion method	12.8	0.11	—	750	15% CO <sub>2</sub> (N <sub>2</sub> balance)	25	—	5% H <sub>2</sub> (N <sub>2</sub> balance)	—	20	15.0	NiO		[656]
Ca <sub>1</sub> Ni <sub>0.1</sub> Ce <sub>0.017</sub> (molar ratio)	Sol-gel combustion method	22.5	0.20	—	750	15% CO <sub>2</sub> (N <sub>2</sub> balance)	25	—	5% H <sub>2</sub> (N <sub>2</sub> balance)	—	20	14.2	NiO, CeO	Dispersing CaO on inert supports	[656]
Ca <sub>1</sub> Ni <sub>0.1</sub> Ce <sub>0.033</sub> (molar ratio)	Sol-gel combustion method	20.7	0.14	—	750	15% CO <sub>2</sub> (N <sub>2</sub> balance)	25	—	5% H <sub>2</sub> (N <sub>2</sub> balance)	—	20	14.1	NiO, CeO		[656]
Formic acid-modified (10 vol%) CaO-based adsorbent	—	2.91	0.0071	6.82	650	15% CO <sub>2</sub> (N <sub>2</sub> balance)	20	850	100% N <sub>2</sub>	5	20	13.63	Formic acid	Surface modification	[657]
Citric acid-modified (10 vol%) CaO	—	5.23	0.022	2.134	650	15% CO <sub>2</sub> (N <sub>2</sub> balance)	5	850	100% N <sub>2</sub>	5	20	8.64	Citric acid		[641]
Acetic acid-modified (10 vol%) CaO	—	4.45	0.021	6.126	650	15% CO <sub>2</sub> (N <sub>2</sub> balance)	5	850	100% N <sub>2</sub>	5	20	~8.41	Acetic acid		[641]
Formic acid-modified (10 vol%) CaO	—	9.38	0.023	2.368	650	15% CO <sub>2</sub> (N <sub>2</sub> balance)	5	850	100% N <sub>2</sub>	5	20	~8.41	Formic acid		[641]
PDA-CaO	Calcination	62.56	0.40	12.6	700	100% CO <sub>2</sub>	10	900	100% CO <sub>2</sub>	5	10	14.09	Pyridine dithioethylamine		[644]

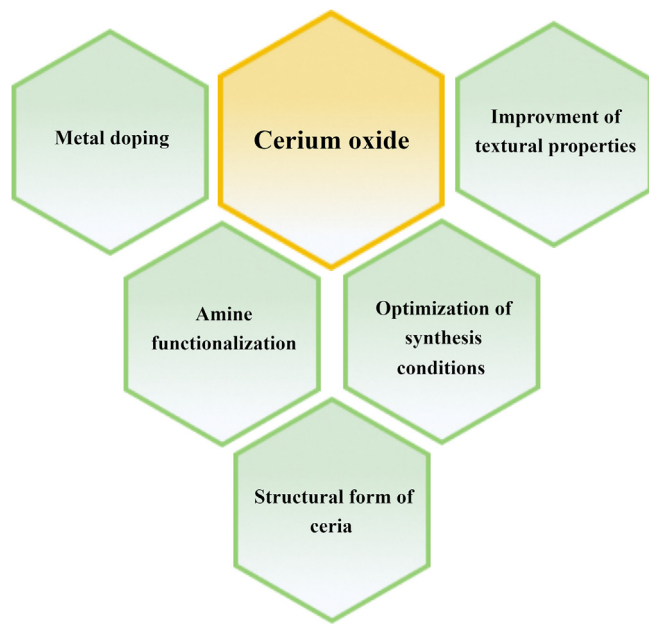


**Fig. 39.** The modification strategies and research directions of cerium oxide-based adsorbents.

Protection Agency) released in 2018, revealed that natural gas units have an average CO<sub>2</sub> emission rate of 407 kg/MWh, while coal units have an average CO<sub>2</sub> emission rate of 989 kg/MWh [672]. Hanak and Manovic [673] determined the technical and economic feasibility of a CO<sub>2</sub> capture system utilizing a molecularly imprinted polymer sorbent based on acrylamide (MIP) within the context of retrofitting a 580 MW coal-fired power plant. The cost of CO<sub>2</sub> avoided was calculated to be 29.3 £/ton of CO<sub>2</sub>. This performance, compared to a CO<sub>2</sub> capture system employing chemical solvents, exhibited superior techno-economic viability. Parametric studies indicated that the sorbent capacity had the most significant impact on the thermodynamic performance of the polymer. Furthermore, the economic performance was influenced not only by the sorbent capacity but also significantly by its cyclic performance. The analysis findings demonstrated a linear relationship between the cost of CO<sub>2</sub> avoided and increasing MIP sorbent makeup, at a rate of 6.8 £/tCO<sub>2</sub> for each one-tenth percent increase in sorbent makeup.

As mentioned earlier in this review, there are several regeneration technologies that are commonly employed during the CO<sub>2</sub> capture process, including PSA, VSA, VPSA, TSA, TPSA, and ESA.

Zanco et al. [674] prepared a comparative techno-economic evaluation for the post-combustion CO<sub>2</sub> capture process based on mature technology for CO<sub>2</sub> separation, such as adsorption using zeolite 13X in conventional fixed beds (either VSA or TSA). The analysis assumed a carbon dioxide source emitting 12% CO<sub>2</sub> v/v (with 95% relative humidity at the inlet conditions of 30 °C and 1.3 bar) to produce a CO<sub>2</sub> stream with 96% purity. Techno-economic assessment revealed that while the studied adsorption process might achieve cost competitiveness on a small scale, particularly for very low recovery rates and small plant sizes, overcoming a significant cost gap is necessary to establish the adsorption process as economically viable. Notably, cost components related to flue gas pre-drying contribute significantly to this disparity. In this context, innovative water-resistant adsorbents combined with more complex process configurations could potentially reverse the observed cost trends. Furthermore, the research highlighted that the unit cost of the commercial adsorbent has a considerably lower impact on investment costs compared to geometric constraints related to

the size and shape of adsorption columns. Finally, optimization of the Pareto front demonstrated that the productivity index is affected by factors such as the volume of zeolite 13X and the metal used in forming the adsorption columns.

Subraveti et al. [675] also conducted a TEA analysis for post-combustion CO<sub>2</sub> capture with cyclic process. Their goal was to determine the cost limitations of PVSA cycles assuming the creation of a 'perfect' cost-free adsorbent. Employing various carbon dioxide compositions and industrial flue gas flow rates as inputs, the researchers enhanced adsorbent characteristics (such as adsorption isotherms and particle morphology) and process design parameters. The objective aimed to examine the lowest possible CO<sub>2</sub> avoidance cost, excluding CO<sub>2</sub> conditioning, transport, and storage expenses. The obtained results revealed insights into the CO<sub>2</sub> concentration in the flue gas significantly influencing the cost limitations of PVSA. The lowest potential CO<sub>2</sub> avoidance costs decrease as the CO<sub>2</sub> concentration increases. By applying a four-step PVSA cycle and altering the pelletized adsorbent's morphology, CO<sub>2</sub> avoidance costs can be reduced by 9–22%. Optimization highlighted that 'ideal' adsorbents for achieving the lowest CO<sub>2</sub> avoidance costs have reasonably linear CO<sub>2</sub> adsorption isotherms and minimal N<sub>2</sub> adsorption. The flue gas flow rate notably impacts the complexity of the PVSA plant in terms of train numbers, equipment, piping, and space requirements. The ultimate cost of CO<sub>2</sub> avoided for PVSA varied from 87.1 to 10.4 €/tonne, corresponding to CO<sub>2</sub> feed concentration of 3.5–30 mol%. When compared with a monoethanolamine-based absorption method, the findings indicated that PVSA could be a potentially favorable separation technique for flue gas streams with high CO<sub>2</sub> concentrations.

PSA technique has also been explored to assess its viability for recovering CO<sub>2</sub> from post-combustion power plant flue gases. In 2008, Ho et al. [676] used commercial adsorbents, including zeolite 13X with a working capacity of 2.2 mol/kg and a CO<sub>2</sub>/N<sub>2</sub> selectivity of 54, to evaluate high-pressure feed and vacuum desorption in their analysis. By utilizing vacuum desorption, the capture cost was reduced from 57 to 51 \$/tonne of CO<sub>2</sub> avoided. With this method, both an 85% CO<sub>2</sub> recovery rate and a product that was 46% CO<sub>2</sub> enriched were achievable. Moreover, the authors found that when combining the novel adsorbent with enhanced processing cycles like depressurization, adsorber bed equalization, and product purging, a CO<sub>2</sub> avoidance cost as low as 30 \$/tonne could be attainable.

#### 4.1. Techno-economic analysis (TEA): principles and procedures

Given the technological solutions discussed, a solid grasp of key engineering data is imperative for multiple aspects, including the development of CO<sub>2</sub> capture materials, designing installations for CO<sub>2</sub> removal from flue gas at pilot or industrial scales (through computer simulations and numerical methods), and especially conducting techno-economic analyses. As briefly mentioned earlier regarding the future prospects of CO<sub>2</sub> adsorbents, these include the working and equilibrium capacity of beds within a specific temperature, pressure, and adsorbate concentration range in flue gas mixtures. Isothermal and kinetic data derived from mathematical models analyzing experimental points are relevant. Mass transfer considerations during the process, along with identification of diffusion mechanisms that govern the adsorption process (surface diffusion, boundary layer effects, and adsorbate diffusion within the internal porous structure of material), are crucial. Additionally, the thermodynamics of adsorption and characteristics of the adsorbent particles within the bed, as well as

the impact of impurities (such as NO<sub>2</sub>, SO<sub>2</sub>, H<sub>2</sub>S) or moisture in the flue gas undergoing separation, should be considered. When these details are verified as integral components of the overall procedure, the technical and economic phase of the analysis can commence. The most crucial engineering data for conducting TEA are depicted in Fig. 40.

In addition to carbon dioxide capture technologies and cyclic adsorption methods, the choice of bed is also pivotal within TEA. When selecting a bed for a specific technology, its functionality must be carefully analyzed. The utilization of a fluidized bed intensifies mass exchange between the gas mixture flowing through its structure and the solid particles, owing to a substantial interface and effective mixing of the material with the gas phase. This acceleration enhances the adsorption process [677,678]. However, the efficacy of gas mixture contact with the bed during fluidization can be compromised, especially by the agglomeration of bed solids at higher temperatures, resulting from van der Waals intermolecular forces for physical adsorption [679,680]. This phenomenon leads to material heterogeneity, characterized by crack and channel formation in the structure. These channels allow the gas phase to bypass adsorbent particles, rendering the equilibrium of CO<sub>2</sub> adsorption ineffective [681,682]. In contrast, an adsorbent in the form of a fixed bed possesses a compact structure with specific internal and external surfaces and consistent pore morphology. This directly impacts the material's adsorption capacity during the process, resulting in a higher concentration of adsorbent solids compared to a fluidized bed. However, adsorption on a fixed bed also presents challenges, including undesirable heat gradients, process control complexities, and, crucially, difficulties in regeneration during CO<sub>2</sub> desorption.

In 2021, Danaci et al. [683] published guidelines for TEA on adsorption processes, categorizing them into two main sections: technical and economic issues. The aforementioned engineering data forms an integral part of this determination. In each section, the authors presented key factors with substantial influence, along with the consequences of decisions made during the TEA phase and recommended practices. Among these factors, parameters of the bed type were highlighted for comprehensive consideration throughout the procedure and as a reference point for the covered topics. Regarding technical considerations, they highlighted essential aspects that demand attention, as follows:

- Feed flow rates of CO<sub>2</sub> must be accurately determined for appropriate sizing and calculation of process equipment components, process design, and economic assessment. These calculations should reflect the actual flow rate in the specific application.

- Cycle time of the CO<sub>2</sub> capture process, which defines the time required for effective CO<sub>2</sub> adsorption and desorption to enable efficient adsorbent reuse. This factor has an immediate impact on productivity.
- Cycle scheduling, given that adsorption cycles often employ multiple beds for CO<sub>2</sub> capture and separation. This parameter involves effectively managing the cycle of each bed within the installation to meet process requirements.
- Vacuum pump curves, vital for adsorption processes involving vacuum regeneration stages like VPSA. Vacuum pump performance can vary across changing operating conditions.
- Mechanical design considerations, where determining fundamental mechanical aspects of the process equipment design, particularly the thickness of the adsorption columns, is necessary during the TEA stage.
- Evaluation of energy requirements, noting that in adsorption processes, heat input is noticeable during thermal regeneration steps in processes like TSA. Additionally, blowers, compressors, and vacuum pumps demand energy for processes like VPSA.
- Emphasis on the understanding that scaling and equilibrium models should not be used for detailed process design or cost estimation. Instead, they are more aptly suited for deliberate selection to identify the most promising adsorbents.

In terms of process economics, the authors emphasized the importance of several key aspects. These include IBL costing methods (Inside Battery Limits), which focus on the primary process equipment items involved in converting the feed into the final product. The authors also highlighted the significance of novel technologies. For instance, fluidized beds for moving bed TSA and rotary adsorbers for continuous TSA are being explored for adsorption processes. Additionally, estimating the cost of the adsorbent, particularly when it's not yet commercialized, can be contentious, underscoring the importance of concentrating on scale-up considerations. Lastly, the concern of other capital costs completes the spectrum of factors.

Overall, a significant objective of TEA studies is to develop cost-effective process equipment designs tailored to the physical and chemical properties of the adsorbent. Moreover, the wide array of regeneration technologies available in different modes, process conditions, reactor configurations, and types of adsorbents offers substantial potential for process enhancement. In a broader sense, given their affordability, widespread availability, and versatility across various applications, CO<sub>2</sub> capture materials emerge as an intriguing choice for CCUS technologies. Furthermore, key aspects related to scaling up and the barriers that require addressing for the successful commercialization of a given adsorbent have been highlighted.

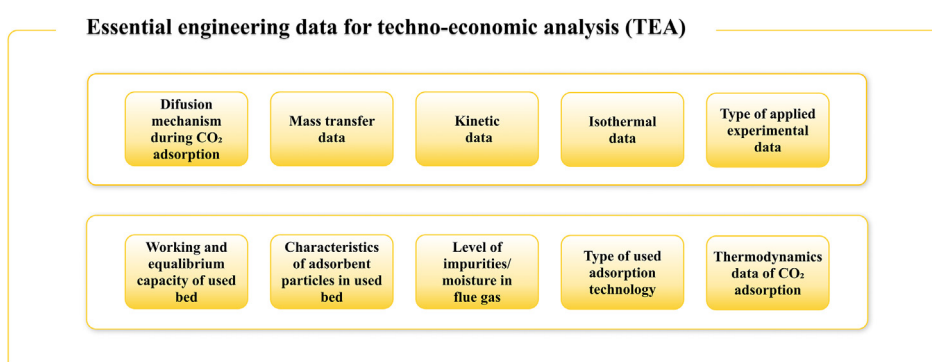


**Fig. 40.** Essential engineering data for techno-economic analysis.

## 5. Summary and future directions

This review thoroughly addresses the latest modification strategies, scientific advancements, and future research directions concerning selected CO<sub>2</sub> capture materials under investigation at various scales. These solid CO<sub>2</sub> adsorbents exhibit considerable potential for CO<sub>2</sub> removal from flue gas, offering advantages over traditional liquid amine absorption methods in terms of regeneration energy efficiency and cost-effectiveness. However, they also confront certain limitations and challenges that need to be overcome before they can be scaled up for diverse industrial applications, defining the specific knowledge gaps for each material type. Among the existing adsorbents, critical parameters for improvement include working adsorption capacity, reduced production costs, cycle longevity, thermal stability, resistance to moisture and impurities, and durability across multiple cycles. To achieve technologically and economically viable systems, novel porous materials with modified strategies have been developed to enhance CO<sub>2</sub> capture capabilities significantly. This emphasizes the importance of collecting data on factors influencing effective adsorption system design, an aspect warranting special attention. In-depth analysis of these factors enables a more accurate portrayal of carbon dioxide adsorption behavior on individual materials, identifying parameters impacting performance such as temperature, CO<sub>2</sub> concentration or partial pressure in the flue gas, thermodynamic attributes of the process, controlling mass transport rates, textural properties of the adsorbent bed (specific surface area, chemical properties, porosity, pore volume), moisture and impurity levels in the flue gas stream, and thorough theoretical evaluations. Furthermore, scrutinizing these criteria for a specific adsorbent application can yield cost reductions in CO<sub>2</sub> capture. Additionally, adsorbents are routinely evaluated for their capacity, selectivity, and regenerability across multiple cycles. Understanding their mechanisms, which precisely elucidate the interactions between adsorbent and adsorbate, as well as CO<sub>2</sub> storage within their structures, is crucial. An approach to address this involves integrating structural, sorption equilibrium, kinetics, spectroscopic, and thermodynamic studies with molecular simulations and modeling of adsorption equations. This combination validates theoretical assumptions and offers valuable insights for facilitating their scalable implementation. Another crucial aspect of this review lies in the techno-economic analysis of various CO<sub>2</sub> capture materials in practical applications, a topic extensively discussed. The results unequivocally highlight the promise and necessity of such analyses in assessing the actual viability of adsorbent use across industries. Within each section of the TEA, specific criteria are essential considerations during its execution.

In conclusion, this paper highlights several performance indicators and outlines directions for future research activities in the field of CO<sub>2</sub> capture materials, as follows:

- Simplify the synthesis process to reduce production costs, shorten preparation time, and facilitate parameter analysis affecting adsorbent characteristics.
- Explore existing synthesis methods to identify optimal conditions, parameters specific to adsorbent groups, and innovative material structures for enhanced CO<sub>2</sub> uptake.
- Enhance new synthesis methods that utilize affordable raw materials and chemicals, significantly lowering production costs (e.g., waste biomass, industrial byproducts).
- Focus on environmentally friendly synthesis approaches using ecologically safe solvents to minimize ecological impact and energy consumption.

- Emphasize materials with highly developed specific surface area, mesoporosity, and microporosity to improve CO<sub>2</sub> adsorption kinetics and equilibrium working capacity.
- Select the most suitable adsorbent type for specific industrial applications, considering synthesis approach, material cost, production process, life cycle evaluation, and modification strategies.
- Improve resistance of materials to moisture, NO<sub>x</sub>, and SO<sub>x</sub> in flue gas by investigating long-term effects and concentrations of these factors, especially for zeolites, silica-based adsorbents, and MOFs.
- Study the close interaction and influence of water vapor and impurities on CO<sub>2</sub> uptake, essential for optimizing CO<sub>2</sub> removal from flue gases.
- Develop a research reference path for mature adsorbent types, covering process conditions, preparation, and chemical characteristics, applicable to novel and innovative materials.
- Focus on reducing textural degradation during adsorption and desorption operations, particularly for metal oxides, to enhance thermal stability.
- Conduct CO<sub>2</sub> capture tests under real flue gas conditions, such as low pressure, high temperature, certain moisture levels, or using different types of adsorbent beds.
- Research well-known and new materials for composite synthesis, contributing to a comprehensive database and selection of modification strategies.
- Investigate natural materials, biomass residues, and industrial waste as raw materials for cost-effective CO<sub>2</sub> capture material synthesis, aligning with waste management and circular economy principles.
- Explore biomass as a support material for enhancing the dispersion of metal oxides in modification processes.
- Create a comprehensive engineering data database for specific material groups to enhance TEA analysis.
- Develop general guidelines for CO<sub>2</sub> capture materials within suitable process condition ranges (temperature, pressure, gas concentration, desired CO<sub>2</sub> purity), application types (pre-combustion capture, post-combustion capture, and oxy-fuel combustion), textural properties, and performance criteria.
- Utilize techno-economic analysis to compare promising adsorbents for industrial purposes, outlining criteria specific to different material groups, technological variants, scalability, and stability costs.

In summary, the considerations presented in this review demonstrate clear trends in CO<sub>2</sub> capture materials research and modifications, evident from the substantial number of published papers between 2017 and 2021. Various types of CO<sub>2</sub> adsorbents, including carbon-based materials, amine-based materials, MOFs, silica, zeolites, alumina, and polymers, have been developed to varying degrees. When comparing their developmental paths and research trends, certain commonalities and patterns emerge, suggesting the relevance of a generic approach to sorbent development. The general approach for creating novel CO<sub>2</sub> capture materials is shown in Fig. 41. A prominent research trend involves the utilization of waste biomass and industrial residues as raw materials, aligning with green synthesis principles. This calls for a detailed analysis of their thermochemical conversion to obtain intermediates like biochar or hydrochar, characterized by specific elemental composition and solid phase percentages. Furthermore, the activation process plays a crucial role in enhancing specific surface area and porosity. Another notable research avenue is the functionalization of amines, a widely adopted technique extensively documented in literature. Adsorbents modified through this approach exhibit comparable CO<sub>2</sub> uptake values to materials with more time-consuming and costly synthesis procedures. Another

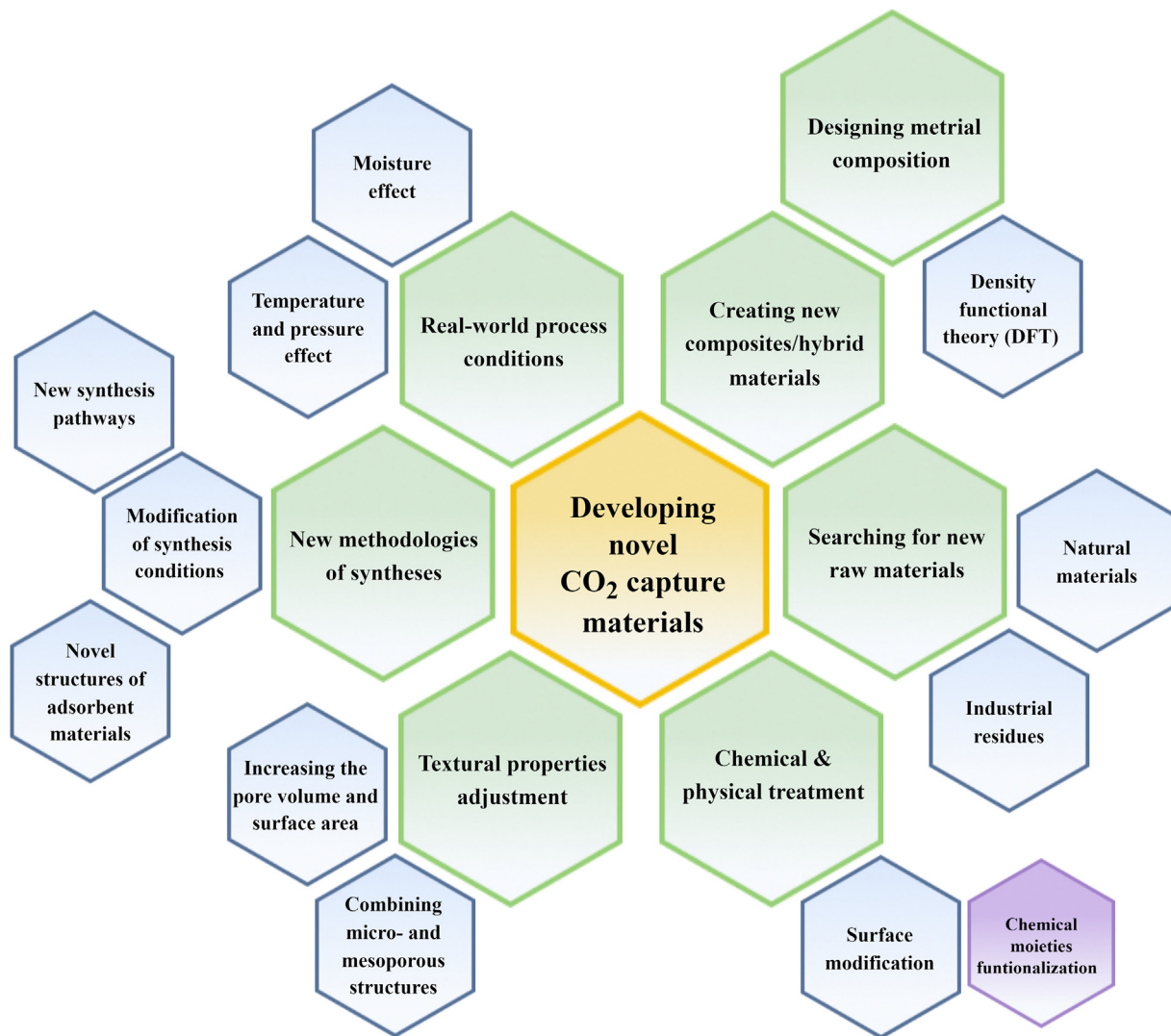


**Fig. 41.** The generic research paths for the development of novel CO<sub>2</sub> capture materials.

research direction involves the creation of hybrid materials based on diverse adsorbents, yielding unique properties for CO<sub>2</sub> adsorption from flue gases. In conclusion, a key recommendation and knowledge gap in CO<sub>2</sub> capture materials research is the combination of the aforementioned methodologies.

#### Credit author statement

Bartosz Dziejarski: Conceptualization, Methodology, Validation, Formal analysis, Investigation, Data curation, Writing – original draft, Writing – review & editing, Visualization, Project administration.

Jarosław Serafin: Investigation, Writing – original draft.

Renata Krzyżyska: Conceptualization, Investigation, Supervision.

Klas Andersson: Conceptualization, Investigation, Supervision.

#### Declaration of competing interest

The authors declare that they have no known competing financial interests or personal relationships that could have appeared to influence the work reported in this paper.

#### Data availability

No data was used for the research described in the article.

#### References

- [1] T.R. Anderson, E. Hawkins, P.D. Jones, CO<sub>2</sub>, the greenhouse effect and global warming: from the pioneering work of Arrhenius and Callendar to today's Earth System Models, *Endeavour* 40 (3) (2016) 178–187, <https://doi.org/10.1016/j.endeavour.2016.07.002>.
- [2] V. Ramanathan, Y. Feng, Air pollution, greenhouse gases and climate change: global and regional perspectives, *Atmos. Environ.* 43 (1) (2009) 37–50, <https://doi.org/10.1016/j.atmosenv.2008.09.063>.
- [3] S.I. Seneviratne, N. Nicholls, D. Easterling, C.M. Goodess, S. Kanae, J. Kossin, Y. Luo, J. Marengo, K. McInnes, M. Rahimi, M. Reichstein, A. Sorteberg, C. Vera, X. Zhang, Changes in climate extremes and their impacts on the natural physical environment, in: C.B. Field, V. Barros, T.F. Stocker, D. Qin, D.J. Dokken, K.L. Ebi, M.D. Mastrandrea, K.J. Mach, G.-K. Plattner, S.K. Allen, M. Tignor, P.M. Midgley (Eds.), *Managing the Risks of Extreme Events and Disasters to Advance Climate Change Adaptation. A Special Report of Working Groups I and II of the Intergovernmental Panel on Climate Change (IPCC)*, Cambridge University Press, Cambridge, UK, and New York, NY, USA, 2012, pp. 109–230.
- [4] Summary for Policymakers, in: V. Masson-Delmotte, P. Zhai, H.O. Pörtner, D. Roberts, J. Skea, P.R. Shukla, A. Pirani, W. Moufouma-Okia, C. Péan, R. Pidcock, S. Connors, J.B.R. Matthews, Y. Chen, X. Zhou, M.I. Gomis, E. Lonnoy, T. Maycock, M. Tignor, T. Waterfield (Eds.), *Global Warming of 1.5°C. An IPCC Special Report on the Impacts of Global Warming of 1.5°C*

- above Pre-industrial Levels and Related Global Greenhouse Gas Emission Pathways, in the Context of Strengthening the Global Response to the Threat of Climate Change, Sustainable Development, and Efforts to, Eradicate Poverty, Cambridge University Press, Cambridge, UK and New York, NY, USA, 2018, pp. 3–24, <https://doi.org/10.1017/9781009157940.001>.
- [5] IEA, Global Energy Review 2021, IEA, Paris, 2021. <https://www.iea.org/reports/global-energy-review-2021>.
- [6] IPCC, 2022: summary for Policymakers, in: P.R. Shukla, J. Skea, R. Slade, A. Al Khourdajie, R. van Diemen, D. McCollum, M. Pathak, S. Some, P. Vyas, R. Fradera, M. Belkacemi, A. Hasija, G. Lisboa, S. Luz, J. Malley (Eds.), Climate Change 2022: Mitigation of Climate Change. Contribution of Working Group III to the Sixth Assessment Report of the Intergovernmental Panel on Climate Change, Cambridge University Press, Cambridge, UK and New York, NY, USA, 2022, <https://doi.org/10.1017/9781009157926.001>.
- [7] IEA, Transforming Industry through CCUS, IEA, Paris, 2019. <https://www.iea.org/reports/transforming-industry-through-ccus>.
- [8] B.P. Spigarelli, S.K. Kawatra, Opportunities and challenges in carbon dioxide capture, *J. CO<sub>2</sub> Util.* 1 (2013) 69–87, <https://doi.org/10.1016/j.jcou.2013.03.002>.
- [9] F.M. Orr Jr., CO<sub>2</sub> capture and storage: are we ready? *Energy Environ. Sci.* 2 (5) (2009) 449–458, <https://doi.org/10.1039/B822107N>.
- [10] J.D. Figueiroa, T. Fout, S. Plasynski, H. McIlvried, R.D. Srivastava, Advances in CO<sub>2</sub> capture technology—the US Department of Energy's carbon sequestration Program, *Int. J. Greenh. Gas Control* 2 (1) (2008) 9–20, [https://doi.org/10.1016/S1750-5836\(07\)00094-1](https://doi.org/10.1016/S1750-5836(07)00094-1).
- [11] M. Pardakhti, T. Jafari, Z. Tobin, B. Dutta, E. Moharreri, N.S. Shemshaki, S. Suib, R. Srivastava, Trends in solid adsorbent materials development for CO<sub>2</sub> capture, *ACS Appl. Mater. Interfaces* 11 (38) (2019) 34533–34559, <https://doi.org/10.1021/acsmami.9b0487>.
- [12] J. Rouquerol, F. Rouquerol, P. Llewellyn, G. Maurin, K.S. Sing, Adsorption by Powders and Porous Solids: Principles, Methodology and Applications, Academic Press, 2013, <https://doi.org/10.1016/C2010-0-66232-8>.
- [13] M. Ghaedi (Ed.), Adsorption: Fundamental Processes and Applications, Academic Press, 2021, <https://doi.org/10.1016/B978-0-12-818805-7.00001-1>.
- [14] R.T. Yang, Gas Separation by Adsorption Processes, vol. 1, World Scientific, 1997, <https://doi.org/10.1142/p037>.
- [15] G.T. Rochelle, Amine scrubbing for CO<sub>2</sub> capture, *Science* 325 (5948) (2009) 1652–1654, <https://doi.org/10.1126/science.1176731>.
- [16] R. Idem, M. Wilson, P. Tontiwachwuthikul, A. Chakma, A. Veawab, A. Aroonwilas, D. Gelowitz, Pilot plant studies of the CO<sub>2</sub> capture performance of aqueousMEA and mixed MEA/MDEA solvents at the University of Regina CO<sub>2</sub> capture technology development plant and the boundary dam CO<sub>2</sub> capture demonstration plant, *Ind. Eng. Chem. Res.* 45 (8) (2006) 2414–2420, <https://doi.org/10.1021/ie050569e>.
- [17] M.H. Jenab, M. Vahidi, M. Mehrabi, Solubility of carbon dioxide in aqueous mixtures of DIPA+ MDEA and DIPA+ PZ solutions, *J. Chin. Chem. Soc.* 53 (2) (2006) 283–286, <https://doi.org/10.1002/jccs.200600034>.
- [18] B. Aghel, S. Janati, S. Wongwises, M.S. Shadloo, Review on CO<sub>2</sub> capture by blended amine solutions, *Int. J. Greenh. Gas Control* 119 (2022) 103715, <https://doi.org/10.1016/j.jggc.2022.103715>.
- [19] X. Shen, H. Du, R.H. Mullins, R.R. Kommalapati, Polyethylenimine applications in carbon dioxide capture and separation: from theoretical study to experimental work, *Energy Technol.* 5 (6) (2017) 822–833, <https://doi.org/10.1002/ente.201600694>.
- [20] A. Samanta, A. Zhao, G.K. Shimizu, P. Sarkar, R. Gupta, Post-combustion CO<sub>2</sub> capture using solid sorbents: a review, *Ind. Eng. Chem. Res.* 51 (4) (2012) 1438–1463, <https://doi.org/10.1021/ie020686q>.
- [21] M.B. Yue, L.B. Sun, Y. Cao, Y. Wang, Z.J. Wang, J.H. Zhu, Efficient CO<sub>2</sub> capturer derived from as-synthesized MCM-41 modified with amine, *Chem. Eur. J.* 14 (11) (2008) 3442–3451, <https://doi.org/10.1002/chem.200701467>.
- [22] X. Si, C. Jiao, F. Li, J. Zhang, S. Wang, S. Liu, Z. Li, L. Sun, F. Xu, Z. Gabelica, C. Schick, High and selective CO<sub>2</sub> uptake, H<sub>2</sub> storage and methanol sensing on the amine-decorated 12-connected MOF CAU-1, *Energy Environ. Sci.* 4 (11) (2011) 4522–4527, <https://doi.org/10.1039/C1EE01380G>.
- [23] M.B. Yue, Y. Chun, Y. Cao, X. Dong, J.H. Zhu, CO<sub>2</sub> capture by as-prepared SBA-15 with an occluded organic template, *Adv. Funct. Mater.* 16 (13) (2006) 1717–1722, <https://doi.org/10.1002/adfm.200600427>.
- [24] Z. Liu, Y. Teng, K. Zhang, H. Chen, Y. Yang, CO<sub>2</sub> adsorption performance of different amine-based siliceous MCM-41 materials, *J. Energy Chem.* 24 (3) (2015) 322–330, [https://doi.org/10.1016/S2095-4956\(15\)60318-7](https://doi.org/10.1016/S2095-4956(15)60318-7).
- [25] L. Ghali, A. Abdulkareem, B.S. Ali, S.A. Mazari, Modeling the rate of corrosion of carbon steel using activated diethanolamine solutions for CO<sub>2</sub> absorption, *Chin. J. Chem. Eng.* 28 (8) (2020) 2099–2110, <https://doi.org/10.1016/j.jcce.2020.03.006>.
- [26] X. Guo, L. Ding, K. Kanamori, K. Nakanishi, H. Yang, Functionalization of hierarchically porous silica monoliths with polyethyleneimine (PEI) for CO<sub>2</sub> adsorption, *Microporous Mesoporous Mater.* 245 (2017) 51–57, <https://doi.org/10.1016/j.micromeso.2017.02.076>.
- [27] X.E. Hu, L. Liu, X. Luo, G. Xiao, E. Shiko, R. Zhang, X. Fan, Y. Zhou, Y. Liu, Z. Zeng, C.E. Li, A review of N-functionalized solid adsorbents for post-combustion CO<sub>2</sub> capture, *Appl. Energy* 260 (2020) 114244, <https://doi.org/10.1016/j.apenergy.2019.114244>.
- [28] X. Zhao, Q. Cui, B. Wang, X. Yan, S. Singh, F. Zhang, X. Gao, Y. Li, Recent progress of amine modified sorbents for capturing CO<sub>2</sub> from flue gas, *Chin. J. Chem. Eng.* 26 (11) (2018) 2292–2302, <https://doi.org/10.1016/j.cjche.2018.04.009>.
- [29] P. Zhao, G. Zhang, H. Yan, Y. Zhao, The latest development on amine functionalized solid adsorbents for post-combustion CO<sub>2</sub> capture: analysis review, *Chin. J. Chem. Eng.* 35 (2021) 17–43, <https://doi.org/10.1016/j.cjche.2020.11.028>.
- [30] S. Ahmed, A. Ramli, S. Yusup, M. Farooq, Adsorption behavior of tetraethylenepentamine-functionalized Si-MCM-41 for CO<sub>2</sub> adsorption, *Chem. Eng. Res. Des.* 122 (2017) 33–42, <https://doi.org/10.1016/j.cherd.2017.04.004>.
- [31] T. Gelles, S. Lawson, A.A. Rownaghi, F. Rezaei, Recent advances in development of amine functionalized adsorbents for CO<sub>2</sub> capture, *Adsorption* 26 (1) (2020) 5–50, <https://doi.org/10.1007/s10450-019-00151-0>.
- [32] N. Rao, M. Wang, Z. Shang, Y. Hou, G. Fan, J. Li, CO<sub>2</sub> adsorption by amine-functionalized MCM-41: a comparison between impregnation and grafting modification methods, *Energy Fuels* 32 (1) (2018) 670–677, <https://doi.org/10.1021/acs.energyfuels.7b02906>.
- [33] R. Serna-Guerrero, Y. Belmabkhout, A. Sayari, Modeling CO<sub>2</sub> adsorption on amine-functionalized mesoporous silica: 1. A semi-empirical equilibrium model, *Chem. Eng. J.* 161 (1–2) (2010) 173–181, <https://doi.org/10.1016/j.cej.2010.04.024>.
- [34] R. Serna-Guerrero, Y. Belmabkhout, A. Sayari, Further investigations of CO<sub>2</sub> capture using triamine-grafted pore-expanded mesoporous silica, *Chem. Eng. J.* 158 (3) (2010) 513–519, <https://doi.org/10.1016/j.cej.2010.01.041>.
- [35] T. Yanagisawa, T. Shimizu, K. Kuroda, C. Kato, The preparation of alkyltrimethylammonium–kanemite complexes and their conversion to microporous materials, *Bull. Chem. Soc. Jpn.* 63 (4) (1990) 988–992, <https://doi.org/10.1246/bcsj.63.988>.
- [36] T. Yanagisawa, T. Shimizu, K. Kuroda, C. Kato, Trimethylsilyl derivatives of alkyltrimethylammonium–kanemite complexes and their conversion to microporous SiO<sub>2</sub> materials, *Bull. Chem. Soc. Jpn.* 63 (5) (1990) 1535–1537, <https://doi.org/10.1246/bcsj.63.1535>.
- [37] J.S. Beck, J.C. Vartuli, W.J. Roth, M.E. Leonowicz, C.T. Kresge, K.D. Schmitt, C.T.W. Chu, D.H. Olson, E.W. Sheppard, S.B. McCullen, J.B. Higgins, J. Schlenker, A new family of mesoporous molecular sieves prepared with liquid crystal templates, *J. Am. Chem. Soc.* 114 (27) (1992) 10834–10843, <https://doi.org/10.1021/ja00053a020>.
- [38] A.C. Kresge, M.E. Leonowicz, W.J. Roth, J.C. Vartuli, J.S. Beck, Ordered mesoporous molecular sieves synthesized by a liquid-crystal template mechanism, *Nature* 359 (6397) (1992) 710–712, <https://doi.org/10.1038/359710a0>.
- [39] M.C. Burleigh, S. Dai, Functionalized nanoporous adsorbents for environmental remediation, *Nanoporous Mater. Sci. Eng.* (2004) 756–771, [https://doi.org/10.1142/9781860946561\\_0024](https://doi.org/10.1142/9781860946561_0024).
- [40] D. Zhao, J. Feng, Q. Huo, N. Melosh, G.H. Fredrickson, B.F. Chmelka, G.D. Stucky, Triblock copolymer syntheses of mesoporous silica with periodic 50 to 300 angstrom pores, *Science* 279 (5350) (1998) 548–552, <https://doi.org/10.1126/science.279.5350.548>.
- [41] T. Asefa, Z. Tao, Mesoporous silica and organosilica materials—review of their synthesis and organic functionalization, *Can. J. Chem.* 90 (12) (2012) 1015–1031, <https://doi.org/10.1139/v2012-094>.
- [42] G. Sun, Q. Huang, S. Huang, Q. Wang, H. Li, H. Liu, S. Wan, X. Zhang, J. Wang, Vanadium oxide supported on MSU-1 as a highly active catalyst for dehydrogenation of isobutane with CO<sub>2</sub>, *Catalysts* 6 (3) (2016) 41, <https://doi.org/10.3390/catal6030041>.
- [43] Y. Lv, F. Zhang, Y. Dou, Y. Zhai, J. Wang, H. Liu, X. Xia, B. Tu, D. Zhao, A comprehensive study on KOH activation of ordered mesoporous carbons and their supercapacitor application, *J. Mater. Chem.* 22 (1) (2012) 93–99, <https://doi.org/10.1039/C1JM12742J>.
- [44] M. Ojeda, M. Mazaj, S. Garcia, J. Xuan, M.M. Maroto-Valer, N.Z. Logar, Novel amine-impregnated mesostructured silica materials for CO<sub>2</sub> capture, *Energy Proc.* 114 (2017) 2252–2258, <https://doi.org/10.1016/j.egypro.2017.03.1362>.
- [45] Y. Belmabkhout, R. Serna-Guerrero, A. Sayari, Adsorption of CO<sub>2</sub> from dry gases on MCM-41 silica at ambient temperature and high pressure. 1: pure CO<sub>2</sub> adsorption, *Chem. Eng. Sci.* 64 (17) (2009) 3721–3728, <https://doi.org/10.1016/j.ces.2009.03.017>.
- [46] T.L. Chew, A.L. Ahmad, S. Bhatia, Ordered mesoporous silica (OMS) as an adsorbent and membrane for separation of carbon dioxide (CO<sub>2</sub>), *Adv. Colloid Interface Sci.* 153 (1–2) (2010) 43–57, <https://doi.org/10.1016/j.cis.2009.12.001>.
- [47] L.K.G. Bhatta, S. Subramanyam, M.D. Chengala, S. Olivera, K. Venkatesh, Progress in hydrotalcite like compounds and metal-based oxides for CO<sub>2</sub> capture: a review, *J. Clean. Prod.* 103 (2015) 171–196, <https://doi.org/10.1016/j.jclepro.2014.12.059>.
- [48] X. Liu, J. Li, L. Zhou, D. Huang, Y. Zhou, Adsorption of CO<sub>2</sub>, CH<sub>4</sub> and N<sub>2</sub> on ordered mesoporous silica molecular sieve, *Chem. Phys. Lett.* 415 (4–6) (2005) 198–201, <https://doi.org/10.1016/j.cplett.2005.09.009>.
- [49] C. Yu, B. Tian, X. Liu, J. Fan, H. Yang, D.Y. Zhao, Advances in mesoporous materials templated by nonionic block copolymers, *Nanoporous Mater. Sci. Eng.* (2004) 14–46, [https://doi.org/10.1142/9781860946561\\_0002](https://doi.org/10.1142/9781860946561_0002).
- [50] S. Kumar, M.M. Malik, R. Purohit, Synthesis methods of mesoporous silica materials, *Mater. Today: Proc.* 4 (2) (2017) 350–357, <https://doi.org/10.1016/j.matpr.2017.01.032>.
- [51] H. Li, X. Chen, D. Shen, F. Wu, R. Pleixats, J. Pan, Functionalized silica nanoparticles: classification, synthetic approaches and recent advances in

- adsorption applications, *Nanoscale* 13 (38) (2021) 15998–16016, <https://doi.org/10.1039/D1NR04048K>.
- [52] N.H. Khdary, M.A. Ghanem, M.E. Abdelsalam, M.M. Al-Garadah, Sequestration of CO<sub>2</sub> using Cu nanoparticles supported on spherical and rod-shape mesoporous silica, *J. Saudi Chem. Soc.* 22 (3) (2018) 343–351, <https://doi.org/10.1016/j.jscs.2016.05.004>.
- [53] N.H. Khdary, M.A. Ghanem, Metal–organic–silica nanocomposites: copper, silver nanoparticles–ethylenediamine–silica gel and their CO<sub>2</sub> adsorption behaviour, *J. Mater. Chem. 22* (24) (2012) 12032–12038, <https://doi.org/10.1039/C2JM31104F>.
- [54] N.H. Khdary, M.A. Ghanem, M.G. Merajuddine, F.M.B. Manie, Incorporation of Cu, Fe, Ag, and Au nanoparticles in mercapto-silica (MOS) and their CO<sub>2</sub> adsorption capacities, *J. CO<sub>2</sub> Util.* 5 (2014) 17–23, <https://doi.org/10.1016/j.jcou.2013.11.003>.
- [55] S.S. Fatima, A. Borhan, M. Ayoub, N. Abd Ghani, Development and progress of functionalized silica-based adsorbents for CO<sub>2</sub> capture, *J. Mol. Liq.* 338 (2021) 116913, <https://doi.org/10.1016/j.molliq.2021.116913>.
- [56] C. Chen, S. Zhang, K.H. Row, W.S. Ahn, Amine–silica composites for CO<sub>2</sub> capture: a short review, *J. Energy Chem.* 26 (5) (2017) 868–880, <https://doi.org/10.1016/j.jecchem.2017.07.001>.
- [57] S. Zhang, C. Chen, W.S. Ahn, Recent progress on CO<sub>2</sub> capture using amine-functionalized silica, *Curr. Opin. Green Sustain. Chem.* 16 (2019) 26–32, <https://doi.org/10.1016/j.cogsc.2018.11.011>.
- [58] E.S. Sanz-Pérez, B. Lobato, M.A. Lopez-Antón, A. Arencibia, R. Sanz, M.R. Martínez-Tarazona, Effectiveness of amino-functionalized sorbents for CO<sub>2</sub> capture in the presence of Hg, *Fuel* 267 (2020) 117250, <https://doi.org/10.1016/j.fuel.2020.117250>.
- [59] Z. Shen, Q. Cai, C. Yin, Q. Xia, J. Cheng, X. Li, Y. Wang, Facile synthesis of silica nanosheets with hierarchical pore structure and their amine-functionalized composite for enhanced CO<sub>2</sub> capture, *Chem. Eng. Sci.* 217 (2020) 115528, <https://doi.org/10.1016/j.ces.2020.115528>.
- [60] R. Sanz, G. Calleja, A. Arencibia, E.S. Sanz-Pérez, CO<sub>2</sub> adsorption on branched polyethylenimine-impregnated mesoporous silica SBA-15, *Appl. Surf. Sci.* 256 (17) (2010) 5323–5328, <https://doi.org/10.1016/j.apsusc.2009.12.070>.
- [61] X. Wang, C. Song, Temperature-programmed desorption of CO<sub>2</sub> from polyethylenimine-loaded SBA-15 as molecular basket sorbents, *Catal. Today* 194 (1) (2012) 44–52, <https://doi.org/10.1016/j.cattod.2012.08.008>.
- [62] A. Heydari-Gorji, Y. Yang, A. Sayari, Effect of the pore length on CO<sub>2</sub> adsorption over amine-modified mesoporous silicas, *Energy Fuels* 25 (9) (2011) 4206–4210, <https://doi.org/10.1021/ef200765f>.
- [63] S. Ahmed, A. Ramli, S. Yusup, Development of polyethylenimine-functionalized mesoporous Si-MCM-41 for CO<sub>2</sub> adsorption, *Fuel Process. Technol.* 167 (2017) 622–630, <https://doi.org/10.1016/j.fuproc.2017.07.036>.
- [64] H. Thakkar, S. Eastman, A. Al-Mamoori, A. Hajari, A.A. Rownaghi, F. Rezaei, Formulation of aminosilica adsorbents into 3D-printed monoliths and evaluation of their CO<sub>2</sub> capture performance, *ACS Appl. Mater. Interfaces* 9 (8) (2017) 7489–7498, <https://doi.org/10.1021/acsmami.6b16732>.
- [65] W.J. Son, J.S. Choi, W.S. Ahn, Adsorptive removal of carbon dioxide using polyethylenimine-loaded mesoporous silica materials, *Microporous Mesoporous Mater.* 113 (1–3) (2008) 31–40, <https://doi.org/10.1016/j.micromeso.2007.10.049>.
- [66] J. Jiao, J. Cao, Y. Xia, L. Zhao, Improvement of adsorbent materials for CO<sub>2</sub> capture by amine functionalized mesoporous silica with worm-hole framework structure, *Chem. Eng. J.* 306 (2016) 9–16, <https://doi.org/10.1016/j.cej.2016.07.041>.
- [67] X. Hou, L. Zhuang, B. Ma, S. Chen, H. He, F. Yin, Silanol-rich platelet silica modified with branched amine for efficient CO<sub>2</sub> capture, *Chem. Eng. Sci.* 181 (2018) 315–325, <https://doi.org/10.1016/j.ces.2018.02.015>.
- [68] H. Zhang, A. Goepert, S. Kar, G.S. Prakash, Structural parameters to consider in selecting silica supports for polyethylenimine based CO<sub>2</sub> solid adsorbents. Importance of pore size, *J. CO<sub>2</sub> Util.* 26 (2018) 246–253, <https://doi.org/10.1016/j.jcou.2018.05.004>.
- [69] S. Park, K. Choi, H.J. Yu, Y.J. Won, C. Kim, M. Choi, S.H. Cho, J.H. Lee, S.Y. Lee, J.S. Lee, Thermal stability enhanced tetraethylpentamine/silica adsorbents for high performance CO<sub>2</sub> capture, *Ind. Eng. Chem. Res.* 57 (13) (2018) 4632–4639, <https://doi.org/10.1021/acs.iecr.7b04912>.
- [70] Y. Fan, F. Rezaei, X. Yang, Mixed alkanolamine-polyethylenimine functionalized silica for CO<sub>2</sub> capture, *Energy Technol.* 7 (2) (2019) 253–262, <https://doi.org/10.1002/ente.201800481>.
- [71] W. Zhang, E. Gao, Y. Li, M.T. Bernards, Y. He, Y. Shi, CO<sub>2</sub> capture with polyamine-based protic ionic liquid functionalized mesoporous silica, *J. CO<sub>2</sub> Util.* 34 (2019) 606–615, <https://doi.org/10.1016/j.jcou.2019.08.012>.
- [72] S. Logathanathan, A.K. Ghoshal, Amine tethered pore-expanded MCM-41: a promising adsorbent for CO<sub>2</sub> capture, *Chem. Eng. J.* 308 (2017) 827–839, <https://doi.org/10.1016/j.cej.2016.09.103>.
- [73] M.J. Lashaki, A. Sayari, CO<sub>2</sub> capture using triamine-grafted SBA-15: the impact of the support pore structure, *Chem. Eng. J.* 334 (2018) 1260–1269, <https://doi.org/10.1016/j.cej.2017.10.103>.
- [74] E.S. Sanz-Pérez, A. Fernández, A. Arencibia, G. Calleja, R. Sanz, Hybrid amine-silica materials: determination of N content by 29Si NMR and application to direct CO<sub>2</sub> capture from air, *Chem. Eng. J.* 373 (2019) 1286–1294, <https://doi.org/10.1016/j.cej.2019.05.117>.
- [75] X. Jiang, Y. Kong, Z. Zhao, X. Shen, Spherical amine grafted silica aerogels for CO<sub>2</sub> capture, *RSC Adv.* 10 (43) (2020) 25911–25917, <https://doi.org/10.1039/D0RA04497K>.
- [76] J.T. Anyanwu, Y. Wang, R.T. Yang, Amine-grafted silica gels for CO<sub>2</sub> capture including direct air capture, *Ind. Eng. Chem. Res.* 59 (15) (2019) 7072–7079, <https://doi.org/10.1021/acs.iecr.9b05228>.
- [77] R. Kishor, A.K. Ghoshal, APTES grafted ordered mesoporous silica KIT-6 for CO<sub>2</sub> adsorption, *Chem. Eng. J.* 262 (2015) 882–890, <https://doi.org/10.1016/j.cej.2014.10.039>.
- [78] E.S. Sanz-Pérez, A. Arencibia, G. Calleja, R. Sanz, Tuning the textural properties of HMS mesoporous silica. Functionalization towards CO<sub>2</sub> adsorption, *Microporous Mesoporous Mater.* 260 (2018) 235–244, <https://doi.org/10.1016/j.micromeso.2017.10.038>.
- [79] J.T. Anyanwu, Y. Wang, R.T. Yang, CO<sub>2</sub> capture (including direct air capture) and natural gas desulfurization of amine-grafted hierarchical bimodal silica, *Chem. Eng. J.* 427 (2022) 131561, <https://doi.org/10.1016/j.cej.2021.131561>.
- [80] R. Sanz, G. Calleja, A. Arencibia, E.S. Sanz-Pérez, CO<sub>2</sub> capture with pore-expanded MCM-41 silica modified with amino groups by double functionalization, *Microporous Mesoporous Mater.* 209 (2015) 165–171, <https://doi.org/10.1016/j.micromeso.2014.10.045>.
- [81] E.S. Sanz-Pérez, T.C.M. Dantas, A. Arencibia, G. Calleja, A.P.M.A. Guedes, A.S. Araujo, R. Sanz, Reuse and recycling of amine-functionalized silica materials for CO<sub>2</sub> adsorption, *Chem. Eng. J.* 308 (2017) 1021–1033, <https://doi.org/10.1016/j.cej.2016.09.109>.
- [82] J. Zhu, B. He, J. Huang, C. Li, T. Ren, Effect of immobilization methods and the pore structure on CO<sub>2</sub> separation performance in silica-supported ionic liquids, *Microporous Mesoporous Mater.* 260 (2018) 190–200, <https://doi.org/10.1016/j.micromeso.2017.10.035>.
- [83] M. Garip, N. Gizli, Ionic liquid containing amine-based silica aerogels for CO<sub>2</sub> capture by fixed bed adsorption, *J. Mol. Liq.* 310 (2020) 113227, <https://doi.org/10.1016/j.molliq.2020.113227>.
- [84] D.V. Quang, A. Dindi, M.R. Abu-Zahra, One-step process using CO<sub>2</sub> for the preparation of amino-functionalized mesoporous silica for CO<sub>2</sub> capture application, *ACS Sustain. Chem. Eng.* 5 (4) (2017) 3170–3178, <https://doi.org/10.1021/acssuschemeng.6b02961>.
- [85] Y. Kong, X. Shen, M. Fan, M. Yang, S. Cui, Dynamic capture of low-concentration CO<sub>2</sub> on amine hybrid silsesquioxane aerogel, *Chem. Eng. J.* 283 (2016) 1059–1068, <https://doi.org/10.1016/j.cej.2015.08.034>.
- [86] W. Klinthong, C.H. Huang, C.S. Tan, One-pot synthesis and pelletizing of polyethylenimine-containing mesoporous silica powders for CO<sub>2</sub> capture, *Ind. Eng. Chem. Res.* 55 (22) (2016) 6481–6491, <https://doi.org/10.1021/acs.iecr.6b00644>.
- [87] X. Wang, L. Chen, Q. Guo, Development of hybrid amine-functionalized MCM-41 sorbents for CO<sub>2</sub> capture, *Chem. Eng. J.* 260 (2015) 573–581, <https://doi.org/10.1016/j.cej.2014.08.107>.
- [88] K. Min, W. Choi, M. Choi, Macroporous silica with thick framework for steam-stable and high-performance poly(ethyleneimine)/silica CO<sub>2</sub> adsorbent, *ChemSusChem* 10 (11) (2017) 2518–2526, <https://doi.org/10.1002/cssc.201700398>.
- [89] L. Zhang, N. Zhan, Q. Jin, H. Liu, J. Hu, Impregnation of polyethylenimine in mesoporous multilamellar silica vesicles for CO<sub>2</sub> capture: a kinetic study, *Ind. Eng. Chem. Res.* 55 (20) (2016) 5885–5891, <https://doi.org/10.1021/acs.iecr.5b04760>.
- [90] X. Liu, F. Gao, J. Xu, L. Zhou, H. Liu, J. Hu, Zeolite@ Mesoporous silica-supported-amine hybrids for the capture of CO<sub>2</sub> in the presence of water, *Microporous Mesoporous Mater.* 222 (2016) 113–119, <https://doi.org/10.1016/j.micromeso.2015.10.006>.
- [91] B. Singh, V. Polshettiwar, Design of CO<sub>2</sub> sorbents using functionalized fibrous nanosilica (KCC-1): insights into the effect of the silica morphology (KCC-1 vs. MCM-41), *J. Mater. Chem. A* 4 (18) (2016) 7005–7019, <https://doi.org/10.1039/C6TA01348A>.
- [92] L. Wang, M. Yao, X. Hu, G. Hu, J. Lu, M. Luo, M. Fan, Amine-modified ordered mesoporous silica: the effect of pore size on CO<sub>2</sub> capture performance, *Appl. Surf. Sci.* 324 (2015) 286–292, <https://doi.org/10.1016/j.apsusc.2014.10.135>.
- [93] W. Zhang, H. Liu, Y. Sun, J. Cakstins, C. Sun, C.E. Snape, Parametric study on the regeneration heat requirement of an amine-based solid adsorbent process for post-combustion carbon capture, *Appl. Energy* 168 (2016) 394–405, <https://doi.org/10.1016/j.apenergy.2016.01.049>.
- [94] Jin Zhou, Xuan Wang, Wei Xing, Carbon-based CO<sub>2</sub> adsorbents, in: *Post-combustion Carbon Dioxide Capture Materials*, 2018, pp. 1–75, <https://doi.org/10.1039/9781788013352-00001>.
- [95] S.Y. Lee, S.J. Park, Determination of the optimal pore size for improved CO<sub>2</sub> adsorption in activated carbon fibers, *J. Colloid Interface Sci.* 389 (1) (2013) 230–235, <https://doi.org/10.1016/j.jcis.2012.09.018>.
- [96] S.H. Moon, J.W. Shim, A novel process for CO<sub>2</sub>/CH<sub>4</sub> gas separation on activated carbon fibers—electric swing adsorption, *J. Colloid Interface Sci.* 298 (2) (2006) 523–528, <https://doi.org/10.1016/j.jcis.2005.12.052>.
- [97] U. Kamran, Y.J. Heo, J.W. Lee, S.J. Park, Functionalized carbon materials for electronic devices: a review, *Micromachines* 10 (4) (2019) 234, <https://doi.org/10.3390/mi10040234>.
- [98] Y. Zhang, S.J. Park, Imidazolium-optimized conductive interfaces in multi-layer graphene nanoplatelet/epoxy composites for thermal management applications and electroactive devices, *Polymer* 168 (2019) 53–60, <https://doi.org/10.1016/j.polymer.2019.01.086>.
- [99] Z. Zhang, Z. Zhu, B. Shen, L. Liu, Insights into biochar and hydrochar production and applications: a review, *Energy* 171 (2019) 581–598, <https://doi.org/10.1016/j.energy.2019.01.035>.

- [100] H.S. Kambo, A. Dutta, A comparative review of biochar and hydrochar in terms of production, physico-chemical properties and applications, *Renew. Sustain. Energy Rev.* 45 (2015) 359–378, <https://doi.org/10.1016/j.rser.2015.01.050>.
- [101] S.K. Das, S. Majhi, P. Mohanty, K.K. Pant, CO-hydrogenation of syngas to fuel using silica supported Fe–Cu–K catalysts: effects of active components, *Fuel Process. Technol.* 118 (2014) 82–89, <https://doi.org/10.1016/j.fuproc.2013.08.014>.
- [102] N. Khan, S. Mohan, P. Dinesha, Regimes of hydrochar yield from hydrothermal degradation of various lignocellulosic biomass: a review, *J. Clean. Prod.* 288 (2021) 125629, <https://doi.org/10.1016/j.jclepro.2020.125629>.
- [103] C. Goel, S. Mohan, P. Dinesha, CO<sub>2</sub> capture by adsorption on biomass-derived activated char: a review, *Sci. Total Environ.* 798 (2021) 149296, <https://doi.org/10.1016/j.scitotenv.2021.149296>.
- [104] S.K. Hoekman, A. Broch, C. Robbins, B. Zielinska, L. Felix, Hydrothermal carbonization (HTC) of selected woody and herbaceous biomass feedstocks, *Biomass Conv. Bioref.* 3 (2) (2013) 113–126, <https://doi.org/10.1007/s13399-012-0066-y>.
- [105] J.A. Libra, K.S. Ro, C. Kammann, A. Funke, N.D. Berge, Y. Neubauer, M.M. Tritici, C. Fuhner, O. Bens, J. Kern, K.H. Emmerich, Hydrothermal carbonization of biomass residuals: a comparative review of the chemistry, processes and applications of wet and dry pyrolysis, *Biofuels* 2 (1) (2011) 71–106, <https://doi.org/10.4155/bfs.10.81>.
- [106] D. Sangare, A. Chartier, M. Moscosa-Santillan, I. Gökalp, S. Bostyn, Kinetic studies of hydrothermal carbonization of avocado stone and analysis of the polycyclic aromatic hydrocarbon contents in the hydrochars produced, *Fuel* 316 (2022) 123163, <https://doi.org/10.1016/j.fuel.2022.123163>.
- [107] M. Sevilla, J.A. Maciá-Agulló, A.B. Fuertes, Hydrothermal carbonization of biomass as a route for the sequestration of CO<sub>2</sub>: chemical and structural properties of the carbonized products, *Biomass Bioenergy* 35 (7) (2011) 3152–3159, <https://doi.org/10.1016/j.biombioe.2011.04.032>.
- [108] C.L.M. Martinez, E. Sermyagina, J. Saari, M.S. de Jesus, M. Cardoso, G.M. de Almeida, E. Vakkilainen, Hydrothermal carbonization of lignocellulosic agro-forest based biomass residues, *Biomass Bioenergy* 147 (2021) 106004, <https://doi.org/10.1016/j.biombioe.2021.106004>.
- [109] J. Fang, L. Zhan, Y.S. Ok, B. Gao, Minireview of potential applications of hydrochar derived from hydrothermal carbonization of biomass, *J. Ind. Eng. Chem.* 57 (2018) 15–21, <https://doi.org/10.1016/j.jiec.2017.08.026>.
- [110] T. Wang, Y. Zhai, Y. Zhu, C. Li, G. Zeng, A review of the hydrothermal carbonization of biomass waste for hydrochar formation: process conditions, fundamentals, and physicochemical properties, *Renew. Sustain. Energy Rev.* 90 (2018) 223–247, <https://doi.org/10.1016/j.rser.2018.03.071>.
- [111] J. Racek, J. Sevcik, T. Chorazy, J. Kucerik, P. Hlavinek, Biochar—recovery material from pyrolysis of sewage sludge: a review, *Waste Biomass Valorizat.* 11 (7) (2020) 3677–3709, <https://doi.org/10.1007/s12649-019-00679-w>.
- [112] W.Y. Chen, D.L. Mattern, E. Okinedo, J.C. Senter, A.A. Mattei, C.W. Redwine, Photochemical and acoustic interactions of biochar with CO<sub>2</sub> and H<sub>2</sub>O: applications in power generation and CO<sub>2</sub> capture, *AIChE J.* 60 (3) (2014) 1054–1065, <https://doi.org/10.1002/aic.14347>.
- [113] R. Chatterjee, B. Sajjadi, D.L. Mattern, W.Y. Chen, T. Zubatiuk, D. Leszczynska, J. Leszczynski, N.O. Egiebor, N. Hammer, Ultrasound cavitation intensified amino functionalization: a feasible strategy for enhancing CO<sub>2</sub> capture capacity of biochar, *Fuel* 225 (2018) 287–298, <https://doi.org/10.1016/j.fuel.2018.03.145>.
- [114] A.R. Zimmerman, Abiotic and microbial oxidation of laboratory-produced black carbon (biochar), *Environ. Sci. Technol.* 44 (4) (2010) 1295–1301, <https://doi.org/10.1021/es903140c>.
- [115] Y.C. Chiang, R.S. Juang, Surface modifications of carbonaceous materials for carbon dioxide adsorption: a review, *J. Taiwan Inst. Chem. Eng.* 71 (2017) 214–234, <https://doi.org/10.1016/j.jtice.2016.12.014>.
- [116] K. Qian, A. Kumar, H. Zhang, D. Bellmer, R. Huhnke, Recent advances in utilization of biochar, *Renew. Sustain. Energy Rev.* 42 (2015) 1055–1064, <https://doi.org/10.1016/j.rser.2014.10.074>.
- [117] Y.S. Ok, D.C. Tsang, N. Bolan, J.M. Novak (Eds.), *Biochar from Biomass and Waste: Fundamentals and Applications*, Elsevier, 2018, <https://doi.org/10.1016/C2016-0-01974-5>.
- [118] S. Jung, Y.K. Park, E.E. Kwon, Strategic use of biochar for CO<sub>2</sub> capture and sequestration, *J. CO<sub>2</sub> Util.* 32 (2019) 128–139, <https://doi.org/10.1016/j.jcou.2019.04.012>.
- [119] S. Shahkarami, R. Azargohar, A.K. Dalai, J. Soltan, Breakthrough CO<sub>2</sub> adsorption in bio-based activated carbons, *J. Environ. Sci.* 34 (2015) 68–76, <https://doi.org/10.1016/j.jes.2015.03.008>.
- [120] X. Zhang, S. Zhang, H. Yang, Y. Feng, Y. Chen, X. Wang, H. Chen, Nitrogen enriched biochar modified by high temperature CO<sub>2</sub>–ammonia treatment: characterization and adsorption of CO<sub>2</sub>, *Chem. Eng. J.* 257 (2014) 20–27, <https://doi.org/10.1016/j.cej.2014.07.024>.
- [121] H. Madzaki, W.A.W.A. KarimGhani, AzilBahariAlias NurZalikhaRebitanum, Carbon dioxide adsorption on sawdust biochar, *Procedia Eng.* 148 (2016) 718–725, <https://doi.org/10.1016/j.proeng.2016.06.591>.
- [122] X. Zhang, J. Wu, H. Yang, J. Shao, X. Wang, Y. Chen, S. Zhang, H. Chen, Preparation of nitrogen-doped microporous modified biochar by high temperature CO<sub>2</sub>–NH<sub>3</sub> treatment for CO<sub>2</sub> adsorption: effects of temperature, *RSC Adv.* 6 (100) (2016) 98157–98166, <https://doi.org/10.1039/C6RA23748C>.
- [123] P. Lahijani, M. Mohammadi, A.R. Mohamed, Metal incorporated biochar as a potential adsorbent for high capacity CO<sub>2</sub> capture at ambient condition, *J. CO<sub>2</sub> Util.* 26 (2018) 281–293, <https://doi.org/10.1016/j.jcou.2018.05.018>.
- [124] A.E. Creamer, B. Gao, S. Wang, Carbon dioxide capture using various metal oxyhydroxide–biochar composites, *Chem. Eng. J.* 283 (2016) 826–832, <https://doi.org/10.1016/j.cej.2015.08.037>.
- [125] A.N. Shafawi, A.R. Mohamed, P. Lahijani, M. Mohammadi, Recent advances in developing engineered biochar for CO<sub>2</sub> capture: an insight into the biochar modification approaches, *J. Environ. Chem. Eng.* 9 (6) (2021) 106869, <https://doi.org/10.1016/j.jece.2021.106869>.
- [126] P.D. Dissanayake, S. You, A.D. Igalavithana, Y. Xia, A. Bhatnagar, S. Gupta, H.W. Kura, S. Kim, J.H. Kwon, D.C.W. Tsang, Y.S. Ok, Biochar-based adsorbents for carbon dioxide capture: a critical review, *Renew. Sustain. Energy Rev.* 119 (2020) 109582, <https://doi.org/10.1016/j.rser.2019.109582>.
- [127] N.A. Zubbri, A.R. Mohamed, N. Kamiuchi, M. Mohammadi, Enhancement of CO<sub>2</sub> adsorption on biochar sorbent modified by metal incorporation, *Environ. Sci. Pollut. Res. Int.* 27 (11) (2020) 11809–11829, <https://doi.org/10.1007/s11356-020-07734-3>.
- [128] M.V. Nguyen, B.K. Lee, A novel removal of CO<sub>2</sub> using nitrogen doped biochar beads as a green adsorbent, *Process Saf. Environ. Protect.* 104 (2016) 490–498, <https://doi.org/10.1016/j.psep.2016.04.007>.
- [129] J. Zhou, D. Li, Y. Wang, Y. Tian, Z. Zhang, L. Wei, W. Feng, Effect of the feedstock type on the volumetric low-pressure CO<sub>2</sub> capture performance of activated carbons, *Energy Fuels* 32 (12) (2018) 12711–12720, <https://doi.org/10.1021/acs.energyfuels.8b02827>.
- [130] F. Montagnaro, A. Silvestre-Albero, J. Silvestre-Albero, F. Rodríguez-Reinoso, A. Erto, A. Lancia, M. Balsamo, Post-combustion CO<sub>2</sub> adsorption on activated carbons with different textural properties, *Microporous Mesoporous Mater.* 209 (2015) 157–164, <https://doi.org/10.1016/j.micromeso.2014.09.037>.
- [131] L. Nie, Y. Mu, J. Jin, J. Chen, J. Mi, Recent developments and consideration issues in solid adsorbents for CO<sub>2</sub> capture from flue gas, *Chin. J. Chem. Eng.* 26 (11) (2018) 2303–2317, <https://doi.org/10.1016/j.cjche.2018.07.012>.
- [132] M. Kwiatkowski, E. Gómez-Delgado, G.V. Nunell, P.R. Bonelli, A.L. Culkierman, Mathematical analysis of the effect of process conditions on the porous structure development of activated carbons derived from Pine cones, *Sci. Rep.* 12 (1) (2022) 15301, <https://doi.org/10.1038/s41598-022-19383-2>.
- [133] J. Silvestre-Albero, A. Wahby, A. Sepúlveda-Escribano, M. Martínez-Escandell, K. Kaneko, F. Rodríguez-Reinoso, Ultrahigh CO<sub>2</sub> adsorption capacity on carbon molecular sieves at room temperature, *Chem. Commun.* 47 (24) (2011) 6840–6842, <https://doi.org/10.1039/C1CC11618E>.
- [134] M.G. Plaza, C. Pevida, B. Arias, J. Fermofo, F. Rubiera, J.J. Pis, A comparison of two methods for producing CO<sub>2</sub> capture adsorbents, *Energy Proc.* 1 (1) (2009) 1107–1113, <https://doi.org/10.1016/j.egypro.2009.01.146>.
- [135] H. Teng, T.S. Yeh, L.Y. Hsu, Preparation of activated carbon from bituminous coal with phosphoric acid activation, *Carbon* 36 (9) (1998) 1387–1395, [https://doi.org/10.1016/S0008-6223\(98\)00127-4](https://doi.org/10.1016/S0008-6223(98)00127-4).
- [136] F. Karacan, U. Ozden, S. Karacan, Optimization of manufacturing conditions for activated carbon from Turkish lignite by chemical activation using response surface methodology, *Appl. Therm. Eng.* 27 (7) (2007) 1212–1218, <https://doi.org/10.1016/j.aplthermaleng.2006.02.046>.
- [137] M.M. Sabzehei, S. Mahnaee, M. Ghaedi, H. Heidari, V.A. Roy, Carbon based materials: a review of adsorbents for inorganic and organic compounds, *Mater. Adv.* 2 (2) (2021) 598–627, <https://doi.org/10.1039/DOMA00087F>.
- [138] A.A. Abd, M.R. Othman, J. Kim, A review on application of activated carbons for carbon dioxide capture: present performance, preparation, and surface modification for further improvement, *Environ. Sci. Pollut. Res. Int.* 28 (32) (2021) 43329–43364, <https://doi.org/10.1007/s11356-021-15121-9>.
- [139] J. Bedia, M. Peñas-Garzón, A. Gómez-Avilés, J.J. Rodriguez, C. Belver, A review on the synthesis and characterization of biomass-derived carbons for adsorption of emerging contaminants from water, *J. Carbon Res.* 4 (4) (2018) 63, <https://doi.org/10.3390/c4040063>.
- [140] B. Sajjadi, W.Y. Chen, N.O. Egiebor, A comprehensive review on physical activation of biochar for energy and environmental applications, *Rev. Chem. Eng.* 35 (6) (2019) 735–776, <https://doi.org/10.1515/revce-2017-0113>.
- [141] N. Abuelnor, A. AlHajaj, M. Khaleel, L.F. Vega, M.R. Abu-Zahra, Activated carbons from biomass-based sources for CO<sub>2</sub> capture applications, *Chemosphere* 282 (2021) 131111, <https://doi.org/10.1016/j.chemosphere.2021.131111>.
- [142] M. Kwiatkowski, J. Serafin, A.M. Booth, B. Michalkiewicz, Computer analysis of the effect of activation temperature on the microporous structure development of activated carbon derived from common polyopoly, *Materials* 14 (11) (2021) 2951, <https://doi.org/10.3390/ma14112951>.
- [143] M. Kwiatkowski, E. Broniek, Application of the LBET class adsorption models to analyze influence of production process conditions on the obtained microporous structure of activated carbons, *Colloids Surf. A Physicochem. Eng. Asp.* 411 (2012) 105–110, <https://doi.org/10.1016/j.colsurfa.2012.06.046>.
- [144] Z. Zhang, T. Wang, L. Ke, X. Zhao, C. Ma, Powder-activated semicokes prepared from coal fast pyrolysis: influence of oxygen and steam atmosphere on pore structure, *Energy Fuels* 30 (2) (2016) 896–903, <https://doi.org/10.1021/acs.energyfuels.5b02488>.
- [145] J. Fu, B. Zhou, Z. Zhang, T. Wang, X. Cheng, L. Lin, C. Ma, One-step rapid pyrolysis activation method to prepare nanostructured activated coke powder, *Fuel* 262 (2020) 116514, <https://doi.org/10.1016/j.fuel.2019.116514>.
- [146] J. Alvarez, G. Lopez, M. Amutio, J. Bilbao, M. Olazar, Physical activation of rice husk pyrolysis char for the production of high surface area activated carbons, *Ind. Eng. Chem. Res.* 54 (29) (2015) 7241–7250, <https://doi.org/10.1021/acs.iecr.5b01589>.

- [147] N. Hagemann, K. Spokas, H.P. Schmidt, R. Kägi, M.A. Böhler, T.D. Bucheli, Activated carbon, biochar and charcoal: linkages and synergies across pyrogenic carbon's ABCs, *Water* 10 (2) (2018) 182, <https://doi.org/10.3390/w10020182>.
- [148] A. Aworn, P. Thiravetyan, W. Nakbanpote, Preparation and characteristics of agricultural waste activated carbon by physical activation having micro-and mesopores, *J. Anal. Appl. Pyrol.* 82 (2) (2008) 279–285, <https://doi.org/10.1016/j.jaat.2008.04.007>.
- [149] M.S. Tam, M.J. Antal, Preparation of activated carbons from macadamia nut shell and coconut shell by air activation, *Ind. Eng. Chem. Res.* 38 (11) (1999) 4268–4276, <https://doi.org/10.1021/ie990346m>.
- [150] M.G. Plaza, A.S. González, J.J. Pis, F. Rubiera, C. Pevida, Production of microporous biochars by single-step oxidation: effect of activation conditions on CO<sub>2</sub> capture, *Appl. Energy* 114 (2014) 551–562, <https://doi.org/10.1016/j.apenergy.2013.09.058>.
- [151] A.K. Dalai, R. Azargohar, Production of activated carbon from biochar using chemical and physical activation: mechanism and modeling, *Mater. Chem. Energy Forest Biomass* 29 (2007) 463–476, <https://doi.org/10.1021/bk-2007-0954.ch029>.
- [152] B. Petrovic, M. Gorbounov, S.M. Soltani, Impact of surface functional groups and their introduction methods on the mechanisms of CO<sub>2</sub> adsorption on porous carbonaceous adsorbents, *Carbon Capture Sci. Technol.* (2022) 100045, <https://doi.org/10.1016/j.ccst.2022.100045>.
- [153] M. Li, R. Xiao, Preparation of a dual pore structure activated carbon from rice husk char as an adsorbent for CO<sub>2</sub> capture, *Fuel Process. Technol.* 186 (2019) 35–39, <https://doi.org/10.1016/j.fuproc.2018.12.015>.
- [154] N.A. Rashidi, S. Yusup, Potential of palm kernel shell as activated carbon precursors through single stage activation technique for carbon dioxide adsorption, *J. Clean. Prod.* 168 (2017) 474–486, <https://doi.org/10.1016/j.jclepro.2017.09.045>.
- [155] M. Danish, V. Parthasarthy, M.K. Al Mesfer, CO<sub>2</sub> capture by low-cost date pits-based activated carbon and silica gel, *Materials* 14 (14) (2021) 3885, <https://doi.org/10.3390/ma14143885>.
- [156] A.E. Ogungbenro, D.V. Quang, K.A. Al-Ali, L.F. Vega, M.R. Abu-Zahra, Physical synthesis and characterization of activated carbon from date seeds for CO<sub>2</sub> capture, *J. Environ. Chem. Eng.* 6 (4) (2018) 4245–4252, <https://doi.org/10.1016/j.jece.2018.06.030>.
- [157] N.S. Nasri, U.D. Hamza, S.N. Ismail, M.M. Ahmed, R. Mohsin, Assessment of porous carbons derived from sustainable palm solid waste for carbon dioxide capture, *J. Clean. Prod.* 71 (2014) 148–157, <https://doi.org/10.1016/j.jclepro.2013.11.053>.
- [158] A.S. González, M.G. Plaza, F. Rubiera, C. Pevida, Sustainable biomass-based carbon adsorbents for post-combustion CO<sub>2</sub> capture, *Chem. Eng. J.* 230 (2013) 456–465, <https://doi.org/10.1016/j.cej.2013.06.118>.
- [159] M. Puig-Gamero, A. Esteban-Arranz, L. Sanchez-Silva, P. Sánchez, Obtaining activated biochar from olive stone using a bench scale high-pressure thermobalance, *J. Environ. Chem. Eng.* 9 (4) (2021) 105374, <https://doi.org/10.1016/j.jece.2021.105374>.
- [160] B. González, J.J. Manyá, Activated olive mill waste-based hydrochars as selective adsorbents for CO<sub>2</sub> capture under postcombustion conditions, *Chem. Eng. Process. Process Intensif.* 149 (2020) 107830, <https://doi.org/10.1016/j.cep.2020.107830>.
- [161] A.S. Ello, L.K. de Souza, A. Trokourey, M. Jaroniec, Coconut shell-based microporous carbons for CO<sub>2</sub> capture, *Microporous Mesoporous Mater.* 180 (2013) 280–283, <https://doi.org/10.1016/j.micromeso.2013.07.008>.
- [162] N.A. Rashidi, S. Yusup, A. Borhan, L.H. Loong, Experimental and modelling studies of carbon dioxide adsorption by porous biomass derived activated carbon, *Clean Technol. Environ. Policy* 16 (7) (2014) 1353–1361, <https://doi.org/10.1007/s10098-014-0788-6>.
- [163] M.G. Plaza, A.S. González, C. Pevida, J.J. Pis, F. Rubiera, Valorisation of spent coffee grounds as CO<sub>2</sub> adsorbents for postcombustion capture applications, *Appl. Energy* 99 (2012) 272–279, <https://doi.org/10.1016/j.apenergy.2012.05.028>.
- [164] J.J. Manyá, B. González, M. Azuara, G. Arner, Ultra-microporous adsorbents prepared from vine shoots-derived biochar with high CO<sub>2</sub> uptake and CO<sub>2</sub>/N<sub>2</sub> selectivity, *Chem. Eng. J.* 345 (2018) 631–639, <https://doi.org/10.1016/j.cej.2018.01.092>.
- [165] J.S. Bae, S. Su, Macadamia nut shell-derived carbon composites for post combustion CO<sub>2</sub> capture, *Int. J. Greenh. Gas Control* 19 (2013) 174–182, <https://doi.org/10.1016/j.ijggc.2013.08.013>.
- [166] A. Alazmi, S.A. Nicolae, P. Modugno, B.E. Hasanov, M.M. Titirici, P.M. Costa, Activated carbon from palm date seeds for CO<sub>2</sub> capture, *Int. J. Environ. Res. Public Health* 18 (22) (2021) 12142, <https://doi.org/10.3390/ijerph182212142>.
- [167] J. Serafin, M. Ouzzine, C. Xing, H. El Ouahabi, A. Kamińska, J. Sreńsek-Nazzal, Activated carbons from the Amazonian biomass andiroba shells applied as a CO<sub>2</sub> adsorbent and a cheap semiconductor material, *J. CO<sub>2</sub> Util.* 62 (2022) 102071, <https://doi.org/10.1016/j.jcou.2022.102071>.
- [168] K.K. Kishibayev, J. Serafin, R.R. Tokpayev, T.N. Khavaza, A.A. Atchabarova, D.A. Abdukhytova, Z.T. Ibraimov, J. Sreńsek-Nazzal, Physical and chemical properties of activated carbon synthesized from plant wastes and shungite for CO<sub>2</sub> capture, *J. Environ. Chem. Eng.* 9 (6) (2021) 106798, <https://doi.org/10.1016/j.jece.2021.106798>.
- [169] M.K. Al Mesfer, Synthesis and characterization of high-performance activated carbon from walnut shell biomass for CO<sub>2</sub> capture, *Environ. Sci. Pollut.* Res. Int. 27 (13) (2020) 15020–15028, <https://doi.org/10.1007/s11356-020-07934-x>.
- [170] Y. Gao, Q. Yue, B. Gao, A. Li, Insight into activated carbon from different kinds of chemical activating agents: a review, *Sci. Total Environ.* 746 (2020) 141094, <https://doi.org/10.1016/j.scitotenv.2020.141094>.
- [171] Y. Kan, Q. Yue, B. Gao, Q. Li, Comparative study of dry-mixing and wet-mixing activated carbons prepared from waste printed circuit boards by NaOH activation, *RSC Adv.* 5 (128) (2015) 105943–105951, <https://doi.org/10.1039/C5RA18840C>.
- [172] B. Petrovic, M. Gorbounov, S.M. Soltani, Influence of surface modification on selective CO<sub>2</sub> adsorption: a technical review on mechanisms and methods, *Microporous Mesoporous Mater.* 312 (2021) 110751, <https://doi.org/10.1016/j.micromeso.2020.110751>.
- [173] M. Asadullah, I. Jahan, M.B. Ahmed, P. Adawiyah, N.H. Malek, M.S. Rahman, Preparation of microporous activated carbon and its modification for arsenic removal from water, *J. Ind. Eng. Chem.* 20 (3) (2014) 887–896, <https://doi.org/10.1016/j.jiec.2013.06.019>.
- [174] J. Sreńsek-Nazzal, W. Kamińska, B. Michalkiewicz, Z.C. Koren, Production, characterization and methane storage potential of KOH-activated carbon from sugarcane molasses, *Ind. Crops Prod.* 47 (2013) 153–159, <https://doi.org/10.1016/j.indcrop.2013.03.004>.
- [175] D.A.S. Maia, J.C.A. de Oliveira, M.S. Nazzaro, K.M. Sapag, R.H. López, S.M.P. de Lucena, D.C.S. de Azevedo, CO<sub>2</sub> gas-adsorption calorimetry applied to the study of chemically activated carbons, *Chem. Eng. Res. Des.* 136 (2018) 753–760, <https://doi.org/10.1016/j.cherd.2018.06.034>.
- [176] J. Xu, L. Chen, H. Qu, Y. Jiao, J. Xie, G. Xing, Preparation and characterization of activated carbon from reedy grass leaves by chemical activation with H<sub>3</sub>PO<sub>4</sub>, *Appl. Surf. Sci.* 320 (2014) 674–680, <https://doi.org/10.1016/j.japsusc.2014.08.178>.
- [177] K. Fu, Q. Yue, B. Gao, Y. Wang, Q. Li, Activated carbon from tomato stem by chemical activation with FeCl<sub>2</sub>, *Colloids Surf. A Physicochem. Eng. Asp.* 529 (2017) 842–849, <https://doi.org/10.1016/j.colsurfa.2017.06.064>.
- [178] M. Kılıç, E. Apaydın-Varol, A.E. Pütün, Preparation and surface characterization of activated carbons from Euphorbia rigida by chemical activation with ZnCl<sub>2</sub>, K<sub>2</sub>CO<sub>3</sub>, NaOH and H<sub>3</sub>PO<sub>4</sub>, *Appl. Surf. Sci.* 261 (15) (2012) 247–254, <https://doi.org/10.1016/j.japsusc.2012.07.155>.
- [179] M.K.B. Gratuito, T. Panyathanmaporn, R.A. Chumnanklang, N.B. Sirinuntawittaya, A. Dutta, Production of activated carbon from coconut shell: optimization using response surface methodology, *Bioresour. Technol.* 99 (11) (2008) 4887–4895, <https://doi.org/10.1016/j.biortech.2007.09.042>.
- [180] B.S. Rathi, P.S. Kumar, Application of adsorption process for effective removal of emerging contaminants from water and wastewater, *Environ. Pollut.* 280 (2021) 116995, <https://doi.org/10.1016/j.envpol.2021.116995>.
- [181] R.V. Siriwardane, M.S. Shen, E.P. Fisher, J.A. Poston, Adsorption of CO<sub>2</sub> on molecular sieves and activated carbon, *Energy Fuels* 15 (2001) 279–284, <https://doi.org/10.1021/ef000241s>.
- [182] T.C. Drage, J.M. Blackman, C. Pevida, C.E. Snape, Evaluation of activated carbon adsorbents for CO<sub>2</sub> capture in gasification, *Energy Fuels* 23 (2009) 2790–2796, <https://doi.org/10.1021/ef8010614>.
- [183] M. Hejazifar, S. Azizian, H. Sarikhani, Q. Li, D. Zhao, Microwave assisted preparation of efficient activated carbon from grapevine rhytidome for the removal of methyl violet from aqueous solution, *J. Anal. Appl. Pyrol.* 92 (1) (2011) 258–266, <https://doi.org/10.1016/j.jaat.2011.06.007>.
- [184] J.M. Illingworth, B. Rand, P.T. Williams, Understanding the mechanism of two-step, pyrolysis-alkali chemical activation of fibrous biomass for the production of activated carbon fibre matting, *Fuel Process. Technol.* 235 (2022) 107348, <https://doi.org/10.1016/j.fuproc.2022.107348>.
- [185] H.M. Mozammel, O. Masahiro, S.C. Bhattacharya, Activated charcoal from coconut shell using ZnCl<sub>2</sub> activation, *Biomass Bioenergy* 22 (5) (2002) 397–400, [https://doi.org/10.1016/S0961-9534\(02\)00015-6](https://doi.org/10.1016/S0961-9534(02)00015-6).
- [186] G. Ravenni, Z. Sárossy, J. Ahrenfeldt, U.B. Henriksen, Activity of chars and activated carbons for removal and decomposition of tar model compounds—a review, *Renew. Sustain. Energy Rev.* 94 (2018) 1044–1056, <https://doi.org/10.1016/j.rser.2018.07.001>.
- [187] Q. Cao, K.C. Xie, Y.K. Lv, W.R. Bao, Process effects on activated carbon with large specific surface area from corn cob, *Bioresour. Technol.* 97 (2006) 110–115, <https://doi.org/10.1016/j.biortech.2005.02.026>.
- [188] Z. Chen, S. Deng, H. Wei, B. Wang, J. Huang, G. Yu, Activated carbons and amine-modified materials for carbon dioxide capture — a review, *Front. Environ. Sci. Eng.* 7 (2013) 326–340, <https://doi.org/10.1007/s11783-013-0510-7>.
- [189] M. Sevilla, C. Falco, M.-M. Titirici, A.B. Fuertes, High-performance CO<sub>2</sub> sorbents from algae, *RSC Adv.* 2 (2012) 12792–12797, <https://doi.org/10.1039/C2RA22552B>.
- [190] X. Zhang, W. Li, A. Lu, Designed porous carbon materials for efficient CO<sub>2</sub> adsorption and separation, *New Carbon Mater.* 30 (2015) 481–501, [https://doi.org/10.1016/S1872-5805\(15\)60203-7](https://doi.org/10.1016/S1872-5805(15)60203-7).
- [191] X. Hu, M. Radosz, K.A. Cybosz, M. Thommes, CO<sub>2</sub>-filling capacity and selectivity of carbon nanopores: synthesis, texture, and poresize distribution from quenched-solid density functional theory (QSDFT), *Environ. Sci. Technol.* 45 (2011) 7068–7074, <https://doi.org/10.1021/es200782s>.
- [192] M. Ouzzine, J. Serafin, J. Sreńsek-Nazzal, Single step preparation of activated biocarbons derived from pomegranate peels and their CO<sub>2</sub> adsorption performance, *J. Anal. Appl. Pyrol.* 160 (2021) 105338, <https://doi.org/10.1016/j.jaat.2021.105338>.

- [193] S. Acevedo, L. Giraldo, J.C. Moreno-Pirajan, Carbonaceous materials prepared from Palm shells for the adsorption of CO<sub>2</sub>. Elemental, proximal, and morphological characterization, Rev. Colomb. Quím. 50 (2021) 30–39, <https://doi.org/10.15446/rev.colomb.quim.v50n2.95020>.
- [194] A.S. Ello, L.K. de Souza, A. Trokourey, M. Jaroniec, Development of micro-porous carbons for CO<sub>2</sub> capture by KOH activation of African palm shells, J. CO<sub>2</sub> Util. 2 (2013) 35–38, <https://doi.org/10.1016/j.jcou.2013.07.003>.
- [195] V. Presser, J. McDonough, S.H. Yeon, Y. Gogotsi, Effect of pore size on carbon dioxide sorption by carbide derived carbon, Energy Environ. Sci. 4 (8) (2011) 3059–3066, <https://doi.org/10.1039/C1EE01176F>.
- [196] H.R. Wei, S.B. Deng, B.Y. Hu, Z.H. Chen, B. Wang, J. Huang, G. Yu, Granular bamboo-derived activated carbon for high CO<sub>2</sub> adsorption: the dominant role of narrow micropores, ChemSusChem 5 (2012) 2354–2360, <https://doi.org/10.1002/cssc.201200570>.
- [197] X.L. Zhu, P.Y. Wang, C. Peng, J. Yang, X.B. Yan, Activated carbon produced from paulownia sawdust for high-performance CO<sub>2</sub> sorbents, Chin. Chem. Lett. 25 (6) (2014) 929–932, <https://doi.org/10.1016/j.ccl.2014.03.039>.
- [198] A. Heidari, H. Younesi, A. Rashidi, A. Ghoreyshi, Adsorptive removal of CO<sub>2</sub> on highly microporous activated carbons prepared from Eucalyptus camaldulensis wood: effect of chemical activation, J. Taiwan Inst. Chem. Eng. 45 (2) (2014) 579–588, <https://doi.org/10.1016/j.jite.2013.06.007>.
- [199] J. Han, L. Zhang, B. Zhao, L. Qin, Y. Wang, F. Xing, The N-doped activated carbon derived from sugarcane bagasse for CO<sub>2</sub> adsorption, Ind. Crops Prod. 128 (2019) 290–297, <https://doi.org/10.1016/j.indcrop.2018.11.028>.
- [200] L. Yue, Q. Xia, L. Wang, L. Wang, H. DaCosta, J. Yang, X. Hu, CO<sub>2</sub> adsorption at nitrogen-doped carbons prepared by K<sub>2</sub>CO<sub>3</sub> activation of urea-modified coconut shell, J. Colloid Interface Sci. 511 (2018) 259–267, <https://doi.org/10.1016/j.jcis.2017.09.040>.
- [201] C.Z. Shen, C.A. Grande, P. Li, J.G. Yu, A.E. Rodrigues, Adsorption equilibria and kinetics of CO<sub>2</sub> and N<sub>2</sub> on activated carbon beads, Chem. Eng. J. 160 (2010) 398–407, <https://doi.org/10.1016/j.cej.2009.12.005>.
- [202] M.G. Plaza, C. Pevida, B. Arias, J. Fermoso, M.D. Casal, C.F. Martín, F. Rubiera, J.J. Pis, Development of low-cost biomass-based adsorbents for post-combustion CO<sub>2</sub> capture, Fuel 88 (2009) 2442–2447, <https://doi.org/10.1016/j.fuel.2009.02.025>.
- [203] X. Ma, R. Chen, K. Zhou, Q. Wu, H. Li, Z. Zeng, L. Li, Activated porous carbon with an ultrahigh surface area derived from waste biomass for acetone adsorption, CO<sub>2</sub> capture, and light hydrocarbon separation, ACS Sustain. Chem. Eng. 8 (31) (2020) 11721–11728, <https://doi.org/10.1021/acssuschemeng.0c03725>.
- [204] J. Serafin, U. Narkiewicz, A.W. Morawski, R.J. Wróbel, B. Michalkiewicz, Highly microporous activated carbons from biomass for CO<sub>2</sub> capture and effective micropores at different conditions, J. CO<sub>2</sub> Util. 18 (2017) 73–79, <https://doi.org/10.1016/j.jcou.2017.01.006>.
- [205] C. Zhang, W. Song, Q. Ma, L. Xie, X. Zhang, H. Guo, Enhancement of CO<sub>2</sub> capture on biomass-based carbon from black locust by KOH activation and ammonia modification, Energy Fuels 30 (5) (2016) 4181–4190, <https://doi.org/10.1021/acs.energyfuels.5b02764>.
- [206] D. Li, T. Ma, R. Zhang, Y. Tian, Y. Qiao, Preparation of porous carbons with high low-pressure CO<sub>2</sub> uptake by KOH activation of rice husk char, Fuel 139 (2015) 68–70, <https://doi.org/10.1016/j.fuel.2014.08.027>.
- [207] H.M. Coromina, D.A. Walsh, R. Mokaya, Biomass-derived activated carbon with simultaneously enhanced CO<sub>2</sub> uptake for both pre and post combustion capture applications, J. Mater. Chem. A 4 (1) (2016) 280–289, <https://doi.org/10.1039/C5TA09202G>.
- [208] A. Alabadi, S. Razzaque, Y. Yang, S. Chen, B. Tan, Highly porous activated carbon materials from carbonized biomass with high CO<sub>2</sub> capturing capacity, Chem. Eng. J. 281 (2015) 606–612, <https://doi.org/10.1016/j.cej.2015.06.032>.
- [209] M.B. Ahmed, M.A.H. Johir, J.L. Zhou, H.H. Ngo, L.D. Nghiem, C. Richardson, M.A. Moni, M.R. Bryant, Activated carbon preparation from biomass feedstock: clean production and carbon dioxide adsorption, J. Clean. Prod. 225 (2019) 405–413, <https://doi.org/10.1016/j.jclepro.2019.03.342>.
- [210] H. Wei, H. Chen, N. Fu, J. Chen, G. Lan, W. Qian, Y. Liu, H. Lin, S. Han, Excellent electrochemical properties and large CO<sub>2</sub> capture of nitrogen-doped activated porous carbon synthesised from waste longan shells, Electrochim. Acta 231 (2017) 403–411, <https://doi.org/10.1016/j.electacta.2017.01.194>.
- [211] A. Toprak, T. Kopac, Carbon dioxide adsorption using high surface area activated carbons from local coals modified by KOH, NaOH and ZnCl<sub>2</sub> agents, Int. J. Chem. React. Eng. 15 (3) (2017), <https://doi.org/10.1515/ijcre-2016-0042>.
- [212] O. Boujibar, A. Souikny, F. Ghamouss, O. Achak, M. Dahbi, T. Chafik, CO<sub>2</sub> capture using N-containing nanoporous activated carbon obtained from argan fruit shells, J. Environ. Chem. Eng. 6 (2) (2018) 1995–2002, <https://doi.org/10.1016/j.jece.2018.03.005>.
- [213] W. Travis, S. Gadipelli, Z. Guo, Superior CO<sub>2</sub> adsorption from waste coffee ground derived carbons, RSC Adv. 5 (2015) 29558–29562, <https://doi.org/10.1039/C4RA13026J>.
- [214] P. Phadungbut, W. Koo-amornpattana, P. Bumroongsri, S. Ratchahat, N. Kunthakudee, W. Jonglertjyuny, B. Chalermsinsuwan, M. Hunsom, Adsorptive purification of CO<sub>2</sub>/H<sub>2</sub> gas mixtures of spent disposable wooden chopstick-derived activated carbon: optimal synthesis condition, Sep. Purif. Technol. 291 (2022) 120948, <https://doi.org/10.1016/j.seppur.2022.120948>.
- [215] J. Serafin, M. Ouzzine, O.F. Cruz Jr., J. Sreńcek-Nazzal, I.C. Gómez, F.Z. Azar, C.A.R. Mafull, D. Hotza, C.R. Rambo, Conversion of fruit waste-derived biomass to highly microporous activated carbon for enhanced CO<sub>2</sub> capture, Waste Manag. 136 (2021) 273–282, <https://doi.org/10.1016/j.wasman.2021.10.025>.
- [216] J. Serafin, K. Kielbasa, B. Michalkiewicz, The new tailored nanoporous carbons from the common polypoly (Polypodium vulgare): the role of textural properties for enhanced CO<sub>2</sub> adsorption, Chem. Eng. J. 429 (2022) 131751, <https://doi.org/10.1016/j.cej.2021.131751>.
- [217] J. Serafin, O.F. Cruz Jr., Promising activated carbons derived from common oak leaves and their application in CO<sub>2</sub> storage, J. Environ. Chem. Eng. 10 (3) (2022) 107642, <https://doi.org/10.1016/j.jece.2022.107642>.
- [218] J. Serafin, B. Dziejarski, O.F.C. Junior, J. Sreńcek-Nazzal, Design of highly microporous activated carbons based on walnut shell biomass for H<sub>2</sub> and CO<sub>2</sub> storage, Carbon 201 (2023) 633–647, <https://doi.org/10.1016/j.carbon.2022.09.013>.
- [219] F. Shen, Y. Wang, L. Li, K. Zhang, R.L. Smith, X. Qi, Porous carbonaceous materials from hydrothermal carbonization and KOH activation of corn stover for highly efficient CO<sub>2</sub> capture, Chem. Eng. Commun. 205 (4) (2018) 423–431, <https://doi.org/10.1080/00986445.2017.1367671>.
- [220] H. Fagnani, C.T. da Silva, M.M. Pereira, A.W. Rinaldi, P.A. Arroyo, M.A. de Barros, CO<sub>2</sub> adsorption in hydrochar produced from waste biomass, SN Appl. Sci. 1 (9) (2019) 1–10, <https://doi.org/10.1007/s42452-019-1055-6>.
- [221] W. Sangchoom, R. Mokaya, Valorization of lignin waste: carbons from hydrothermal carbonization of renewable lignin as superior sorbents for CO<sub>2</sub> and hydrogen storage, ACS Sustain. Chem. Eng. 3 (7) (2015) 1658–1667, <https://doi.org/10.1021/acssuschemeng.5b00351>.
- [222] M. Sevilla, A.B. Fuertes, Sustainable porous carbons with a superior performance for CO<sub>2</sub> capture, Energy Environ. Sci. 4 (5) (2011) 1765–1771, <https://doi.org/10.1039/C0EE00784F>.
- [223] G.G. Huang, Y.F. Liu, X.X. Wu, J.J. Cai, Activated carbons prepared by the KOH activation of a hydrochar from garlic peel and their CO<sub>2</sub> adsorption performance, New Carbon Mater 34 (3) (2019) 247–257, [https://doi.org/10.1016/S1872-5805\(19\)60014-4](https://doi.org/10.1016/S1872-5805(19)60014-4).
- [224] M.G. Plaza, C. Pevida, B. Arias, M.D. Casal, C.F. Martín, J. Fermoso, F. Rubiera, J.J. Pis, Different approaches for the development of low-cost CO<sub>2</sub> adsorbents, J. Environ. Eng. 135 (6) (2009) 426–432, [https://doi.org/10.1061/\(ASCE\)EE.1943-7870.0000009](https://doi.org/10.1061/(ASCE)EE.1943-7870.0000009).
- [225] M.S. Shafeeyan, W.M.A.W. Daud, A. Houshmand, A. Arami-Niya, Ammonia modification of activated carbon to enhance carbon dioxide adsorption: effect of pre-oxidation, Appl. Surf. Sci. 257 (9) (2011) 3936–3942, <https://doi.org/10.1016/j.apusc.2010.11.127>.
- [226] E. Mehrvarz, A.A. Ghoreyshi, M. Jahanshahi, Surface modification of broom sorghum-based activated carbon via functionalization with triethylenetetraamine and urea for CO<sub>2</sub> capture enhancement, Front. Chem. Sci. Eng. 11 (2) (2017) 252–265, <https://doi.org/10.1007/s11705-017-1630-6>.
- [227] A. Boonpoke, S. Chiarakorn, N. Laosiripojana, S. Towprayoon, A. Chidthaisong, Investigation of CO<sub>2</sub> adsorption by bagasse-based activated carbon, Korean J. Chem. Eng. 29 (1) (2012) 89–94, <https://doi.org/10.1007/s11814-011-0143-0>.
- [228] Y. Jin, C.P. Huynh, S.C. Hawkins, S. Su, Expanded graphite/phenolic resin-based carbon composite adsorbents for post-combustion CO<sub>2</sub> capture, RSC Adv. 5 (77) (2015) 62604–62610, <https://doi.org/10.1039/C5RA09853J>.
- [229] J. Park, S.Y. Cho, M. Jung, K. Lee, Y.C. Nah, N.F. Attia, H. Oh, Efficient synthetic approach for nanoporous adsorbents capable of pre-and post-combustion CO<sub>2</sub> capture and selective gas separation, J. CO<sub>2</sub> Util. 45 (2021) 101404, <https://doi.org/10.1016/j.jcou.2020.101404>.
- [230] W. Liang, Z. Liu, J. Peng, X. Zhou, X. Wang, Z. Li, Enhanced CO<sub>2</sub> adsorption and CO<sub>2</sub>/N<sub>2</sub>/CH<sub>4</sub> selectivity of novel carbon composites CPDA@ A-Cs, Energy Fuels 33 (1) (2018) 493–502, <https://doi.org/10.1021/acs.energyfuels.8b03637>.
- [231] H. Chen, Y.J. Zhang, P.Y. He, C.J. Li, L.C. Liu, Novel activated carbon route to low-cost geopolymers based porous composite with high mechanical resistance and enhanced CO<sub>2</sub> capacity, Microporous Mesoporous Mater. 305 (2020) 110282, <https://doi.org/10.1016/j.micromeso.2020.110282>.
- [232] J. Przepiórska, A. Czyżewski, R.A. Pietrzak, B. Tryba, MgO/CaO-loaded porous carbons for carbon dioxide capture: effects accompanying regeneration process, J. Therm. Anal. Calorim. 111 (2013) 357–364, <https://doi.org/10.1007/s10973-012-2354-y>.
- [233] S. Shahkarami, A.K. Dalai, J. Soltan, Enhanced CO<sub>2</sub> adsorption using MgO-impregnated activated carbon: impact of preparation techniques, Ind. Eng. Chem. Res. 55 (20) (2016) 5955–5964, <https://doi.org/10.1021/acs.iecr.5b04824>.
- [234] M. Rostami, M. Mofarahi, R. Karimzadeh, D. Abedi, Preparation and characterization of activated carbon–zeolite composite for gas adsorption separation of CO<sub>2</sub>/N<sub>2</sub> system, J. Chem. Eng. Data 61 (7) (2016) 2638–2646, <https://doi.org/10.1021/acs.jcd.6b00374>.
- [235] T. Okutani, T. Utsumi, M. Ohnishi, Synthesis of Conjunctive Zeolite-Activated Carbon Composite Adsorbent from Rice Hulls for Simultaneous Adsorption of CO<sub>2</sub> and H<sub>2</sub>O, 42nd International Conference on Environmental Systems, 2012, p. 3429, <https://doi.org/10.2514/6.2012-3429>.
- [236] M.J. Regufe, A.F. Ferreira, J.M. Loureiro, Y. Shi, A. Rodrigues, A.M. Ribeiro, New hybrid composite honeycomb monolith with 13X zeolite and activated

- carbon for CO<sub>2</sub> capture, *Adsorption* 24 (3) (2018) 249–265, <https://doi.org/10.1007/s10450-018-9938-1>.
- [237] H. Li, F. Zheng, J. Wang, J. Zhou, X. Huang, L. Chen, P. Hu, J.M. Gao, Q. Zhen, S. Bashir, J.L. Liu, Facile preparation of zeolite-activated carbon composite from coal gangue with enhanced adsorption performance, *Chem. Eng. J.* 390 (2020) 124513, <https://doi.org/10.1016/j.cej.2020.124513>.
- [238] G. Zeng, Z. Yu, M. Du, N. Ai, W. Chen, Z. Gu, B. Chen, Enhanced CO<sub>2</sub> adsorption on activated carbon-modified HKUST-1 composites, *ChemistrySelect* 3 (41) (2018) 11601–11605, <https://doi.org/10.1002/slct.201802443>.
- [239] A.K. Adhikari, K.S. Lin, Improving CO<sub>2</sub> adsorption capacities and CO<sub>2</sub>/N<sub>2</sub> separation efficiencies of MOF-74 (Ni, Co) by doping palladium-containing activated carbon, *Chem. Eng. J.* 284 (2016) 1348–1360, <https://doi.org/10.1016/j.cej.2015.09.086>.
- [240] X. Liu, C. Sun, H. Liu, W.H. Tan, W. Wang, C. Snape, Developing hierarchically ultra-micro/mesoporous biocarbons for highly selective carbon dioxide adsorption, *Chem. Eng. J.* 361 (2019) 199–208, <https://doi.org/10.1016/j.cej.2018.11.062>.
- [241] F.E.C. Othman, N. Yusof, S. Samitsu, N. Abdullah, M.F. Hamid, K. Nagai, M.N.Z. Abidin, M.A. Azali, A.F. Ismail, J. Jaafar, F. Aziz, W.N.W. Salleh, Activated carbon nanofibers incorporated metal oxides for CO<sub>2</sub> adsorption: effects of different type of metal oxides, *J. CO<sub>2</sub> Util.* 45 (2021) 101434, <https://doi.org/10.1016/j.jcou.2021.101434>.
- [242] Y. Liu, P. Ghimire, M. Jaroniec, Copper benzene-1, 3, 5-tricarboxylate (Cu-BTC) metal-organic framework (MOF) and porous carbon composites as efficient carbon dioxide adsorbents, *J. Colloid Interface Sci.* 535 (2019) 122–132, <https://doi.org/10.1016/j.jcis.2018.09.086>.
- [243] R.W. Chang, C.J. Lin, S.Y.H. Liou, M.A. Bañares, M.O. Guerrero-Pérez, R.M.M. Aranda, Enhanced cyclic CO<sub>2</sub>/N<sub>2</sub> separation performance stability on chemically modified N-doped ordered mesoporous carbon, *Catal. Today* 356 (2020) 88–94, <https://doi.org/10.1016/j.cattod.2019.08.004>.
- [244] M. Song, Y. Huang, B. Jin, Y. Wu, J. Wu, Z. Zhong, The influence of different surface-modification treatments on biomass-based carbons and their effects on adsorption of carbon dioxide, *Int. J. Green Energy* 13 (11) (2016) 1084–1089, <https://doi.org/10.1080/15435075.2014.893238>.
- [245] A. Kongnoo, P. Inthrapat, P. Worathanakul, C. Phalakornkule, Diethanolamine impregnated palm shell activated carbon for CO<sub>2</sub> adsorption at elevated temperatures, *J. Environ. Chem. Eng.* 4 (1) (2016) 73–81, <https://doi.org/10.1016/j.jece.2015.11.015>.
- [246] E. Atta-Obeng, B. Dawson-Andoh, E. Felton, G. Dahle, Carbon dioxide capture using amine functionalized hydrothermal carbons from technical lignin, *Waste Biomass Valorization* 10 (9) (2019) 2725–2731, <https://doi.org/10.1007/s12649-018-0281-2>.
- [247] S. Hosseini, I. Bayesti, E. Marahel, F.E. Babadi, L.C. Abdullah, T.S. Choong, Adsorption of carbon dioxide using activated carbon impregnated with Cu promoted by zinc, *J. Taiwan Inst. Chem. Eng.* 52 (2015) 109–117, <https://doi.org/10.1016/j.jtice.2015.02.015>.
- [248] S. Acevedo, L. Giraldo, J.C. Moreno-Piraján, Adsorption of CO<sub>2</sub> on activated carbons prepared by chemical activation with cupric nitrate, *ACS Omega* 5 (18) (2020) 10423–10432, <https://doi.org/10.1021/acsomega.0c00342>.
- [249] M. Younas, L.K. Leong, A.R. Mohamed, S. Sethupathi, CO<sub>2</sub> adsorption by modified palm shell activated carbon (PSAC) via chemical and physical activation and metal impregnation, *Chem. Eng. Commun.* 203 (11) (2016) 1455–1463, <https://doi.org/10.1080/0986445.2016.1201660>.
- [250] W.N.R.W. Isahak, S.Z. Hasan, Z.A.C. Ramli, M.M. Ba-Abbad, M.A. Yarmo, Enhanced physical and chemical adsorption of carbon dioxide using bimetallic copper–magnesium oxide/carbon nanocomposite, *Res. Chem. Intermed.* 44 (2) (2018) 829–841, <https://doi.org/10.1007/s11164-017-3138-6>.
- [251] M. Nowrouzi, H. Younesi, N. Bahramifar, Superior CO<sub>2</sub> capture performance on biomass-derived carbon/metal oxides nanocomposites from Persian ironwood by H<sub>3</sub>PO<sub>4</sub> activation, *Fuel* 223 (2018) 99–114, <https://doi.org/10.1016/j.fuel.2018.03.035>.
- [252] Y. Guo, C. Zhao, C. Li, S. Lu, Application of PEI–K<sub>2</sub>CO<sub>3</sub>/AC for capturing CO<sub>2</sub> from flue gas after combustion, *Appl. Energy* 129 (2014) 17–24, <https://doi.org/10.1016/j.apenergy.2014.05.003>.
- [253] X. Zhu, Q. Wang, Y. Shi, N. Cai, Layered double oxide/activated carbon-based composite adsorbent for elevated temperature H<sub>2</sub>/CO<sub>2</sub> separation, *Int. J. Hydrogen Energy* 40 (30) (2015) 9244–9253, <https://doi.org/10.1016/j.ijhydene.2015.05.116>.
- [254] Q. Ye, J. Jiang, C. Wang, Y. Liu, H. Pan, Y. Shi, Adsorption of low-concentration carbon dioxide on amine-modified carbon nanotubes at ambient temperature, *Energy Fuels* 26 (4) (2012) 2497–2504, <https://doi.org/10.1021/ef201699w>.
- [255] S.K. Smart, A.I. Cassady, G.Q. Lu, D.J. Martin, The biocompatibility of carbon nanotubes, *Carbon* 44 (6) (2006) 1034–1047, <https://doi.org/10.1016/j.carbon.2005.10.011>.
- [256] K. Rahimi, S. Riahi, M. Abbasi, Z. Fakhroueian, Modification of multi-walled carbon nanotubes by 1, 3-diaminopropane to increase CO<sub>2</sub> adsorption capacity, *J. Environ. Manag.* 242 (2019) 81–89, <https://doi.org/10.1016/j.jenvman.2019.04.036>.
- [257] T. Belin, F. Epron, Characterization methods of carbon nanotubes: a review, *Mater. Sci. Eng. B* 119 (2) (2005) 105–118, <https://doi.org/10.1016/j.mseb.2005.02.046>.
- [258] M. Schirowski, G. Abellán, E. Nuin, J. Pampel, C. Dolle, V. Wedler, T.P. Fellinger, E. Speckner, F. Hauke, A. Hirsch, Fundamental insights into the reductive covalent cross-linking of single-walled carbon nanotubes, *J. Am. Chem. Soc.* 140 (9) (2018) 3352–3360, <https://doi.org/10.1021/jacs.7b12910>.
- [259] M.L. Terranova, V. Sessa, M. Rossi, The world of carbon nanotubes: an overview of CVD growth methodologies, *Chem. Vap. Depos.* 12 (6) (2006) 315–325, <https://doi.org/10.1002/cvde.200600030>.
- [260] S. Shukrullah, N.M. Mohamed, M.S. Shaharun, S. Ullah, M.Y. Naz, Effective CO<sub>2</sub> adsorption on pristine and chemically functionalized MWCNTs, *AIP Conf. Proc.* 1787 (1) (2016, November) 050025, <https://doi.org/10.1063/1.4968123>. AIP Publishing LLC.
- [261] T. Kim, J. Shin, K. Lee, Y. Jung, S.B. Lee, S.J. Yang, A universal surface modification method of carbon nanotube fibers with enhanced tensile strength, *Compos. Part A Appl. Sci. Manuf.* 140 (2021) 106182, <https://doi.org/10.1016/j.compositesa.2020.106182>.
- [262] N. Gupta, S.M. Gupta, S.K. Sharma, Carbon nanotubes: synthesis, properties and engineering applications, *Carbon Lett* 29 (5) (2019) 419–447, <https://doi.org/10.1007/s42823-019-00068-2>.
- [263] L. Keller, B. Ohs, J. Lenhart, L. Abduly, P. Blanke, M. Wessling, High capacity polyethylenimine impregnated microtubes made of carbon nanotubes for CO<sub>2</sub> capture, *Carbon* 126 (2018) 338–345, <https://doi.org/10.1016/j.carbon.2017.10.023>.
- [264] M.S. Lee, S.Y. Lee, S.J. Park, Preparation and characterization of multi-walled carbon nanotubes impregnated with polyethylenimine for carbon dioxide capture, *Int. J. Hydrogen Energy* 40 (8) (2015) 3415–3421, <https://doi.org/10.1016/j.ijhydene.2014.12.104>.
- [265] Z. Zhou, S.K. Babijepalli, A.H. Nguyen-Sorenson, C.M. Anderson, J.L. Park, K.J. Stowers, Steam-stable covalently bonded polyethylenimine modified multiwall carbon nanotubes for carbon dioxide capture, *Energy Fuels* 32 (11) (2018) 11701–11709, <https://doi.org/10.1021/acs.energyfuels.8b02864>.
- [266] M. Deng, H.G. Park, Spacer-assisted amine-coiled carbon nanotubes for CO<sub>2</sub> capture, *Langmuir* 35 (13) (2019) 4453–4459, <https://doi.org/10.1021/acs.langmuir.8b03980>.
- [267] M. Irani, A.T. Jacobson, K.A. Gasem, M. Fan, Modified carbon nanotubes/tetraethylenepentamine for CO<sub>2</sub> capture, *Fuel* 206 (2017) 10–18, <https://doi.org/10.1016/j.fuel.2017.05.087>.
- [268] A. Mukhtar, N. Mellon, S. Saqib, A. Khawar, S. Rafiq, S. Ullah, A.G. Al-Sehem, M. Babar, M.A. Bustam, W.A. Khan, M.S. Tahir, CO<sub>2</sub>/CH<sub>4</sub> adsorption over functionalized multi-walled carbon nanotubes; an experimental study, isotherms analysis, mechanism, and thermodynamics, *Microporous Mesoporous Mater.* 294 (2020) 109883, <https://doi.org/10.1016/j.micromeso.2019.109883>.
- [269] M. Konni, S. Doddì, A.S. Dadhich, S.B. Mukkamala, Adsorption of CO<sub>2</sub> by hierarchical structures of f-MWCNTs@Zn/Co-ZIF and N-MWCNTs@Zn/Co-ZIF prepared through in situ growth of ZIFs in CNTs, *Surf. Interfaces* 12 (2018) 20–25, <https://doi.org/10.1016/j.surfin.2018.04.006>.
- [270] L. Keller, B. Ohs, L. Abduly, M. Wessling, Carbon nanotube silica composite hollow fibers impregnated with polyethylenimine for CO<sub>2</sub> capture, *Chem. Eng. J.* 359 (2019) 476–484, <https://doi.org/10.1016/j.cej.2018.11.100>.
- [271] A. Garcia-Gallastegui, D. Iruretagoyena, M. Mokhtar, A.M. Asiri, S.N. Basahel, S.A. Al-Thabaiti, A.O. Alyoubi, D. Chadwick, M.S. Shaffer, Layered double hydroxides supported on multi-walled carbon nanotubes: preparation and CO<sub>2</sub> adsorption characteristics, *J. Mater. Chem. A* 22 (28) (2012) 13932–13940, <https://doi.org/10.1039/C2JM00059H>.
- [272] Y. Zhang, J. Sun, J. Tan, C. Ma, S. Luo, W. Li, S. Liu, Multi-walled carbon nanotubes/carbon foam nanocomposites derived from biomass for CO<sub>2</sub> capture and supercapacitor applications, *Fuel* 305 (2021) 121622, <https://doi.org/10.1016/j.fuel.2021.121622>.
- [273] H. Wang, C. Xu, Y. Zhou, W. Zhao, J. Zhong, W. Huang, R. Chen, Fabrication of hierarchical N-doped carbon nanotubes for CO<sub>2</sub> adsorption, *Nano* 14 (6) (2019) 1950072, <https://doi.org/10.1142/S1793292019500723>.
- [274] Z. Zhou, C.M. Anderson, S.K. Butler, S.K. Thompson, K.J. Whitty, T.C. Shen, K.J. Stowers, Stability and efficiency of CO<sub>2</sub> capture using linear amine polymer modified carbon nanotubes, *J. Mater. Chem. A* 5 (21) (2017) 10486–10494, <https://doi.org/10.1039/C7TA02576A>.
- [275] C. Lu, H. Bai, B. Wu, F. Su, J.F. Hwang, Comparative study of CO<sub>2</sub> capture by carbon nanotubes, activated carbons, and zeolites, *Energy Fuels* 22 (5) (2008) 3050–3056, <https://doi.org/10.1021/ef8000086>.
- [276] J.M. Ngoy, N. Wagner, L. Riboldi, O. Bolland, A CO<sub>2</sub> capture technology using multi-walled carbon nanotubes with polyaspartamide surfactant, *Energy Proc.* 63 (2014) 2230–2248, <https://doi.org/10.1016/j.egypro.2014.11.242>.
- [277] H. Hu, T. Zhang, S. Yuan, S. Tang, Functionalization of multi-walled carbon nanotubes with phenylenediamine for enhanced CO<sub>2</sub> adsorption, *Adsorption* 23 (1) (2017) 73–85, <https://doi.org/10.1007/s10450-016-9820-y>.
- [278] N. Iqbal, X. Wang, J. Yu, B. Ding, Robust and flexible carbon nanofibers doped with amine functionalized carbon nanotubes for efficient CO<sub>2</sub> capture, *Adv. Sustain. Syst.* 1 (3–4) (2017) 1600028, <https://doi.org/10.1002/adsu.201600028>.
- [279] X. He, J. Liu, Y. Jiang, M. Yaseen, H. Guan, J. Sun, X. Cui, D. Liao, Z. Tong, 'Useful' template synthesis of N-doped acicular hollow porous carbon/carbon-nanotubes for enhanced capture and selectivity of CO<sub>2</sub>, *Chem. Eng. J.* 361 (2019) 278–285, <https://doi.org/10.1016/j.cej.2018.12.031>.
- [280] Y.C. Chiang, W.L. Hsu, S.Y. Lin, R.S. Juang, Enhanced CO<sub>2</sub> adsorption on activated carbon fibers grafted with nitrogen-doped carbon nanotubes, *Materials* 10 (5) (2017) 511, <https://doi.org/10.3390/ma10050511>.

- [281] S. Salehi, M. Anbia, A.H. Hosseiny, M. Sepehrian, Enhancement of CO<sub>2</sub> adsorption on polyethylenimine functionalized multiwalled carbon nanotubes/Cd-nanozelite composites, *J. Mol. Struct.* 1173 (2018) 792–800, <https://doi.org/10.1016/j.molstruc.2018.07.056>.
- [282] S.A.M.I. Ullah, M.A. Bustam, A.E. Elkhalifah, N.A.D.I.A. Riaz, G.I.R.M.A. Gonfa, A.M. Shariff, Synthesis, CO<sub>2</sub> adsorption performance of modified MIL-101 with multi-wall carbon nanotubes, in: Advanced Materials Research, vol. 1133, Trans Tech Publications Ltd, 2016, pp. 486–490, <https://doi.org/10.4028/www.scientific.net/AMR.1133.486>.
- [283] G.E. Gadd, P.J. Evans, S. Kennedy, M. James, M. Elcombe, D. Cassidy, S. Morica, J. Holmes, N. Webb, P. Dixon, P. Prasad, Gas storage in fullerenes, *Fullerene Sci. Technol.* 7 (6) (1999) 1043–1143, <https://doi.org/10.1080/10641229909350304>.
- [284] L. Bi, J. Yin, X. Huang, Y. Wang, Z. Yang, Graphene pillared with hybrid fullerene and nanotube as a novel 3D framework for hydrogen storage: a DFT and GCMC study, *Int. J. Hydrogen Energy* 45 (35) (2020) 17637–17648, <https://doi.org/10.1016/j.ijhydene.2020.04.227>.
- [285] C.U. Deniz, H. Mert, C. Baykasoglu, Li-doped fullerene pillared graphene nanocomposites for enhancing hydrogen storage: a computational study, *Comput. Mater. Sci.* 186 (2021) 110023, <https://doi.org/10.1016/j.commatsci.2020.110023>.
- [286] G. Xu, Z. Meng, X. Guo, H. Zhu, K. Deng, C. Xiao, Y. Liu, Molecular simulations on CO<sub>2</sub> adsorption and adsorptive separation in fullerene impregnated MOF-177, MOF-180 and MOF-200, *Comput. Mater. Sci.* 168 (2019) 58–64, <https://doi.org/10.1016/j.commatsci.2019.05.039>.
- [287] T.B. Shiell, D.G. McCulloch, J.E. Bradby, B. Haberl, D.R. McKenzie, Neutron diffraction discriminates between models for the nanoarchitecture of graphene sheets in glassy carbon, *J. Non-Cryst. Solids* 554 (2021) 120610, <https://doi.org/10.1016/j.jnoncrysol.2020.120610>.
- [288] G.J. Ogunwale, H. Louis, T.E. Gber, A.S. Adeyinka, Modeling of pristine, Ir-and Au-decorated C<sub>60</sub> fullerenes as sensors for detection of Hydroxyurea and Nitrosoure drugs, *J. Environ. Chem. Eng.* (2022) 108802, <https://doi.org/10.1016/j.jece.2022.108802>.
- [289] C.S. Liu, X.J. Ye, X. Wang, X. Yan, Metalized B<sub>40</sub> fullerene as a novel material for storage and optical detection of hydrogen: a first-principles study, *RSC Adv.* 6 (62) (2016) 56907–56912, <https://doi.org/10.1039/C6RA08378A>.
- [290] H. Dong, B. Lin, K. Gilmore, T. Hou, S.T. Lee, Y. Li, B<sub>40</sub> fullerene: an efficient material for CO<sub>2</sub> capture, storage and separation, *Curr. Appl. Phys.* 15 (9) (2015) 1084–1089, <https://doi.org/10.1016/j.cap.2015.06.008>.
- [291] G. Gao, F. Ma, Y. Jiao, Q. Sun, Y. Jiao, E. Wacławik, A. Du, Modelling CO<sub>2</sub> adsorption and separation on experimentally-realized B<sub>40</sub> fullerene, *Comput. Mater. Sci.* 108 (2015) 38–41, <https://doi.org/10.1016/j.commatsci.2015.06.005>.
- [292] M.D. Esrafilii, P. Mousavian, Ca coated B<sub>40</sub> fullerene: a promising material for CO<sub>2</sub> storage and separation, *Chem. Phys. Lett.* 781 (2021) 138991, <https://doi.org/10.1016/j.cplett.2021.138991>.
- [293] M. Qu, G. Qin, A. Du, J. Fan, Q. Sun, B<sub>80</sub> fullerene: a promising metal-free photocatalyst for efficient conversion of CO<sub>2</sub> to HCOOH, *J. Phys. Chem. C* 123 (39) (2019) 24193–24199, <https://doi.org/10.1021/acs.jpcc.9b07562>.
- [294] A.A. Khan, R. Ahmad, I. Ahmad, X. Su, Selective adsorption of CO<sub>2</sub> from gas mixture by P-decorated C<sub>24</sub>N<sub>24</sub> fullerene assisted by an electric field: a DFT approach, *J. Mol. Graph. Model.* 103 (2021) 107806, <https://doi.org/10.1016/j.jmgm.2020.107806>.
- [295] A.A. Khan, I. Ahmad, R. Ahmad, Influence of electric field on CO<sub>2</sub> removal by P-doped C<sub>60</sub>-fullerene: a DFT study, *Chem. Phys. Lett.* 742 (2020) 137155, <https://doi.org/10.1016/j.cplett.2020.137155>.
- [296] J. Wang, L. Huang, R. Yang, Z. Zhang, J. Wu, Y. Gao, Q. Wang, D. O'Hare, Z. Zhong, Recent advances in solid sorbents for CO<sub>2</sub> capture and new development trends, *Energy Environ. Sci.* 7 (11) (2014) 3478–3518, <https://doi.org/10.1039/C4EE01647E>.
- [297] S. Somiya, *Handbook of Advanced Ceramics: Materials, Applications, Processing, and Properties*, Academic Press, 2013, <https://doi.org/10.1016/C2010-0-66261-4>.
- [298] H.B. Zhang, J.W. Wang, Q. Yan, W.G. Zheng, C. Chen, Z.Z. Yu, Vacuum-assisted synthesis of graphene from thermal exfoliation and reduction of graphite oxide, *J. Mater. Chem.* 21 (14) (2011) 5392–5397, <https://doi.org/10.1039/C1JM10099H>.
- [299] H. Yuan, L.Y. Meng, S.J. Park, KOH-activated graphite nanofibers as CO<sub>2</sub> adsorbents, *Carbon Lett.* 19 (2016) 99–103, <https://doi.org/10.5714/CL.2016.19.099>.
- [300] A.K. Mishra, S. Ramaprabhu, Study of CO<sub>2</sub> adsorption in low cost graphite nanoplatelets, *IJCEA* 1 (3) (2010) 266–269, <https://doi.org/10.7763/IJCEA.2010.V1.I4.6>.
- [301] G.Z. Kyzas, A.C. Mitropoulos (Eds.), *Advanced Low-Cost Separation Techniques in Interface Science*, Academic Press, 2019, <https://doi.org/10.1016/B978-0-12-814178-6.00001-7>.
- [302] G.J. Shin, K. Rhee, S.J. Park, Improvement of CO<sub>2</sub> capture by graphite oxide in presence of polyethylenimine, *Int. J. Hydrogen Energy* 41 (32) (2016) 14351–14359, <https://doi.org/10.1016/j.ijhydene.2016.05.162>.
- [303] Y. Zhao, H. Ding, Q. Zhong, Preparation and characterization of aminated graphite oxide for CO<sub>2</sub> capture, *Appl. Surf. Sci.* 258 (10) (2012) 4301–4307, <https://doi.org/10.1016/j.apsusc.2011.12.085>.
- [304] Y. Zhang, Y. Chi, C. Zhao, Y. Liu, Y. Zhao, L. Jiang, Y. Song, CO<sub>2</sub> adsorption behavior of graphite oxide modified with Tetraethylpentamine, *J. Chem. Eng. Data* 63 (1) (2018) 202–207, <https://doi.org/10.1021/acs.jced.7b00824>.
- [305] S.M. Hong, S.H. Kim, K.B. Lee, Adsorption of carbon dioxide on 3-aminopropyl-triethoxysilane modified graphite oxide, *Energy Fuels* 27 (6) (2013) 3358–3363, <https://doi.org/10.1021/ef400467w>.
- [306] Z. Bian, J. Xu, S. Zhang, X. Zhu, H. Liu, J. Hu, Interfacial growth of metal organic framework/graphite oxide composites through pickering emulsion and their CO<sub>2</sub> capture performance in the presence of humidity, *Langmuir* 31 (26) (2015) 7410–7417, <https://doi.org/10.1021/acs.langmuir.5b01171>.
- [307] A. Policicchio, Y. Zhao, Q. Zhong, R.G. Agostino, T.J. Bandosz, Cu-BTC/aminated graphite oxide composites as high-efficiency CO<sub>2</sub> capture media, *ACS Appl. Mater. Interfaces* 6 (1) (2014) 101–108, <https://doi.org/10.1021/am404952z>.
- [308] Y. Zhao, M. Seredych, Q. Zhong, T.J. Bandosz, Superior performance of copper based MOF and aminated graphite oxide composites as CO<sub>2</sub> adsorbents at room temperature, *ACS Appl. Mater. Interfaces* 5 (11) (2013) 4951–4959, <https://doi.org/10.1021/am404952z>.
- [309] H. Espinosa-Jiménez, H. Domínguez, CO<sub>2</sub> adsorption on a modified graphite surface with sodium dodecyl sulfate surfactants: a molecular dynamics study, *Rev. Mex. Fis.* 65 (1) (2019) 20–24.
- [310] X. Li, Q. Xue, X. Chang, L. Zhu, C. Ling, H. Zheng, Effects of sulfur doping and humidity on CO<sub>2</sub> capture by graphite split pore: a theoretical study, *ACS Appl. Mater. Interfaces* 9 (9) (2017) 8336–8343, <https://doi.org/10.1021/acsm.6b14281>.
- [311] E. Kusnini, C.S. Utami, A. Usman, N. Nasruddin, K.A. Tito, CO<sub>2</sub> capture using graphite waste composites and ceria, *Int. J. Technol.* 9 (2) (2018) 287–296, <https://doi.org/10.14716/ijtech.v9i2.1031>.
- [312] E. Kusnini, A.K. Sasongko, N. Nasruddin, A. Usman, Improvement of carbon dioxide capture using graphite waste/Fe<sub>3</sub>O<sub>4</sub> composites, *Int. J. Technol.* 8 (8) (2017) 1436, <https://doi.org/10.14716/ijtech.v8i8.697>.
- [313] M. Seredych, E. Rodríguez-Castellón, T.J. Bandosz, Alterations of S-doped porous carbon-rGO composites surface features upon CO<sub>2</sub> adsorption at ambient conditions, *Carbon* 107 (2016) 501–509, <https://doi.org/10.1016/j.carbon.2016.06.028>.
- [314] L.Y. Meng, S.J. Park, Effect of heat treatment on CO<sub>2</sub> adsorption of KOH-activated graphite nanofibers, *J. Colloid Interface Sci.* 352 (2) (2010) 498–503, <https://doi.org/10.1016/j.jcis.2010.08.048>.
- [315] P. Ying, T. Liang, Y. Du, J. Zhang, X. Zeng, Z. Zhong, Thermal transport in planar sp2-hybridized carbon allotropes: a comparative study of biphenylene network, pentaheptite and graphene, *Int. J. Heat Mass Transf.* 183 (2022) 122060, <https://doi.org/10.1016/j.ijheatmasstransfer.2021.122060>.
- [316] C. Liu, X. Huang, Y.Y. Wu, X. Deng, Z. Zheng, Z. Xu, D. Hui, Advance on the dispersion treatment of graphene oxide and the graphene oxide modified cement-based materials, *Nanotechnol. Rev.* 10 (1) (2021) 34–49, <https://doi.org/10.1515/ntrrev-2021-0003>.
- [317] T. Wang, M.D. Quinn, S.M. Notley, Enhanced electrical, mechanical and thermal properties by exfoliating graphene platelets of larger lateral dimensions, *Carbon* 129 (2018) 191–198, <https://doi.org/10.1016/j.carbon.2017.12.034>.
- [318] D.R. Dreyer, R.S. Ruoff, C.W. Bielawski, From conception to realization: an historical account of graphene and some perspectives for its future, *Angew. Chem. Int. Ed.* 49 (49) (2010) 9336–9344, <https://doi.org/10.1002/anie.201003024>.
- [319] D.M. D'Alessandro, B. Smit, J.R. Long, Carbon dioxide capture: prospects for new materials, *Angew. Chem. Int. Ed.* 49 (35) (2010) 6058–6082, <https://doi.org/10.1002/anie.201000431>.
- [320] B.S. Ge, T. Wang, H.X. Sun, W. Gao, H.R. Zhao, Preparation of mixed matrix membranes based on polyimide and aminated graphene oxide for CO<sub>2</sub> separation, *Polym. Adv. Technol.* 29 (4) (2018) 1334–1343, <https://doi.org/10.1002/pat.4245>.
- [321] M.D. Stoller, S. Park, Y. Zhu, J. An, R.S. Ruoff, Graphene-based ultracapacitors, *Nano Lett.* 8 (10) (2008) 3498–3502, <https://doi.org/10.1021/nl802558y>.
- [322] H. Koolivand, A. Sharif, M.R. Kashani, M. Karimi, M.K. Salooki, M.A. Semsarzadeh, Functionalized graphene oxide/polyimide nanocomposites as highly CO<sub>2</sub>-selective membranes, *J. Polym. Res.* 21 (11) (2014) 1–12, <https://doi.org/10.1007/s10965-014-0599-9>.
- [323] M. Khajouei, M. Najafi, S.A. Jafari, Development of ultrafiltration membrane via in-situ grafting of nano-GO/PSF with anti-biofouling properties, *Chem. Eng. Res. Des.* 142 (2019) 34–43, <https://doi.org/10.1016/j.cherd.2018.11.033>.
- [324] S. Gadipelli, Z.X. Guo, Graphene-based materials: synthesis and gas sorption, storage and separation, *Prog. Mater. Sci.* 69 (2015) 1–60, <https://doi.org/10.1016/j.pmatsci.2014.10.004>.
- [325] G. Reina, J.M. González-Domínguez, A. Criado, E. Vázquez, A. Bianco, M. Prato, Promises, facts and challenges for graphene in biomedical applications, *Chem. Soc. Rev.* 46 (15) (2017) 4400–4416, <https://doi.org/10.1039/C7CS00363C>.
- [326] S. Ullah, M.A. Bustam, A.G. Al-Sehemi, M.A. Assiri, F.A.A. Kareem, A. Mukhtar, M. Ayoub, G. Gonfa, Influence of post-synthetic graphene oxide (GO) functionalization on the selective CO<sub>2</sub>/CH<sub>4</sub> adsorption behavior of MOF-200 at different temperatures; an experimental and adsorption isotherms study, *Microporous Mesoporous Mater.* 296 (2020) 110002, <https://doi.org/10.1016/j.micromeso.2020.110002>.
- [327] B. Szczęśniak, J. Choma, Graphene-containing microporous composites for selective CO<sub>2</sub> adsorption, *Microporous Mesoporous Mater.* 292 (2020) 109761, <https://doi.org/10.1016/j.micromeso.2019.109761>.
- [328] S. Shang, Z. Tao, C. Yang, A. Hanif, L. Li, D.C. Tsang, Q. Gu, J. Shang, Facile synthesis of CuBTC and its graphene oxide composites as efficient adsorbents

- for CO<sub>2</sub> capture, *Chem. Eng. J.* 393 (2020) 124666, <https://doi.org/10.1016/j.cej.2020.124666>.
- [329] M. Kwiatkowski, A. Policicchio, M. Seredych, T.J. Bandosz, Evaluation of CO<sub>2</sub> interactions with S-doped nanoporous carbon and its composites with a reduced GO: effect of surface features on an apparent physical adsorption mechanism, *Carbon* 98 (2016) 250–258, <https://doi.org/10.1016/j.carbon.2015.11.019>.
- [330] N. Polikatos, I. Barbarin, T. Cordero-Lanzac, A. Gonzalez, R. Zangi, R. Tomovska, Reduced graphene oxide/polymer monolithic materials for selective CO<sub>2</sub> capture, *Polymers* 12 (4) (2020) 936, <https://doi.org/10.3390/polym12040936>.
- [331] S. Rodríguez-García, R. Santiago, D. López-Díaz, M.D. Merchán, M.M. Velázquez, J.L.G. Fierro, J. Palomar, Role of the structure of graphene oxide sheets on the CO<sub>2</sub> adsorption properties of nanocomposites based on graphene oxide and polyaniline or Fe<sub>3</sub>O<sub>4</sub>-nanoparticles, *ACS Sustain. Chem. Eng.* 7 (14) (2019) 12464–12473, <https://doi.org/10.1021/acssuschemeng.9b02035>.
- [332] S. Chowdhury, G.K. Parshetti, R. Balasubramanian, Post-combustion CO<sub>2</sub> capture using mesoporous TiO<sub>2</sub>/graphene oxide nanocomposites, *Chem. Eng. J.* 263 (2015) 374–384, <https://doi.org/10.1016/j.cej.2014.11.037>.
- [333] G.C.A. Gunathilake, G.G.T.A. Ranathunge, R.S. Dassanayake, S.D. Illesinghe, A.S. Manchanda, C.S. Kalpage, R.M.G. Rajapakse, G.G.P. Karunaratne, Emerging investigator series: synthesis of magnesium oxide nanoparticles fabricated on a graphene oxide nanocomposite for CO<sub>2</sub> sequestration at elevated temperatures, *Environ. Sci.: Nano* 7 (4) (2020) 1225–1239, <https://doi.org/10.1039/C9EN01442J>.
- [334] S. Stanly, E.J. Jelmy, C.P.R. Nair, H. John, Carbon dioxide adsorption studies on modified montmorillonite clay/reduced graphene oxide hybrids at low pressure, *J. Environ. Chem. Eng.* 7 (5) (2019) 103344, <https://doi.org/10.1016/j.jece.2019.103344>.
- [335] S. Yun, H. Lee, W.E. Lee, H.S. Park, Multiscale textured, ultralight graphene monoliths for enhanced CO<sub>2</sub> and SO<sub>2</sub> adsorption capacity, *Fuel* 174 (2016) 36–42, <https://doi.org/10.1016/j.fuel.2016.01.068>.
- [336] A.I. Pruna, A. Barjola, A.C. Cárcel, B. Alonso, E. Giménez, Effect of varying amine functionalities on CO<sub>2</sub> capture of carboxylated graphene oxide-based cryogels, *Nanomaterials* 10 (8) (2020) 1446, <https://doi.org/10.3390/nano10081446>.
- [337] A. Pruna, A.C. Cárcel, A. Benedito, E. Giménez, Effect of synthesis conditions on CO<sub>2</sub> capture of ethylenediamine-modified graphene aerogels, *Appl. Surf. Sci.* 487 (2019) 228–235, <https://doi.org/10.1016/j.apsusc.2019.05.098>.
- [338] M. Nováček, O. Jankovský, J. Luxa, D. Sedmidubský, M. Pumera, V. Fila, M. Lhotka, K. Klímová, S. Matejkova, Z. Sofer, Tuning of graphene oxide composition by multiple oxidations for carbon dioxide storage and capture of toxic metals, *J. Mater. Chem. A* 5 (6) (2017) 2739–2748, <https://doi.org/10.1039/C6TA03631G>.
- [339] K. Xia, R. Xiong, Y. Chen, D. Liu, Q. Tian, Q. Gao, B. Han, C. Zhou, Tuning the pore structure and surface chemistry of porous graphene for CO<sub>2</sub> capture and H<sub>2</sub> storage, *Colloids Surf. A Physicochem. Eng. Asp.* 622 (2021) 126640, <https://doi.org/10.1016/j.colsurfa.2021.126640>.
- [340] S. Chowdhury, R. Balasubramanian, Three-dimensional graphene-based porous adsorbents for postcombustion CO<sub>2</sub> capture, *Ind. Eng. Chem. Res.* 55 (29) (2016) 7906–7916, <https://doi.org/10.1021/acs.iecr.5b04052>.
- [341] S. Liu, W. Peng, H. Sun, S. Wang, Physical and chemical activation of reduced graphene oxide for enhanced adsorption and catalytic oxidation, *Nanoscale* 6 (2) (2014) 766–771, <https://doi.org/10.1039/C3NR04282K>.
- [342] Y. Hosseini, M. Najafi, S. Khalili, M. Jahanshahi, M. Peyravi, Assembly of amine-functionalized graphene oxide for efficient and selective adsorption of CO<sub>2</sub>, *Mater. Chem. Phys.* 270 (2021) 124788, <https://doi.org/10.1016/j.matchemphys.2021.124788>.
- [343] Y. He, Y. Xia, J. Zhao, Y. Song, L. Yi, L. Zhao, One-step fabrication of PEI-modified GO particles for CO<sub>2</sub> capture, *Appl. Phys. A* 125 (3) (2019) 1–9, <https://doi.org/10.1007/s00339-019-2435-x>.
- [344] Y. Liu, B. Sajjadi, W.Y. Chen, R. Chatterjee, Ultrasound-assisted amine functionalized graphene oxide for enhanced CO<sub>2</sub> adsorption, *Fuel* 247 (2019) 10–18, <https://doi.org/10.1016/j.fuel.2019.03.011>.
- [345] L. An, S. Liu, L. Wang, J. Wu, Z. Wu, C. Ma, Q. Yu, X. Hu, Novel nitrogen-doped porous carbons derived from graphene for effective CO<sub>2</sub> capture, *Ind. Eng. Chem. Res.* 58 (8) (2019) 3349–3358, <https://doi.org/10.1021/acs.iecr.8b06122>.
- [346] A.H. Ruhami, C.N.C. Hitam, M.A.A. Aziz, N.H.A. Hamid, H.D. Setiabudi, L.P. Teh, The role of surface and structural functionalisation on graphene adsorbent nanomaterial for CO<sub>2</sub> adsorption application: recent progress and future prospects, *Renew. Sustain. Energy Rev.* 167 (2022) 112840, <https://doi.org/10.1016/j.rser.2022.112840>.
- [347] R. Balasubramanian, S. Chowdhury, Recent advances and progress in the development of graphene-based adsorbents for CO<sub>2</sub> capture, *J. Mater. Chem. A* 3 (44) (2015) 21968–21989, <https://doi.org/10.1039/C5TA04822B>.
- [348] N. Hsan, P.K. Dutta, S. Kumar, R. Bera, N. Das, Chitosan grafted graphene oxide aerogel: synthesis, characterization and carbon dioxide capture study, *Int. J. Biol. Macromol.* 125 (2019) 300–306, <https://doi.org/10.1016/j.ijbiomac.2018.12.071>.
- [349] Y. Zhao, Y. Cao, Q. Zhong, CO<sub>2</sub> capture on metal-organic framework and graphene oxide composite using a high-pressure static adsorption apparatus, *J. Clean Energy Technol.* 2 (1) (2014) 34–37, <https://doi.org/10.7763/JCET.2014.V2.86>.
- [350] A.M. Varghese, K.S.K. Reddy, N. Bhoria, S. Singh, J. Pokhrel, G.N. Karanikolos, Enhancing effect of UV activation of graphene oxide on carbon capture performance of metal-organic framework/graphene oxide hybrid adsorbents, *Chem. Eng. J.* 420 (2021) 129677, <https://doi.org/10.1016/j.cej.2021.129677>.
- [351] Y. Cao, Y. Zhao, Z. Lv, F. Song, Q. Zhong, Preparation and enhanced CO<sub>2</sub> adsorption capacity of UiO-66/graphene oxide composites, *J. Ind. Eng. Chem.* 27 (2015) 102–107, <https://doi.org/10.1016/j.jiec.2014.12.021>.
- [352] R. Krishna, J.M. van Baten, A comparison of the CO<sub>2</sub> capture characteristics of zeolites and metal-organic frameworks, *Sep. Purif. Technol.* 87 (2012) 120–126, <https://doi.org/10.1016/j.seppur.2011.11.031>.
- [353] Z. Bao, L. Yu, Q. Ren, X. Lu, S. Deng, Adsorption of CO<sub>2</sub> and CH<sub>4</sub> on a magnesium-based metal organic framework, *J. Colloid Interface Sci.* 353 (2) (2011) 549–556, <https://doi.org/10.1016/j.jcis.2010.09.06>.
- [354] H.R. Abid, G.H. Pham, H.M. Ang, M.O. Tade, S. Wang, Adsorption of CH<sub>4</sub> and CO<sub>2</sub> on Zr-metal organic frameworks, *J. Colloid Interface Sci.* 366 (1) (2012) 120–124, <https://doi.org/10.1016/j.jcis.2011.09.060>.
- [355] M. Younas, M. Rezakazemi, M. Daud, M.B. Wazir, S. Ahmad, N. Ullah, S. Ramakrishna, Recent progress and remaining challenges in post-combustion CO<sub>2</sub> capture using metal-organic frameworks (MOFs), *Prog. Energy Combust. Sci.* 80 (2020) 100849, <https://doi.org/10.1016/j.jpecs.2020.100849>.
- [356] N. Kundu, S. Sarkar, Porous organic frameworks for carbon dioxide capture and storage, *J. Environ. Chem. Eng.* 9 (2) (2021) 105090, <https://doi.org/10.1016/j.jece.2021.105090>.
- [357] M. Ding, R.W. Flagg, H.L. Jiang, O.M. Yaghi, Carbon capture and conversion using metal-organic frameworks and MOF-based materials, *Chem. Soc. Rev.* 48 (10) (2019) 2783–2828, <https://doi.org/10.1039/C8CS00829A>.
- [358] S. Mandal, S. Natarajan, P. Mani, A. Pankajakshan, Post-synthetic modification of metal-organic frameworks toward applications, *Adv. Funct. Mater.* 31 (4) (2021) 2006291, <https://doi.org/10.1002/adfm.202006291>.
- [359] G.P. Yang, L. Hou, L.F. Ma, Y.Y. Wang, Investigation on the prime factors influencing the formation of entangled metal-organic frameworks, *CrystEngComm* 15 (14) (2013) 2561–2578, <https://doi.org/10.1039/C3CE26435A>.
- [360] D.M. Chen, X.P. Zhang, W. Shi, P. Cheng, Microporous metal-organic framework based on a bifunctional linker for selective sorption of CO<sub>2</sub> over N<sub>2</sub> and CH<sub>4</sub>, *Inorg. Chem.* 54 (11) (2015) 5512–5518, <https://doi.org/10.1021/acs.inorgchem.5b00561>.
- [361] R. Poloni, K. Lee, R.F. Berger, B. Smit, J.B. Neaton, Understanding trends in CO<sub>2</sub> adsorption in metal-organic frameworks with open-metal sites, *J. Phys. Chem. Lett.* 5 (5) (2014) 861–865, <https://doi.org/10.1021/jz500202x>.
- [362] J. Qian, Q. Li, L. Liang, T.T. Li, Y. Hu, S. Huang, A microporous MOF with open metal sites and Lewis basic sites for selective CO<sub>2</sub> capture, *Dalton Trans.* 46 (41) (2017) 14102–14106, <https://doi.org/10.1039/C7DT03255B>.
- [363] J. Yang, Y. Wang, L. Li, Z. Zhang, J. Li, Protection of open-metal V (III) sites and their associated CO<sub>2</sub>/CH<sub>4</sub>/N<sub>2</sub>/O<sub>2</sub>/H<sub>2</sub>O adsorption properties in mesoporous V-MOFs, *J. Colloid Interface Sci.* 456 (2015) 197–205, <https://doi.org/10.1016/j.jcis.2015.06.036>.
- [364] S.E.M. Elhenawy, M. Khraisheh, F. AlMomani, G. Walker, Metal-organic frameworks as a platform for CO<sub>2</sub> capture and chemical processes: adsorption, membrane separation, catalytic-conversion, and electrochemical reduction of CO<sub>2</sub>, *Catalysts* 10 (11) (2020) 1293, <https://doi.org/10.3390/catal10111293>.
- [365] S. Kumar, S. Jain, M. Nehra, N. Dilbaghi, G. Marrazza, K.H. Kim, Green synthesis of metal-organic frameworks: a state-of-the-art review of potential environmental and medical applications, *Coord. Chem. Rev.* 420 (2020) 213407, <https://doi.org/10.1016/j.ccr.2020.213407>.
- [366] H. Furukawa, N. Ko, Y.B. Go, N. Aratani, S.B. Choi, E. Choi, A.O. Yazaydin, R.Q. Snurr, M. O'keeffe, J. Kim, O.M. Yaghi, Ultrahigh porosity in metal-organic frameworks, *Science* 329 (5990) (2010) 424–428, <https://doi.org/10.1126/science.1192160>.
- [367] O.K. Farha, A.Ö. Yazaydin, I. Eryazici, C.D. Malliakas, B.G. Hauser, M.G. Kanatzidis, S.T. Nguyen, R.Q. Snurr, J.T. Hupp, De novo synthesis of a metal-organic framework material featuring ultrahigh surface area and gas storage capacities, *Nat. Chem.* 2 (11) (2010) 944–948, <https://doi.org/10.1038/nchem.834>.
- [368] A.A. Azmi, M.A.A. Aziz, Mesoporous adsorbent for CO<sub>2</sub> capture application under mild condition: a review, *J. Environ. Chem. Eng.* 7 (2) (2019) 103022, <https://doi.org/10.1016/j.jece.2019.103022>.
- [369] Z. Hu, Y. Wang, B.B. Shah, D. Zhao, CO<sub>2</sub> capture in metal-organic framework adsorbents: an engineering perspective, *Adv. Sustain. Syst.* 3 (1) (2019) 1800080, <https://doi.org/10.1002/adsu.201800080>.
- [370] B. Chen, S. Ma, E.J. Hurtado, E.B. Lobkovsky, H.C. Zhou, A triply interpenetrated microporous metal-organic framework for selective sorption of gas molecules, *Inorg. Chem.* 46 (21) (2007) 8490–8492, <https://doi.org/10.1021/ic7014034>.
- [371] B. Chen, S. Ma, F. Zapata, F.R. Fronczek, E.B. Lobkovsky, H.C. Zhou, Rationally designed micropores within a metal-organic framework for selective sorption of gas molecules, *Inorg. Chem.* 46 (4) (2007) 1233–1236, <https://doi.org/10.1021/ic0616434>.
- [372] H. Wu, R.S. Reali, D.A. Smith, M.C. Trachtenberg, J. Li, Highly selective CO<sub>2</sub> capture by a flexible microporous metal-organic framework (MMOF)

- material, *Chem. Eur J.* 16 (47) (2010) 13951–13954, <https://doi.org/10.1002/chem.201002683>.
- [373] H.M. Wen, C. Liao, L. Li, A. Alsalme, Z. Alothman, R. Krishna, H. Wu, W. Zhou, J. Hu, B. Chen, A metal–organic framework with suitable pore size and dual functionalities for highly efficient post-combustion CO<sub>2</sub> capture, *J. Mater. Chem. A* 7 (7) (2019) 3128–3134, <https://doi.org/10.1039/C8TA11596F>.
- [374] W. Fan, X. Wang, X. Liu, B. Xu, X. Zhang, W. Wang, X. Wang, Y. Wang, F. Dai, D. Yuan, D. Sun, Regulating C<sub>2</sub>H<sub>2</sub> and CO<sub>2</sub> storage and separation through pore environment modification in a microporous Ni-MOF, *ACS Sustain. Chem. Eng.* 7 (2) (2018) 2134–2140, <https://doi.org/10.1021/acssuschemeng.8b04783>.
- [375] C. Song, J. Hu, Y. Ling, Y. Feng, R. Krishna, D.L. Chen, Y. He, The accessibility of nitrogen sites makes a difference in selective CO<sub>2</sub> adsorption of a family of isostructural metal–organic frameworks, *J. Mater. Chem. A* 3 (38) (2015) 19417–19426, <https://doi.org/10.1039/C5TA05481H>.
- [376] T. Xu, L. Fan, Z. Jiang, P. Zhou, Z. Li, H. Lu, Y. He, Immobilization of N-oxide functionality into NbO-type MOFs for significantly enhanced C<sub>2</sub>H<sub>2</sub>/CH<sub>4</sub> and CO<sub>2</sub>/CH<sub>4</sub> separations, *Dalton Trans.* 49 (21) (2020) 7174–7181, <https://doi.org/10.1039/D0DT01081B>.
- [377] L.T. Yang, L.G. Qiu, S.M. Hu, X. Jiang, A.J. Xie, Y.H. Shen, Rapid hydrothermal synthesis of MIL-101 (Cr) metal–organic framework nanocrystals using expanded graphite as a structure-directing template, *Inorg. Chem. Commun.* 35 (2013) 265–267, <https://doi.org/10.1016/j.inoche.2013.06.034>.
- [378] S. Kayal, A. Chakraborty, Activated carbon (type Maxsorb-III) and MIL-101 (Cr) metal organic framework based composite adsorbent for higher CH<sub>4</sub> storage and CO<sub>2</sub> capture, *Chem. Eng. J.* 334 (2018) 780–788, <https://doi.org/10.1016/j.cej.2017.10.080>.
- [379] D. Qian, C. Lei, G.P. Hao, W.C. Li, A.H. Lu, Synthesis of hierarchical porous carbon monoliths with incorporated metal–organic frameworks for enhancing volumetric based CO<sub>2</sub> capture capability, *ACS Appl. Mater. Interfaces* 4 (11) (2012) 6125–6132, <https://doi.org/10.1021/am301772k>.
- [380] C. Chen, N. Feng, Q. Guo, Z. Li, X. Li, J. Ding, L. Wang, H. Wan, G. Guan, Template-directed fabrication of MIL-101 (Cr)/mesoporous silica composite: layer-packed structure and enhanced performance for CO<sub>2</sub> capture, *J. Colloid Interface Sci.* 513 (2018) 891–902, <https://doi.org/10.1016/j.jcis.2017.12.014>.
- [381] A. Chakraborty, T.K. Maji, Mg-MOF-74@ SBA-15 hybrids: synthesis, characterization, and adsorption properties, *Apl. Mater.* 2 (12) (2014) 124107, <https://doi.org/10.1063/1.4902816>.
- [382] N.E. Tari, A. Tadjarodi, J. Tammanloo, S. Fatemi, One pot microwave synthesis of MCM-41/Cu based MOF composite with improved CO<sub>2</sub> adsorption and selectivity, *Microporous Mesoporous Mater.* 231 (2016) 154–162, <https://doi.org/10.1016/j.micromeso.2016.05.027>.
- [383] C. Chen, B. Li, L. Zhou, Z. Xia, N. Feng, J. Ding, L. Wang, H. Wan, G. Guan, Synthesis of hierarchically structured hybrid materials by controlled self-assembly of metal–organic framework with mesoporous silica for CO<sub>2</sub> adsorption, *ACS Appl. Mater. Interfaces* 9 (27) (2017) 23060–23071, <https://doi.org/10.1021/acsami.7b08117>.
- [384] P.L. Llewellyn, S. Bourrelly, C. Serre, Y. Filinchuk, G. Férey, How hydration drastically improves adsorption selectivity for CO<sub>2</sub> over CH<sub>4</sub> in the flexible chromium terephthalate MIL-53, *Angew. Chem.* 118 (46) (2006) 7915–7918, <https://doi.org/10.1002/ange.200602278>.
- [385] J. Yu, P.B. Balbuena, Water effects on postcombustion CO<sub>2</sub> capture in Mg-MOF-74, *J. Phys. Chem. C* 117 (7) (2013) 3383–3388, <https://doi.org/10.1021/jp311118x>.
- [386] R. Aniruddha, I. Sreedhar, B.M. Reddy, MOFs in carbon capture–past, present and future, *J. CO<sub>2</sub> Util.* 42 (2020) 101297, <https://doi.org/10.1016/j.jcou.2020.101297>.
- [387] Z. Zhang, Y. Zhao, Q. Gong, Z. Li, J. Li, MOFs for CO<sub>2</sub> capture and separation from flue gas mixtures: the effect of multifunctional sites on their adsorption capacity and selectivity, *Chem. Commun.* 49 (7) (2013) 653–661, <https://doi.org/10.1039/C2CC35561B>.
- [388] S. Ma, X.S. Wang, E.S. Manis, C.D. Collier, H.C. Zhou, Metal–organic framework based on a trinickel secondary building unit exhibiting gas-sorption hysteresis, *Inorg. Chem.* 46 (9) (2007) 3432–3434, <https://doi.org/10.1021/ic070338v>.
- [389] M. Zhang, L. Zhang, Z. Xiao, Q. Zhang, R. Wang, F. Dai, D. Sun, Pentptycene-based luminescent Cu (II) MOF exhibiting selective gas adsorption and unprecedentedly high-sensitivity detection of Nitroaromatic compounds (NACs), *Sci. Rep.* 6 (1) (2016) 1–10, <https://doi.org/10.1038/srep20672>.
- [390] Q. Yan, Y. Lin, P. Wu, L. Zhao, L. Cao, L. Peng, C. Kong, L. Chen, Designed synthesis of functionalized two-dimensional metal–organic frameworks with preferential CO<sub>2</sub> capture, *ChemPlusChem* 78 (1) (2013) 86–91, <https://doi.org/10.1002/cplu.201200270>.
- [391] A.R. Millward, O.M. Yaghi, Metal–organic frameworks with exceptionally high capacity for storage of carbon dioxide at room temperature, *J. Am. Chem. Soc.* 127 (51) (2005) 17998–17999, <https://doi.org/10.1021/ja0570032>.
- [392] S. Bourrelly, P.L. Llewellyn, C. Serre, F. Millange, T. Loiseau, G. Férey, Different adsorption behaviors of methane and carbon dioxide in the isotropic nanoporous metal terephthalates MIL-53 and MIL-47, *J. Am. Chem. Soc.* 127 (39) (2005) 13519–13521, <https://doi.org/10.1021/ja054668v>.
- [393] P. Cui, J.J. Li, J. Dong, B. Zhao, Modulating CO<sub>2</sub> adsorption in metal–organic frameworks via metal-ion doping, *Inorg. Chem.* 57 (10) (2018) 6135–6141, <https://doi.org/10.1021/acs.inorgchem.8b00730>.
- [394] Y. Cao, Y. Zhao, F. Song, Q. Zhong, Alkali metal cation doping of metal–organic framework for enhancing carbon dioxide adsorption capacity, *J. Energy Chem.* 23 (4) (2014) 468–474, [https://doi.org/10.1016/S2095-4956\(14\)60173-X](https://doi.org/10.1016/S2095-4956(14)60173-X).
- [395] C.R. Wade, M. Dinca, Investigation of the synthesis, activation, and isosteric heats of CO<sub>2</sub> adsorption of the isostructural series of metal–organic frameworks M<sub>n</sub>(BTC)<sub>n</sub> (M= Cr, Fe, Ni, Cu, Mo, Ru), *Dalton Trans.* 41 (26) (2012) 7391–7938, <https://doi.org/10.1039/C2DT30372H>.
- [396] D.H. Hong, M.P. Suh, Selective CO<sub>2</sub> adsorption in a metal–organic framework constructed from an organic ligand with flexible joints, *Chem. Commun.* 48 (73) (2012) 9168–9170, <https://doi.org/10.1039/C2CC34482C>.
- [397] T.K. Prasad, M.P. Suh, Control of interpenetration and gas-sorption properties of metal–organic frameworks by a simple change in ligand design, *Chem. Eur J.* 18 (28) (2012) 8673–8680, <https://doi.org/10.1002/chem.201200456>.
- [398] B. Zheng, R. Yun, J. Bai, Z. Lu, L. Du, Y. Li, Expanded porous MOF-505 analogue exhibiting large hydrogen storage capacity and selective carbon dioxide adsorption, *Inorg. Chem.* 52 (6) (2013) 2823–2829, <https://doi.org/10.1021/ic301598n>.
- [399] D. Yuan, D. Zhao, D. Sun, H.C. Zhou, An isoreticular series of metal–organic frameworks with dendritic hexacarboxylate ligands and exceptionally high gas-uptake capacity, *Angew. Chem.* 122 (31) (2010) 5485–5489, <https://doi.org/10.1002/ange.201001009>.
- [400] J. Park, J.R. Li, Y.P. Chen, J. Yu, A.A. Yakovenko, Z.U. Wang, L.B. Sun, P.B. Balbuena, H.C. Zhou, A versatile metal–organic framework for carbon dioxide capture and cooperative catalysis, *Chem. Commun.* 48 (80) (2012) 9995–9997, <https://doi.org/10.1039/C2CC34622B>.
- [401] H.J. Park, Y.E. Cheon, M.P. Suh, Post-synthetic reversible incorporation of organic linkers into porous metal–organic frameworks through single-crystal-to-single-crystal transformations and modification of gas-sorption properties, *Chem. Eur J.* 16 (38) (2010) 11662–11669, <https://doi.org/10.1002/chem.201001549>.
- [402] Z. Hu, Y. Wang, S. Farooq, D. Zhao, A highly stable metal–organic framework with optimum aperture size for CO<sub>2</sub> capture, *AIChE J.* 63 (9) (2017) 4103–4114, <https://doi.org/10.1002/aic.15837>.
- [403] H.R. Abid, Z.H. Rada, X. Duan, H. Sun, S. Wang, Enhanced CO<sub>2</sub> adsorption and selectivity of CO<sub>2</sub>/N<sub>2</sub> on amino-MIL-53 (Al) synthesized by polar co-solvents, *Energy Fuels* 32 (4) (2017) 4502–4510, <https://doi.org/10.1021/acs.energyfuels.7b03240>.
- [404] F. Martínez, R. Sanz, G. Orcajo, D. Briones, V. Yáñez, Amino-impregnated MOF materials for CO<sub>2</sub> capture at post-combustion conditions, *Chem. Eng. Sci.* 142 (2016) 55–61, <https://doi.org/10.1016/j.ces.2015.11.033>.
- [405] T. Xu, Z. Jiang, P. Liu, H. Chen, X. Lan, D. Chen, L. Li, Y. He, Immobilization of oxygen atoms in the pores of microporous metal–organic frameworks for C<sub>2</sub>H<sub>2</sub> separation and purification, *ACS Appl. Nano Mater.* 3 (3) (2020) 2911–2919, <https://doi.org/10.1021/acsnano.0c00162>.
- [406] P.J. Milner, R.L. Siegelman, A.C. Forse, M.I. Gonzalez, T. Runčevski, J.D. Martell, J.A. Reimer, J.R. Long, A diaminopropane-appended metal–organic framework enabling efficient CO<sub>2</sub> capture from coal flue gas via a mixed adsorption mechanism, *J. Am. Chem. Soc.* 139 (38) (2017) 13541–13553, <https://doi.org/10.1021/jacs.7b07612>.
- [407] H.J. Park, D.W. Lim, W.S. Yang, T.R. Oh, M.P. Suh, A highly porous metal–organic framework: structural transformations of a guest-free MOF depending on activation method and temperature, *Chem. Eur J.* 17 (26) (2011) 7251–7260, <https://doi.org/10.1002/chem.201003376>.
- [408] A. Taheri, E.G. Babakhani, J.T. Darian, S. Pakseresht, Hybrid MIL-101 (Cr)@MIL-53 (Al) composite for carbon dioxide capture from biogas, *RSC Adv.* 9 (26) (2019) 15141–15150, <https://doi.org/10.1039/C8RA10619C>.
- [409] C.J. Doonan, D.J. Tranchmontagne, T.G. Glover, J.R. Hunt, O.M. Yaghi, Exceptional ammonia uptake by a covalent organic framework, *Nat. Chem.* 2 (3) (2010) 235–238, <https://doi.org/10.1038/nchem.548>.
- [410] B. Li, Y. Zhang, R. Krishna, K. Yao, Y. Han, Z. Wu, D. Ma, Z. Shi, T. Pham, B. Space, J. Liu, P.K. Thallapally, J. Liu, M. Chrzanowski, S. Ma, Introduction of π-complexation into porous aromatic framework for highly selective adsorption of ethylene over ethane, *J. Am. Chem. Soc.* 136 (24) (2014) 8654–8660, <https://doi.org/10.1021/ja502119z>.
- [411] R. Dawson, E. Stöckel, J.R. Holst, D.J. Adams, A.I. Cooper, Microporous organic polymers for carbon dioxide capture, *Energy Environ. Sci.* 4 (10) (2011) 4239–4245, <https://doi.org/10.1039/C1EE01971F>.
- [412] G. Liu, Y. Wang, C. Shen, Z. Ju, D. Yuan, A facile synthesis of microporous organic polymers for efficient gas storage and separation, *J. Mater. Chem. A* 3 (6) (2015) 3051–3058, <https://doi.org/10.1039/C4TA05349D>.
- [413] Y. Xie, T.T. Wang, X.H. Liu, K. Zou, W.Q. Deng, Capture and conversion of CO<sub>2</sub> at ambient conditions by a conjugated microporous polymer, *Nat. Commun.* 4 (1) (2013) 1–7, <https://doi.org/10.1038/ncomms2960>.
- [414] N. Du, H.B. Park, G.P. Robertson, M.M. Dal-Cin, T. Visser, L. Scoles, M.D. Guiver, Polymer nanosieve membranes for CO<sub>2</sub>-capture applications, *Nat. Mater.* 10 (5) (2011) 372–375, <https://doi.org/10.1038/nmat2989>.
- [415] C. Xu, N. Hedin, Microporous adsorbents for CO<sub>2</sub> capture—a case for microporous polymers? *Mater. Today* 17 (8) (2014) 397–403, <https://doi.org/10.1016/j.mattod.2014.05.007>.
- [416] M.G. Mohamed, A.F. El-Mahdy, M.G. Kotp, S.W. Kuo, Advances in porous organic polymers: syntheses, structures, and diverse applications, *Mater. Adv.* 3 (2022) 707–733, <https://doi.org/10.1039/D1MA00771H>.

- [417] C. Sarkar, N. Das, J. Mondal, Presenting porous–organic–polymers as next-generation invigorating materials for nanoreactors, *Chem. Commun.* 57 (69) (2021) 8550–8567, <https://doi.org/10.1039/D1CC02616J>.
- [418] Q. Sun, B. Aguilera, Y. Song, S. Ma, Tailored porous organic polymers for task-specific water purification, *Acc. Chem. Res.* 53 (4) (2020) 812–821, <https://doi.org/10.1021/acs.accounts.0c0007>.
- [419] T.H. Pham, B.K. Lee, J. Kim, C.H. Lee, Enhancement of CO<sub>2</sub> capture by using synthesized nano-zoelite, *J. Taiwan Inst. Chem. Eng.* 64 (2016) 220–226, <https://doi.org/10.1016/j.jite.2016.04.026>.
- [420] M. Razavian, S. Fatemi, M. Masoudi-Nejad, A comparative study of CO<sub>2</sub> and CH<sub>4</sub> adsorption on silicalite-1 fabricated by sonication and conventional method, *Adsorpt. Sci. Technol.* 32 (1) (2014) 73–87, <https://doi.org/10.1260/0263-6174.32.1.73>.
- [421] H. Gao, Q. Li, S. Ren, Progress on CO<sub>2</sub> capture by porous organic polymers, *Curr. Opin. Green Sustain. Chem.* 16 (2019) 33–38, <https://doi.org/10.1016/j.cogsc.2018.11.015>.
- [422] P. Banjha, A. Modak, A. Bhaumik, Porous organic polymers for CO<sub>2</sub> storage and conversion reactions, *ChemCatChem* 11 (1) (2019) 244–257, <https://doi.org/10.1002/cctc.201801046>.
- [423] W. Wang, M. Zhou, D. Yuan, Carbon dioxide capture in amorphous porous organic polymers, *J. Mater. Chem. A* 5 (4) (2017) 1334–1347, <https://doi.org/10.1039/C6TA09234A>.
- [424] H. Li, J. Li, A. Thomas, Y. Liao, Ultra-high surface area nitrogen-doped carbon aerogels derived from a schiff-base porous organic polymer aerogel for CO<sub>2</sub> storage and supercapacitors, *Adv. Funct. Mater.* 29 (40) (2019) 1904785, <https://doi.org/10.1002/adfm.201904785>.
- [425] R. Luo, M. Chen, X. Liu, W. Xu, J. Li, B. Liu, Y. Fang, Recent advances in CO<sub>2</sub> capture and simultaneous conversion into cyclic carbonates over porous organic polymers having accessible metal sites, *J. Mater. Chem. A* 8 (36) (2020) 18408–18424, <https://doi.org/10.1039/DOTA06142E>.
- [426] R. Bera, M. Ansari, A. Alam, N. Das, Triptycene, phenolic-OH, and Azofunctionalized porous organic polymers: efficient and selective CO<sub>2</sub> capture, *ACS Appl. Polym. Mater.* 1 (5) (2019) 959–968, <https://doi.org/10.1021/acspolym.8b00264>.
- [427] L. Shao, Y. Li, J. Huang, Y.N. Liu, Synthesis of triazine-based porous organic polymers derived N-enriched porous carbons for CO<sub>2</sub> capture, *Ind. Eng. Chem. Res.* 57 (8) (2018) 2856–2865, <https://doi.org/10.1021/acs.iecr.7b04533>.
- [428] S. Kramer, N.R. Bennedsen, S. Kegnæs, Porous organic polymers containing active metal centers as catalysts for synthetic organic chemistry, *ACS Catal.* 8 (8) (2018) 6961–6982, <https://doi.org/10.1021/ascatal.8b01167>.
- [429] D. Ma, K. Liu, J. Li, Z. Shi, Bifunctional metal-free porous organic framework heterogeneous catalyst for efficient CO<sub>2</sub> conversion under mild and cocatalyst-free conditions, *ACS Sustain. Chem. Eng.* 6 (11) (2018) 15050–15055, <https://doi.org/10.1021/acssuschemeng.8b03517>.
- [430] A.I. Cooper, Conjugated microporous polymers, *Adv. Mater.* 21 (12) (2009) 1291–1295, <https://doi.org/10.1002/adma.200801971>.
- [431] J.X. Jiang, F. Su, A. Trewin, C.D. Wood, N.L. Campbell, H. Niu, C. Dickinson, A.Y. Ganin, M.J. Rosseinsky, Y.Z. Khimyak, A.I. Cooper, Conjugated microporous poly(aryleneethynylene) networks, *Angew. Chem.* 119 (45) (2007) 8728–8732, <https://doi.org/10.1002/anie.200890021>.
- [432] J.S.M. Lee, A.I. Cooper, Advances in conjugated microporous polymers, *Chem. Rev.* 120 (4) (2020) 2171–2214, <https://doi.org/10.1021/acs.chemrev.9b00399>.
- [433] X. Wang, Y. Zhao, L. Wei, C. Zhang, J.X. Jiang, Nitrogen-rich conjugated microporous polymers: impact of building blocks on porosity and gas adsorption, *J. Mater. Chem. A* 3 (2015) 21185–21193, <https://doi.org/10.1039/C5TA05230K>.
- [434] C. Yao, D. Cui, Y. Zhu, W. Xie, S. Zhang, G. Xu, Y. Xu, Synthetic control of the polar units in poly (thiophene carbazole) porous networks for effective CO<sub>2</sub> capture, *New J. Chem.* 43 (18) (2019) 6838–6842, <https://doi.org/10.1039/C9NJ00688E>.
- [435] J. Chen, T. Qiu, W. Yan, C.F. Faul, Exploiting Hansen solubility parameters to tune porosity and function in conjugated microporous polymers, *J. Mater. Chem. A* 8 (43) (2020) 22657–22665, <https://doi.org/10.1039/DOTA05563H>.
- [436] M.Y. Wang, Q.J. Zhang, Q.Q. Shen, Q.Y. Li, S.J. Ren, Truxene-based conjugated microporous polymers via different synthetic methods, *Chin. J. Polym. Sci.* 38 (2) (2020) 151–157, <https://doi.org/10.1007/s10118-019-2321-1>.
- [437] H. Li, B. Meng, S.M. Mahurin, S.H. Chai, K.M. Nelson, D.C. Baker, S. Dai, Carbohydrate based hyper-crosslinked organic polymers with–OH functional groups for CO<sub>2</sub> separation, *J. Mater. Chem. A* 3 (42) (2015) 20913–20918, <https://doi.org/10.1039/C5TA03213J>.
- [438] R. Dawson, D.J. Adams, A.I. Cooper, Chemical tuning of CO<sub>2</sub> sorption in robust nanoporous organic polymers, *Chem. Sci.* 2 (6) (2011) 1173–1177, <https://doi.org/10.1039/C1SC00100K>.
- [439] Y. Liao, Z. Cheng, W. Zuo, A. Thomas, C.F. Faul, Nitrogen-rich conjugated microporous polymers: facile synthesis, efficient gas storage, and heterogeneous catalysis, *ACS Appl. Mater. Interfaces* 9 (44) (2017) 38390–38400, <https://doi.org/10.1021/acsami.7b09553>.
- [440] Y. Sang, J. Huang, Benzimidazole-based hyper-cross-linked poly (ionic liquid)s for efficient CO<sub>2</sub> capture and conversion, *Chem. Eng. J.* 385 (2020) 123973, <https://doi.org/10.1016/j.cej.2019.123973>.
- [441] Z. Xie, Y. Wei, X. Zhao, Y. Li, S. Ding, L. Chen, Facile construction of butadiynylene based conjugated porous polymers by cost-effective Glaser coupling, *Mater. Chem. Front.* 1 (5) (2017) 867–872, <https://doi.org/10.1039/C6QM00190D>.
- [442] Y. Xu, S. Wu, S. Ren, J. Ji, Y. Yue, J. Shen, Nitrogen-doped porous carbon materials generated via conjugated microporous polymer precursors for CO<sub>2</sub> capture and energy storage, *RSC Adv.* 7 (52) (2017) 32496–32501, <https://doi.org/10.1039/C7RA05551J>.
- [443] J.X. Jiang, F. Su, A. Trewin, C.D. Wood, H. Niu, J.T. Jones, Y.Z. Khimyak, A.I. Cooper, Synthetic control of the pore dimension and surface area in conjugated microporous polymer and copolymer networks, *J. Am. Chem. Soc.* 130 (24) (2008) 7710–7720, <https://doi.org/10.1021/ja8010176>.
- [444] Y. Liu, S. Wang, X. Meng, Y. Ye, X. Song, Z. Liang, Increasing the surface area and CO<sub>2</sub> uptake of conjugated microporous polymers via a post-knitting method, *Mater. Chem. Front.* 5 (14) (2021) 5319–5327, <https://doi.org/10.1039/D1QM00371B>.
- [445] C. Zhang, X. Yang, Y. Zhao, X. Wang, M. Yu, J.X. Jiang, Bifunctionalized conjugated microporous polymers for carbon dioxide capture, *Polymer* 61 (2015) 36–41, <https://doi.org/10.1016/j.polymer.2015.01.072>.
- [446] L. Wang, W. Xie, G. Xu, S. Zhang, C. Yao, Y. Xu, Synthesis of thiophene-based conjugated microporous polymers for high iodine and carbon dioxide capture, *Polym. Adv. Technol.* 33 (2) (2022) 584–590, <https://doi.org/10.1002/pat.5540>.
- [447] C. Xu, Y. Zhu, C. Yao, W. Xie, G. Xu, S. Zhang, Y. Zhao, Y. Xu, Facile synthesis of tetraphenylethene-based conjugated microporous polymers as adsorbents for CO<sub>2</sub> and organic vapor uptake, *New J. Chem.* 44 (2) (2020) 317–321, <https://doi.org/10.1039/C9NJ04562G>.
- [448] D. Cui, C. Yao, Y. Xu, Conjugated microporous polymers with azide groups: a new strategy for postsynthetic fluoride functionalization and effectively enhanced CO<sub>2</sub> adsorption properties, *Chem. Commun.* 53 (83) (2017) 11422–11425, <https://doi.org/10.1039/C7CC06528K>.
- [449] J.X. Jiang, A. Trewin, F. Su, C.D. Wood, H. Niu, J.T. Jones, Y.Z. Khimyak, A.I. Cooper, Microporous poly (tri (4-ethynylphenyl) amine) networks: synthesis, properties, and atomistic simulation, *Macromolecules* 42 (7) (2009) 2658–2666, <https://doi.org/10.1021/ma802625d>.
- [450] S. Ren, R. Dawson, A. Laybourn, J.X. Jiang, Y. Khimyak, D.J. Adams, A.I. Cooper, Functional conjugated microporous polymers: from 1, 3, 5-benzene to 1, 3, 5-triazine, *Polym. Chem.* 3 (4) (2012) 928–934, <https://doi.org/10.1039/C2PY00585A>.
- [451] K. Geng, T. He, R. Liu, S. Dalapati, K.T. Tan, Z. Li, S. Tao, Y. Gong, Q. Jiang, D. Jiang, Covalent organic frameworks: design, synthesis, and functions, *Chem. Rev.* 120 (16) (2020) 8814–8933, <https://doi.org/10.1021/acs.chemrev.9b00550>.
- [452] Z. Li, X. Feng, Y. Zou, Y. Zhang, H. Xia, X. Liu, Y. Mu, A 2D azine-linked covalent organic framework for gas storage applications, *Chem. Commun.* 50 (89) (2014) 13825–13828, <https://doi.org/10.1039/C4CC05665E>.
- [453] Y. Zeng, R. Zou, Y. Zhao, Covalent organic frameworks for CO<sub>2</sub> capture, *Adv. Mater.* 28 (15) (2016) 2855–2873, <https://doi.org/10.1002/adma.201505004>.
- [454] H. Furukawa, O.M. Yaghi, Storage of hydrogen, methane, and carbon dioxide in highly porous covalent organic frameworks for clean energy applications, *J. Am. Chem. Soc.* 131 (25) (2009) 8875–8883, <https://doi.org/10.1021/ja9015765>.
- [455] J. Ozdemir, I. Mosleh, M. Abolhassani, L.F. Greenlee, R.R. Beitle Jr., M.H. Beyzavi, Covalent organic frameworks for the capture, fixation, or reduction of CO<sub>2</sub>, *Front. Energy Res.* 77 (2019), <https://doi.org/10.3389/fenrg.2019.00077>.
- [456] Y. Tian, S.Q. Xu, C. Qian, Z.F. Pang, G.F. Jiang, X. Zhao, Two-dimensional dual-pore covalent organic frameworks obtained from the combination of two D2h symmetrical building blocks, *Chem. Commun.* 52 (78) (2016) 11704–11707, <https://doi.org/10.1039/C6CC06637B>.
- [457] N. Huang, X. Chen, R. Krishna, D. Jiang, Two-dimensional covalent organic frameworks for carbon dioxide capture through channel-wall functionalization, *Angew. Chem.* 127 (10) (2015) 3029–3033, <https://doi.org/10.1002/anie.201411262>.
- [458] B. Dong, L. Wang, S. Zhao, R. Ge, X. Song, Y. Wang, Y. Gao, Immobilization of ionic liquids to covalent organic frameworks for catalyzing the formylation of amines with CO<sub>2</sub> and phenylsilane, *Chem. Commun.* 52 (44) (2016) 7082–7085, <https://doi.org/10.1039/C6CC03058K>.
- [459] Z. Li, Y. Zhi, X. Feng, X. Ding, Y. Zou, X. Liu, Y. Mu, An azine-linked covalent organic framework: synthesis, characterization and efficient gas storage, *Chem. Eur. J.* 21 (34) (2015) 12079–12084, <https://doi.org/10.1002/chem.201501206>.
- [460] O. Buyukcakir, S.H. Je, S.N. Talapaneni, D. Kim, A. Coskun, Charged covalent triazine frameworks for CO<sub>2</sub> capture and conversion, *ACS Appl. Mater. Interfaces* 9 (8) (2017) 7209–7216, <https://doi.org/10.1021/acsami.6b16769>.
- [461] X. Liu, H. Li, Y. Zhang, B. Xu, A. Sigen, H. Xia, Y. Mu, Enhanced carbon dioxide uptake by metalloporphyrin-based microporous covalent triazine framework, *Polym. Chem.* 4 (8) (2013) 2445–2448, <https://doi.org/10.1039/C3PY00083D>.
- [462] X. Li, Q. Su, K. Luo, H. Li, G. Li, Q. Wu, Construction of a highly heteroatom-functionalized covalent organic framework and its CO<sub>2</sub> capture capacity and CO<sub>2</sub>/N<sub>2</sub> selectivity, *Mater. Lett.* 282 (2021) 128704, <https://doi.org/10.1016/j.matlet.2020.128704>.
- [463] A.A. Olajire, Recent advances in the synthesis of covalent organic frameworks for CO<sub>2</sub> capture, *J. CO<sub>2</sub> Util.* 17 (2017) 137–161, <https://doi.org/10.1016/j.jcou.2016.12.003>.

- [464] Q. Gao, X. Li, G.H. Ning, H.S. Xu, C. Liu, B. Tian, W. Tang, K.P. Loh, Covalent organic framework with frustrated bonding network for enhanced carbon dioxide storage, *Chem. Mater.* 30 (5) (2018) 1762–1768, <https://doi.org/10.1021/acs.chemmater.8b00117>.
- [465] Y. Zhi, P. Shao, X. Feng, H. Xia, Y. Zhang, Z. Shi, Y. Mu, X. Liu, Covalent organic frameworks: efficient, metal-free, heterogeneous organocatalysts for chemical fixation of CO<sub>2</sub> under mild conditions, *J. Mater. Chem. A* 6 (2) (2018) 374–382, <https://doi.org/10.1039/C7TA08629F>.
- [466] Z. Kahveci, T. Islamoglu, G.A. Shar, R. Ding, H.M. El-Kaderi, Targeted synthesis of a mesoporous triptycene-derived covalent organic framework, *CrysEngComm* 15 (8) (2013) 1524–1527, <https://doi.org/10.1039/C2CE26487K>.
- [467] Y. Liu, X. Fan, X. Jia, B. Zhang, H. Zhang, A. Zhang, Q. Zhang, Hypercrosslinked polymers: controlled preparation and effective adsorption of aniline, *J. Mater. Sci.* 51 (18) (2016) 8579–8592, <https://doi.org/10.1007/s10853-016-0118-y>.
- [468] Z. Fu, J. Jia, J. Li, C. Liu, Transforming waste expanded polystyrene foam into hyper-crosslinked polymers for carbon dioxide capture and separation, *Chem. Eng. J.* 323 (2017) 557–564, <https://doi.org/10.1016/j.cej.2017.04.090>.
- [469] F. Björnerbäck, N. Hedin, Highly porous hypercrosslinked polymers derived from biobased molecules, *ChemSusChem* 12 (4) (2019) 839–847, <https://doi.org/10.1002/cssc.201802681>.
- [470] K.A. Fayemiwo, N. Chiarasumran, S.A. Nabavi, K.N. Loponov, V. Manovic, B. Benyahia, G.T. Vladisavljević, Eco-friendly fabrication of a highly selective amide-based polymer for CO<sub>2</sub> capture, *Ind. Eng. Chem. Res.* 58 (39) (2019) 18160–18167, <https://doi.org/10.1021/acs.iecr.9b02347>.
- [471] Y. Liu, X. Jia, J. Liu, X. Fan, B. Zhang, A. Zhang, Q. Zhang, Synthesis and evaluation of N, O-doped hypercrosslinked polymers and their performance in CO<sub>2</sub> capture, *Appl. Organomet. Chem.* 33 (8) (2019) e5025, <https://doi.org/10.1002/aoc.5025>.
- [472] K.A. Fayemiwo, G.T. Vladisavljević, S.A. Nabavi, B. Benyahia, D.P. Hanak, K.N. Loponov, V. Manović, Nitrogen-rich hyper-crosslinked polymers for low-pressure CO<sub>2</sub> capture, *Chem. Eng. J.* 334 (2018) 2004–2013, <https://doi.org/10.1016/j.cej.2017.11.106>.
- [473] L. Pan, Q. Chen, J.H. Zhu, J.G. Yu, Y.J. He, B.H. Han, Hypercrosslinked porous polycarbazoles via one-step oxidative coupling reaction and Friedel–Crafts alkylation, *Polym. Chem.* 6 (13) (2015) 2478–2487, <https://doi.org/10.1039/C4PY01797H>.
- [474] J.H. Zhu, Q. Chen, Z.Y. Sui, L. Pan, J. Yu, B.H. Han, Preparation and adsorption performance of cross-linked porous polycarbazoles, *J. Mater. Chem. A* 2 (38) (2014) 16181–16189, <https://doi.org/10.1039/C4TA01537A>.
- [475] D. Chang, M. Yu, C. Zhang, Y. Zhao, R. Kong, F. Xie, J.X. Jiang, Indolo [3, 2-b] carbazole-containing hypercrosslinked microporous polymer networks for gas storage and separation, *Microporous Mesoporous Mater.* 228 (2016) 231–236, <https://doi.org/10.1016/j.micromeso.2016.03.038>.
- [476] X. Zhu, S. Ding, C.W. Abney, K.L. Browning, R.L. Sacci, G.M. Veith, C. Tian, S. Dai, Superacid-promoted synthesis of highly porous hypercrosslinked polycarbazoles for efficient CO<sub>2</sub> capture, *Chem. Commun.* 53 (54) (2017) 7645–7648, <https://doi.org/10.1039/C7CC03620E>.
- [477] H. Ramezanipour Penchah, P. Najafi, A. Ghaemi, H. Ghanadzadeh Gilani, Characterization of hypercrosslinked polymer adsorbent based on carbazole to achieve higher CO<sub>2</sub> capture, *Environ. Prog. Sustain. Energy* 40 (4) (2021), [https://doi.org/10.1002/ep.13586 e13586](https://doi.org/10.1002/ep.13586).
- [478] L. Shao, M. Liu, J. Huang, Y.N. Liu, CO<sub>2</sub> capture by nitrogen-doped porous carbons derived from nitrogen-containing hyper-cross-linked polymers, *J. Colloid Interface Sci.* 513 (2018) 304–313, <https://doi.org/10.1016/j.jcis.2017.11.043>.
- [479] L. Shao, S. Wang, M. Liu, J. Huang, Y.N. Liu, Triazine-based hyper-cross-linked polymers derived porous carbons for CO<sub>2</sub> capture, *Chem. Eng. J.* 339 (2018) 509–518, <https://doi.org/10.1016/j.cej.2018.01.14>.
- [480] S. Wang, L. Shao, Y. Sang, J. Huang, Hollow hyper-cross-linked polymer microspheres for efficient rhodamine B adsorption and CO<sub>2</sub> capture, *J. Chem. Eng. Data* 64 (4) (2019) 1662–1670, <https://doi.org/10.1021/acs.jced.8b01197>.
- [481] X. Jiang, Y. Liu, J. Liu, X. Fu, Y. Luo, Y. Lyu, Hypercrosslinked conjugated microporous polymers for carbon capture and energy storage, *New J. Chem.* 41 (10) (2017) 3915–3919, <https://doi.org/10.1039/C7NJ00105C>.
- [482] Y. Liu, X. Chen, X. Jia, X. Fan, B. Zhang, A. Zhang, Q. Zhang, Hydroxyl-based hyper-cross-linked microporous polymers and their excellent performance for CO<sub>2</sub> capture, *Ind. Eng. Chem. Res.* 57 (50) (2018) 17259–17265, <https://doi.org/10.1021/acs.iecr.8b05004>.
- [483] H. Yi, H. Deng, X. Tang, Q. Yu, X. Zhou, H. Liu, Adsorption equilibrium and kinetics for SO<sub>2</sub>, NO, CO<sub>2</sub> on zeolites FAU and LTA, *J. Hazard. Mater.* 203 (2012) 111–117, <https://doi.org/10.1016/j.jhazmat.2011.11.091>.
- [484] J.A. Silva, K. Schumann, A.E. Rodrigues, Sorption and kinetics of CO<sub>2</sub> and CH<sub>4</sub> in binderless beads of 13X zeolite, *Microporous Mesoporous Mater.* 158 (2012) 219–228, <https://doi.org/10.1016/j.micromeso.2012.03.042>.
- [485] Z. Zhang, W. Zhang, X. Chen, Q. Xia, Z. Li, Adsorption of CO<sub>2</sub> on zeolite 13X and activated carbon with higher surface area, *Separ. Sci. Technol.* 45 (5) (2010) 710–719, <https://doi.org/10.1080/01496390903571192>.
- [486] Z. Zhao, X. Cui, J. Ma, R. Li, Adsorption of carbon dioxide on alkali-modified zeolite 13X adsorbents, *Int. J. Greenh. Gas Control* 1 (3) (2007) 355–359, [https://doi.org/10.1016/S1750-5836\(07\)00072-2](https://doi.org/10.1016/S1750-5836(07)00072-2).
- [487] F. Rezaei, A. Mosca, J. Hedlund, P.A. Webley, M. Grahn, J. Mouzon, The effect of wall porosity and zeolite film thickness on the dynamic behavior of adsorbents in the form of coated monoliths, *Sep. Purif. Technol.* 81 (2) (2011) 191–199, <https://doi.org/10.1016/j.seppur.2011.07.027>.
- [488] O.G. Nik, B. Nohair, S. Kaligaine, Aminosilanes grafting on FAU/EMT zeolite: effect on CO<sub>2</sub> adsorptive properties, *Microporous Mesoporous Mater.* 143 (1) (2011) 221–229, <https://doi.org/10.1016/j.micromeso.2011.03.002>.
- [489] S. Kumar, R. Srivastava, J. Koh, Utilization of zeolites as CO<sub>2</sub> capturing agents: advances and future perspectives, *J. CO<sub>2</sub> Util.* 41 (2020) 101251, <https://doi.org/10.1016/j.jcou.2020.101251>.
- [490] Y. Yuan, H. You, L. Ricardez-Sandoval, Recent advances on first-principles modeling for the design of materials in CO<sub>2</sub> capture technologies, *Chin. J. Chem. Eng.* 27 (7) (2019) 1554–1565, <https://doi.org/10.1016/j.cjche.2018.10.017>.
- [491] A. Zukal, C.O. Arean, M.R. Delgado, P. Nachtigall, A. Pulido, J. Mayerová, J. Cejka, Combined volumetric, infrared spectroscopic and theoretical investigation of CO<sub>2</sub> adsorption on Na-A zeolite, *Microporous Mesoporous Mater.* 146 (1–3) (2011) 97–105, <https://doi.org/10.1016/j.micromeso.2011.03.034>.
- [492] P. Nachtigall, M.R. Delgado, D. Nachtigallova, C.O. Areán, The nature of cationic adsorption sites in alkaline zeolites—single, dual and multiple cation sites, *Phys. Chem. Chem. Phys.* 14 (5) (2012) 1552–1569, <https://doi.org/10.1039/C2CP23237E>.
- [493] A.V. Larin, A. Mace, A.A. Rybakov, A. Laaksonen, Carbonate “door” in the NaKA zeolite as the reason of higher CO<sub>2</sub> uptake relative to N<sub>2</sub>, *Microporous Mesoporous Mater.* 162 (2012) 98–104, <https://doi.org/10.1016/j.micromeso.2012.06.005>.
- [494] M. Fischer, R.G. Bell, A dispersion-corrected density-functional theory study of small molecules adsorbed in alkali-exchanged chabazites, *Crystal. Mater.* 228 (2013) 124–133, <https://doi.org/10.1524/zkri.2012.1562>.
- [495] H.V. Thang, L. Graciár, P. Nachtigall, O. Bludský, C.O. Areán, E. Frýdová, R. Bulanek, Adsorption of CO<sub>2</sub> in FAU zeolites: effect of zeolite composition, *Catal. Today* 227 (2014) 50–56, <https://doi.org/10.1016/j.cattod.2013.10.036>.
- [496] E. García-Pérez, J.B. Parra Soto, M.C. Ovín Ania, A. García Sánchez, J.M. Van Baten, R. Krishna, D. Dubbeldam, S. Calero, A computational study of CO<sub>2</sub>, N<sub>2</sub>, and CH<sub>4</sub> adsorption in zeolites, *Adsorption* 13 (2007) 469–476, <https://doi.org/10.1007/s10450-007-9039-z>.
- [497] M.W. Ackley, S.U. Rege, H. Saxena, Application of natural zeolites in the purification and separation of gases, *Microporous Mesoporous Mater.* 61 (1–3) (2003) 25–42, [https://doi.org/10.1016/S1387-1811\(03\)00353-6](https://doi.org/10.1016/S1387-1811(03)00353-6).
- [498] V. Garshabi, M. Jahangiri, M. Anbia, Equilibrium CO<sub>2</sub> adsorption on zeolite 13X prepared from natural clays, *Appl. Surf. Sci.* 393 (2017) 225–233, <https://doi.org/10.1016/j.apsusc.2016.09.161>.
- [499] C. Chen, D.W. Park, W.S. Ahn, CO<sub>2</sub> capture using zeolite 13X prepared from bentonite, *Appl. Surf. Sci.* 292 (2014) 63–67, <https://doi.org/10.1016/j.apsusc.2013.11.064>.
- [500] A.W. Chester, E.G. Derouane, *Zeolite Characterization and Catalysis*, vol. 360, EUA, Springer, New York, 2009, <https://doi.org/10.1007/978-1-4419-0678-5>.
- [501] D. Barthomeuf, Framework induced basicity in zeolites, *Microporous Mesoporous Mater.* 66 (1) (2003) 1–14, <https://doi.org/10.1016/j.micromeso.2003.08.006>.
- [502] H. Khanmohammadi, B. Bayati, J. Rahbar-Shahrouzi, A.A. Babaloo, A. Ghorbani, Molecular simulation of the ion exchange behavior of Cu<sup>2+</sup>, Cd<sup>2+</sup> and Pb<sup>2+</sup> ions on different zeolites exchanged with sodium, *J. Environ. Chem. Eng.* 7 (3) (2019) 103040, <https://doi.org/10.1016/j.je.2019.103040>.
- [503] C.H. Yu, C.H. Huang, C.S. Tan, A review of CO<sub>2</sub> capture by absorption and adsorption, *Aerosol Air Qual. Res.* 12 (5) (2012) 745–769, <https://doi.org/10.4209/aaqr.2012.05.0132>.
- [504] D.E. Beving, C.R. O'Neill, Y. Yan, Hydrophilic and antimicrobial low-silica-zeolite LTA and high-silica-zeolite MFI hybrid coatings on aluminum alloys, *Microporous Mesoporous Mater.* 108 (1–3) (2008) 77–85, <https://doi.org/10.1016/j.micromeso.2007.03.029>.
- [505] D. Xu, G.R. Swindlehurst, H. Wu, D.H. Olson, X. Zhang, M. Tsapatsis, On the synthesis and adsorption properties of single-unit-cell hierarchical zeolites made by rotational intergrowths, *Adv. Funct. Mater.* 24 (2) (2014) 201–208, <https://doi.org/10.1002/adfm.201301975>.
- [506] M.M. Zagho, M.K. Hassan, M. Khraisheh, M.A.A. Al-Maadeed, S. Nazarenko, A review on recent advances in CO<sub>2</sub> separation using zeolite and zeolite-like materials as adsorbents and fillers in mixed matrix membranes (MMMs), *Chem. Eng. J. Adv.* 6 (2021) 100091, <https://doi.org/10.1016/j.cej.2021.100091>.
- [507] J. Gong, C. Wang, C. Zeng, L. Zhang, Hydrothermal preparation of hierarchical SAPO-34 constructed by nano-sheets using rapeseed pollen extract as water and its CO<sub>2</sub> adsorption property, *Microporous Mesoporous Mater.* 221 (2016) 128–136, <https://doi.org/10.1016/j.micromeso.2015.09.035>.
- [508] Y. Han, G. Hwang, H. Kim, B.Z. Haznedaroglu, B. Lee, Amine-impregnated millimeter-sized spherical silica foams with hierarchical mesoporous–macroporous structure for CO<sub>2</sub> capture, *Chem. Eng. J.* 259 (2015) 653–662, <https://doi.org/10.1016/j.cej.2014.08.043>.
- [509] N. Gargiulo, A. Verlotta, A. Peluso, P. Aprea, D. Caputo, Modeling the performances of a CO<sub>2</sub> adsorbent based on polyethylenimine-functionalized macro-/mesoporous silica monoliths, *Microporous Mesoporous Mater.* 215 (2015) 1–7, <https://doi.org/10.1016/j.micromeso.2015.05.025>.

- [510] X. Wang, Q. Guo, T. Kong, Tetraethylenepentamine-modified MCM-41/silica gel with hierarchical mesoporous structure for CO<sub>2</sub> capture, *Chem. Eng. J.* 273 (2015) 472–480, <https://doi.org/10.1016/j.cej.2015.03.098>.
- [511] K. Na, M. Choi, R. Ryoo, Recent advances in the synthesis of hierarchically nanoporous zeolites, *Microporous Mesoporous Mater.* 166 (2013) 3–19, <https://doi.org/10.1016/j.micromeso.2012.03.054>.
- [512] L.H. Chen, X.Y. Li, J.C. Rooke, Y.H. Zhang, X.Y. Yang, Y. Tang, F.S. Xiao, B.L. Su, Hierarchically structured zeolites: synthesis, mass transport properties and applications, *J. Mater. Chem.* 22 (34) (2012) 17381–17403, <https://doi.org/10.1039/C2JM31957H>.
- [513] D. Panda, E.A. Kumar, S.K. Singh, Introducing mesoporosity in zeolite 4A bodies for rapid CO<sub>2</sub> capture, *J. CO<sub>2</sub> Util.* 40 (2020) 101223, <https://doi.org/10.1016/j.jcou.2020.101223>.
- [514] A.A. Dabbawala, I. Ismail, B.V. Vaithilingam, K. Polychronopoulou, G. Singaravel, S. Morin, M. Berthod, Y. Al Wahedi, Synthesis of hierarchical porous Zeolite-Y for enhanced CO<sub>2</sub> capture, *Microporous Mesoporous Mater.* 303 (2020) 110261, <https://doi.org/10.1016/j.micromeso.2020.110261>.
- [515] Q. Liu, P. He, X. Qian, Z. Fei, Z. Zhang, X. Chen, J. Tang, M. Cui, X. Qiao, Y. Shi, Enhanced CO<sub>2</sub> adsorption performance on hierarchical porous ZSM-5 zeolite, *Energy Fuels* 31 (12) (2017) 13933–13941, <https://doi.org/10.1021/acs.energyfuels.7b02543>.
- [516] D. Bonenfant, M. Kharoune, P. Niquette, M. Mimeault, R. Hausler, Advances in principal factors influencing carbon dioxide adsorption on zeolites, *Sci. Technol. Adv. Mater.* 9 (1) (2008) 013007, <https://doi.org/10.1088/1468-6996/9/1/013007>.
- [517] M. Sun, Q. Gu, A. Hanif, T. Wang, J. Shang, Transition metal cation-exchanged SSZ-13 zeolites for CO<sub>2</sub> capture and separation from N<sub>2</sub>, *Chem. Eng. J.* 370 (2019) 1450–1458, <https://doi.org/10.1016/j.cej.2019.03.234>.
- [518] Z. Liang, M. Marshall, A.L. Chaffee, CO<sub>2</sub> adsorption-based separation by metal organic framework (Cu-BTC) versus zeolite (13X), *Energy Fuels* 23 (5) (2009) 2785–2789, <https://doi.org/10.1021/ef800938e>.
- [519] Q. Wang, J. Luo, Z. Zhong, A. Borgna, CO<sub>2</sub> capture by solid adsorbents and their applications: current status and new trends, *Energy Environ. Sci.* 4 (1) (2011) 42–55, <https://doi.org/10.1039/C0EE00064G>.
- [520] D. Saha, Z. Bao, F. Jia, S. Deng, Adsorption of CO<sub>2</sub>, CH<sub>4</sub>, N<sub>2</sub>O, and N<sub>2</sub> on MOF-5, MOF-177, and zeolite 5A, *Environ. Sci. Technol.* 44 (5) (2010) 1820–1826, <https://doi.org/10.1021/es9032309>.
- [521] W. Shao, L. Zhang, L. Li, R.L. Lee, Adsorption of CO<sub>2</sub> and N<sub>2</sub> on synthesized NaY zeolite at high temperatures, *Adsorption* 15 (5) (2009) 497–505, <https://doi.org/10.1007/s10450-009-9200-y>.
- [522] S.K. Wahono, J. Stalin, J. Addai-Mensah, W. Skinner, A. Vinu, K. Vasilev, Physico-chemical modification of natural mordenite-clinoptilolite zeolites and their enhanced CO<sub>2</sub> adsorption capacity, *Microporous Mesoporous Mater.* 294 (2020) 109871, <https://doi.org/10.1016/j.micromeso.2019.109871>.
- [523] T.H. Nguyen, S. Kim, M. Yoon, T.H. Bae, Hierarchical zeolites with amine-functionalized mesoporous domains for carbon dioxide capture, *ChemSusChem* 9 (5) (2016) 455–461, <https://doi.org/10.1002/cssc.201600004>.
- [524] Y. Wang, T. Du, Y. Song, S. Che, X. Fang, L. Zhou, Amine-functionalized mesoporous ZSM-5 zeolite adsorbents for carbon dioxide capture, *Solid State Sci.* 73 (2017) 27–35, <https://doi.org/10.1016/j.solidstatedsciences.2017.09.004>.
- [525] C. Chen, S.S. Kim, W.S. Cho, W.S. Ahn, Polyethylenimine-incorporated zeolite 13X with mesoporosity for post-combustion CO<sub>2</sub> capture, *Appl. Surf. Sci.* 332 (2015) 167–171, <https://doi.org/10.1016/j.apusc.2015.01.106>.
- [526] R. Kodasma, J. Fermoso, A. Sanna, Li-LSX-zeolite evaluation for post-combustion CO<sub>2</sub> capture, *Chem. Eng. J.* 358 (2019) 1351–1362, <https://doi.org/10.1016/j.cej.2018.10.063>.
- [527] S.J. Chen, M. Zhu, Y. Fu, Y.X. Huang, Z.C. Tao, W.L. Li, Using 13X, LiX, and LiPdAgX zeolites for CO<sub>2</sub> capture from post-combustion flue gas, *Appl. Energy* 191 (2017) 87–98, <https://doi.org/10.1016/j.apenergy.2017.01.031>.
- [528] E. Davarpanah, M. Armandi, S. Hernández, D. Fino, R. Arletti, S. Bensaïd, M. Piumenti, CO<sub>2</sub> capture on natural zeolite clinoptilolite: effect of temperature and role of the adsorption sites, *J. Environ. Manag.* 275 (2020) 111229, <https://doi.org/10.1016/j.jenvman.2020.111229>.
- [529] S.T. Yang, J. Kim, W.S. Ahn, CO<sub>2</sub> adsorption over ion-exchanged zeolite beta with alkali and alkaline earth metal ions, *Microporous Mesoporous Mater.* 135 (1–3) (2010) 90–94, <https://doi.org/10.1016/j.micromeso.2010.06.015>.
- [530] P. Murge, S. Dinda, S. Roy, Zeolite-based sorbent for CO<sub>2</sub> capture: preparation and performance evaluation, *Langmuir* 35 (46) (2019) 14751–14760, <https://doi.org/10.1021/acs.langmuir.9b02259>.
- [531] S. Bocheva, I. Marinov, D. Zgureva-Filipova, Studies on the CO<sub>2</sub> capture by coal fly ash zeolites: process design and simulation, *Energies* 14 (24) (2021) 8279, <https://doi.org/10.3390/en14248279>.
- [532] Z. Zhang, Y. Xiao, B. Wang, Q. Sun, H. Liu, Waste is a misplayed resource: synthesis of zeolites from fly ash for CO<sub>2</sub> capture, *Energy Proc.* 114 (2017) 2537–2544, <https://doi.org/10.1016/j.egypro.2017.08.036>.
- [533] N. Czuma, I. Casanova, P. Baran, J. Szczurowski, K. Zarębska, CO<sub>2</sub> sorption and regeneration properties of fly ash zeolites synthesized with the use of differentiated methods, *Sci. Rep.* 10 (1) (2020) 1–9, <https://doi.org/10.1038/s41598-020-58591-6>.
- [534] L. Valencia, W. Rosas, A. Aguilar-Sánchez, A.P. Mathew, A.E. Palmqvist, Bio-based micro-/meso-/macroporous hybrid foams with ultrahigh zeolite loadings for selective capture of carbon dioxide, *ACS Appl. Mater. Interfaces* 11 (43) (2019) 40424–40431, <https://doi.org/10.1021/acsami.9b11399>.
- [535] S. Kumar, R. Bera, N. Das, J. Koh, Chitosan-based zeolite-Y and ZSM-5 porous biocomposites for H<sub>2</sub> and CO<sub>2</sub> storage, *Carbohydr. Polym.* 232 (2020) 115808, <https://doi.org/10.1016/j.carbpol.2019.115808>.
- [536] A.T. Tabereaux, R.D. Peterson, Aluminum Production, Treatise on Process Metallurgy, Elsevier, 2014, pp. 839–917, <https://doi.org/10.1016/B978-0-08-096988-6.00023-7>.
- [537] C. Gunathilake, M. Gangoda, M. Jaroniec, Mesoporous alumina with amidoxime groups for CO<sub>2</sub> sorption at ambient and elevated temperatures, *Ind. Eng. Chem. Res.* 55 (19) (2016) 5598–5607, <https://doi.org/10.1021/acs.iecr.6b00674>.
- [538] J.C.P. Broekhoff, B.G. Linsen, *Studies on pore systems in adsorbents and catalysts*, in: B.G. Linsen (Ed.), *Physical and Chemical Aspects of Adsorbents and Catalysts*, Academic Press, Londres, 1970, p. 47.
- [539] S.C. Lee, M.S. Cho, S.Y. Jung, C.K. Ryu, J.C. Kim, Effects of alumina phases on CO<sub>2</sub> sorption and regeneration properties of potassium-based alumina sorbents, *Adsorption* 20 (2) (2014) 331–339, <https://doi.org/10.1007/s10450-013-9596-2>.
- [540] T. Seki, M. Onaka, Mesoporous alumina: synthesis, characterization, and catalysis, *Adv. Nanomater.* (2009) 481–521, <https://doi.org/10.1002/978327628940.ch15>.
- [541] X. Xu, S.K. Megarajan, Y. Zhang, H. Jiang, Ordered mesoporous alumina and their composites based on evaporation induced self-assembly for adsorption and catalysis, *Chem. Mater.* 32 (1) (2019) 3–26, <https://doi.org/10.1021/acs.chemmater.9b03873>.
- [542] S.T. Bararpour, D. Karami, N. Mahinpey, Investigation of the effect of alumina-aerogel support on the CO<sub>2</sub> capture performance of K<sub>2</sub>CO<sub>3</sub>, *Fuel* 242 (2019) 124–132, <https://doi.org/10.1016/j.fuel.2018.12.123>.
- [543] S.T. Bararpour, D. Karami, N. Mahinpey, Post-combustion CO<sub>2</sub> capture using supported K<sub>2</sub>CO<sub>3</sub>: comparing physical mixing and incipient wetness impregnation preparation methods, *Chem. Eng. Res. Des.* 137 (2018) 319–328, <https://doi.org/10.1016/j.cherd.2018.07.027>.
- [544] P. Wang, J. Sun, Y. Guo, C. Zhao, W. Li, G. Wang, S. Lei, P. Lu, Structurally improved, urea-templated, K<sub>2</sub>CO<sub>3</sub>-based sorbent pellets for CO<sub>2</sub> capture, *Chem. Eng. J.* 374 (2019) 20–28, <https://doi.org/10.1016/j.cej.2019.05.091>.
- [545] A. Ertu, M. Balsamo, L.P. Paduano, A. Lancia, F. Di Natale, Utilization of alumina-supported K<sub>2</sub>CO<sub>3</sub> as CO<sub>2</sub>-selective sorbent: a promising strategy to mitigate the carbon footprint of the maritime sector, *J. CO<sub>2</sub> Util.* 24 (2018) 139–148, <https://doi.org/10.1016/j.jcou.2017.12.014>.
- [546] S.T. Bararpour, D. Karami, N. Mahinpey, Utilization of mesoporous alumina-based supports synthesized by a surfactant-assisted technique for post-combustion CO<sub>2</sub> capture, *J. Environ. Chem. Eng.* 9 (4) (2021) 105661, <https://doi.org/10.1016/j.jece.2021.105661>.
- [547] G.L. Seah, L. Wang, L.F. Tan, C. Tipjanrawee, W.A. Sasangka, A.K. Usadi, J.M. McConnachie, K.W. Tan, Ordered mesoporous alumina with tunable morphologies and pore sizes for CO<sub>2</sub> capture and dye separation, *ACS Appl. Mater. Interfaces* 13 (30) (2021) 36117–36129, <https://doi.org/10.1021/acsami.1c06151>.
- [548] D. Yuan, X. Zhu, L. Chen, J. Hu, G. Xie, D. Yin, C.T. Au, S.F. Yin, Layer-by-layer self-assembly of sodium tripolyphosphate/chitosan composites on mesoporous alumina for CO<sub>2</sub> adsorption, *Mater. Chem. Phys.* 230 (2019) 93–99, <https://doi.org/10.1016/j.matchemphys.2019.03.040>.
- [549] Y. Zhou, M. Chang, X. Zang, L. Zheng, Y. Wang, L. Wu, X. Han, Y. Chen, Y. Yu, Z. Zhang, The polymeric ionic liquids/mesoporous alumina composites: synthesis, characterization and CO<sub>2</sub> capture performance test, *Polym. Test.* 81 (2020) 106109, <https://doi.org/10.1016/j.polymertesting.2019.106109>.
- [550] X. Li, Z. Wang, R. Feng, J. Huang, Y. Fang, CO<sub>2</sub> capture on aminosilane functionalized alumina-extracted residue of catalytic gasification coal ash, *Energy* 221 (2021) 119642, <https://doi.org/10.1016/j.energy.2020.119642>.
- [551] N.K. Mohammad, A. Ghaemi, K. Tahvildari, Hydroxide modified activated alumina as an adsorbent for CO<sub>2</sub> adsorption: experimental and modeling, *Int. J. Greenh. Gas Control* 88 (2019) 24–37, <https://doi.org/10.1016/j.ijggc.2019.05.029>.
- [552] L. Sun, M. Yin, S. Tang, Bi-functionalized ionic liquid-grafted mesoporous alumina: synthesis, characterization and CO<sub>2</sub>/N<sub>2</sub> selectivity, *J. Environ. Chem. Eng.* 9 (5) (2021) 105829, <https://doi.org/10.1016/j.jece.2021.105829>.
- [553] V. Hiremath, B.T. Shiferraw, J.G. Seo, MgO insertion endowed strong basicity in mesoporous alumina framework and improved CO<sub>2</sub> sorption capacity, *J. CO<sub>2</sub> Util.* 42 (2020) 101294, <https://doi.org/10.1016/j.jcou.2020.101294>.
- [554] L. Sun, S. Tang, Synthesis of bi-functionalized ionic liquid—mesoporous alumina composite material and its CO<sub>2</sub> capture capacity, *Korean J. Chem. Eng.* 36 (10) (2019) 1708–1715, <https://doi.org/10.1007/s11814-019-0360-5>.
- [555] F.C. Yu, N. Phalak, Z. Sun, L.S. Fan, Activation strategies for calcium-based sorbents for CO<sub>2</sub> capture: a perspective, *Ind. Eng. Chem. Res.* 51 (4) (2012) 2133–2142, <https://doi.org/10.1021/ie00802y>.
- [556] H. Jeon, Y.J. Min, S.H. Ahn, S.M. Hong, J.S. Shin, J.H. Kim, K.B. Lee, Graft copolymer templated synthesis of mesoporous MgO/TiO<sub>2</sub> mixed oxide nanoparticles and their CO<sub>2</sub> adsorption capacities, *Colloids Surf. A Physicochem. Eng. Asp.* 414 (2012) 75–81, <https://doi.org/10.1016/j.colsurfa.2012.08.009>.
- [557] L. Li, X. Wen, X. Fu, F. Wang, N. Zhao, F. Xiao, W. Wei, Y. Sun, MgO/Al<sub>2</sub>O<sub>3</sub> sorbent for CO<sub>2</sub> capture, *Energy Fuels* 24 (10) (2010) 5773–5780, <https://doi.org/10.1021/ef100817f>.

- [558] S. Kumar, V. Drozd, A. Durygin, S.K. Saxena, Capturing CO<sub>2</sub> Emissions in the iron industries using a magnetite–iron mixture, *Energy Technol.* 4 (5) (2016) 560–564, <https://doi.org/10.1002/ente.201500451>.
- [559] C. Salvador, D. Lu, E.J. Anthony, J.C. Abanades, Enhancement of CaO for CO<sub>2</sub> capture in an FBC environment, *Chem. Eng. J.* 96 (1–3) (2003) 187–195, <https://doi.org/10.1016/j.cej.2003.08.011>.
- [560] M.V. Dagaonkar, H.J. Heeres, A.A.C.M. Beenackers, V.G. Pangarkar, The application of fine TiO<sub>2</sub> particles for enhanced gas absorption, *Chem. Eng. J.* 92 (1–3) (2003) 151–159, [https://doi.org/10.1016/S1385-8947\(02\)00188-2](https://doi.org/10.1016/S1385-8947(02)00188-2).
- [561] P. Liang, Y. Qin, B. Hu, T. Peng, Z. Jiang, Nanometer-size titanium dioxide microcolumn on-line preconcentration of trace metals and their determination by inductively coupled plasma atomic emission spectrometry in water, *Anal. Chim. Acta* 440 (2) (2001) 207–213, [https://doi.org/10.1016/S0003-2670\(01\)01010-8](https://doi.org/10.1016/S0003-2670(01)01010-8).
- [562] W. Li, Z. Wu, J. Wang, A.A. Elzatahry, D. Zhao, A perspective on mesoporous TiO<sub>2</sub> materials, *Chem. Mater.* 26 (1) (2014) 287–298, <https://doi.org/10.1021/cm4014859>.
- [563] Y. Nie, W.N. Wang, Y. Jiang, J. Fortner, P. Biswas, Crumpled reduced graphene oxide–amine–titanium dioxide nanocomposites for simultaneous carbon dioxide adsorption and photoreduction, *Catal. Sci. Technol.* 6 (16) (2016) 6187–6196, <https://doi.org/10.1039/C6CY00828C>.
- [564] A. Crake, K.C. Christoforidis, R. Godin, B. Moss, A. Kafizas, S. Zafeiratos, J.R. Durrant, C. Petit, Titanium dioxide/carbon nitride nanosheet nanocomposites for gas phase CO<sub>2</sub> photoreduction under UV-visible irradiation, *Appl. Catal. B Environ.* 242 (2019) 369–378, <https://doi.org/10.1016/j.apcatb.2018.10.023>.
- [565] L. Wang, P. Jin, J. Huang, H. She, Q. Wang, Integration of copper (II)-porphyrin zirconium metal–organic framework and titanium dioxide to construct Z-scheme system for highly improved photocatalytic CO<sub>2</sub> reduction, *ACS Sustain. Chem. Eng.* 7 (18) (2019) 15660–15670, <https://doi.org/10.1021/acssuschemeng.9b03773>.
- [566] M. Nasr, C. Eid, R. Habchi, P. Miele, M. Bechelany, Recent progress on titanium dioxide nanomaterials for photocatalytic applications, *ChemSusChem* 11 (18) (2018) 3023–3047, <https://doi.org/10.1002/cssc.201800874>.
- [567] A. Zhou, Y. Dou, C. Zhao, J. Zhou, X.Q. Wu, J.R. Li, A leaf-branch TiO<sub>2</sub>/carbon@MOF composite for selective CO<sub>2</sub> photoreduction, *Appl. Catal. B Environ.* 264 (2020) 118519, <https://doi.org/10.1016/j.apcatb.2019.118519>.
- [568] N. Shehzad, M. Tahir, K. Johari, T. Murugesan, M. Hussain, Improved interfacial bonding of graphene-TiO<sub>2</sub> with enhanced photocatalytic reduction of CO<sub>2</sub> into solar fuel, *J. Environ. Chem. Eng.* 6 (6) (2018) 6947–6957, <https://doi.org/10.1016/j.jece.2018.10.065>.
- [569] O. Shtyka, V. Shatsila, R. Ciesielski, A. Kedziora, W. Maniukiewicz, S. Dubkov, D. Gromov, A. Tarasov, J. Rogowski, A. Stadnichenko, P. Lazarenko, R. Ryazanov, M.I. Szynkowska-Józwik, T. Maniecki, Adsorption and photocatalytic reduction of carbon dioxide on TiO<sub>2</sub>, *Catalysts* 11 (1) (2020) 47, <https://doi.org/10.3390/catal11010047>.
- [570] G. Jiang, Q. Huang, S.D. Kenarsari, X. Hu, A.G. Russell, M. Fan, X. Shen, A new mesoporous amine-TiO<sub>2</sub> based pre-combustion CO<sub>2</sub> capture technology, *Appl. Energy* 147 (2015) 214–223, <https://doi.org/10.1016/j.apenergy.2015.01.081>.
- [571] Y. Liao, S.W. Cao, Y. Yuan, Q. Gu, Z. Zhang, C. Xue, Efficient CO<sub>2</sub> capture and photoreduction by amine-functionalized TiO<sub>2</sub>, *Chem. Eur. J.* 20 (33) (2014) 10220–10222, <https://doi.org/10.1002/chem.20140321>.
- [572] C.C. Aquino, G. Richner, M. Chee Kimling, D. Chen, G. Puxty, P.H. Feron, R.A. Caruso, Amine-functionalized titania-based porous structures for carbon dioxide postcombustion capture, *J. Phys. Chem. C* 117 (19) (2013) 9747–9757, <https://doi.org/10.1021/jp312118e>.
- [573] K. Müller, D. Lu, S.D. Senanayake, D.E. Starr, Monoethanolamine adsorption on TiO<sub>2</sub> (110): bonding, structure, and implications for use as a model solid-supported CO<sub>2</sub> capture material, *J. Phys. Chem. C* 118 (3) (2014) 1576–1586, <https://doi.org/10.1021/jp409098p>.
- [574] J. Kapica-Kozar, E. Piróg, E. Kusiak-Nejman, R.J. Wrobel, A. Gęsickiewicz-Puchalska, A.W. Morawski, U. Narkiewicz, B. Michalkiewicz, Titanium dioxide modified with various amines used as sorbents of carbon dioxide, *New J. Chem.* 41 (4) (2017) 1549–1557, <https://doi.org/10.1039/C6NJ02808J>.
- [575] M. Ota, Y. Hirota, Y. Uchida, N. Nishiyama, CO<sub>2</sub> adsorption property of amine-modified amorphous TiO<sub>2</sub> nanoparticles with a high surface area, *Colloids Interfaces* 2 (3) (2018) 25, <https://doi.org/10.3390/colloids2030025>.
- [576] J.C. Yu, L. Zhang, Z. Zheng, J. Zhao, Synthesis and characterization of phosphated mesoporous titanium dioxide with high photocatalytic activity, *Chem. Mater.* 15 (11) (2003) 2280–2286, <https://doi.org/10.1021/cm0340781>.
- [577] Z. Huang, P. Dong, Y. Zhang, X. Nie, X. Wang, X. Zhang, A ZIF-8 decorated TiO<sub>2</sub> grid-like film with high CO<sub>2</sub> adsorption for CO<sub>2</sub> photoreduction, *J. CO<sub>2</sub> Util.* 24 (2018) 369–375, <https://doi.org/10.1016/j.jcou.2018.01.024>.
- [578] S.F. Wu, Y.Q. Zhu, Behavior of CaTiO<sub>3</sub>/nano-CaO as a CO<sub>2</sub> reactive adsorbent, *Ind. Eng. Chem. Res.* 49 (6) (2010) 2701–2706, <https://doi.org/10.1021/ie900900r>.
- [579] M. Alfe, P. Ammendola, V. Gargiulo, F. Raganati, R. Chirone, Magnetite loaded carbon fine particles as low-cost CO<sub>2</sub> adsorbent in a sound assisted fluidized bed, *Proc. Combust. Inst.* 35 (3) (2015) 2801–2809, <https://doi.org/10.1016/j.proci.2014.06.037>.
- [580] S. Kumar, S.K. Saxena, A comparative study of CO<sub>2</sub> sorption properties for different oxides, *Mater. Renew. Sustain. Energy* 3 (3) (2014) 1–15, <https://doi.org/10.1007/s40243-014-0030-9>.
- [581] Y. Kim, E. Worrell, International comparison of CO<sub>2</sub> emission trends in the iron and steel industry, *Energy Pol.* 30 (10) (2002) 827–838, [https://doi.org/10.1016/S0301-4215\(01\)00130-6](https://doi.org/10.1016/S0301-4215(01)00130-6).
- [582] A. Hakim, T.S. Marliza, N.M. Abu Tahari, R.W. Wan Isahak, R.M. Yusop, W.M. Mohamed Hisham, A.M. Yarmo, Studies on CO<sub>2</sub> adsorption and desorption properties from various types of iron oxides (FeO, Fe<sub>2</sub>O<sub>3</sub>, and Fe<sub>3</sub>O<sub>4</sub>), *Ind. Eng. Chem. Res.* 55 (29) (2016) 7888–7897, <https://doi.org/10.1021/acs.iecr.5b04091>.
- [583] E.Y.M. Mendoza, A.S. Santos, E.V. López, V. Drozd, A. Durygin, J. Chen, S.K. Saxena, Iron oxides as efficient sorbents for CO<sub>2</sub> capture, *J. Mater. Res. Technol.* 8 (3) (2019) 2944–2956, <https://doi.org/10.1016/j.jmrt.2019.05.002>.
- [584] V. Hiremath, H.J. Kwon, I.S. Jung, S. Kwon, S.H. Kwon, S.G. Lee, H.C. Lee, J.G. Seo, Mg-ion inversion in Mg@MgO–Al<sub>2</sub>O<sub>3</sub> oxides: the origin of basic sites, *ChemSusChem* 12 (12) (2019) 2810–2818, <https://doi.org/10.1002/cssc.201900072>.
- [585] M.B. Jensen, L.G. Pettersson, O. Swang, U. Olsbye, CO<sub>2</sub> sorption on MgO and CaO surfaces: a comparative quantum chemical cluster study, *J. Phys. Chem. B* 109 (35) (2005) 16774–16781, <https://doi.org/10.1021/jp052037h>.
- [586] N.N. Meis, J.H. Bitter, K.P. de Jong, Support and size effects of activated hydroxalites for precombustion CO<sub>2</sub> capture, *Ind. Eng. Chem. Res.* 49 (3) (2010) 1229–1235, <https://doi.org/10.1021/ie901114d>.
- [587] P. Li, R. Chen, Y. Lin, W. Li, General approach to facile synthesis of MgO-based porous ultrathin nanosheets enabling high-efficiency CO<sub>2</sub> capture, *Chem. Eng. J.* 404 (2021) 126459, <https://doi.org/10.1016/j.cej.2020.126459>.
- [588] A. Hassanzadeh, J. Abbasian, Regenerable MgO-based sorbents for high-temperature CO<sub>2</sub> removal from syngas: 1. Sorbent development, evaluation, and reaction modeling, *Fuel* 89 (6) (2010) 1287–1297, <https://doi.org/10.1016/j.fuel.2009.11.017>.
- [589] K. Zhang, X.S. Li, Y. Duan, D.L. King, P. Singh, L. Li, Roles of double salt formation and NaNO<sub>3</sub> in Na<sub>2</sub>CO<sub>3</sub>-promoted MgO absorbent for intermediate temperature CO<sub>2</sub> removal, *Int. J. Greenh. Gas Control* 12 (2013) 351–358, <https://doi.org/10.1016/j.ijggc.2012.11.013>.
- [590] G. Xiao, R. Singh, A. Chaffee, P. Webley, Advanced adsorbents based on MgO and K<sub>2</sub>CO<sub>3</sub> for capture of CO<sub>2</sub> at elevated temperatures, *Int. J. Greenh. Gas Control* 5 (4) (2011) 634–639, <https://doi.org/10.1016/j.ijggc.2011.04.002>.
- [591] Y. Guo, C. Tan, P. Wang, J. Sun, W. Li, C. Zhao, P. Lu, Magnesium-based basic mixtures derived from earth-abundant natural minerals for CO<sub>2</sub> capture in simulated flue gas, *Fuel* 243 (2019) 298–305, <https://doi.org/10.1016/j.fuel.2019.01.108>.
- [592] A. Dal Pozzo, A. Armutulu, M. Rekhtina, P.M. Abdala, C.R. Müller, CO<sub>2</sub> uptake and cyclic stability of MgO-based CO<sub>2</sub> sorbents promoted with alkali metal nitrates and their eutectic mixtures, *ACS Appl. Energy Mater.* 2 (2) (2019) 1295–1307, <https://doi.org/10.1021/acsael.8b01852>.
- [593] S. Jin, G. Bang, L. Liu, C.H. Lee, Synthesis of mesoporous MgO–CeO<sub>2</sub> composites with enhanced CO<sub>2</sub> capture rate via controlled combustion, *Micro-porous Mesoporous Mater.* 288 (2019) 109587, <https://doi.org/10.1016/j.micromeso.2019.109587>.
- [594] X. Feng, F. Pan, B.Z. Tran, Y. Li, Photocatalytic CO<sub>2</sub> reduction on porous TiO<sub>2</sub> synergistically promoted by atomic layer deposited MgO overcoating and photodeposited silver nanoparticles, *Catal. Today* 339 (2020) 328–336, <https://doi.org/10.1016/j.cattod.2019.03.012>.
- [595] V. Hiremath, M.L.T. Trivino, J.G. Seo, Eutectic mixture promoted CO<sub>2</sub> sorption on MgO-TiO<sub>2</sub> composite at elevated temperature, *J. Environ. Sci.* 76 (2019) 80–88, <https://doi.org/10.1016/j.jes.2018.03.028>.
- [596] A.H. Ruhami, M.A.A. Aziz, A.A. Jalil, Magnesium oxide-based adsorbents for carbon dioxide capture: current progress and future opportunities, *J. CO<sub>2</sub> Util.* 43 (2021) 101357, <https://doi.org/10.1016/j.jcou.2020.101357>.
- [597] V.A. Tuan, C.H. Lee, Preparation of rod-like MgO by simple precipitation method for CO<sub>2</sub> capture at ambient temperature, *Vietnam J. Chem.* 56 (2) (2018) 197–202, <https://doi.org/10.1002/vjch.201800013>.
- [598] M. Bhagyalakshmi, J.Y. Lee, H.T. Jang, Synthesis of mesoporous magnesium oxide: its application to CO<sub>2</sub> chemisorption, *Int. J. Greenh. Gas Control* 4 (1) (2010) 51–56, <https://doi.org/10.1016/j.ijggc.2009.08.001>.
- [599] K. Ho, S. Jin, M. Zhong, A.T. Vu, C.H. Lee, Sorption capacity and stability of mesoporous magnesium oxide in post-combustion CO<sub>2</sub> capture, *Mater. Chem. Phys.* 198 (2017) 154–161, <https://doi.org/10.1016/j.matchemphys.2017.06.002>.
- [600] A.M. Alkadem, M.A. Elgzoly, S.A. Onaizi, Novel amine-functionalized magnesium oxide adsorbents for CO<sub>2</sub> capture at ambient conditions, *J. Environ. Chem. Eng.* 8 (4) (2020) 103968, <https://doi.org/10.1016/j.jece.2020.103968>.
- [601] T. Boningari, S.N.R. Inturi, V.I. Manousiouthakis, P.G. Smirniotis, Facile synthesis of flame spray pyrolysis-derived magnesium oxide nanoparticles for CO<sub>2</sub> sorption: effect of precursors, morphology, and structural properties, *Ind. Eng. Chem. Res.* 57 (28) (2018) 9054–9061, <https://doi.org/10.1021/acs.iecr.8b00188>.
- [602] N. Yang, P. Ning, K. Li, J. Wang, MgO-based adsorbent achieved from magnesite for CO<sub>2</sub> capture in simulate wet flue gas, *J. Taiwan Inst. Chem. Eng.* 86 (2018) 73–80, <https://doi.org/10.1016/j.jtice.2018.02.006>.

- [603] K.K. Han, Y. Zhou, W.G. Lin, J.H. Zhu, One-pot synthesis of foam-like magnesia and its performance in CO<sub>2</sub> adsorption, *Microporous Mesoporous Mater.* 169 (2013) 112–119, <https://doi.org/10.1016/j.micromeso.2012.11.004>.
- [604] W. Gao, T. Zhou, B. Louis, Q. Wang, Hydrothermal fabrication of high specific surface area mesoporous MgO with excellent CO<sub>2</sub> adsorption potential at intermediate temperatures, *Catalysts* 7 (4) (2017) 116, <https://doi.org/10.3390/catal7040116>.
- [605] W. Gao, T. Zhou, Q. Wang, Controlled synthesis of MgO with diverse basic sites and its CO<sub>2</sub> capture mechanism under different adsorption conditions, *Chem. Eng. J.* 336 (2018) 710–720, <https://doi.org/10.1016/j.cej.2017.12.025>.
- [606] Y. Guo, C. Tan, P. Wang, J. Sun, W. Li, C. Zhao, P. Lu, Structure-performance relationships of magnesium-based CO<sub>2</sub> adsorbents prepared with different methods, *Chem. Eng. J.* 379 (2020) 122277, <https://doi.org/10.1016/j.cej.2019.122277>.
- [607] Y. Hu, X. Liu, Z. Zhou, W. Liu, M. Xu, Pelletization of MgO-based sorbents for intermediate temperature CO<sub>2</sub> capture, *Fuel* 187 (2017) 328–337, <https://doi.org/10.1016/j.fuel.2016.09.066>.
- [608] G.B. Elvira, G.C. Francisco, S.M. Victor, M.L.R. Alberto, MgO-based adsorbents for CO<sub>2</sub> adsorption: influence of structural and textural properties on the CO<sub>2</sub> adsorption performance, *J. Environ. Sci.* 57 (2017) 418–428, <https://doi.org/10.1016/j.jes.2016.11.016>.
- [609] S. Kumar, S.K. Saxena, V. Drozd, A. Durygin, An experimental investigation of mesoporous MgO as a potential pre-combustion CO<sub>2</sub> sorbent, *Mater. Renew. Sustain. Energy* 4 (2) (2015) 1–8, <https://doi.org/10.1007/s40243-015-0050-0>.
- [610] W.J. Liu, H. Jiang, K. Tian, Y.W. Ding, H.Q. Yu, Mesoporous carbon stabilized MgO nanoparticles synthesized by pyrolysis of MgCl<sub>2</sub> preloaded waste biomass for highly efficient CO<sub>2</sub> capture, *Environ. Sci. Technol.* 47 (16) (2013) 9397–9403, <https://doi.org/10.1021/es401286p>.
- [611] M. Bhagiyalakshmi, P. Hemalatha, M. Ganesh, P.M. Mei, H.T. Jang, A direct synthesis of mesoporous carbon supported MgO sorbent for CO<sub>2</sub> capture, *Fuel* 90 (4) (2011) 1662–1667, <https://doi.org/10.1016/j.fuel.2010.10.050>.
- [612] Y. Guo, C. Tan, J. Sun, W. Li, J. Zhang, C. Zhao, Biomass ash stabilized MgO adsorbents for CO<sub>2</sub> capture application, *Fuel* 259 (2020) 116298, <https://doi.org/10.1016/j.fuel.2019.116298>.
- [613] X. Fu, N. Zhao, J. Li, F. Xiao, W. Wei, Y. Sun, Carbon dioxide capture by MgO-modified MCM-41 materials, *Adsorpt. Sci. Technol.* 27 (6) (2009) 593–601, <https://doi.org/10.1260/0263-6174.27.6.593>.
- [614] H. Burri, R. Anjum, R.B. Gurram, H. Mitta, S. Mutyala, M. Jonnalagadda, Mesoporous carbon supported MgO for CO<sub>2</sub> capture and separation of CO<sub>2</sub>/N<sub>2</sub>, *Korean J. Chem. Eng.* 36 (9) (2019) 1482–1488, <https://doi.org/10.1007/s11814-019-0346-3>.
- [615] S. Zhang, W. Cai, J. Yu, C. Ji, N. Zhao, A facile one-pot cation-anion double hydrolysis approach to the synthesis of supported MgO/γ-Al<sub>2</sub>O<sub>3</sub> with enhanced adsorption performance towards CO<sub>2</sub>, *Chem. Eng. J.* 310 (2017) 216–225, <https://doi.org/10.1016/j.cej.2016.10.114>.
- [616] Q. Pu, Y. Wang, X. Wang, Z. Shao, S. Wen, J. Wang, Q. Wang, Biomass-derived carbon/MgO-Al<sub>2</sub>O<sub>3</sub> composite with superior dynamic CO<sub>2</sub> uptake for post combustion capture application, *J. CO<sub>2</sub> Util.* 54 (2021) 101756, <https://doi.org/10.1016/j.jcou.2021.101756>.
- [617] A. Chen, Y. Yu, Y. Li, Y. Li, M. Jia, Solid-state grinding synthesis of ordered mesoporous MgO/carbon spheres composites for CO<sub>2</sub> capture, *Mater. Lett.* 164 (2016) 520–523, <https://doi.org/10.1016/j.matlet.2015.11.043>.
- [618] S. Liu, X. Zhang, J. Li, N. Zhao, W. Wei, Y. Sun, Preparation and application of stabilized mesoporous MgO-ZrO<sub>2</sub> solid base, *Catal. Commun.* 9 (7) (2008) 1527–1532, <https://doi.org/10.1016/j.catcom.2007.12.007>.
- [619] Z. Xu, T. Jiang, H. Zhang, Y. Zhao, X. Ma, S. Wang, Efficient MgO-doped CaO sorbent pellets for high temperature CO<sub>2</sub> capture, *Front. Chem. Sci. Eng.* 15 (3) (2021) 698–708, <https://doi.org/10.1007/s11705-020-1981-2>.
- [620] J.L. Chen, X.Y.M. Dong, C.L. Shi, S.H. Li, Y. Wang, J.H. Zhu, Fabrication of strong solid base FeO–MgO for warm CO<sub>2</sub> capture, *Clean Soil Air Water* 47 (8) (2019) 1800447, <https://doi.org/10.1002/clen.201800447>.
- [621] C.H. Lee, S. Mun, K.B. Lee, Characteristics of Na–Mg double salt for high-temperature CO<sub>2</sub> sorption, *Chem. Eng. J.* 258 (2014) 367–373, <https://doi.org/10.1016/j.cej.2014.07.082>.
- [622] Y. Qiao, J. Wang, Y. Zhang, W. Gao, T. Harada, L. Huang, T.A. Hatton, Q. Wang, Alkali nitrates molten salt modified commercial MgO for intermediate-temperature CO<sub>2</sub> capture: optimization of the Li/Na/K ratio, *Ind. Eng. Chem. Res.* 56 (6) (2017) 1509–1517, <https://doi.org/10.1021/acs.iecr.6b04793>.
- [623] J. Ding, C. Yu, J. Lu, X. Wei, W. Wang, G. Pan, Enhanced CO<sub>2</sub> adsorption of MgO with alkali metal nitrates and carbonates, *Appl. Energy* 263 (2020) 114681, <https://doi.org/10.1016/j.apenergy.2020.114681>.
- [624] W. Gao, M.A. Vasiliades, C.M. Damaskinos, M. Zhao, W. Fan, Q. Wang, T.R. Reina, A.M. Efstratiou, Molten salt-promoted MgO adsorbents for CO<sub>2</sub> capture: transient kinetic studies, *Environ. Sci. Technol.* 55 (8) (2021) 4513–4521, <https://doi.org/10.1021/acs.est.0c08731>.
- [625] S.J. Park, Y. Kim, C.W. Jones, NaNO<sub>3</sub>-promoted mesoporous MgO for high-capacity CO<sub>2</sub> capture from simulated flue gas with isothermal regeneration, *ChemSusChem* 13 (11) (2020) 2988–2995, <https://doi.org/10.1002/cssc.202000259>.
- [626] H. Cui, Q. Zhang, Y. Hu, C. Peng, X. Fang, Z. Cheng, V.V. Galvita, Z. Zhou, Ultrafast and stable CO<sub>2</sub> capture using alkali metal salt-promoted MgO–CaCO<sub>3</sub> sorbents, *ACS Appl. Mater. Interfaces* 10 (24) (2018) 20611–20620, <https://doi.org/10.1021/acsami.8b05829>.
- [627] P. Kasikamphaiboon, U. Khunjan, CO<sub>2</sub> adsorption from biogas using amine-functionalized MgO, *Int. J. Chem. Eng.* (2018), <https://doi.org/10.1155/2018/1706405>.
- [628] S.A. Salaudeen, B. Acharya, A. Dutta, CaO-based CO<sub>2</sub> sorbents: a review on screening, enhancement, cyclic stability, regeneration and kinetics modeling, *J. CO<sub>2</sub> Util.* 23 (2018) 179–199, <https://doi.org/10.1016/j.jcou.2017.11.012>.
- [629] L. Li, D.L. King, Z. Nie, C. Howard, Magnesia-stabilized calcium oxide absorbents with improved durability for high temperature CO<sub>2</sub> capture, *Ind. Eng. Chem. Res.* 48 (23) (2009) 10604–10613, <https://doi.org/10.1021/ie901166b>.
- [630] P. Gruene, A.G. Belova, T.M. Yegulalp, R.J. Farrauto, M.J. Castaldi, Dispersed calcium oxide as a reversible and efficient CO<sub>2</sub> sorbent at intermediate temperatures, *Ind. Eng. Chem. Res.* 50 (7) (2011) 4042–4049, <https://doi.org/10.1021/je102475d>.
- [631] K. Han, C. Lu, S. Cheng, G. Zhao, Y. Wang, J. Zhao, Effect of characteristics of calcium-based sorbents on the sulfation kinetics, *Fuel* 84 (14–15) (2005) 1933–1939, <https://doi.org/10.1016/j.fuel.2005.04.001>.
- [632] C.H. Huang, K.P. Chang, C.T. Yu, P.C. Chiang, C.F. Wang, Development of high-temperature CO<sub>2</sub> sorbents made of CaO-based mesoporous silica, *Chem. Eng. J.* 161 (1–2) (2010) 129–135, <https://doi.org/10.1016/j.cej.2010.04.045>.
- [633] C. Luo, Y. Zheng, Y. Xu, N. Ding, Q. Shen, C. Zheng, Wet mixing combustion synthesis of CaO-based sorbents for high temperature cyclic CO<sub>2</sub> capture, *Chem. Eng. J.* 267 (2015) 111–116, <https://doi.org/10.1016/j.cej.2015.01.005>.
- [634] N.H. Florin, A.T. Harris, Screening CaO-based sorbents for CO<sub>2</sub> capture in biomass gasifiers, *Energy Fuels* 22 (4) (2008) 2734–2742, <https://doi.org/10.1021/ef700751g>.
- [635] M. Heidari, M. Tahmasebpoor, S.B. Mousavi, C. Pevida, CO<sub>2</sub> capture activity of a novel CaO adsorbent stabilized with (ZrO<sup>2+</sup> Al<sub>2</sub>O<sub>3</sub>+ CeO<sub>2</sub>)-based additive under mild and realistic calcium looping conditions, *J. CO<sub>2</sub> Util.* 53 (2021) 101747, <https://doi.org/10.1016/j.jcou.2021.101747>.
- [636] N. Wang, Y. Feng, X. Guo, Atomistic mechanisms study of the carbonation reaction of CaO for high-temperature CO<sub>2</sub> capture, *Appl. Surf. Sci.* 532 (2020) 147425, <https://doi.org/10.1016/j.apsusc.2020.147425>.
- [637] J.C. Abanades, D. Alvarez, Conversion limits in the reaction of CO<sub>2</sub> with lime, *Energy Fuels* 17 (2) (2003) 308–315, <https://doi.org/10.1021/ef020152a>.
- [638] R. Barker, The reactivity of calcium oxide towards carbon dioxide and its use for energy storage, *J. Appl. Chem. Biotechnol.* 24 (4–5) (1974) 221–227, <https://doi.org/10.1002/jctb.2720240405>.
- [639] S.K. Bhatia, D.D. Perlmuter, Effect of the product layer on the kinetics of the CO<sub>2</sub>-lime reaction, *AIChE J.* 29 (1) (1983) 79–86, <https://doi.org/10.1002/aic.690290111>.
- [640] H. Sun, C. Wu, B. Shen, X. Zhang, Y. Zhang, J. Huang, Progress in the development and application of CaO-based adsorbents for CO<sub>2</sub> capture—a review, *Mater. Today Sustain.* 1 (2018) 1–27, <https://doi.org/10.1016/j.mtsust.2018.08.001>.
- [641] A. Nawar, M. Ali, A.H. Khoja, A. Waqas, M. Anwar, M. Mahmood, Enhanced CO<sub>2</sub> capture using organic acid structure modified waste eggshell derived CaO sorbent, *J. Environ. Chem. Eng.* 9 (1) (2021) 104871, <https://doi.org/10.1016/j.je.2020.104871>.
- [642] F.N. Ridha, V. Manovic, A. Macchi, E.J. Anthony, CO<sub>2</sub> capture at ambient temperature in a fixed bed with CaO-based sorbents, *Appl. Energy* 140 (2015) 297–303, <https://doi.org/10.1016/j.apenergy.2014.11.030>.
- [643] K. Liu, B. Zhao, Y. Wu, F. Li, Q. Li, J. Zhang, Bubbling synthesis and high-temperature CO<sub>2</sub> adsorption performance of CaO-based adsorbents from carbide slag, *Fuel* 269 (2020) 117481, <https://doi.org/10.1016/j.fuel.2020.117481>.
- [644] S.L. Hsieh, F.Y. Li, P.Y. Lin, D.E. Beck, R. Kirankumar, G.J. Wang, S. Hsieh, CaO recovered from eggshell waste as a potential adsorbent for greenhouse gas CO<sub>2</sub>, *J. Environ. Manag.* 297 (2021) 113430, <https://doi.org/10.1016/j.jenvman.2021.113430>.
- [645] C. Luo, Y. Zheng, C. Zheng, J. Yin, C. Qin, B. Feng, Manufacture of calcium-based sorbents for high temperature cyclic CO<sub>2</sub> capture via a sol–gel process, *Int. J. Greenh. Gas Control* 12 (2013) 193–199, <https://doi.org/10.1016/j.ijggc.2012.11.011>.
- [646] P. Jamrunroj, S. Wongsakulphasatch, A. Maneedaeng, C.K. Cheng, S. Assabumrungrat, Surfactant assisted CaO-based sorbent synthesis and their application to high-temperature CO<sub>2</sub> capture, *Powder Technol.* 344 (2019) 208–221, <https://doi.org/10.1016/j.powtec.2018.12.011>.
- [647] Y. Xu, B. Xiaoy, Y. Feng, W. Yang, Y. Lv, Mn-promoted CaO-based adsorbents with enhanced CO<sub>2</sub> uptake performance, *J. Nat. Gas Sci. Eng.* 94 (2021) 104029, <https://doi.org/10.1016/j.jngse.2021.104029>.
- [648] X. Zhang, Z. Li, Y. Peng, W. Su, X. Sun, J. Li, Investigation on a novel CaO–Y<sub>2</sub>O<sub>3</sub> sorbent for efficient CO<sub>2</sub> mitigation, *Chem. Eng. J.* 243 (2014) 297–304, <https://doi.org/10.1016/j.cej.2014.01.017>.
- [649] M. Zhang, Y. Peng, Y. Sun, P. Li, J. Yu, Preparation of CaO–Al<sub>2</sub>O<sub>3</sub> sorbent and CO<sub>2</sub> capture performance at high temperature, *Fuel* 111 (2013) 636–642, <https://doi.org/10.1016/j.fuel.2013.03.078>.
- [650] F. Gao, J. Huang, H. Sun, J. Hu, M. Wang, J. Mi, C. Wu, CO<sub>2</sub> capture using mesocellular siliceous foam (MCF)-supported CaO, *J. Energy Inst.* 92 (5) (2019) 1591–1598, <https://doi.org/10.1016/j.joei.2018.07.015>.
- [651] H. Sun, C.M. Parlett, M.A. Isaacs, X. Liu, G. Adwek, J. Wang, B. Shen, J. Huang, C. Wu, Development of Ca/KIT-6 adsorbents for high temperature CO<sub>2</sub>

- capture, *Fuel* 235 (2019) 1070–1076, <https://doi.org/10.1016/j.fuel.2018.07.044>.
- [652] S.S. Kazi, A. Aranda, J. Meyer, J. Mastin, High performance CaO-based sorbents for pre-and post-combustion CO<sub>2</sub> capture at high temperature, *Energy Proc.* 63 (2014) 2207–2215, <https://doi.org/10.1016/j.egypro.2014.11.240>.
- [653] M. Broda, A.M. Kierzkowska, C.R. Müller, Influence of the calcination and carbonation conditions on the CO<sub>2</sub> uptake of synthetic Ca-based CO<sub>2</sub> sorbents, *Environ. Sci. Technol.* 46 (19) (2012) 10849–10856, <https://doi.org/10.1021/es302757e>.
- [654] N. Gao, K. Chen, C. Quan, Development of CaO-based adsorbents loaded on charcoal for CO<sub>2</sub> capture at high temperature, *Fuel* 260 (2020) 116411, <https://doi.org/10.1016/j.fuel.2019.116411>.
- [655] T. Jiang, H. Zhang, Y. Zhao, C. Qin, S. Wang, X. Ma, Kilogram-scale production and pelletization of Al-promoted CaO-based sorbent for CO<sub>2</sub> capture, *Fuel* 301 (2021) 121049, <https://doi.org/10.1016/j.fuel.2021.121049>.
- [656] H. Sun, J. Wang, J. Zhao, B. Shen, J. Shi, J. Huang, C. Wu, Dual functional catalytic materials of Ni over Ce-modified CaO sorbents for integrated CO<sub>2</sub> capture and conversion, *Appl. Catal. B Environ.* 244 (2019) 63–75, <https://doi.org/10.1016/j.apcatb.2018.11.040>.
- [657] F.N. Ridha, V. Manovic, Y. Wu, A. Macchi, E.J. Anthony, Post-combustion CO<sub>2</sub> capture by formic acid-modified CaO-based sorbents, *Int. J. Greenh. Gas Control* 16 (2013) 21–28, <https://doi.org/10.1016/j.ijggc.2013.02.026>.
- [658] R.J. Gorte, Ceria in catalysis: from automotive applications to the water–gas shift reaction, *AIChE J.* 56 (5) (2010) 1126–1135, <https://doi.org/10.1002/aic.12234>.
- [659] P. Fornasiero, G.R. Rao, J. Kašpar, F. L'erario, M. Graziani, Reduction of NO by CO over Rh/CeO<sub>2</sub>–ZrO<sub>2</sub> catalysts: evidence for a support-promoted catalytic activity, *J. Catal.* 175 (2) (1998) 269–279, <https://doi.org/10.1006/jcat.1998.1999>.
- [660] Y. Pu, Y. Luo, X. Wei, J. Sun, L. Li, W. Zou, L. Dong, Synergistic effects of Cu<sub>2</sub>O-decorated CeO<sub>2</sub> on photocatalytic CO<sub>2</sub> reduction: surface Lewis acid/base and oxygen defect, *Appl. Catal. B Environ.* 254 (2019) 580–586, <https://doi.org/10.1016/j.apcatb.2019.04.093>.
- [661] G.R. Rao, Influence of metal particles on the reduction properties of ceria-based materials studied by TPR, *Bull. Mater. Sci.* 22 (2) (1999) 89–94, <https://doi.org/10.1007/BF02745559>.
- [662] G.R. Rao, P. Fornasiero, R. Di Monte, J. Kašpar, G. Vlaic, G. Balducci, S. Meriani, G. Gubitoso, A. CremonaM. Graziani, Reduction of NO over partially reduced metal-loaded CeO<sub>2</sub>–ZrO<sub>2</sub> solid solutions, *J. Catal.* 162 (1) (1996) 1–9, <https://doi.org/10.1006/jcat.1996.0254>.
- [663] A. Trovarelli, Catalytic properties of ceria and CeO<sub>2</sub>-containing materials, *Catal. Rev.* 38 (4) (1996) 439–520, <https://doi.org/10.1080/01614949608006464>.
- [664] R. Juárez, P. Concepción, A. Corma, H. García, Ceria nanoparticles as heterogeneous catalyst for CO<sub>2</sub> fixation by  $\omega$ -aminoalcohols, *Chem. Commun.* 46 (23) (2010) 4181–4183, <https://doi.org/10.1039/C001955K>.
- [665] V.R.B. Gurrum, S.S. Enumula, S. Mutyalala, R. Pochamoni, P.S. Prasad, D.R. Burri, S.R.R. Kamaraju, The advantage of ceria loading over V<sub>2</sub>O<sub>5</sub>/Al<sub>2</sub>O<sub>3</sub> catalyst for vapor phase oxidative dehydrogenation of ethylbenzene to styrene using CO<sub>2</sub> as a soft oxidant, *Appl. Petrochem. Res.* 6 (4) (2016) 427–437, <https://doi.org/10.1007/s13203-016-0163-0>.
- [666] K. Reed, A. Cormack, A. Kulkarni, M. Mayton, D. Sayle, F. Klaessig, B. Stadler, Exploring the properties and applications of nanoceria: is there still plenty of room at the bottom? *Environ. Sci.: Nano* 1 (5) (2014) 390–405, <https://doi.org/10.1039/C4EN00079J>.
- [667] C. Walkley, S. Das, S. Seal, J. Erlichman, K. Heckman, L. Ghibelli, E. Traversa, J.F. McGinnis, W.T. Self, Catalytic properties and biomedical applications of cerium oxide nanoparticles, *Environ. Sci.: Nano* 2 (1) (2015) 33–53, <https://doi.org/10.1039/C4EN00138A>.
- [668] K. Yoshikawa, H. Sato, M. Kaneeda, J.N. Kondo, Synthesis and analysis of CO<sub>2</sub> adsorbents based on cerium oxide, *J. CO<sub>2</sub> Util.* 8 (2014) 34–38, <https://doi.org/10.1016/j.jcou.2014.10.001>.
- [669] M. Li, U. Tumuluri, Z. Wu, S. Dai, Effect of dopants on the adsorption of carbon dioxide on ceria surfaces, *ChemSusChem* 8 (21) (2015) 3651–3660, <https://doi.org/10.1002/cssc.201500899>.
- [670] C. Słosowski, S. Marre, P. Dagault, O. Babot, T. Toupane, C. Aymonier, CeO<sub>2</sub> nanopowders as solid sorbents for efficient CO<sub>2</sub> capture/release processes, *J. CO<sub>2</sub> Util.* 20 (2017) 52–58, <https://doi.org/10.1016/j.jcou.2017.03.023>.
- [671] A.A. Azmi, A.H. Ruhami, M.A.A. Aziz, Efficient 3-aminopropyltrimethoxysilane functionalised mesoporous ceria nanoparticles for CO<sub>2</sub> capture, *Mater. Today Chem.* 16 (2020) 100273, <https://doi.org/10.1016/j.mtchem.2020.100273>.
- [672] <https://www.epa.gov/energy/emissions-generation-resource-integrated-database-egrid>.
- [673] D.P. Hanak, V. Manovic, Techno-economic feasibility assessment of CO<sub>2</sub> capture from coal-fired power plants using molecularly imprinted polymer, *Fuel* 214 (2018) 512–520, <https://doi.org/10.1016/j.fuel.2017.10.107>.
- [674] S.E. Zanco, J.F. Pérez-Calvo, A. Gasós, B. Cordiano, V. Becattini, M. Mazzotti, Postcombustion CO<sub>2</sub> capture: a comparative techno-economic assessment of three technologies using a solvent, an adsorbent, and a membrane, *ACS Eng. Au* 1 (1) (2021) 50–72, <https://doi.org/10.1021/acsengineeringau.1c00002>.
- [675] S.G. Subraveti, S. Roussanaly, R. Anantharaman, L. Riboldi, A. Rajendran, How much can novel solid sorbents reduce the cost of post-combustion CO<sub>2</sub> capture? A techno-economic investigation on the cost limits of pressure–vacuum swing adsorption, *Appl. Energy* 306 (2022) 117955, <https://doi.org/10.1016/j.apenergy.2021.117955>.
- [676] M.T. Ho, G.W. Allinson, D.E. Wiley, Reducing the cost of CO<sub>2</sub> capture from flue gases using pressure swing adsorption, *Ind. Eng. Chem. Res.* 47 (14) (2008) 4883–4890, <https://doi.org/10.1021/ie070831e>.
- [677] J.M. Valverde, F. Pontiga, C. Soria-Hoyo, M.A.S. Quintanilla, H. Moreno, F.J. Duran, M.J. Espín, Improving the gas–solids contact efficiency in a fluidized bed of CO<sub>2</sub> adsorbent fine particles, *Phys. Chem. Chem. Phys.* 13 (33) (2011) 14909, <https://doi.org/10.1039/C1CP21939A>.
- [678] D. Geldart, Types of gas fluidization, *Powder Technol.* 7 (5) (1973) 285–292, [https://doi.org/10.1016/0032-5910\(73\)80037-3](https://doi.org/10.1016/0032-5910(73)80037-3).
- [679] F.R.M. Nascimento, A.M. González, E.E.S. Lora, A. Ratner, J.C.E. Palacio, R. Reinaldo, Bench-scale bubbling fluidized bed systems around the world-Bed agglomeration and collapse: a comprehensive review, *Int. J. Hydrogen Energy* 46 (36) (2021) 18740–18766, <https://doi.org/10.1016/j.ijhydene.2021.03.036>.
- [680] J. Yan, T. Shen, P. Wang, X. Yin, X. Zhu, S. Jiang, L. Shen, Redox performance of manganese ore in a fluidized bed thermogravimetric analyzer for chemical looping combustion, *Fuel* 295 (2021) 120564, <https://doi.org/10.1016/j.fuel.2021.120564>.
- [681] R.F. Nascimento, J.G. Rosa, M.F. Ávila, O.P. Taranto, Pea protein isolate fluid dynamics and characterization obtained by agglomeration in pulsed fluidized bed, *Part. Sci. Technol.* 39 (7) (2021) 809–819, <https://doi.org/10.1080/02726351.2020.1830209>.
- [682] M. Imani, M. Tahmasebpoor, P.E. Sánchez-Jiménez, J.M. Valverde, V. Moreno, Improvement in cyclic CO<sub>2</sub> capture performance and fluidization behavior of eggshell-derived CaCO<sub>3</sub> particles modified with acetic acid used in calcium looping process, *J. CO<sub>2</sub> Util.* 65 (2022) 102207, <https://doi.org/10.1016/j.jcou.2022.102207>.
- [683] D. Danaci, P.A. Webley, C. Petit, Guidelines for techno-economic analysis of adsorption processes, *Front. Chem. Eng.* 30 (2021), <https://doi.org/10.3389/feng.2020.602430>.